Substrate-selective Inhibition of Cyclooxygenase-2:
Molecular Determinants, Probe Development, and *In Vivo* Effects.

By

Daniel John Hermanson

Dissertation

Submitted to the Faculty of the

Graduate School of Vanderbilt University

in partial fulfillment of the requirements

for the degree of

DOCTOR OF PHILOSOPHY

in

Chemistry

May, 2014

Nashville, Tennessee

Approved:

Lawrence J. Marnett, Ph.D.

H. Alex Brown, Ph.D.

Bruce D. Carter, Ph.D.

Sachin Patel, M.D. Ph.D.

Ned A. Porter, Ph.D.

ACKNOWLEDGEMENTS

LIST OF TABLES

LIST OF FIGURES

LIST OF ABBREVIATIONS

2-AG	2-arachidonoyl glycerol
2-OG	2-oleoyl glycerol
AA	arachidonic acid
ACN	acetonitrile
AEA	arachidonoyl ethanolamide (anandamide)
BMDM	bone-marrow derived macrophage
CB	cannabinoid receptor
CID	collision induced dissociation
COX	cyclooxygenase
CNS	central nervous system
DAG	diacylglycerol
DAGL	diacylglycerol lipase
DMEM	Dulbecco's modified Eagle medium
DMSO	dimethyl sulfoxide
DRG	dorsal root ganglion
-EA	ethanolamide
EGF	epidermal growth factor
ERAD	endoplasmic reticulum associated degradation system
ERK	extracellular signal-related kinase
ESI	electrospray ionization
EtOAc	ethyl acetate
FAAH	fatty acid amide hydrolase
FBS	fetal bovine serum
-G	glyceryl ester
GI	gastrointestinal

GPCR	G-protein coupled receptor
HETE	hydroxyeicosatetraenoic acid
HPLC	high-performance liquid chromatography
IC_{50}	half maximal inhibitory concentration
IFNγ	interferonγ
IL	interleukin
IP_3	inositol tris-phospahte
IPA	isopropanol
LC	liquid chromatography
LPS	lipopolysaccharide
MAG	monoacyl glycerol
MAGL	monoacyl glycerol lipase
MAPK	mitogen-activated protein kinase
MeOH	methanol
MS	mass spectrometry
NAE	*N*-acylethanolamide
NAPE	*N*-arachidonoylphosphatidylethanolamine
NSAID	non-steroidal anti-inflammatory drug
OEA	oleoyl ethanolamide
PBS	phosphate buffered saline
PC	phosphatidyl choline
PI	phosphatidyl inositol
PIP_2	phosphatidyl inositol 4,5-*bis*phosphate
PG	prostaglandin
PKC	protein kinase C
PL	phospholipase

PLA   phospholipase A

PLC   phospholipase C

PLD   phospholipase D

PPA   5-phenyl-4-pentenyl alcohol

PPAR   peroxisome proliferator activated receptor

PPHP   5-phenyl-4-pentenyl hydroperoxide

POX   peroxidase

S.E.M.   standard error measure

SRM   selected reaction monitoring

THC   tetrahydrocannabinol

TRPV1   transient receptor potential vanilloid receptor 1

TxA$_2$ thromboxane

WT   wild-type

TABLE OF CONTENTS

CHAPTER I

INTRODUCTION

Cyclooxygenase Structure and Function

Cyclooxygenase Biochemistry and Pharmacology

The cyclooxygenase (COX) enzyme was first prepared and characterized in 1967 from sheep vesicular gland.[1] Further work identified that the COX enzyme exists in two separate isoforms, COX-1 and COX-2. COX-1 was first purified and identified in 1976 from bovine and sheep vesicular glands, while COX-2 was discovered in 1991.[2-4] The COX enzymes are membrane-bound homodimers that localize to the nuclear envelope, the lumen of the endoplasmic reticulum, and Golgi apparatus.[5] The COX enzymes consist of three domains, an epidermal growth factor (EGF)-like domain a membrane-binding domain, and a catalytic domain (Figure 1). In addition, the COX enzymes associate with a molecule of heme (Fe^{3+} protoporphyrin IX), which is required for catalysis.[3,6]
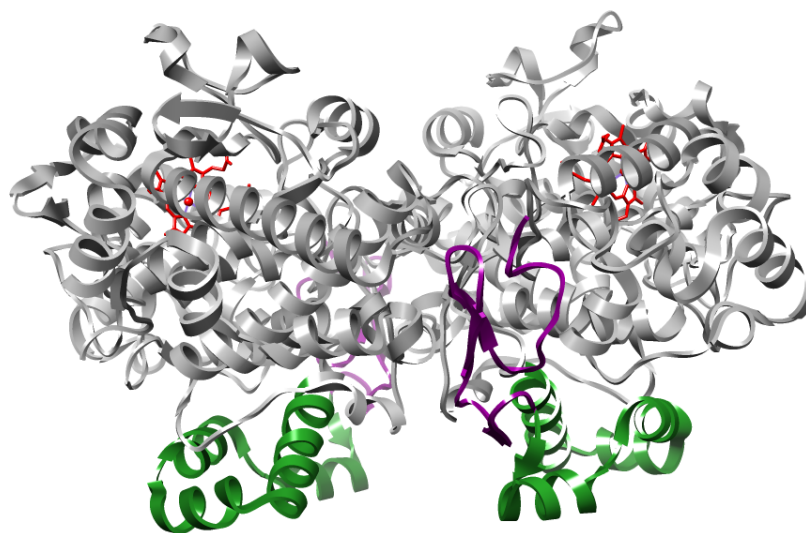
Figure 1: Structure of COX enzyme domains. The epidermal growth factor-like domain is shown in purple, the membrane-binding domain in green, and the catalytic domain is shown in grey. Heme is pictured in red. PDB ID: 3PGH.

The COX enzymes catalyze the conversion of arachidonic acid (AA) to prostaglandin endoperoxide H_2 (PGH_2) in two steps at two separate active sites. The cyclooxygenase active site catalyzes the *bis*-dioxygenation and cyclization of AA to form the hydroperoxy endoperoxide prostaglandin G_2 (PGG_2).[7] PGG_2 then exits the

1

cyclooxygenase active site and diffuses to the peroxidase active site, where a two-electron reduction of PGG_2 occurs to form the hydroxy endoperoxide PGH_2.[8] Although the two active sites are structurally separate, the cyclooxygenase reaction is functionally dependent upon the two-electron oxidation of the heme at the peroxidase active site. This two-electron oxidation of heme at the peroxidase activate site is coupled to the two-electron reduction of a hydroperoxide substrate, such as PGG_2.[9] The oxidation of the heme results in the formation of a ferryloxo protoporphyrin radical cation $((PPIX^{\bullet})^{+}Fe^{4+}O)$, which has been termed Compound I.[10,11] After formation, Compound I can abstract the phenolic hydrogen of Tyr-385 in the cyclooxygenase active site to form a tyrosyl radical, which can then initiate the cyclooxygenase reaction.

The free radical mechanism of the cyclooxygenase reaction was initially identified through biochemical and isotopic labeling studies.[1,12,13] The binding of AA within the L-shape of the cyclooxygenase active site positions its 13-pro-(S)-hydrogen adjacent to the tyrosyl radical at amino acid 385. The tyrosyl radical then abstracts the 13-pro-(S)-hydrogen of AA to form a carbon-centered arachidonyl radical, which can be trapped at carbon 11 by molecular oxygen to produce an 11-(R)-peroxyl radical (Figure 2). The 11-(R)-peroxyl radical then undergoes two cyclizations to form a bicyclic endoperoxide and an allylic radical between carbons 13 and 15. The allylic radical then reacts with a second molecule of molecular oxygen to form a peroxyl radical at carbon 15. Finally, the peroxyl radical abstracts the phenolic hydrogen of Tyr-385 to generate PGG_2 and regenerate the tyrosyl radical, which can further catalyze fatty acid oxygenation. PGG_2 then diffuses out of the cyclooxygenase active site and into the peroxidase active site, where it is reduced to form PGH_2. COX can also generate alternate products that result from no cyclization such as 11-hydroperoxyeicosatetraenoic acid (11-HpETE) if the 11-(R)-peroxyl radical does not undergo cyclization to form the endoperoxide ring at carbon 9 or 15-HpETE if molecular oxygen reacts with the initial arachidonyl radical at carbon 15.
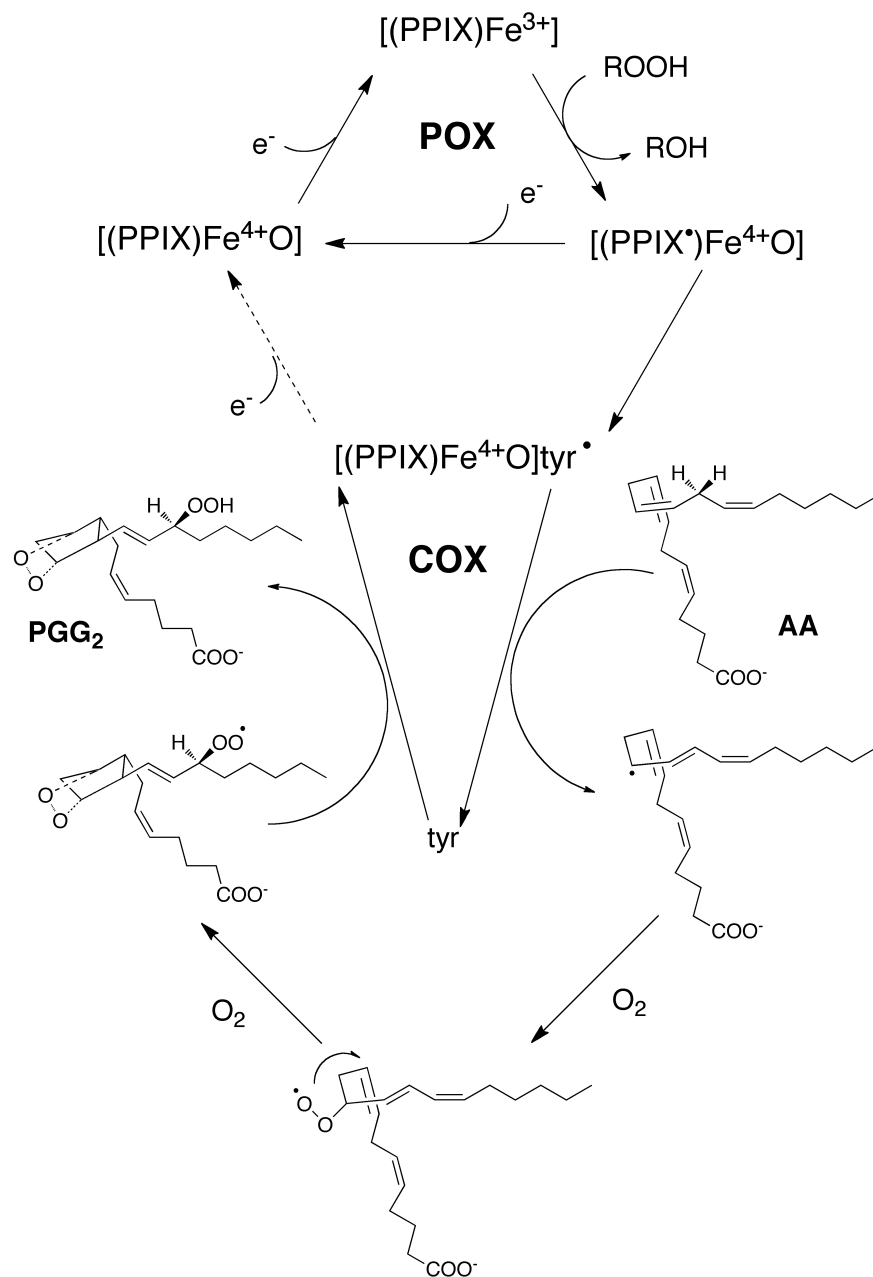
Figure 2: The mechanism of the cyclooxygenase reaction. In the peroxidase (POX) active site, the heme moiety $((PPIX)Fe^{3+})$ undergoes a two-electron oxidation to form Compound I $((PPIX•)Fe^{4+}O)$, while the hydroperoxide substrate (ROOH) undergoes a two-electron reduction. The enzyme can be brought back to its resting state by two subsequent one-electron reductions or the radical can abstract the phenolic hydrogen of Tyr-385 in the COX active site. When AA is bound within the cyclooxygenase (COX) active site, the tyrosyl radical can abstract the 13-pro-(*S*) hydrogen and initiate a series of radical rearrangements and two additions of molecular to form the hydroperoxy endoperoxide PGG_2. The radical is then transferred back to the tyrosine residue to allow the initiation of subsequent catalytic cycles.

The generation of PGH_2 from AA by the COX enzymes represents the committed step in the synthesis of prostaglandins (PGs). After synthesis by the COX enzymes, PGH_2 is processed by tissue specific synthases to form the prostaglandins PGE_2, PGD_2, and $PGF_{2\alpha}$, as well as prostacyclin (PGI_2) and thromboxane (TXA_2)

(Figure 3).[14] The prostanoids are bioactive lipids that mediate a plethora of physiological and pathophysiological processes through their actions at discrete G-protein coupled receptors (GPCRs) and nuclear receptors.[15-17] The differential expression of PG synthases and PG GPCR isoforms results in a complex, non-uniform response to COX action that is tissue-specific. For example, PGE_2 potentiates platelet aggregation, regulates kidney function, and provides gastrointestinal cytoprotection.[18-21] PGD_2 produces anti-inflammatory effects via Nrf2 and is cytoprotective in models of acute brain injury and heart ischemia-reperfusion injury.[22-24] PGI_2 is a potent vasodilator and anti-thrombotic agent, whereas TXA_2 induces vasoconstriction and thrombosis.[25-27] Prostanoids also have prevalent roles in pain, fever, inflammation, and tumorigenesis.[26,28-30]
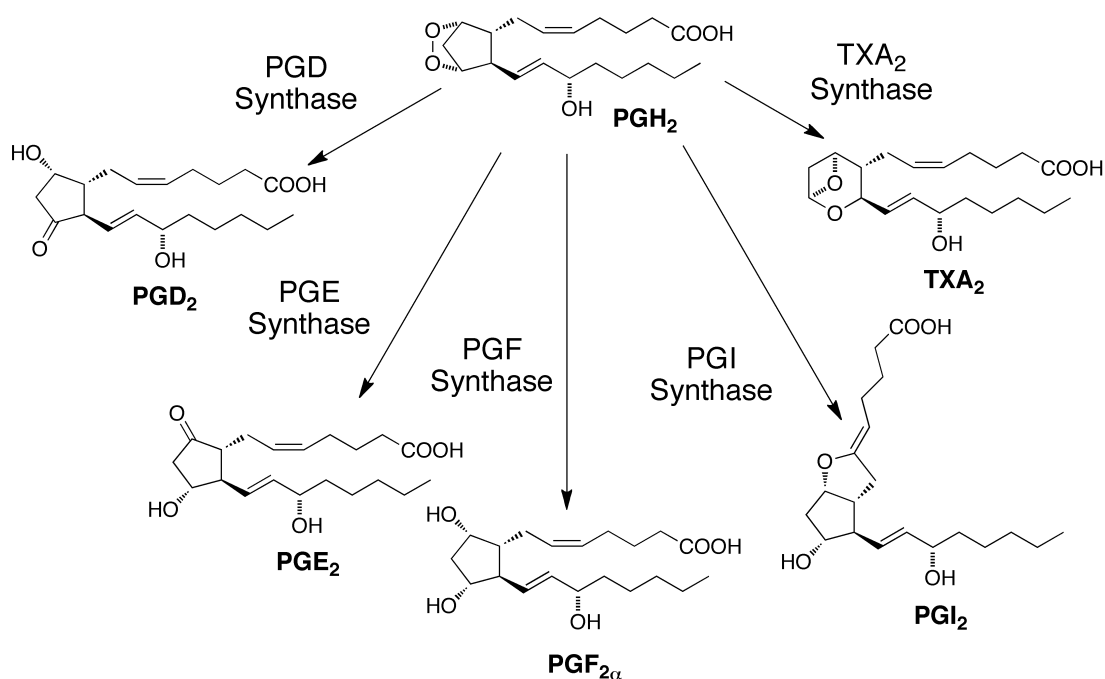
Figure 3: Formation of PGs from PGH_2. PGH_2 is processed by tissue specific synthases to form the prostaglandins PGD_2, PGE_2, and $PGF_{2\alpha}$, prostacyclin (PGI_2), and thromboxane (TXA_2).

Cyclooxygenase Structure

The first three-dimensional structure of COX-1 was published in 1994, followed two years later by the crystal structure of COX-2.[31,32] A 14-amino acid deletion at the N-terminus of COX-2 causes the numbers of most COX-2 amino acids to be 14 units lower than those of COX-1, but by convention, the amino acids of both isoforms are referred to by the numbering of COX-1. Comparison of the crystal structures of COX-1 and COX-2 reveals that the two isoforms have virtually superimposable structures.

4

Each monomer is comprised of three domains: an EGF-like domain, a membrane binding domain, and a large globular catalytic domain, which houses the COX and POX active sites.[31-33] The COX enzymes are present as homodimers with an extensive dimer interface created by the EGF-like and catalytic domains.[34] The EGF-like domain is made up by resides 34-72 of the *N*-terminus and its precise function remains unknown. However, it has been suggested that this domain may initiate or maintain interactions necessary for the insertion of COX into the membrane bilayer or homodimer formation.[35]

COX-2 associates with the outer leaflet of phospholipid bilayers with its membrane-binding domain, which is composed of residues 73-116 and contains four short amphipathic α-helices (A-D). The helices are positioned orthogonal to one another, creating a hydrophobic surface for insertion into the membrane bilayer. The helices of the membrane-binding domain also form an open area termed the "lobby", which substrates and inhibitors travel through to enter the active site located within the catalytic domain.

The catalytic domain is structurally homologous to mammalian myeloperoxidase, suggesting that the COX enzymes evolved from soluble heme-dependent peroxidases.[35] The catalytic domain is largely composed of α-helices. The COX active site is composed of an L-shaped hydrophobic channel that extends from the membrane-binding domain into the interior of the catalytic domain. Within the COX channel, a constriction site composed of Arg-120, Tyr-355 and Glu-524 separates the catalytic and membrane-binding domains. The catalytic residue, Tyr-385, is located at the turn of the L-shaped channel. While the COX-1 and COX-2 active sites are relatively similar, the COX-2 active site is 20-30% larger than that of COX-1 due to the substitution of Ile-523 in COX-1 for Val-523 in COX-2 (Figure 4).[36] COX-2 also contains substitutions of Val-434 and Arg-513 compared to Ile-434 and His-513 in COX-1. The POX active site is located in a solvent-accessible groove at the top of the catalytic domain. The POX active site consists of a heme binding pocket formed by His-388 as the proximal heme ligand and Gln-203 and His-207 distal to the heme (Figure 5).[31] Mutation of His-388, Gln-203, or His-207 causes a dramatic reduction in POX activity, but the mutation of Gln-203 retains full COX activity.[11,37,38]
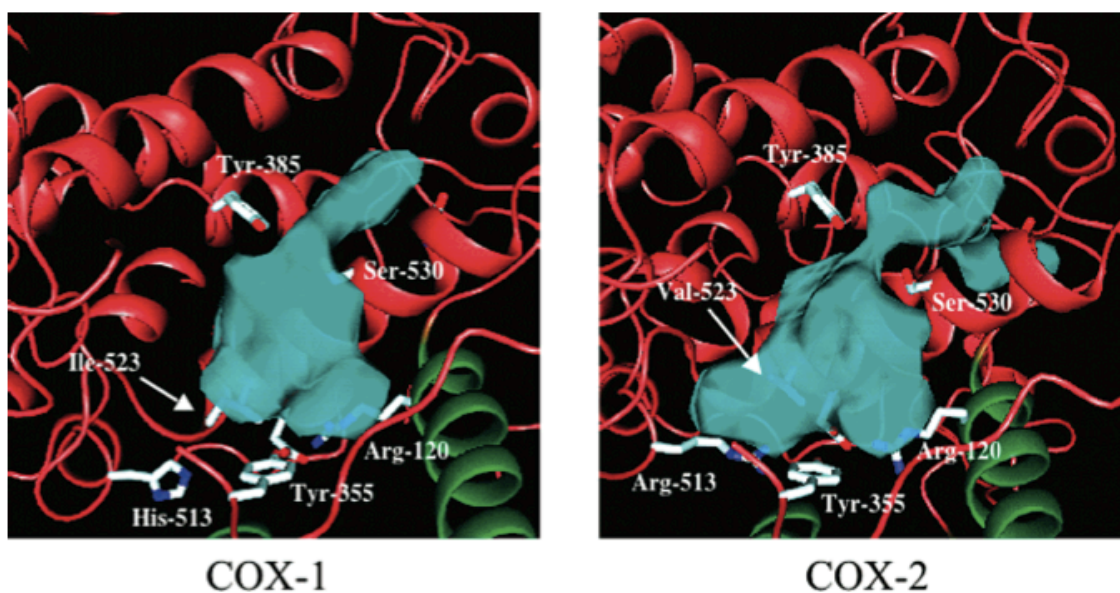
Figure 4: COX active site structures in COX-1 and COX-2. Substitution of Ile-523 in COX-1 for Val-523 in COX-2 increases the solvent-accessible surface area of the COX active site of COX-2. Reproduced from.[18]
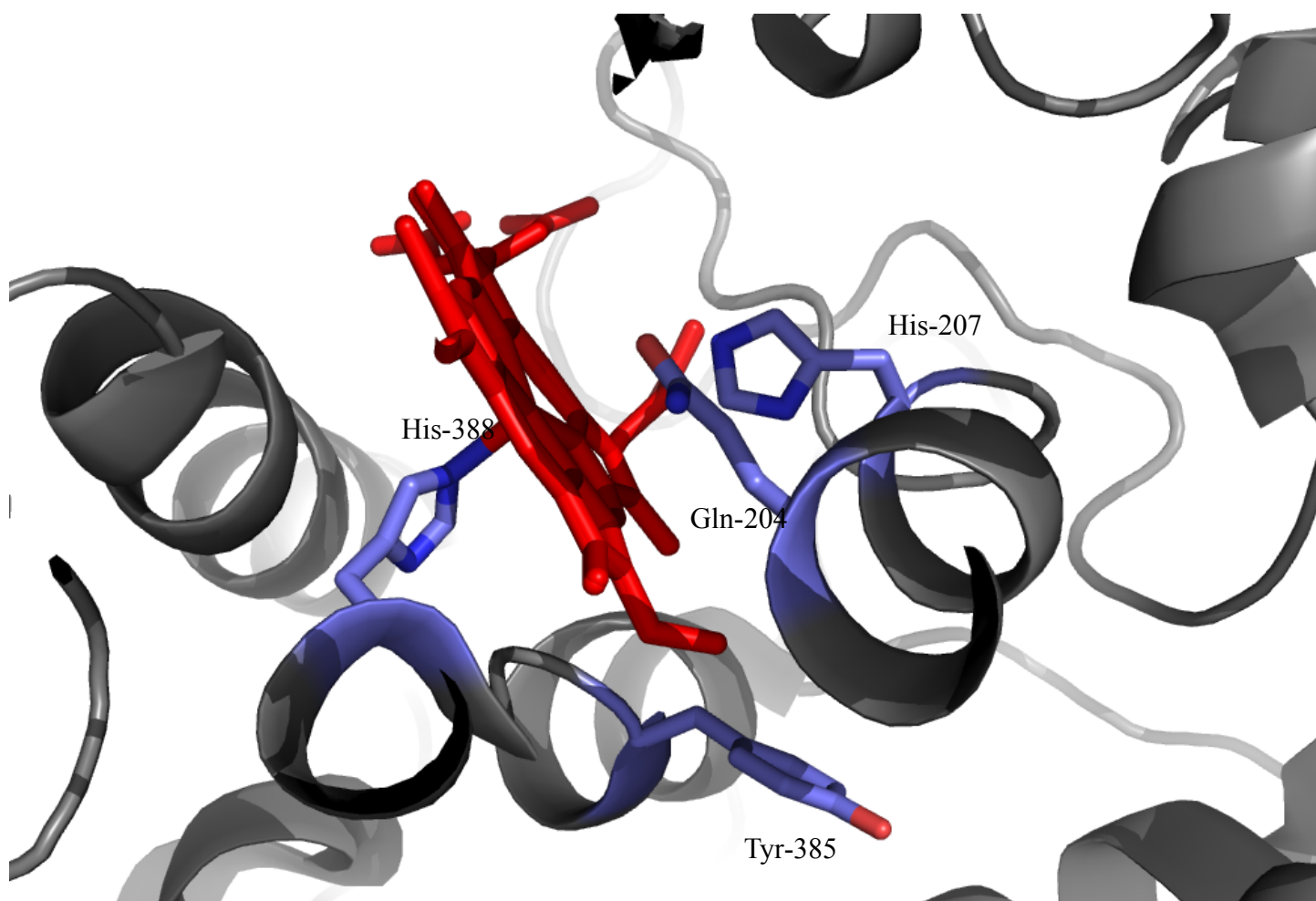
Figure 5: Structure of the POX active site. Heme (red) is bound in the POX active site by coordination to His-388, Gln-203, and His-207. The catalytic Tyr-385 is positioned below the heme. PDB ID: 1Q4G.

Crystal structures of AA bound to COX-2 have identified the basis of substrate binding to the COX active site.[39,40] The COX-2 crystal structure identified that AA binds in two distinct conformations to the two monomers of COX-2. In the productive conformation, AA binds in an L-shaped conformation with its carboxylic acid hydrogen-bonded to Tyr-355 at the base of the active site and the fatty acid tail projecting into the catalytic site with the ω-tail in a hydrophobic groove above Ser-530 and Leu-534 (Figure 6). This conformation positions the 13-pro-(*S*)-hydrogen of AA for abstraction by the catalytic Tyr-385 radical. In the non-productive conformation, AA binds in an inverted fashion with its carboxylic acid coordinated to Tyr-385 and Ser-530 at the apex of the COX active site.[41] In this orientation, the 13-pro-(*S*)-hydrogen is over 10 Å away from the catalytic Tyr-385 and cannot be abstracted to initiate the COX reaction. AA makes 49 interactions with the active site of COX-1 and 54 interactions with COX-2 active site residues.[39,40] Mutation of either Val-349 or Trp-387 causes a shift in the product profile of both COX-1 and COX-2, such that an increased amount 11- or 15-HpETE is formed, while the amount of the PGG$_2$ is correspondingly decreased.[42] This occurs with mutation of Trp-387 to Phe due to elimination of the interactions of COX-2 with C-11 and C-12 of AA, leading to greater conformational flexibility of the 11-peroxyl radical and suboptimal alignment for endoperoxide formation.[42,43]
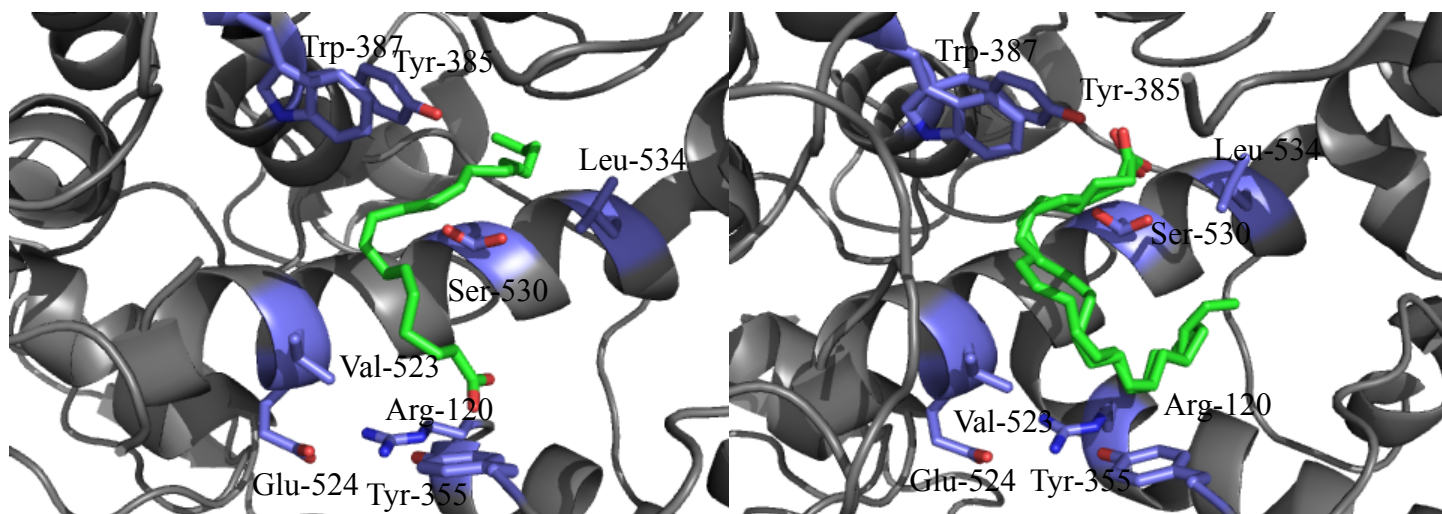
Figure 6: Crystal structures of the productive and non-productive conformations of AA within the COX active site. In the productive binding mode of AA (left), the carboxylate moiety of AA (green) participates in hydrogen-bonding interactions with Tyr-355 at the constriction site of COX-2. The catalytic residue, Tyr-385, is positioned above the 13-pro-(*S*)-hydrogen. In contrast, AA is shown in two possible arrangements in non-productive conformations in the active site of COX-2 (right). The carboxylate of AA is coordinated to Tyr-385 and Ser-530 at the top of the COX active site. PDB ID: 3HS5.

Ser-530 also plays a role in promoting cyclization and PGG$_2$ stereochemistry.[42] When Ser-530 is mutated to Thr in either murine or human COX-2, the ratio of PG to HpETE products is similar to that of wild-type COX-2, but there is a dramatic shift in the stereochemistry around C-15 to the (R)-conformation.[44] Mutation of Ser-530 to Met or Val in COX-2 also results in almost complete stereochemical inversion of the oxygenation at C-15 and leads to increased amounts of HpETE products. Because both polar and non-polar substitutions for Ser-530 alter the stereospecificity of the COX-2 reaction, the stereochemistry of the reaction is regulated by steric interactions between the substrate and Ser-530.

COX Enzyme Regulation and Isoforms

Although COX-2 shares 60% sequence identity with COX-1 and performs the same enzymatic reaction, the two isoforms have several principal structural and function differences. *Ptgs-1*, the gene coding for COX-1, is constitutively expressed through the body and encodes a relatively stable 2.8 kb mRNA. In contrast, *Ptgs-2*, the gene for COX-2, is an immediate early gene that is expressed in response to stimuli such as cytokines, growth factors, and tumor promoters.[4,45] The *Ptgs-2* gene encodes a 4 kb mRNA that contains an instability sequence in the 3'-untranslated region, which leads to rapid turnover.[46] Although true in some settings, the dogma that COX-1 is constitutively expressed and COX-2 is solely an inducible isoform has been challenged by several recent studies. COX-2 is constitutively expressed in the cerebral cortex, kidney, and spinal cord myelin sheaths.[47-49] The constitutive expression of COX-2 in these tissues and the induction of COX-1 in some settings suggest that there are other important differences between the isoforms.

The activity and stability of the COX enzymes are regulated by several mechanisms after protein translation. While COX-1 protein is quite stable, COX-2 is a target of the endoplasmic reticulum-associated degradation pathway.[50] This is due to the fact that while COX-1 has three *N*-glycosylation sites, COX-2 contains an additional *N*-glycosylation site at Asn-594 due to an additional 19 amino acids at the C-terminus. This additional glycosylation at Asn-594 mediates the endoplasmic reticulum-associated degradation pathway and mutation of Asn-594 to remove this glycosylation site increases the stability of COX-2.

Additionally, The COX enzymes are suicide-inactivated by a first-order, irreversible hydroperoxide-dependent process.[51] The oxoferryl heme produces radical species that can lead to either heme or protein

modification and subsequent loss of enzymatic activity.[52] This suicide inactivation may serve as an alternative regulatory mechanism for COX activity, as reducing co-substrates prevent COX suicide inactivation.[53] In contrast, a hydroperoxide product of platelet lipoxygenase, 12-HpETE, inactivates COX in platelets.[54] Thus, oxidative processes modulate COX action.

Although the two COX isoforms catalyze the same reactions and have similar sequences, the two COX isoforms are not functionally transposable. Insertion of the *Ptgs-1* gene after the regulatory sequence controlling *Ptgs-2* expression in mice causes functional differences.[55] In these knock-in mice, stimuli that induce COX-2 expression cause COX-1 expression. Despite the fact that the urinary levels of PGEM (the metabolite of PGE_2) are restored relative to COX-2 null mice, there is a decrease in PGI_2 levels. The differences in PG production could be a result of the marked difference between hydroperoxide activation sensitivity, as COX-2 is activated at much lower hydroperoxide levels than COX-1.[56] The hydroperoxide sensitivity difference between COX-2 and COX-1 is mediated by the mutation of His-383 in COX-1 to Thr-383 in COX-2.[57] Additionally, COX-1 and COX-2 may interact with specific downstream PG synthases, which may account for some of the differences observed in the knock-in mice.[58]

<div align="center">The Endocannabinoid System</div>

Endocannabinoid biology

The endocannabinoid system consists of the endogenous cannabinoids (endocannabinoids, eCBs), cannabinoid receptors, and the enzymes responsible for the synthesis and degradation of eCBs. The endocannabinoid system was initially identified as the target of Δ^9-tetrohydrocannabinol (THC), the psychoactive component of *Cannabis sativa*.[59] After decades of research, the cannabinoid receptor 1 (CB₁) was cloned and its brain localization mapped in 1990.[60,61] A second peripheral cannabinoid receptor, CB₂, was identified in 1993.[62] Arachidonoyl ethanolamide (anandamide, AEA) was the first endogenous ligand identified for the CB₁ and CB₂ receptors.[63] The second eCB, 2-arachidonoyl glycerol (2-AG), was discovered in 1997.[64] Both AEA and 2-AG are carboxylate-modified AA derivatives and act as neuromodulators.

AA, 2-AG, and AEA are synthesized from phospholipids via discrete pathways in an "on demand" fashion. A primary source of AA is the hydrolysis of phospholipids at the *sn*-2 position by cytosolic phospholipase A$_2$ (cPLA$_2$). There are six identified isoforms of cPLA$_2$ found in mice, α, β, γ, δ, ε, and ζ. These isoforms are expressed in different tissues and respond to different stimuli. In activated macrophages, AA formation is primarily mediated by the action of cPLA$_2$α, a 85-kDa protein containing an *N*-terminal C2 domain and a *C*-terminal catalytic domain.[65] Importantly, cPLA$_2$α hydrolysis of phospholipid substrate has high substrate specificity for phospholipids containing AA at the *sn*-2 position.[36] The activity of cPLA$_2$α is regulated by intracellular calcium and calcium binding to the C2 domain causes localization of the enzyme to the phospholipid membrane.[66] After translocation to the membrane, cPLA$_2$α utilizes an active site Ser-228/Asp-549 dyad within the α/β hydrolase domain to catalyze the hydrolysis of the *sn*-2 position of phospholipids containing AA including phosphatidylcholine (PC), phosphatidylethanolamine (PE), phosphatidylserine (PS), and phosphatidylinositol (PI).[37] In addition to calcium, cPLA$_2$α activation is also mediated by phosphorylation by MAP kinase, ceramide-1-phosphate, and phosphatidylinositol 4,5-bis phosphate (PIP$_2$).[38,67-69]

While cytosolic phospholipase A$_2$ (cPLA$_2$) has been identified as a primary synthetic route for AA in many settings, recent studies have identified 2-AG hydrolysis as a major source of AA (and hence PGs) in the brain.[70,71] Multiple pathways have been described for the synthesis of 2-AG (Figure 7). The primary synthetic route for 2-AG is the phospholipase C (PLC)-diacylglycerol lipase (DAGL) pathway.[72] PLC hydrolyzes 2-arachidonoyl-PI to form arachidonoyl-diacylglycerols (DAGs), which are then hydrolyzed to 2-AG by DAGL.[73,74] In neurons, 2-AG is synthesized by PLCβ isoforms in response to the stimulation of G$_{q/11}$-coupled receptors.[75] These receptors include the group I metabotropic glutamate receptors, mGluR1 and mGluR5, and the muscarinic acetylcholine receptor M1.[76] Alternatively, DAGs can be formed by the hydrolysis of either phosphatidic acid (PA) in ionomycin stimulated neuroblastoma cells or PC in phorbol ester treated mouse ear tissue.[77,78] Alternative routes that do not involve the formation of DAGs have also been identified, such as the hydrolysis of PI by PLA$_1$ to form lyso-PI (LPI), followed by LPI-PLC hydrolysis to form 2-AG or the hydrolysis of phospholipids by phospholipase D (PLD) to form 2-arachidonoyl-lysophosphatidic acid (LPA)

and then dephosphorylation to form 2-AG.[79-81] Thus, 2-AG biosynthesis can occur through multiple routes depending on the stimulation method and tissue of interest.
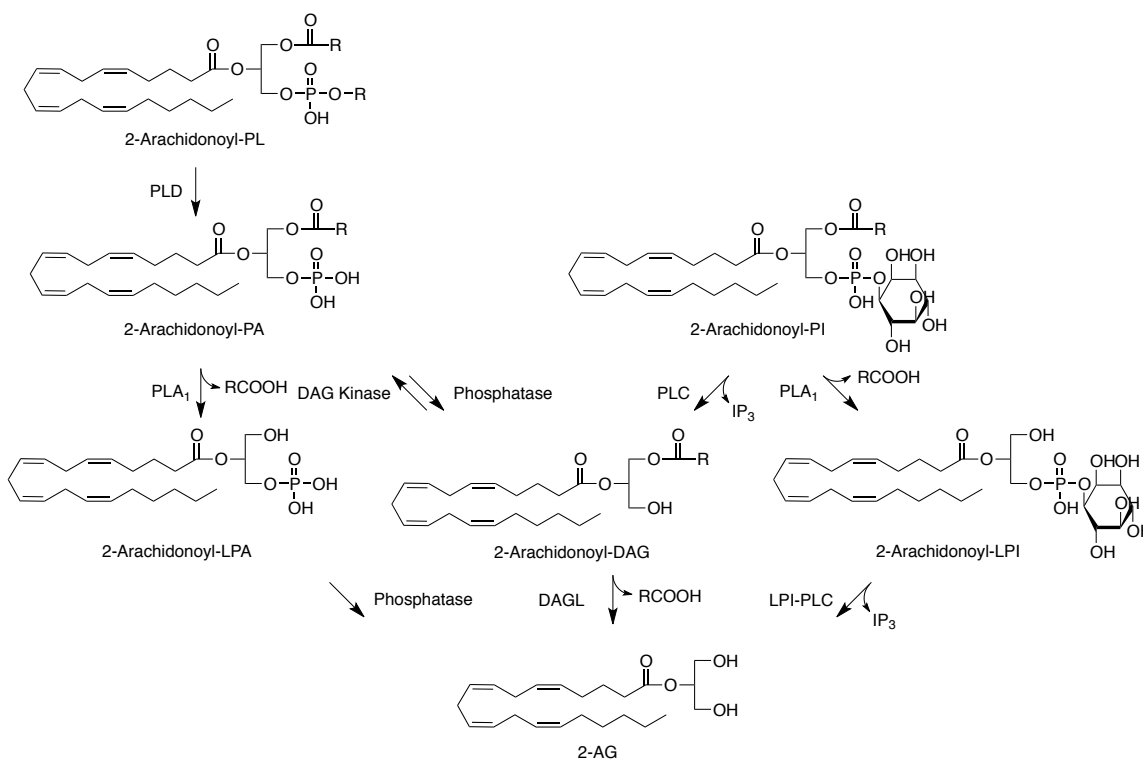
Figure 7: Biosynthetic routes of 2-AG.

DAGL is a membrane-associated enzyme that preferentially hydrolyzes DAGs at the *sn*-1 position.[82,83] In most mammals there are two DAGL isoforms, α and β, and each contains a lipase-3 motif, a serine lipase motif, and four putative transmembrane domains.[84] DAGLα is primarily expressed in the nervous system and pancreas in humans and mice and co-localizes with $G_{q/11}$-coupled receptors and PLCβ in neurons.[60] In neuroblastoma cells DAGLα mediates the mGluR-dependent formation of 2-AG and in DAGLα-deficient mice there is a reduction in brain 2-AG levels.[85-87] In contrast, DAGLβ is the major source of 2-AG in macrophage cell lines as evidenced by a reduction in the levels of 2-AG upon treatment with selective DAGLβ inhibitors or genetic deletion of DAGLβ.[88]

AEA can also be synthesized through multiple distinct pathways. Classically, AEA is synthesized through a transacylation-phosphodiesterase pathway in the brain (Figure 8).[89] The first step in this pathway involves the transfer of AA by an *N*-acyltransferase (NAT) onto the terminal amine of PE to form *N*-arachidonoyl-PE (NAPE).[90-92] NAT is stimulated by Ca^{2+} and utilizes PC, 1-acyl-lyso-PC, PE, or cardiolipin as

the AA donor.[93-95] NAPE is then hydrolyzed by NAPE-PLD to form AEA and PA.[96,97] NAPE-PLD utilizes zinc as a co-factor and is activated by PE and divalent cations such as Ca^{2+} and Mg^{2+}.[98,99] Alternate pathways to synthesize AEA from NAPE have also been described. NAPE can be converted to 1-acyl-lyso-NAPE by secretory PLA_2 ($sPLA_2$) isoforms and then converted to AEA by a lyso-PLD enzyme.[100] NAPE can also be double *O*-deacylated by α/β-hydrolase domain 4 (ABHD4) to form glycerophospho-AEA (Gp-AEA), which can then be hydrolyzed to AEA and glycerol 3-phosphate by glycerophosphodiester phosphodiesterase 1 (GDE1).[101,102] However, GDE1$^{-/-}$ mice do not have lower levels of brain AEA despite having no formation of Gp-AEA or lyso-NAPE in brain homogenates.[103] In lipopolysaccharide (LPS) treated RAW 264.7 macrophages, NAPE can also be hydrolyzed by PLC to form phospho-AEA (p-AEA), which is then dephosphorylated by protein tyrosine phosphatase non-receptor type 22 (PTPN22) or SH2-containing inositol phosphatase 1 (SHIP1) to generate AEA.[104-106]
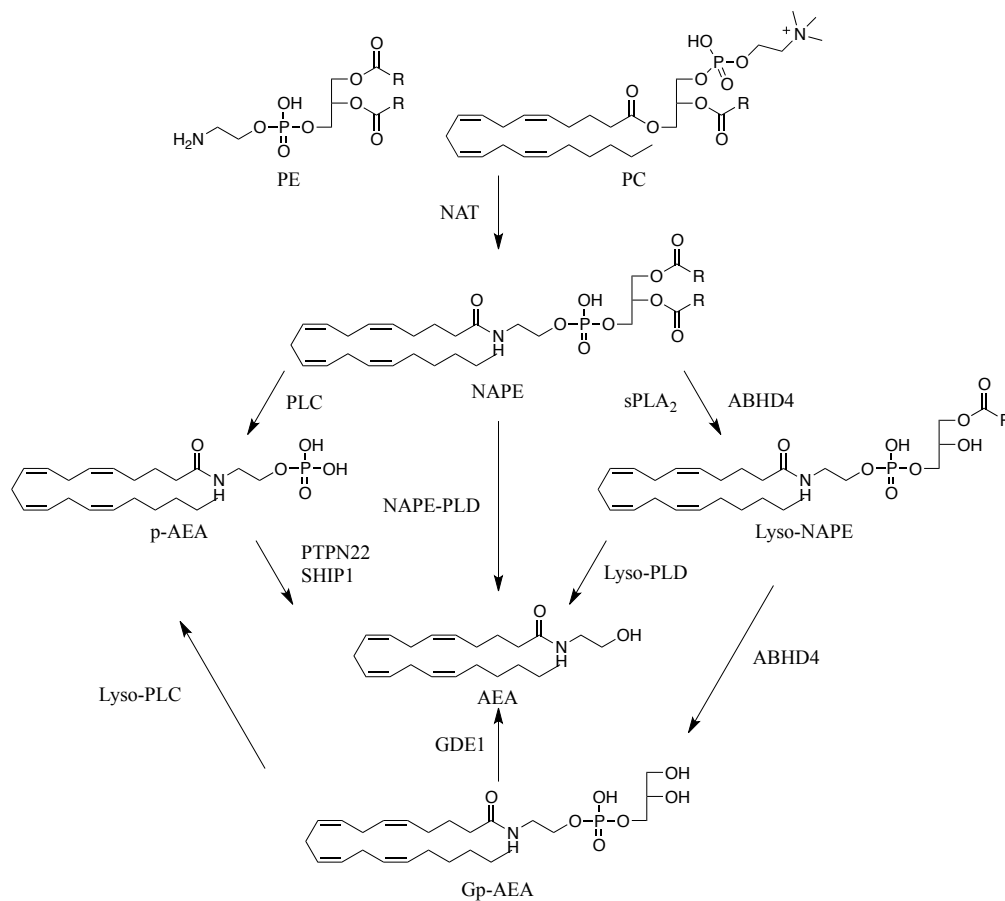
Figure 8: Biosynthetic pathways for AEA.

Endocannabinoid Function and Degradation

After being synthesized, AEA and 2-AG activate CB_1 and CB_2 receptors to exert biological actions. The CB receptors are GPCRs that couple to $G_{i/o}$ and inhibit adenylyl cyclase and activate MAP kinase.[107] The CB_2 receptor is widely expressed in immune cells, while the CB_1 receptor is expressed in the central nervous system, particularly in areas involved in nociception, including periaqueductal gray matter, the dorsal horn of the spinal cord, and dorsal root ganglion neurons.[98,108-110] CB_1 activation mediates the inhibition of either inhibitory GABAergic or excitatory glutamatergic neurotransmitter release from axon terminals in the central nervous system.[111-114] Activation of synaptic CB_1 receptors by either endogenous or exogenous agonists inhibits neurotransmitter release directly through inhibitory coupling to voltage-dependent calcium channels or through activation of potassium channels, which truncates action potential duration and diminishes the amount of neurotransmitter release per action potential.[105,107,115-117] These effects are mediated through the direct interaction of βγ G-protein subunits with the ion channels.[106]

CB receptor activation by AEA and 2-AG occurs in response to neuronal activation and the resulting "on-demand" synthesis and release of the eCBs. After synthesis and release, the eCBs activate CB_1 receptors on axon terminals to inhibit the release of GABA or glutamate.[118] In the case of inhibitory GABAergic neurons, eCBs exhibit depolarization-induced suppression of inhibition (DSI), while in excitatory glutamatergic neurons eCBs exhibit depolarization-induced suppression of excitation (DSE).[119,120] Thus, eCBs action can lead to both excitatory responses or inhibit responses in neurons. In addition, activation of CB_1 receptors by eCBs can also modulate long-term depression (LTD) and long-term potentiation (LTP).[121,122] The mechanism of retrograde signaling exhibited by eCBs differs considerably from those of classic neurotransmitters system (e.g., cholinergic, aminoacidergic, and monoamigeric), where depolarization of the presynaptic neuron by an action potential results in the release of neurotransmitters, which then traverse the synaptic cleft to bind and activate their cognate receptors on the postsynaptic neuron.

In addition to having a distinct signaling mechanism from classic neurotransmitters, eCBs also differ in their release and clearance from axon terminals. Most classic neurotransmitters are water-soluble and are packaged, stored, and released in synaptic vesicles.[123] Following release into the extracellular space and

postsynaptic receptor activation, classic neurotransmitter signaling is terminated by a combination of cellular reuptake and enzymatic degradation. Inhibition of neurotransmitter clearance through blockade of reuptake, such as selective serotonin reuptake inhibitors, or metabolism, such as monoamine oxidase inhibitors, is a widely employed strategy for both therapeutic pharmacological treatments and drugs of abuse.[124,125] AEA and 2-AG levels, and therefore their effect on CB receptors, are primarily regulated by their "on demand" synthesis from membrane phospholipids and subsequent enzymatic inactivation. Pharmacological inhibition of eCB inactivating enzymes enhances eCB signaling and is a promising strategy for therapeutic interventions. AEA is primarily degraded by the enzyme fatty acid amide hydrolase (FAAH) to form AA and ethanolamine.[126-128] Similarly, 2-AG is primarily degraded by hydrolysis to AA and glycerol by several enzymes including monoacylglycerol lipase (MAGL), α/β-hydrolase domain 6 (ABHD6), α/β-hydrolase domain 12 (ABHD12), carboxylesterases 1 and 2 (CES1 and CES2), and palmitoylprotein thioesterase 1 (PPT1).[60,129-132] Thus, AEA and 2-AG are biosynthesized and degraded by distinct sets of enzymes.

FAAH is a 60-kDa integral membrane protein and is highly expressed in the mammalian brain, where it localizes to intracellular membranes of postsynaptic somata and dendrites.[133] FAAH and CB_1 exhibit complementary subcellular distributions in many brain regions including the neocortex, cerebellar cortex, and hippocampus.[134] FAAH contains an active site serine nucleophile and utilizes a lysine residue as a catalytic base that allows it to hydrolyze both amides and esters, in contrast to the histidine residue utilized by most serine hydrolases.[135] Mice bearing a targeted deletion of the *Faah* gene (FAAH$^{-/-}$) have been generated and confirm FAAH's role as the principal hydrolase of AEA *in vivo*.[136] FAAH$^{-/-}$ mice exhibit anti-nociceptive, anti-inflammatory, anxiolytic, and anti-depressive phenotypes without motor or cognitive defects.[134] Several selective pharmacological inhibitors for FAAH have been developed and validated. The first selective FAAH inhibitor was URB597, a carbamate compound that irreversibly carbamoylates the catalytic serine nucleophile.[137,138] URB597 administration increases AEA and other *N*-acylethanolamide (NAE) levels *in vivo* and reduces pain, anxiety, depression, and nausea in rodents.[132,139-141] In contrast to direct CB_1 agonists, URB597 does not cause hypothermia, hypolocomotion, catalepsy, or increased appetite.[132] However, URB597 also inhibits multiple CES enzymes in the liver and has a relatively short half-life *in vivo*, limiting its use in

chronic dosing studies.[142-144] A significant pharmaceutical effort to develop a series of FAAH inhibitors has been undertaken by Pfizer. This effort resulted in a series of covalent and irreversible urea-based FAAH inhibitors with exceptional potency, selectivity, and duration of action *in vivo*.[145-147] The most widely used compound, PF-3845, selectively blocks FAAH activity in mouse brain for up to 24 hours after a single 10 mg/kg i.p. dose and maximally elevates AEA for 7-12 hours.[142] PF-3845 was further optimized for human clinical trials to PF-04457845 and this compound is efficacious in rat models of inflammatory and non-inflammatory pain.[148,149] Despite inhibiting FAAH activity and elevating plasma AEA and other NAE levels in humans, PF-04457845 failed to show efficacy in Phase II clinical trials in patients with osteoarthritic knee pain.[150,151]

The primary hydrolytic enzyme for 2-AG in the brain is MAGL, which accounts for 85% of 2-AG hydrolysis in mouse brain membranes.[152] MAGL is a 33-kDa soluble serine hydrolase that contains a serine-histidine-aspartic acid catalytic triad and peripherally associates with cell membranes.[153-155] MAGL is highly expressed in the cerebellum, cortex, thalamus, and hippocampus, where it is primarily localized to presynaptic axon terminals.[129,154] MAGL is highly selective for the hydrolysis of monoacyl glycerols (MAGs), with negligible activity on DAGs, triacylglycerols, phospholipids, or cholesterol esters.[156] The primary selective MAGL inhibitor utilized is JZL184, which is an *in vivo* active inhibitor and elevates brain 2-AG levels and elicits a subset of cannabinoid behaviors.[157,158] JZL184 enhances eCB retrograde signaling, attenuates neuropathic pain, and produces anxiolytic effects.[159-161] However, JZL184 has also been shown to inhibit CES1 and CES2, which also can hydrolyze 2-AG, and FAAH.[162] Second generation MAGL inhibitors with *O*-hexafluoroisopropyl carbamate scaffolds, such as KML29, have superior selectivity toward MAGL over other serine hydrolases.[163]

Although MAGL is the primary 2-AG hydrolytic enzyme in the brain, ABHD6 also modulates 2-AG levels. ABHD6 is a 30-kDa integral membrane serine hydrolase with an intracellular orientation.[149] The murine microglial BV2 cell line efficiently hydrolyzes 2-AG despite lacking MAGL expression, and this hydrolysis is mediated by ABHD6.[164] ABHD6 is abundantly expressed in the brain and multiple peripheral tissues and cell types.[165,166] In the brain, ABHD6 is expressed in cortical areas and preferentially localizes to postsynaptic

15

dendrites adjacent to presynaptic CB_1 receptors.[163] ABHD6 regulates 2-AG degradation and signaling in primary murine neurons and cortical slices as well as Neuro2A cells.[163,164] The ABHD6 inhibitor WWL70 produces CB_1 and CB_2-mediated anti-inflammatory and neuroprotective effects in a mouse model of traumatic brain injury.[167] More recent studies have identified a series of potent and selective 2-substituted-piperidyl-1,2,3-triazole ABHD6 inhibitors that are active *in vivo*.[168]

Inhibition of eCB degradation by FAAH and MAGL has demonstrated a multitude of therapeutic effects. Inhibition of FAAH reduces nociceptive and hyperalgesic behavior in acute, inflammatory, and neuropathic pain models.[169] Complete inhibition of FAAH by PF-3845, at a 10 mg/kg i.p. dose, or MAGL by JZL184, at a 40 mg/kg i.p. dose, produces antinociceptive effects in tests of acute thermal pain, visceral pain, neuropathic pain, and inflammatory pain.[154,155,166,170-175] These effects are mediated by CB_1 and/or CB_2 receptor activation depending on the model and inhibition mode used.

In addition to analgesic effects, FAAH and MAGL inhibitors have demonstrated anxiolytic effects in preclinical models of anxiety and depression.[176] URB597 produces anxiolytic effects in multiple preclinical models of anxiety, including the elevated zero maze and elevated plus maze in both acute and chronic settings in a CB_1-dependent manner.[132,177,178] JZL184 also produces anxiolytic-like effects in rats in the elevated zero maze and elevated plus maze, however, these effects are CB_2-dependent. In highly aversive contexts, JZL184 produces anxiolytic-like effects in the elevated plus maze in a CB_1-dependent manner.[157] FAAH inhibition by URB597 or PF-3845 and MAGL inhibition by JZL184 also decrease anxiety as measured in the marble burying assay in mice through a CB_1-receptor dependent mechanism.[179,180] These studies demonstrate the pleiotropic therapeutic effects of eCB augmentation via FAAH and MAGL inhibition and the resulting modulation of cannabinoid receptor signaling.

Oxygenation of Endocannabinoids by Cyclooxygenase-2

In addition to the oxygenation of AA, COX-2 also catalyzes the oxygenation of AEA and 2-AG to form prostaglandin ethanolamides (PG-EAs) and prostaglandin glyceryl esters (PG-Gs), respectively (Figure 9).[181,182] Kinetic studies identified that the oxygenation of AEA by COX-2 occurs with an approximately 6 fold higher

16

K_m relative to AA.[183,184] In contrast, the oxygenation of 2-AG by COX-2 is as efficient as that of AA as evidenced by steady-state kinetic analyses indicating that AA and 2-AG have comparable k_{cat}/K_m values.[32] Thus, COX-2 can utilize neutral ester and amide derivatives of AA as substrates.
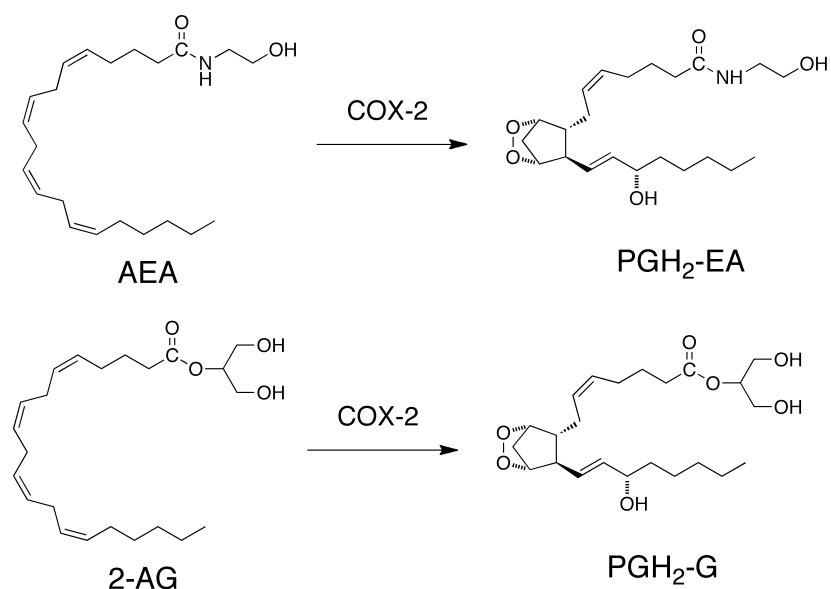
Figure 9: Oxygenation of AEA and 2-AG by COX-2.

Initial studies on the amino acid determinants of eCB oxygenation by COX-2 using site-directed mutagenesis identified the constriction site as a major determinant of eCB oxygenation. Mutation of Arg-120 to Gln causes a 9-fold reduction in 2-AG oxygenation and a 3-fold reduction in AEA oxygenation relative to wild-type enzyme, while mutation of Glu-524 to Leu reduces the oxygenation of 2-AG, AEA, and AA.[184,185] Interestingly, Tyr-355 mutation to Phe has no effect on eCB oxygenation but decreases AA oxygenation. The lack of eCB oxygenation by COX-1 predicts that the side pocket comprised of Val-523, Arg-513, and Val-434 in COX-2 may bind the eCBs. Mutation of all three COX-2 side pocket residues to their COX-1 counterparts, Val-523 to Ile, Arg-513 to His, and Val-434 to Ile, causes a 75% reduction in 2-AG and AEA oxygenation but has no effect on AA oxygenation.[184,185]

More recently, a crystal structure of murine COX-2 complexed to 1-AG (an isomerization from 2-AG to 1-AG occurred over the course of the crystallization) has been solved. The COX-2:1-AG structure identifies that, like AA, 1-AG binds in both a productive and non-productive conformation to the two monomers of COX-2 (Figure 10).[186] In the productive conformation, the ω tail of 1-AG is projected into the hydrophobic channel at

the apex of the COX active site with the 13-pro-(*S*)-hydrogen positioned for abstraction by Tyr-385 and the 2,3-dihydroxypropyl of 1-AG bound in a pocket vacated by rotation of Leu-531. In contrast to the inversion of AA in the non-productive conformation, the non-productive conformation of 1-AG has the same overall binding orientation as observed in its productive conformation but lacks sufficient insertion of its ω tail into the hydrophobic channel to bring the 13-pro-(*S*)-hydrogen close enough for abstraction by Tyr-385.[40,186] Of note, the side pocket of COX-2 does not serve as a binding site for 1-AG in the crystal structure and mutation of Arg-513 to His had no effect on either AA or 1-AG binding in structures with R513H mutant enzyme.[186] This is in contrast to the site-directed mutagenesis studies, which suggested that the constriction site residues and side pocket are important for eCB oxygenation. However, both sets of studies agree that the overall binding orientation and reaction mechanisms for eCB oxygenation and AA oxygenation are the same.
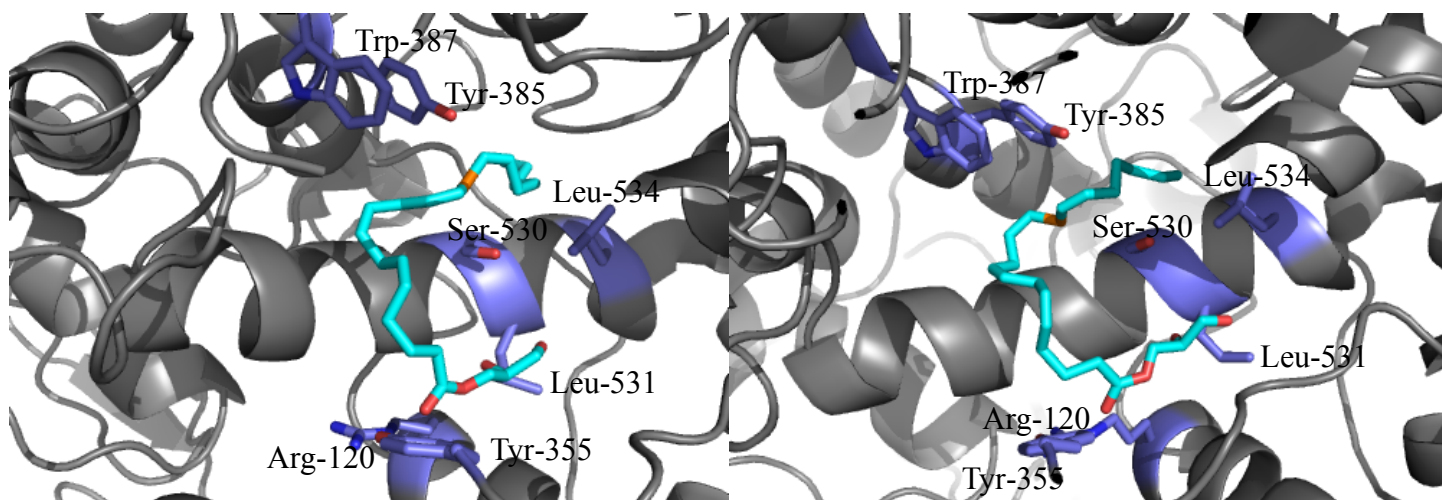
Figure 10: Crystal structure of the productive and non-productive conformations of 1-AG in the COX active site. 1-AG (teal) bound to the COX active site in the productive conformation (left) and non-productive conformation (right). C-13 of 1-AG is highlighted in orange, to indicate the change in distance between Tyr-385 in the two conformations. PDB ID: 3MDL.

While PGH$_2$ is converted to PGE$_2$, PGD$_2$, PGF$_{2\alpha}$, PGI$_2$, and TxA$_2$ by downstream synthases, PGH$_2$-EA and PGH$_2$-G are not good substrates for thromboxane synthase; thus, they each form PGE$_2$, PGD$_2$, PGF$_{2\alpha}$, and PGI$_2$ ethanolamide or glycerol analogs, but not TxA$_2$ products.[187] The production of PG-EAs has been demonstrated in several settings including in FAAH knockout mice treated with AEA, lipopolysaccharide-stimulated mouse dorsal root ganglia cultures, mouse renal medulla, rat spinal cord, and in mouse adipocytes.[188-192] PG-Gs have been detected in rat paws and multiple stimulated macrophage cell lines including

18

RAW 264.7 cells, resident peritoneal macrophages, and J774 macrophages.[193-197] Several studies have demonstrated that PG-Gs are unstable due to enzymatic hydrolysis to PGs, which may account for the fewer reports of their formation *in vivo* compared to PG-EAs.[131,132,198]

Emerging evidence reveals that PG-EAs and PG-Gs have discrete functions that appear to be mediated by receptors distinct from classical PG receptors. PGE_2-EA reduces the expression of IL-12p40 in activated macrophages and microglial cells.[199] AEA also negatively regulates IL-12p40 production, thereby inhibiting the expression of the cytokines IL-12 and IL-23. The inhibitory effects of AEA and PGE_2-EA on IL-12p40 are partially reduced by an EP_2 receptor antagonist, but not an EP_4 receptor antagonist. These results indicate that the specific activation of EP_2 may play a role in the down regulation of IL-12p40 induction by AEA and PGE_2-EA. A structural analog of $PGF_{2\alpha}$-EA, bimatoprost, is an ocular hypotensive agent marketed for the treatment of glaucoma and ocular hypertension.[200] Neither bimatoprost nor $PGF_{2\alpha}$-EA exhibits significant activity at PG receptors. Extensive ocular distribution and metabolism studies indicate that bimatoprost exerts its effects as the intact, $PGF_{2\alpha}$-EA-like molecule through signaling via a heterodimer comprised of the F prostanoid (FP) receptor and a splice variant of the FP receptor with a truncated C-terminus.[201,202] More recently, $PGF_{2\alpha}$-EA has also been shown to negatively regulate adipogenesis.[192]

PGE_2-G, but not PGE_2, potently mobilizes Ca^{2+} and stimulates a transient increase in inositol 1,4,5 phosphate (IP_3) levels, activation of PKC, and ERK phosphorylation.[203] The affinity of PGE_2-G for E prostanoid receptors is at least two orders of magnitude lower than that of PGE_2, and binding to the thromboxane, prostacyclin, D prostanoid, or F prostanoid receptors are negligible. PGE_2-G also causes a concentration-dependent increase in the frequency of miniature inhibitory post-synaptic currents (mIPSCs) in mouse hippocampal neurons.[204] The frequency of mIPSCs is also increased by PGD_2-G, $PGF_{2\alpha}$-G, and PGD_2-EA, but not by PGE_2-EA and $PGF_{2\alpha}$-EA, while 2-AG and AEA reduce the frequency of mIPSCs. The ability of PG-Gs and PG-EAs to increase the frequency of mIPSCs is not due to hydrolysis to PGs or binding to PG receptors, as classical PGs act to reduce the frequency of mIPSCs or have no effect. Treatment with an IP_3 receptor agonist or a MAPK inhibitor blocks the PGE_2-G-mediated increase in the frequency of mIPSCs. PGE_2-G also increases the frequency of miniature excitatory postsynaptic currents (mEPSCs) in mouse hippocampal

neurons in culture through the MAPK and IP$_3$ signaling pathways.[205] PGE$_2$-G may be neurotoxic, as it causes a dose-dependent increase in terminal transferase dUTP nick end labeling (TUNEL) staining and time-dependent cleavage of caspase-3 in rat hippocampal neurons. PGE$_2$-G also induces hyperalgesia through modulation of NF-κB in carrageenan-treated rat paws.[193] In contrast, PGD$_2$-G exhibits anti-inflammatory activity in isolated macrophages and *in vivo*.[197]

A study in human vascular endothelial cells has suggested that PGI$_2$-G may activate the nuclear receptor PPARδ.[206] Treatment of human umbilical vein endothelial cells expressing COX-2 with 2-AG leads to PPARδ activation in a non-CB$_1$ or CB$_2$-dependent manner. Both COX-2 and prostacyclin synthase activity were required for 2-AG-induced PPARδ activation, suggesting that 2-AG is converted to PGI$_2$-G, which can then activate PPARδ. The COX-2-PGI$_2$-G-PPARδ pathway appears to lead to the attenuation of prothombotic tissue factor gene expression. Taken together, these studies have identified distinct functions of PG-EAs and PG-Gs that are mediated by signaling at non-prostanoid receptors.

<div align="center">Inhibition of Cyclooxygenases</div>

Non-steroidal anti-inflammatory drugs

Natural products have been used in the treatment of pain, fever, and inflammation since ancient times. Egyptians used myrtle leaf extracts to treat pain and fever as early as 1550 BC and the Greeks utilized willow bark and leaf extracts for the same purpose around 500 BC. In 1763, Edward Stone presented a scientific study of the anti-pyretic effects of willow bark to the Royal Society of London. Henri Leroux then isolated and identified salicin as the active analgesic and anti-pyretic ingredient in willow bark in 1829. An industrial process for synthesizing salicylic acid from phenol was developed in the mid 19th century and the first factory, Salicylic Acid Works, for producing a drug was built in 1874.[207]

After the advent of mass production, salicylic acid was widely used but several notable issues arose. The drug was not very potent and required several grams to be taken per day to be effective. Salicylic acid treatments also lead to gastric irritation and poor tolerance, leading to the need for an improved drug. Felix Hoffman acetylated the hydroxyl group of salicylic acid to create acetylsalicylic acid, which improved the taste

and gastric tolerance. Acetylsalicylic acid was unveiled as aspirin in 1899 by Hoffman's company, Bayer, and became the best selling drug worldwide. Further drug discovery efforts identified several other anti-inflammatory and analgesic drugs using animal models of pain and inflammation. However, the mechanism of action was not discovered until 1971, when it was found that treating guinea pig lung with aspirin, sodium salicylate, or indomethacin causes a dose-dependent decrease in PG biosynthesis and treatment of platelets with aspirin leads to inhibition of PG biosynthesis.[208,209] These studies identified the COX enzyme as the molecular target of non-steroidal anti-inflammatory drugs (NSAIDs).

Further studies into aspirin identified that it inhibits PG production in both a time- and concentration-dependent manner.[210] Incorporation of aspirin radioactivity into COX when incubated with [^{3}H]-aspirin revealed that it inhibits COX through covalent modification of the enzyme at Ser-530 by acetylation.[211-213] A crystal structure with an aspirin analog revealed that acetylation of Ser-530 leads to steric blockade of the catalytic residue, Tyr-385, which prevents catalysis.[214] Although aspirin inhibits both COX-1 and COX-2, it preferentially inhibits COX-1. This preferential inhibition leads to sustained inhibition of COX-1 in platelets at low doses, which leads to inhibition of TxA$_2$ biosynthesis and vasoconstriction.[215] Thus, aspirin is commonly taken to reduce cardiovascular risk.

While aspirin remains a commonly used NSAID, it is the only COX inhibitor that covalently modifies the enzyme. All other NSAIDs act in one of two possible kinetic modes of inhibition: competitive and rapidly reversible, or time-dependent, functionally irreversible inhibitors.[210] Rapid, reversible inhibitors interact with the COX enzymes in a single-step kinetic mechanism governed by the concentration of substrate and the dissociation constant, K$_I$ (Figure 11). In contrast, time-dependent inhibitors associated with the COX enzymes via a two-step process by which the inhibitor associates with the enzyme in an analogous bimolecular association, but a time-dependent second step leads to the formation of a more tightly associated inhibitor-enzyme complex.[210]

$$\text{Rapid, reversible inhibition} \qquad E + I \underset{k_{-1}}{\overset{k_1}{\rightleftharpoons}} EI$$

$$\text{Slow, tight inhibition} \qquad E + I \underset{k_{-1}}{\overset{k_1}{\rightleftharpoons}} EI \underset{k_{-2}}{\overset{k_2}{\rightleftharpoons}} EI^*$$
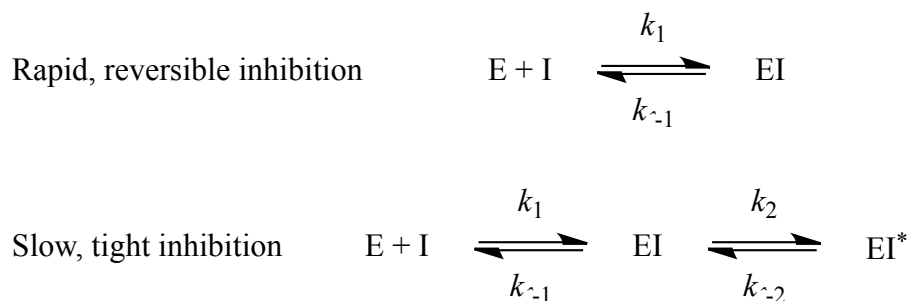
Figure 11: Kinetic modes of COX-2 inhibition.

Several seminal studies on the phenylpropionic acid class of inhibitors have identified the determinants of COX inhibition and kinetics. The two kinetic modes of inhibition do not appear to be mediated by specific binding modes, as (*S*)-ibuprofen, a rapid, reversible inhibitor, and (*S*)-flurbiprofen, a slow, tight binding inhibitor, exhibit different kinetic modes of inhibition but bind similarly to the COX active site (Figure 12).[31,32,216] Both inhibitors hydrogen-bond and ion-pair with Arg-120 and Tyr-355 at the constriction site of COX and mutation of these residues abrogates inhibition of both COX-1 and COX-2.[217,218]
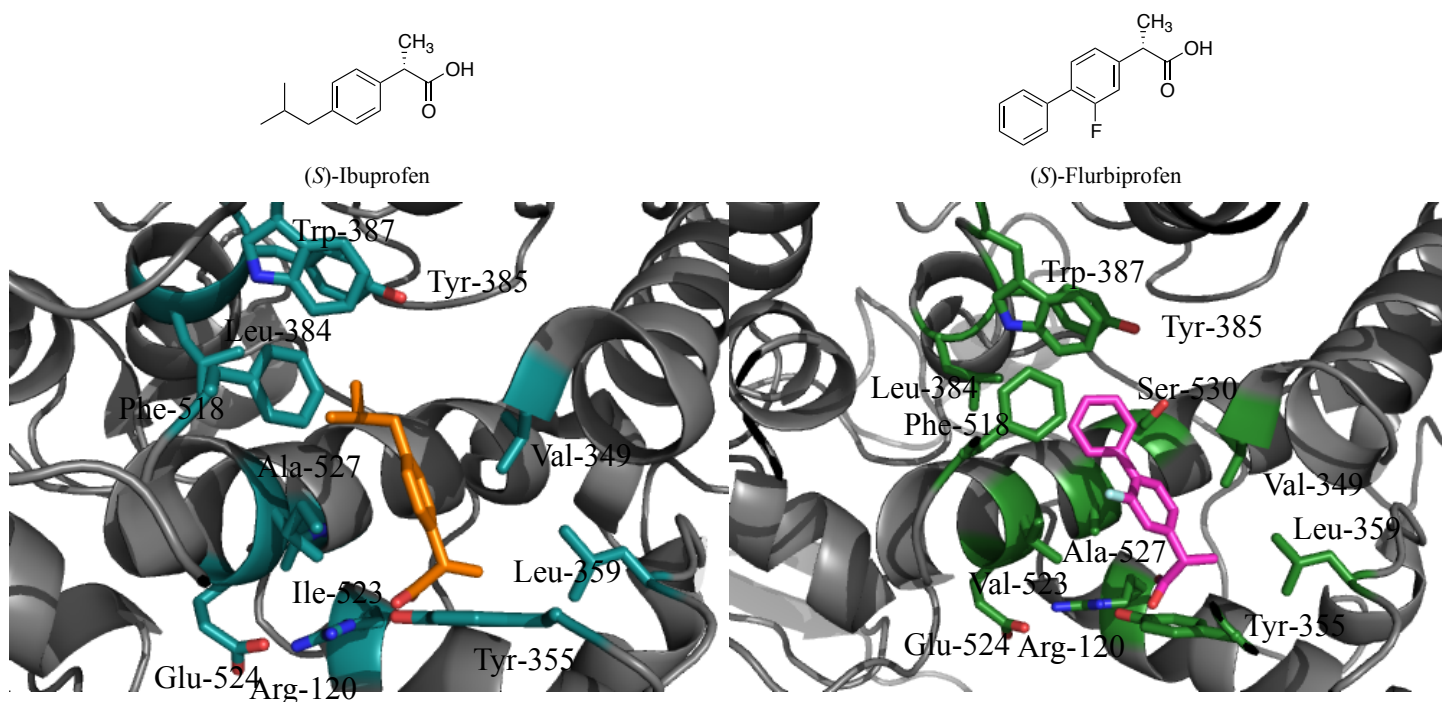
Figure 12: Crystal structures of (*S*)-ibuprofen and (*S*)-flurbiprofen bound to COX-1 and COX-2. The crystal structure of (*S*)-ibuprofen (orange) bound to COX-1 reveals hydrogen bonding and ion-pairing interactions between its carboxylate and Tyr-355 and Arg-120 (left, PDB ID: 1EQG). (*S*)-flurbiprofen (pink) binds in the COX-2 active site in an analogous manner (right, PDB ID: 3PGH).

In addition to the hydrogen bonding and ion-pairing interactions between the carboxylic acid of phenylpropionic acids, such as ibuprofen and flurbiprofen, there are several other interactions that may account for their kinetic differences. The (S)-α-methyl group participates in Van der Waals interactions with Val-349 and Leu-359 at the base of the active site.[31,32] A notable difference in binding between ibuprofen and flurbiprofen is that the second phenyl ring of flurbiprofen interacts with amino acid residues at the apex of the COX active site, while the isobutyl group of ibuprofen does not.[216]

A striking example of the subtle differences that may give rise to differential inhibitor kinetics has been identified through a study of flurbiprofen and its methyl ester. Whereas flurbiprofen acts as a slow, tight binding inhibitor, flurbiprofen methyl ester acts as a rapid, reversible inhibitor.[216] Crystal structures of the two molecules bound to COX revealed no major differences in the interactions between the two inhibitors and the enzyme, suggesting that the kinetic mode of inhibition is not due to different interactions between an inhibitor and the enzyme that are evident from the crystal structures.[216]

The second major class of NSAIDs is the arylacetic acids. The first arylacetic acid to be identified as an inhibitor of PG biosynthesis was indomethacin.[210] Indomethacin is a slow, tight binding inhibitor and several studies have elucidated the molecular determinants of indomethacin inhibition of COX.[219] The crystal structure of indomethacin bound to COX-2 reveals that it binds to the COX active site and forms ion-pairing and hydrogen-bonding interactions between its carboxylic acid and Arg-120 and Tyr-355, as with the phenylpropionic acids (Figure 13). Interestingly, the interaction between indomethacin and Arg-120 is essential for time-dependent inhibition of COX-1, but not COX-2, and modification of the carboxylic acid of indomethacin to neutral esters or amides results in COX-2-selective inhibitors.[220-222] A second important determinant of kinetic inhibition by indomethacin is the insertion of its 2'-methyl group into a hydrophobic pocket formed by Val-349, Ala-527, Ser-530, and Leu-531.[223] Mutation of Val-349 to Leu decreases the potency of indomethacin and causes indomethacin to become a rapid-reversible inhibitor. Removal of the methyl group, as in the case of 2'-*des*methyl-indomethacin, results in a rapid-reversible inhibitor of both COX-1 and COX-2.[224]

A second member of the arylacetic acid class of NSAIDs, diclofenac, exhibits some striking differences from indomethacin and phenylpropionic acids. While diclofenac acts as a time-dependent inhibitor of COX-1 and COX-2, it binds in an inverted fashion to the COX active site with its carboxylic acid hydrogen-bonded to Ser-530 and Tyr-385 at the bend of the channel.[225] In stark contrast to indomethacin and phenylpropionic acids and in agreement with this binding mode, mutations of Arg-120 or Tyr-355 have no effect on the inhibition of diclofenac, but mutation of Ser-530 to Ala or Met eliminates its inhibition.[195,226] Despite the inverted orientation of its carboxylic acid, diclofenac also inserts a chlorine atom into the hydrophobic pocket formed by Val-349, Ala-527, Ser-530, and Leu-531 in an analogous fashion to the 2'-methyl group of indomethacin. Thus, NSAIDs can exhibit multiple binding orientations within the COX active site, but each binding mode involves both hydrophilic and hydrophobic interactions.
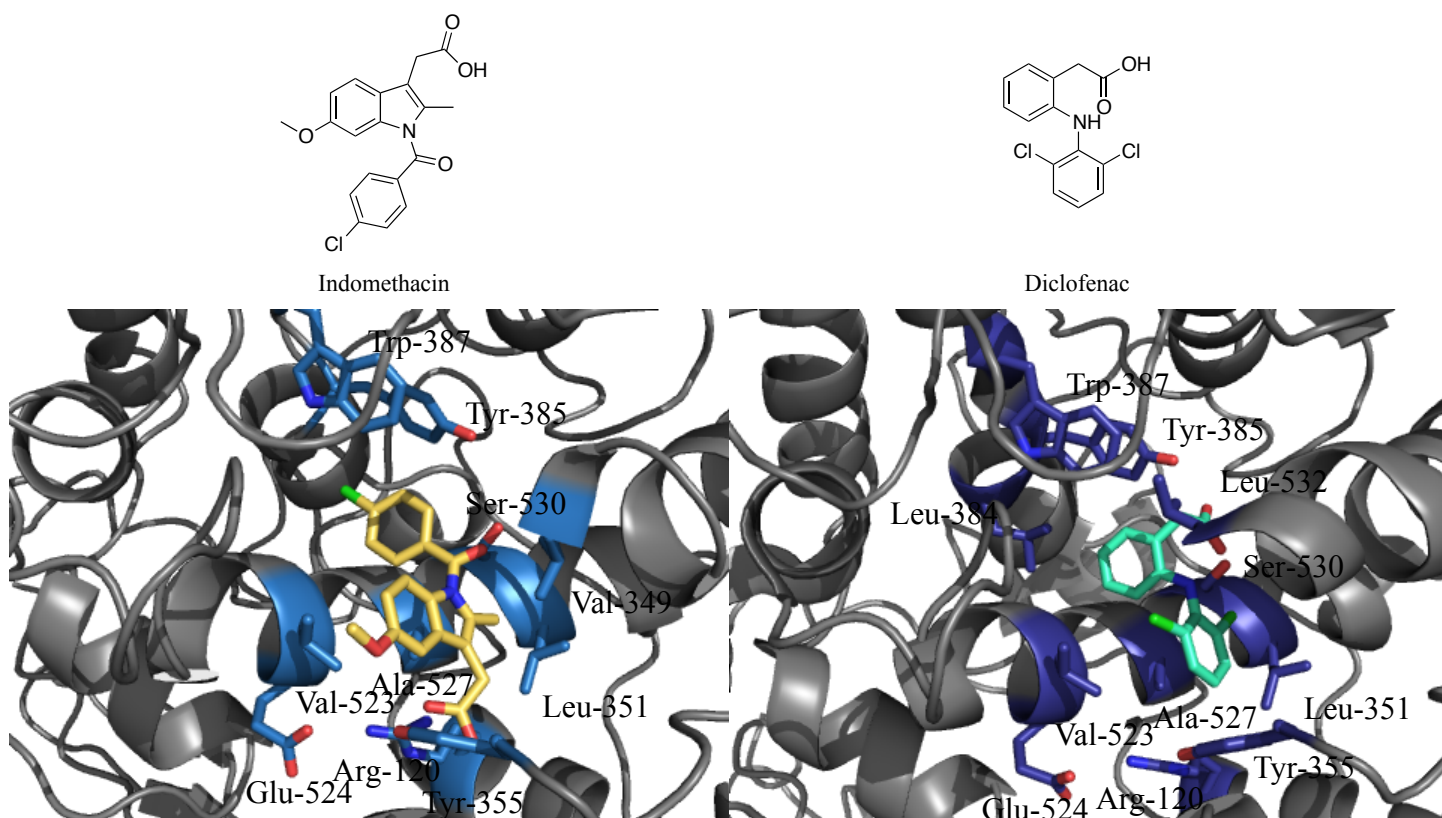
Figure 13: Binding of Indomethacin and Diclofenac to COX-2. Indomethacin (yellow) coordinates to constriction site residues Arg-120 and Tyr-355. The 2′-methyl group inserts into a small hydrophobic pocket comprised of Ser-530, Val-349, Leu-531, and Ala-527 (left, PDB ID: 4COX). In contrast, diclofenac (green) binds in an inverted conformation in the active site with the carboxylate hydrogen-bonded to Ser-530 and Tyr-385 (right, PDB ID: 1PXX).

The discovery of COX-2 as a second inducible isoform of COX lead to concerted drug discovery efforts to develop COX-2-selective inhibitors. These efforts were spurred on by the association of COX-2 with inflammation, pain, and fever, while COX-1 has been attributed to the negative side effects of NSAIDs, particularly gastrointestinal bleeding. Multiple animal models and human clinical trials have since demonstrated that COX-2-selective inhibitors have anti-inflammatory effects and present decreased gastrointestinal complications.[227-229]

The majority of COX-2-selective inhibitors are diarylheterocycles. The first diarylheterocycle, DuP-697, is an aryl methyl sulfonyl compound that was developed by Dupont-Merck before COX-2 was discovered. DuP-697 inhibits PG biosynthesis in macrophages, but not platelets, in agreement with the fact that platelets primarily express COX-1, while macrophages primarily express COX-2.[230,231] Kinetic studies indicate that diarylheterocycles are rapid, reversible inhibitors of COX-1, but time-dependent inhibitors of COX-2.[232] Surprisingly, diarylheterocycles exhibit a three-step inhibition mechanism with COX-2 consisting of an initial association of inhibitor with enzyme followed by two unimolecular events.[233-235] While the first two events are similar to traditional time-dependent NSAIDs, the third step results in the formation of a pseudo-irreversible inhibitor-enzyme complex.[234,235]

The molecular determinants of COX-2 selective inhibition by diarylheterocycles have been elucidated through extensive structure-activity studies, site-directed mutagenesis, and crystal structures. COX-2 selective inhibition requires a heterocycle or carbocycle with two aromatic rings at adjacent positions and a 4-sulfonamide or 4-methylsulfone substitution on one of the phenyl rings.[236] A crystal structure of the COX-2 selective inhibitor SC-558 revealed that the substituted phenyl ring interacts with Leu-352, Tyr-355, Phe-518, and Val-523 while the sulfonamide or sulfone group interacts with His-90, Gln-192, and Arg-513.[223] The COX-2 selectivity arises due to the substitution of Val-523 to Ile in COX-1 and mutation of Val-523 to Ile in COX-2 abrogates time-dependent inhibition of COX-2 by diarylheterocycles.[237,238] The secondary shell substitutions of Arg-513 and Val-434 in COX-2 for His and Ile in COX-1 also regulate the ability of diarylheterocycles to bind in the side pocket.[223,239]

In addition to the diarylheterocycles, an analog of diclofenac, lumiracoxib, is also a COX-2-selective inhibitor. As with diclofenac, lumiracoxib binds in an inverted conformation with its carboxylic acid hydrogen bonded to Ser-530 and Tyr-385 at the bend of the COX active site. Lumiracoxib is a COX-2 selective inhibitor due to the insertion of its methyl group into a hydrophobic pocket next to Leu-384, where in COX-1 there are larger secondary shell residues that clash with the methyl group.[240] Removal of the methyl group from lumiracoxib results in a non-selective COX-1 and COX-2 inhibitor.[241]

Side effects of selective COX-2 inhibitors

While COX-2 selective inhibitors display reduced gastrointestinal toxicity than non-selective COX inhibitors, the Vioxx Gastrointestinal Outcome Research (VIGOR) study suggested that this COX-2-selective inhibitor has an increased risk of cardiovascular events.[228] The VIGOR study examined the efficacy and safety of the COX-2 selective inhibitor rofecoxib (Vioxx) in comparison to the non-selective NSAID naproxen in patients with rheumatoid arthritis. While rofecoxib is as efficacious as naproxen for the treatment of rheumatoid arthritis, patients taking rofecoxib had fewer adverse gastrointestinal events compared to naproxen. However, patients treated with rofecoxib exhibited a 4-fold increase in acute myocardial infarction compared to those treated with naproxen. The apparent increase in cardiovascular toxicity with rofecoxib compared to naproxen was attributed to a cardioprotective effect of naproxen. The long half-life of naproxen in humans leads to sustained inhibition of COX-1 in platelets, which reduces the production of the prothrombotic and atherogenic product TxA_2.[242] When patients are treated with naproxen at doses of 500 mg twice daily, the biosynthesis of platelet-derived TxA_2 is inhibited throughout the dosage interval.

Another study examining the efficacy and safety of COX-2-selective inhibitors was the Celecoxib Long-term Arthritis Safety Study (CLASS). The CLASS trial compared celecoxib to diclofenac and ibuprofen in patients with osteoarthritis or rheumatoid arthritis.[229] Initial reports indicated that celecoxib was associated with fewer gastrointestinal events compared to the traditional NSAIDS, but no statistically significant differences were observed after twelve months of follow up, consistent with reports that celecoxib and diclofenac show a similar degree of COX-2 selectivity in the human whole blood assay.[243,244] In contrast to the VIGOR study, no

significant differences in the incidence of cardiovascular events between the celecoxib, diclofenac, and ibuprofen groups was found.

Additional studies evaluated the cardiovascular risk of rofecoxib in the Adenomatous Polyp Prevention on Vioxx (APPROVE) trial. COX-2-selective inhibitors are possible therapeutic agents in human colon cancers due to the role that COX-2 overexpression plays in tumorigenesis. In agreement with this, patients who received 25 mg of rofecoxib had a 24% reduction in colon polyp recurrence after treatment for three years. However, the rofecoxib treatment group also had a 2-fold increase in cardiovascular events, including myocardial infarction and stroke, compared to placebo.[245,246] This increase in cardiovascular events reported in the APPROVE trial led to the immediate withdrawal of rofecoxib from the market. In a parallel study, the Adenoma Prevention with Celecoxib (APC) trial measured polyp recurrence in patients receiving either 200 or 400 mg celecoxib twice daily compared to placebo. Celecoxib treatment resulted in a dose-dependent reduction in the recurrence of polyps following treatment. However, celecoxib also increased cardiovascular events in a dose-dependent manner with a 2.6-fold increase in patients allocated to low-dose celecoxib and a 3.4-fold increase in the high-dose group. These clinical trials reveal that COX-2-selective inhibitors are effective therapeutics for arthritis and colon polyp recurrence, but prolonged use of COX-2-selective inhibitors is associated with an increased risk of cardiovascular events.

Several studies have examined the underlying mechanisms of the cardiovascular toxicity of COX-2-selective inhibitors. The most prominent hypothesis is that the cardiovascular toxicity of COX-2-selective inhibitors occurs from the inhibition of PGI_2 or PGI_2-G production by vascular endothelial cells, both of which have anti-thrombotic and anti-atherogenic effects.[206,247] Importantly, although COX-2-selective inhibitors have increased cardiovascular toxicity relative to placebo, meta-analyses of clinical trials have identified that traditional NSAIDs including ibuprofen, indomethacin, and diclofenac, also have an increased cardiovascular risk similar to that of celecoxib.[248-250] The only exception identified thus far is that naproxen, a non-selective inhibitor of COX-1 and COX-2, does not increase cardiovascular events. The lack of cardiovascular toxicity of naproxen may be due to its persistent inhibition of TxA_2 biosynthesis throughout the dosing interval, which is not observed with other commonly used NSAIDs.[251]

27

Cyclooxygenase Subunit Communication

A growing body of evidence has identified that although the two monomers of COX are composed of identical sequences, they are functional heterodimers. Initial studies identified monomer cooperation by determining that binding of only one molecule of a slow, tight-binding inhibitor such as (*S*)-flurbiprofen, indomethacin, or diclofenac, is sufficient to inhibit oxygenation by both COX monomers.[219] The generation of COX heterodimers consisting of a wild-type monomer and a G533A monomer identified that these heterodimers retain maximal catalytic activity despite the fact that G533A results in the improper positioning of AA and G533A homodimers have impaired AA oxygenation relative to wild-type homodimers.[252,253]

As with substrate utilization, inhibitors also demonstrate intriguing behavior in heterodimers. (*S*)-flurbiprofen does not inhibit R120Q COX-2 homodimers, but it is a potent time-dependent inhibitor of a heterodimer consisting of a wild-type monomer and a R120Q monomer, as it is with wild-type COX-2 homodimers.[252] These studies with heterodimers are in agreement with the early findings that COX enzymes exhibit half-of-sites reactivity with only a single functional monomer and a single association of heme with the dimer.[254] Additionally, they are in agreement with the structures revealing that substrates bind in a productive conformation in one monomer and a non-productive conformation in the second monomer.[235,241]

More recent efforts have identified portions of the enzyme that mediate dimer crosstalk. The COX-2 monomers can be identified as a catalytic subunit, which binds a heme prosthetic group, and an allosteric subunit, which does not.[255,256] Cross-linking studies have identified that binding of an inhibitor to COX-2 alters two loops located at the dimer interface: one containing Ser-126 and Pro-127 and a second containing Ser-531 and Ala-543.[257] A crystal structure of the COX-2 selective inhibitor celecoxib bound to COX-1 identified an alternate conformation of the loop consisting of residues 121-129 (Figure 14).[258] In this alternate conformation the loop positions Ser-126 adjacent to Glu-543, which may form the basis of subunit communication. Movement of the loop consisting of residues 121-129 is also apparent in the crystal structure of (*S*)-flurbiprofen bound to the COX heterodimer consisting of a wild-type monomer and a R120Q monomer, revealing that multiple inhibitors cause movement of this loop.[259]
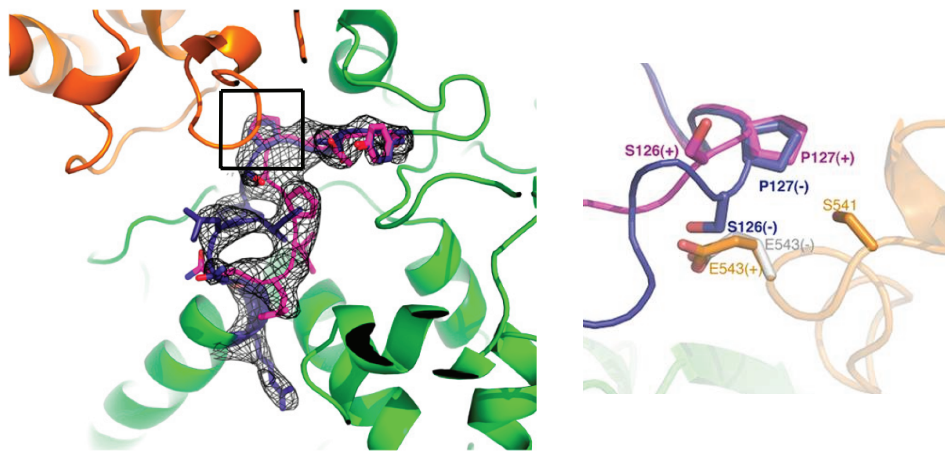
Figure 14: Conformational changes in the dimer interface upon binding of celecoxib to COX-1. The loop consisting of residues 121-129 exists in different conformations upon binding of celecoxib to COX-1, shown in blue and purple. Reproduced from.[258]

A particularly striking example of dimer crosstalk has been revealed in our laboratory. Despite the fact that AA and 2-AG have comparable k_{cat}/K_m ratios for oxygenation, inhibition of COX-2 oxygenation of 2-AG by the rapid-reversible inhibitors (*S*)-ibuprofen and mefenamic acid occurs at much lower inhibitor concentrations than inhibition of COX-2 oxygenation of AA.[260,261] Surprisingly, kinetic studies revealed that (*S*)-ibuprofen and mefenamic acid act as non-competitive inhibitors of 2-AG oxygenation by COX-2, but competitive inhibitors of AA oxygenation (Figure 15).
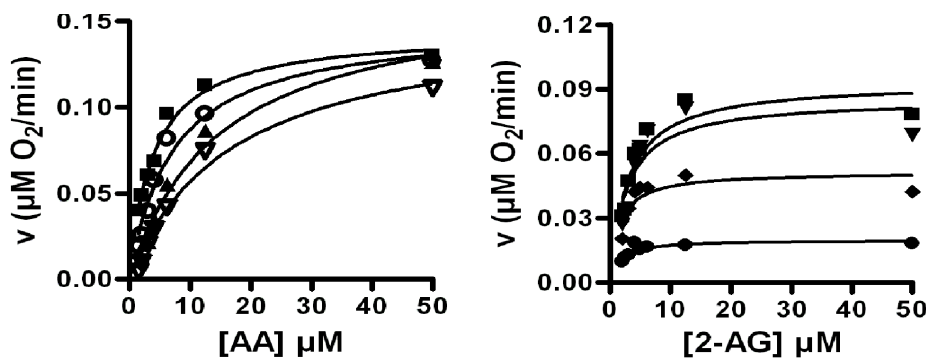
Figure 15: Inhibition of COX-2 oxygenation of AA and 2-AG by ibuprofen. Ibuprofen acts as a competitive inhibitor of AA (left), but a non-competitive inhibitor of 2-AG (right). Reproduced from.[261]

These studies reveal that (*S*)-ibuprofen and mefenamic acid inhibit COX-2 oxygenation of AA and 2-AG through different inhibition mechanisms and with different potencies. Given the potential for dimer cross-talk upon binding of an inhibitor to one monomer, a model was hypothesized (Figure 16).[252] Binding of a single molecule of either (*S*)-ibuprofen or mefenamic acid to the first monomer is sufficient to inhibit 2-AG

29

oxygenation in the second monomer, but not AA. To inhibit AA oxygenation in the second monomer, a second inhibitor molecule needs to bind to the second active site. This model is consistent with the kinetic data indicating that (*S*)-ibuprofen and mefenamic acid are non-competitive inhibitors of 2-AG oxygenation and competitive inhibitors of AA oxygenation. The model also accounts for the differences in inhibition potencies between 2-AG and AA as the binding of (*S*)-ibuprofen to the first monomer increases the K_I of the second binding event. Thus, the model accounts for both the difference in inhibition modes and inhibition potencies between the two substrates.
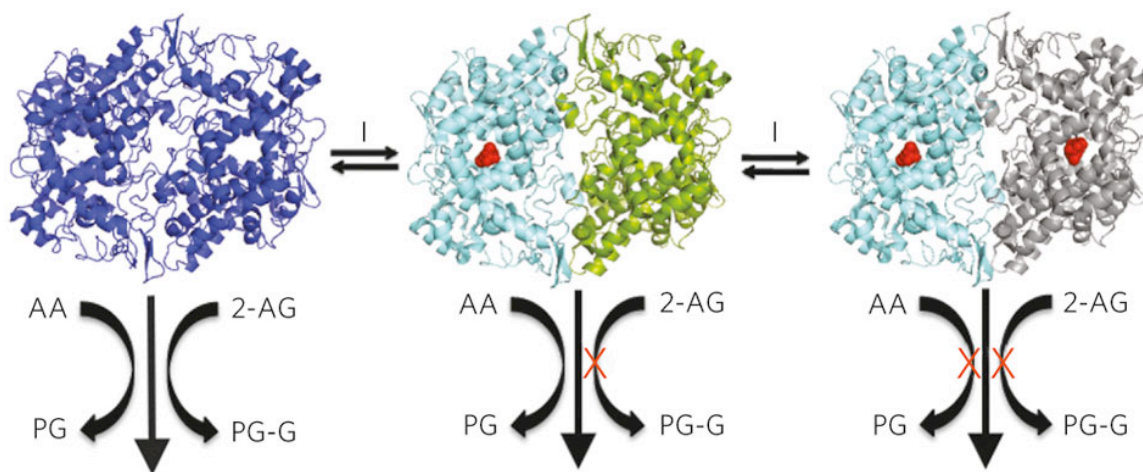
Figure 16: Model for differential inhibition of 2-AG and AA oxygenation by COX-2. Reproduced from.[262]

Dissertation Aims

The major goal of the research described herein was to provide further insight into substrate-selective COX-2 inhibition. These studies will provide an understanding of the mechanisms by which NSAIDs function and identify the biological effects of COX-2 inhibition. Taken together with previous studies, these studies are critical to developing novel therapeutic agents with beneficial effects and potentially reduced side-effect profiles. An investigation of the molecules that exhibit substrate-selective inhibition and the molecular mechanisms of substrate-selective COX-2 inhibition are presented in chapter II. These studies comprise analyses of the COX-2 inhibitors that exhibit substrate-selective inhibition, the identification of novel substrate-selective inhibitors and their binding modes, and the enzymatic mechanism of substrate-selective inhibition *in vitro*. We then furthered our examination of substrate-selective COX-2 inhibition by developing cellular model systems to study the effects of substrate-selective COX-2 inhibitors, which is discussed in chapter III. After validating several substrate-selective COX-2 inhibitors *in vitro* and in cellular systems, we sought to characterize the effects of substrate-selective COX-2 inhibition *in vivo* in chapter IV. These studies lead to the development of novel substrate-selective COX-2 inhibitors and the characterization of the biochemical and behavioral effects of a series of NSAIDs. We then characterized the pharmacokinetics and pharmacodynamics of the *in vivo* substrate-selective inhibitor of LM-4131 in chapter V. The short half-life and lack of substrate-selective COX-2 inhibition displayed by LM-4131 led to the characterization of alternative *in vivo* substrate-selective COX-2 inhibitors, which is discussed in chapter VI. As outlined in chapter VII we also determined the biosynthetic route of PG-Gs in multiple macrophage cell lines. Chapter VIII contains a summary of this research and a discussion of the repercussions.

References

1. Hamberg, M. & Samuelsson, B. Oxygenation of unsaturated fatty acids by the vesicular gland of sheep. *The Journal of biological chemistry* **242**, 5344-5354 (1967).
2. Hemler, M. & Lands, W.E. Purification of the cyclooxygenase that forms prostaglandins. Demonstration of two forms of iron in the holoenzyme. *The Journal of biological chemistry* **251**, 5575-5579 (1976).
3. Miyamoto, T., Ogino, N., Yamamoto, S. & Hayaishi, O. Purification of prostaglandin endoperoxide synthetase from bovine vesicular gland microsomes. *The Journal of biological chemistry* **251**, 2629-2636 (1976).
4. Xie, W.L., Chipman, J.G., Robertson, D.L., Erikson, R.L. & Simmons, D.L. Expression of a mitogen-responsive gene encoding prostaglandin synthase is regulated by mRNA splicing. *Proceedings of the National Academy of Sciences of the United States of America* **88**, 2692-2696 (1991).
5. Morita, I.*, et al.* Different intracellular locations for prostaglandin endoperoxide H synthase-1 and -2. *The Journal of biological chemistry* **270**, 10902-10908 (1995).
6. Ogino, N., Ohki, S., Yamamoto, S. & Hayaishi, O. Prostaglandin endoperoxide synthetase from bovine vesicular gland microsomes. Inactivation and activation by heme and other metalloporphyrins. *The Journal of biological chemistry* **253**, 5061-5068 (1978).
7. Hamberg, M. & Samuelsson, B. Detection and isolation of an endoperoxide intermediate in prostaglandin biosynthesis. *Proceedings of the National Academy of Sciences of the United States of America* **70**, 899-903 (1973).
8. Ohki, S., Ogino, N., Yamamoto, S. & Hayaishi, O. Prostaglandin hydroperoxidase, an integral part of prostaglandin endoperoxide synthetase from bovine vesicular gland microsomes. *The Journal of biological chemistry* **254**, 829-836 (1979).
9. Dietz, R., Nastainczyk, W. & Ruf, H.H. Higher oxidation states of prostaglandin H synthase. Rapid electronic spectroscopy detected two spectral intermediates during the peroxidase reaction with prostaglandin G2. *European journal of biochemistry / FEBS* **171**, 321-328 (1988).
10. Smith, W.L. & Lands, W.E. Oxygenation of polyunsaturated fatty acids during prostaglandin biosynthesis by sheep vesicular gland. *Biochemistry* **11**, 3276-3285 (1972).
11. Landino, L.M., Crews, B.C., Gierse, J.K., Hauser, S.D. & Marnett, L.J. Mutational analysis of the role of the distal histidine and glutamine residues of prostaglandin-endoperoxide synthase-2 in peroxidase catalysis, hydroperoxide reduction, and cyclooxygenase activation. *The Journal of biological chemistry* **272**, 21565-21574 (1997).
12. Samuelsson, B. On the Incorporation of Oxygen in the Conversion of 8, 11, 14-Eicosatrienoic Acid to Prostaglandin E1. *Journal of the American Chemical Society* **87**, 3011-3013 (1965).
13. Hamberg, M. & Samuelsson, B. On the mechanism of the biosynthesis of prostaglandins E-1 and F-1-alpha. *The Journal of biological chemistry* **242**, 5336-5343 (1967).
14. Smith, W. Molecular biology of prostanoid biosynthetic enzymes and receptors. *Advances in experimental medicine and biology* **400B**, 989-1011 (1997).
15. Funk, C.D. Prostaglandins and leukotrienes: advances in eicosanoid biology. *Science* **294**, 1871-1875 (2001).
16. Rizzo, G. & Fiorucci, S. PPARs and other nuclear receptors in inflammation. *Current opinion in pharmacology* **6**, 421-427 (2006).
17. Bos, C.L., Richel, D.J., Ritsema, T., Peppelenbosch, M.P. & Versteeg, H.H. Prostanoids and prostanoid receptors in signal transduction. *The international journal of biochemistry & cell biology* **36**, 1187-1205 (2004).
18. Rouzer, C.A. & Marnett, L.J. Non-redundant functions of cyclooxygenases: oxygenation of endocannabinoids. *The Journal of biological chemistry* **283**, 8065-8069 (2008).
19. Shio, H. & Ramwell, P. Effect of Prostaglandin E2 and Aspirin on Secondary Aggregation of Human Platelets. *Nature-New Biol* **236**, 45-& (1972).
20. Patrono, C. & Dunn, M.J. The Clinical-Significance of Inhibition of Renal Prostaglandin Synthesis. *Kidney Int* **32**, 1-12 (1987).

21. Robert, A. Gastrointestinal Cytoprotection by Prostaglandins. *Gastroen Clin Biol* **8**, 819-827 (1984).
22. Ahmad, A.S., Ahmad, M., Maruyama, T., Narumiya, S. & Dore, S. Neuroprotective Effect of PGD2 DP1 Receptor Against Acute Brain Damage in Young and in Aged Mice. *Stroke* **41**, E382-E382 (2010).
23. Katsumata, Y., *et al.* Lipocalin-type prostaglandin D synthase-mediated biosynthesis of PGD2 and its metabolites 15-deoxy-delta 12,14-PGJ2 synergistically stimulate nrf2 and protect hearts from ischemia/reperfusion injury. *Am J Resp Crit Care* **183**, 687-687 (2011).
24. Kim, K., *et al.* Anti-inflammatory Activity Of PGD2 Is Mediated By Nrf2. *Am J Resp Crit Care* **181**(2010).
25. Fitzgerald, G.A., Catella, F. & Oates, J.A. Eicosanoid Biosynthesis in Human Cardiovascular-Disease. *Hum Pathol* **18**, 248-252 (1987).
26. Murata, T., *et al.* Altered pain perception and inflammatory response in mice lacking prostacyclin receptor. *Nature* **388**, 678-682 (1997).
27. Thomas, D.W., *et al.* Coagulation defects and altered hemodynamic responses in mice lacking receptors for thromboxane A(2). *Journal of Clinical Investigation* **102**, 1994-2001 (1998).
28. Sheng, H.M., *et al.* Inhibition of human colon cancer cell growth by selective inhibition of cyclooxygenase-2. *Journal of Clinical Investigation* **99**, 2254-2259 (1997).
29. Hwang, D., Scollard, D., Byrne, J. & Levine, E. Expression of cyclooxygenase-1 and cyclooxygenase-2 in human breast cancer. *J Natl Cancer I* **90**, 455-460 (1998).
30. Samad, T.A., Sapirstein, A. & Woolf, C.J. Prostanoids and pain: unraveling mechanisms and revealing therapeutic targets. *Trends Mol Med* **8**, 390-396 (2002).
31. Picot, D., Loll, P.J. & Garavito, R.M. The X-ray crystal structure of the membrane protein prostaglandin H2 synthase-1. *Nature* **367**, 243-249 (1994).
32. Kurumbail, R.G., *et al.* Structural basis for selective inhibition of cyclooxygenase-2 by anti-inflammatory agents. *Nature* **384**, 644-648 (1996).
33. Rouzer, C.A. & Marnett, L.J. Cyclooxygenases: structural and functional insights. *J Lipid Res* **50**, S29 - S34 (2009).
34. Van der Ouderaa, F.J., Buytenhek, M., Nugteren, D.H. & Van Dorp, D.A. Purification and characterisation of prostaglandin endoperoxide synthetase from sheep vesicular glands. *Biochim Biophys Acta* **487**, 315-331 (1977).
35. Picot, D. & Garavito, R.M. Prostaglandin H synthase: implications for membrane structure. *FEBS letters* **346**, 21-25 (1994).
36. Luong, C., *et al.* Flexibility of the NSAID binding site in the structure of human cyclooxygenase-2. *Nature structural biology* **3**, 927-933 (1996).
37. Shimokawa, T. & Smith, W.L. Essential histidines of prostaglandin endoperoxide synthase. His-309 is involved in heme binding. *The Journal of biological chemistry* **266**, 6168-6173 (1991).
38. Liu, J., *et al.* Prostaglandin endoperoxide H synthases: peroxidase hydroperoxide specificity and cyclooxygeanse activation. *The Journal of biological chemistry* **282**, 18233-18244 (2007).
39. Malkowski, M.G., Ginell, S.L., Smith, W.L. & Garavito, R.M. The productive conformation of arachidonic acid bound to prostaglandin synthase. *Science* **289**, 1933-1937 (2000).
40. Vecchio, A.J., Simmons, D.M. & Malkowski, M.G. Structural basis of fatty acid substrate binding to cyclooxygenase-2. *The Journal of biological chemistry* **285**, 22152-22163 (2010).
41. Kiefer, J.R., *et al.* Structural insights into the stereochemistry of the cyclooxygenase reaction. *Nature* **405**, 97-101 (2000).
42. Thuresson, E.D., *et al.* Prostaglandin endoperoxide H synthase-1: the functions of cyclooxygenase active site residues in the binding, positioning, and oxygenation of arachidonic acid. *The Journal of biological chemistry* **276**, 10347-10357 (2001).
43. Harman, C.A., Rieke, C.J., Garavito, R.M. & Smith, W.L. Crystal structure of arachidonic acid bound to a mutant of prostaglandin endoperoxide H synthase-1 that forms predominantly 11-hydroperoxyeicosatetraenoic acid. *The Journal of biological chemistry* **279**, 42929-42935 (2004).

44. Schneider, C*., et al.* Control of prostaglandin stereochemistry at the 15-carbon by cyclooxygenases-1 and -2. A critical role for serine 530 and valine 349. *The Journal of biological chemistry* **277**, 478-485 (2002).

45. Newton, R*., et al.* Superinduction of COX-2 mRNA by cycloheximide and interleukin-1beta involves increased transcription and correlates with increased NF-kappaB and JNK activation. *FEBS letters* **418**, 135-138 (1997).

46. Faour, W.H., Mancini, A., He, Q.W. & Di Battista, J.A. T-cell-derived interleukin-17 regulates the level and stability of cyclooxygenase-2 (COX-2) mRNA through restricted activation of the p38 mitogen-activated protein kinase cascade: role of distal sequences in the 3'-untranslated region of COX-2 mRNA. *The Journal of biological chemistry* **278**, 26897-26907 (2003).

47. Kaufmann, W.E., Worley, P.F., Pegg, J., Bremer, M. & Isakson, P. COX-2, a synaptically induced enzyme, is expressed by excitatory neurons at postsynaptic sites in rat cerebral cortex. *Proceedings of the National Academy of Sciences of the United States of America* **93**, 2317-2321 (1996).

48. Harris, R.C*., et al.* Cyclooxygenase-2 is associated with the macula densa of rat kidney and increases with salt restriction. *The Journal of clinical investigation* **94**, 2504-2510 (1994).

49. Yoshikawa, K*., et al.* Preferential localization of prostamide/prostaglandin F synthase in myelin sheaths of the central nervous system. *Brain research* **1367**, 22-32 (2011).

50. Mbonye, U.R*., et al.* The 19-amino acid cassette of cyclooxygenase-2 mediates entry of the protein into the endoplasmic reticulum-associated degradation system. *The Journal of biological chemistry* **281**, 35770-35778 (2006).

51. Wu, G., Wei, C.H., Kulmacz, R.J., Osawa, Y. & Tsai, A.L. A mechanistic study of self-inactivation of the peroxidase activity in prostaglandin H synthase-1. *Journal of Biological Chemistry* **274**, 9231-9237 (1999).

52. Wu, G*., et al.* Oxyferryl heme and not tyrosyl radical is the likely culprit in prostaglandin H synthase-1 peroxidase inactivation. *Biochemistry* **46**, 534-542 (2007).

53. Markey, C.M., Alward, A., Weller, P.E. & Marnett, L.J. Quantitative studies of hydroperoxide reduction by prostaglandin H synthase. Reducing substrate specificity and the relationship of peroxidase to cyclooxygenase activities. *The Journal of biological chemistry* **262**, 6266-6279 (1987).

54. Siegel, M.I., McConnell, R.T., Abrahams, S.L., Porter, N.A. & Cuatrecasas, P. Regulation of arachidonate metabolism via lipoxygenase and cyclo-oxygenase by 12-HPETE, the product of human platelet lipoxygenase. *Biochemical and biophysical research communications* **89**, 1273-1280 (1979).

55. Yu, Y*., et al.* Targeted cyclooxygenase gene (ptgs) exchange reveals discriminant isoform functionality. *The Journal of biological chemistry* **282**, 1498-1506 (2007).

56. Kulmacz, R.J. Regulation of cyclooxygenase catalysis by hydroperoxides. *Biochemical and biophysical research communications* **338**, 25-33 (2005).

57. Bambai, B., Rogge, C.E., Stec, B. & Kulmacz, R.J. Role of Asn-382 and Thr-383 in activation and inactivation of human prostaglandin H synthase cyclooxygenase catalysis. *The Journal of biological chemistry* **279**, 4084-4092 (2004).

58. Ueno, N., Takegoshi, Y., Kamei, D., Kudo, I. & Murakami, M. Coupling between cyclooxygenases and terminal prostanoid synthases. *Biochemical and biophysical research communications* **338**, 70-76 (2005).

59. Mechoulam, R. & Gaoni, Y. A Total Synthesis of Dl-Delta-1-Tetrahydrocannabinol, the Active Constituent of Hashish. *Journal of the American Chemical Society* **87**, 3273-3275 (1965).

60. Matsuda, L.A., Lolait, S.J., Brownstein, M.J., Young, A.C. & Bonner, T.I. Structure of a Cannabinoid Receptor and Functional Expression of the Cloned Cdna. *Nature* **346**, 561-564 (1990).

61. Herkenham, M*., et al.* Cannabinoid Receptor Localization in Brain. *Proceedings of the National Academy of Sciences of the United States of America* **87**, 1932-1936 (1990).

62. Munro, S., Thomas, K.L. & Abushaar, M. Molecular Characterization of a Peripheral Receptor for Cannabinoids. *Nature* **365**, 61-65 (1993).

63. Devane, W.A*., et al.* Isolation and Structure of a Brain Constituent That Binds to the Cannabinoid Receptor. *Science* **258**, 1946-1949 (1992).

64. Stella, N., Schweitzer, P. & Piomelli, D. A second endogenous cannabinoid that modulates long-term potentiation. *Nature* **388**, 773-778 (1997).
65. Clark, J.D., *et al.* A Novel Arachidonic Acid-Selective Cytosolic Pla2 Contains a Ca2+-Dependent Translocation Domain with Homology to Pkc and Gap. *Cell* **65**, 1043-1051 (1991).
66. Leslie, C.C., Voelker, D.R., Channon, J.Y., Wall, M.M. & Zelarney, P.T. Properties and Purification of an Arachidonoyl-Hydrolyzing Phospholipase-A2 from a Macrophage Cell-Line, Raw-264.7. *Biochimica Et Biophysica Acta* **963**, 476-492 (1988).
67. Lin, L.L., *et al.* Cpla2 Is Phosphorylated and Activated by Map Kinase. *Cell* **72**, 269-278 (1993).
68. Nakamura, H., Hirabayashi, T., Shimizu, M. & Murayama, T. Ceramide-1-phosphate activates cytosolic phospholipase A2 alpha directly and by PKC pathway. *Biochem Pharmacol* **71**, 850-857 (2006).
69. Mosior, M., Six, D.A. & Dennis, E.A. Group IV cytosolic phospholipase A(2) binds with high affinity and specificity to phosphatidylinositol 4,5-bisphosphate resulting in dramatic increases in activity. *Journal of Biological Chemistry* **273**, 2184-2191 (1998).
70. Sharp, J.D., *et al.* Molecular-Cloning and Expression of Human Ca2+-Sensitive Cytosolic Phospholipase-A2. *Journal of Biological Chemistry* **266**, 14850-14853 (1991).
71. Nomura, D.K., *et al.* Endocannabinoid Hydrolysis Generates Brain Prostaglandins That Promote Neuroinflammation. *Science* **334**, 809-813 (2011).
72. Prescott, S.M. & Majerus, P.W. Characterization of 1,2-Diacylglycerol Hydrolysis in Human-Platelets - Demonstration of an Arachidonoyl-Monoacylglycerol Intermediate. *Journal of Biological Chemistry* **258**, 764-769 (1983).
73. Sugiura, T., Kishimoto, S., Oka, S. & Gokoh, M. Biochemistry, pharmacology and physiology of 2-arachidonoylglycerol, an endogenous cannabinoid receptor ligand. *Prog Lipid Res* **45**, 405-446 (2006).
74. Ueda, N., Tsuboi, K., Uyama, T. & Ohnishi, T. Biosynthesis and degradation of the endocannabinoid 2-arachidonoylglycerol. *Biofactors* **37**, 1-7 (2011).
75. Fukami, K., Inanobe, S., Kanemaru, K. & Nakamura, Y. Phospholipase C is a key enzyme regulating intracellular calcium and modulating the phosphoinositide balance. *Prog Lipid Res* **49**, 429-437 (2010).
76. Kano, M., Ohno-Shosaku, T., Hashimotodani, Y., Uchigashima, M. & Watanabe, M. Endocannabinoid-Mediated Control of Synaptic Transmission. *Physiol Rev* **89**, 309-380 (2009).
77. Bisogno, T., Melck, D., De Petrocellis, L. & Di Marzo, V. Phosphatidic acid as the biosynthetic precursor of the endocannabinoid 2-arachidonoylglycerol in intact mouse neuroblastoma cells stimulated with ionomycin. *J Neurochem* **72**, 2113-2119 (1999).
78. Oka, S., *et al.* Evidence for the involvement of the cannabinoid CB2 receptor and its endogenous ligand 2-arachidonoylglycerol in 12-O-tetradecanoylphorbol-13-acetate-induced acute inflammation in mouse ear. *Journal of Biological Chemistry* **280**, 18488-18497 (2005).
79. Ueda, H., Kobayashi, T., Kishimoto, M., Tsutsumi, T. & Okuyama, H. A Possible Pathway of Phosphoinositide Metabolism through Edta-Insensitive Phospholipase-a(1) Followed by Lysophosphoinositide-Specific Phospholipase-C in Rat-Brain. *J Neurochem* **61**, 1874-1881 (1993).
80. Tsutsumi, T., *et al.* Lysophosphoinositide-Specific Phospholipase-C in Rat-Brain Synaptic Plasma-Membranes. *Neurochem Res* **19**, 399-406 (1994).
81. Nakane, S., *et al.* 2-arachidonoyl-sn-glycero-3-phosphate, an arachidonic acid-containing lysophosphatidic acid: occurrence and rapid enzymatic conversion to 2-arachidonoyl-sn-glycerol, a cannabinoid receptor ligand, in rat brain. *Arch Biochem Biophys* **402**, 51-58 (2002).
82. Okazaki, T., *et al.* Diacylglycerol Metabolism and Arachidonic-Acid Release in Human-Fetal Membranes and Decidua Vera. *Journal of Biological Chemistry* **256**, 7316-7321 (1981).
83. Chau, L.Y. & Tai, H.H. Release of Arachidonate from Diglyceride in Human-Platelets Requires the Sequential Action of a Diglyceride Lipase and a Monoglyceride Lipase. *Biochemical and biophysical research communications* **100**, 1688-1695 (1981).
84. Bisogno, T., *et al.* Cloning of the first sn1-DAG lipases points to the spatial and temporal regulation of endocannabinoid signaling in the brain. *J Cell Biol* **163**, 463-468 (2003).
85. Jung, K.M., *et al.* A key role for diacylglycerol lipase-alpha in metabotropic glutamate receptor-dependent endocannabinoid mobilization. *Mol Pharmacol* **72**, 612-621 (2007).

86. Tanimura, A*., et al.* The Endocannabinoid 2-Arachidonoylglycerol Produced by Diacylglycerol Lipase alpha Mediates Retrograde Suppression of Synaptic Transmission. *Neuron* **65**, 320-327 (2010).

87. Gao, Y*., et al.* Loss of Retrograde Endocannabinoid Signaling and Reduced Adult Neurogenesis in Diacylglycerol Lipase Knock-out Mice. *J Neurosci* **30**, 2017-2024 (2010).

88. Hsu, K.L*., et al.* DAGL beta inhibition perturbs a lipid network involved in macrophage inflammatory responses. *Nat Chem Biol* **8**, 999-1007 (2012).

89. Schmid, H.H.O., Schmid, P.C. & Natarajan, V. N-Acylated Glycerophospholipids and Their Derivatives. *Prog Lipid Res* **29**, 1-43 (1990).

90. Ueda, N., Tsuboi, K. & Uyama, T. Enzymological studies on the biosynthesis of N-acylethanolamines. *Bba-Mol Cell Biol L* **1801**, 1274-1285 (2010).

91. Schmid, H.H.O. Pathways and mechanisms of N-acylethanolamine biosynthesis: can anandamide be generated selectively? *Chem Phys Lipids* **108**, 71-87 (2000).

92. Wellner, N., Diep, T.A., Janfelt, C. & Hansen, H.S. N-acylation of phosphatidylethanolamine and its biological functions in mammals. *Bba-Mol Cell Biol L* **1831**, 652-662 (2013).

93. Cadas, H., diTomaso, E. & Piomelli, D. Occurrence and biosynthesis of endogenous cannabinoid precursor, N-arachidonoyl phosphatidylethanolamine, in rat brain. *J Neurosci* **17**, 1226-1242 (1997).

94. Jin, X.H*., et al.* cDNA cloning and characterization of human and mouse Ca2+-independent phosphatidylethanolamine N-acyltransferases. *Bba-Mol Cell Biol L* **1791**, 32-38 (2009).

95. Jin, X.H*., et al.* Discovery and characterization of Ca2+-independent phosphatidylethanolarnine N-acyltransferase generating the anandarnide precursor and its congeners. *Journal of Biological Chemistry* **282**, 3614-3623 (2007).

96. Okamoto, Y., Wang, J., Morishita, J. & Ueda, N. Biosynthetic pathways of the endocannabinoid anandamide. *Chem Biodivers* **4**, 1842-1857 (2007).

97. Okamoto, Y., Morishita, J., Tsuboi, K., Tonai, T. & Ueda, N. Molecular characterization of a phospholipase D generating anandamide and its congeners. *Journal of Biological Chemistry* **279**, 5298-5305 (2004).

98. Wang, J*., et al.* Functional analysis of the purified anandamide-generating phospholipase D as a member of the metallo-beta-lactamase family. *Journal of Biological Chemistry* **281**, 12325-12335 (2006).

99. Wang, J., Okamoto, Y., Tsuboi, K. & Ueda, N. The stimulatory effect of phosphatidylethanolamine on N-acylphosphatidylethanolamine-hydrolyzing phospholipase D (NAPE-PLD). *Neuropharmacology* **54**, 8-15 (2008).

100. Sun, Y.X*., et al.* Biosynthesis of anandamide and N-palmitoylethanolamine by sequential actions of phospholipase A(2) and lysophospholipase D. *Biochem J* **380**, 749-756 (2004).

101. Simon, G.M. & Cravatt, B.F. Endocannabinoid biosynthesis proceeding through glycerophospho-N-acyl ethanolamine and a role for alpha/beta-hydrolase 4 in this pathway. *Journal of Biological Chemistry* **281**, 26465-26472 (2006).

102. Simon, G.M. & Cravatt, B.F. Anandamide biosynthesis catalyzed by the phosphodiesterase GDE1 and detection of glycerophospho-n-acyl ethanolamine precursors in mouse brain. *Journal of Biological Chemistry* **283**, 9341-9349 (2008).

103. Simon, G.M. & Cravatt, B.F. Characterization of mice lacking candidate N-acyl ethanolamine biosynthetic enzymes provides evidence for multiple pathways that contribute to endocannabinoid production in vivo. *Mol Biosyst* **6**, 1411-1418 (2010).

104. Liu, J*., et al.* A biosynthetic pathway for anandamide. *Proceedings of the National Academy of Sciences of the United States of America* **103**, 13345-13350 (2006).

105. Liu, J*., et al.* Lipopolysaccharide induces anandamide synthesis in macrophages via CD14/MAPK/phosphoinositide 3-kinase/NF-kappa B independently of platelet-activating factor. *Journal of Biological Chemistry* **278**, 45034-45039 (2003).

106. Liu, J*., et al.* Multiple pathways involved in the biosynthesis of anandamide. *Neuropharmacology* **54**, 1-7 (2008).

107. Howlett, A.C*., et al.* International Union of Pharmacology. XXVII. Classification of cannabinoid receptors. *Pharmacol Rev* **54**, 161-202 (2002).

108. Tsou, K., Brown, S., Sanudo-Pena, M.C., Mackie, K. & Walker, J.M. Immunohistochemical distribution of cannabinoid CB1 receptors in the rat central nervous system. *Neuroscience* **83**, 393-411 (1998).

109. Hohmann, A.G. & Herkenham, M. Localization of central cannabinoid CB1 receptor messenger RNA in neuronal subpopulations of rat dorsal root ganglia: A double-label in situ hybridization study. *Neuroscience* **90**, 923-931 (1999).

110. Bouaboula, M*., et al.* Cannabinoid-Receptor Expression in Human-Leukocytes. *European Journal of Biochemistry* **214**, 173-180 (1993).

111. Hoffman, A.F. & Lupica, C.R. Mechanisms of cannabinoid inhibition of GABA(A) synaptic transmission in the hippocampus. *J Neurosci* **20**, 2470-2479 (2000).

112. Robbe, D., Alonso, G., Duchamp, F., Bockaert, J. & Manzoni, O.J. Localization and mechanisms of action of cannabinoid receptors at the glutamatergic synapses of the mouse nucleus accumbens. *J Neurosci* **21**, 109-116 (2001).

113. Misner, D.L. & Sullivan, J.M. Mechanism of cannabinoid effects on long-term potentiation and depression in hippocampal CA1 neurons. *J Neurosci* **19**, 6795-6805 (1999).

114. Sullivan, J.M. Mechanisms of cannabinoid-receptor-mediated inhibition of synaptic transmission in cultured hippocampal pyramidal neurons. *J Neurophysiol* **82**, 1286-1294 (1999).

115. Mackie, K. & Hille, B. Cannabinoids Inhibit N-Type Calcium Channels in Neuroblastoma Glioma-Cells. *Proceedings of the National Academy of Sciences of the United States of America* **89**, 3825-3829 (1992).

116. Mu, J., Zhuang, S.Y., Kirby, M.T., Hampson, R.E. & Deadwyler, S.A. Cannabinoid receptors differentially modulate potassium A and D currents in hippocampal neurons in culture. *J Pharmacol Exp Ther* **291**, 893-902 (1999).

117. Schweitzer, P. Cannabinoids decrease the K+ M-current in hippocampal CA1 neurons. *J Neurosci* **20**, 51-58 (2000).

118. Alger, B.E. Retrograde signaling in the regulation of synaptic transmission: focus on endocannabinoids. *Prog Neurobiol* **68**, 247-286 (2002).

119. Melis, M*., et al.* Prefrontal cortex stimulation induces 2-arachidonoyl-glycerol-mediated suppression of excitation in dopamine neurons. *J Neurosci* **24**, 10707-10715 (2004).

120. Riegel, A.C. & Lupica, C.R. Independent presynaptic and postsynaptic mechanisms regulate endocannabinoid signaling at multiple synapses in the ventral tegmental area. *J Neurosci* **24**, 11070-11078 (2004).

121. Carlson, G., Wang, Y. & Alger, B.E. Endocannabinoids facilitate the induction of LTP in the hippocampus. *Nat Neurosci* **5**, 723-724 (2002).

122. Kortleven, C., Fasano, C., Thibault, D., Lacaille, J.C. & Trudeau, L.E. The endocannabinoid 2-arachidonoylglycerol inhibits long-term potentiation of glutamatergic synapses onto ventral tegmental area dopamine neurons in mice. *Eur J Neurosci* **33**, 1751-1760 (2011).

123. Sudhof, T.C. A molecular machine for neurotransmitter release: synaptotagmin and beyond. *Nature medicine* **19**, 1227-1231 (2013).

124. Byerley, W.F., Reimherr, F.W., Wood, D.R. & Grosser, B.I. Fluoxetine, a selective serotonin uptake inhibitor, for the treatment of outpatients with major depression. *Journal of clinical psychopharmacology* **8**, 112-115 (1988).

125. Barar, F.S*., et al.* Interactions between catecholamines and tricyclic and monoamine oxidase inhibitor antidepressive agents in man. *British journal of pharmacology* **43**, 472P-473P (1971).

126. Cravatt, B.F*., et al.* Molecular characterization of an enzyme that degrades neuromodulatory fatty-acid amides. *Nature* **384**, 83-87 (1996).

127. Kurahashi, Y., Ueda, N., Suzuki, H., Suzuki, M. & Yamamoto, S. Reversible hydrolysis and synthesis of anandamide demonstrated by recombinant rat fatty-acid amide hydrolase. *Biochemical and biophysical research communications* **237**, 512-515 (1997).

128. Thomas, E.A., Cravatt, B.F., Danielson, P.E., Gilula, N.B. & Sutcliffe, J.G. Fatty acid amide hydrolase, the degradative enzyme for anandamide and oleamide, has selective distribution in neurons within the rat central nervous system. *J Neurosci Res* **50**, 1047-1052 (1997).

129. Marrs, W.R., *et al.* The serine hydrolase ABHD6 controls the accumulation and efficacy of 2-AG at cannabinoid receptors. *Nat Neurosci* **13**, 951-957 (2010).

130. Savinainen, J.R., Saario, S.M. & Laitinen, J.T. The serine hydrolases MAGL, ABHD6 and ABHD12 as guardians of 2-arachidonoylglycerol signalling through cannabinoid receptors. *Acta physiologica* **204**, 267-276 (2012).

131. Xie, S., *et al.* Inactivation of lipid glyceryl ester metabolism in human THP1 monocytes/macrophages by activated organophosphorus insecticides: role of carboxylesterases 1 and 2. *Chemical research in toxicology* **23**, 1890-1904 (2010).

132. Wang, R., *et al.* Identification of Palmitoyl Protein Thioesterase 1 in Human THP1 Monocytes and Macrophages and Characterization of Unique Biochemical Activities for This Enzyme. *Biochemistry* **52**, 7559-7574 (2013).

133. Gulyas, A.I., *et al.* Segregation of two endocannabinoid-hydrolyzing enzymes into pre- and postsynaptic compartments in the rat hippocampus, cerebellum and amygdala. *Eur J Neurosci* **20**, 441-458 (2004).

134. Egertova, M., Giang, D.K., Cravatt, B.F. & Elphick, M.R. A new perspective on cannabinoid signalling: complementary localization of fatty acid amide hydrolase and the CB1 receptor in rat brain. *P Roy Soc B-Biol Sci* **265**, 2081-2085 (1998).

135. Patricelli, M.P. & Cravatt, B.F. Fatty acid amide hydrolase competitively degrades bioactive amides and esters through a nonconventional catalytic mechanism. *Biochemistry* **38**, 14125-14130 (1999).

136. Cravatt, B.F., *et al.* Supersensitivity to anandamide and enhanced endogenous cannabinoid signaling in mice lacking fatty acid amide hydrolase. *Proceedings of the National Academy of Sciences of the United States of America* **98**, 9371-9376 (2001).

137. Kathuria, S., *et al.* Modulation of anxiety through blockade of anandamide hydrolysis. *Nature medicine* **9**, 76-81 (2003).

138. Alexander, J.P. & Cravatt, B.F. Mechanism of carbamate inactivation of FAAH: Implications for the design of covalent inhibitors and in vivo functional probes for enzymes. *Chem Biol* **12**, 1179-1187 (2005).

139. Ahn, K., McKinney, M.K. & Cravatt, B.F. Enzymatic pathways that regulate endocannabinoid signaling in the nervous system. *Chem Rev* **108**, 1687-1707 (2008).

140. Jayamanne, A., *et al.* Actions of the FAAH inhibitor URB597 in neuropathic and inflammatory chronic pain models. *British journal of pharmacology* **147**, 281-288 (2006).

141. Cross-Mellor, S.K., Ossenkopp, K.P., Piomelli, D. & Parker, L.A. Effects of the FAAH inhibitor, URB597, and anandamide on lithium-induced taste reactivity responses: a measure of nausea in the rat. *Psychopharmacology* **190**, 135-143 (2007).

142. Lichtman, A.H., *et al.* Reversible inhibitors of fatty acid amide hydrolase that promote analgesia: Evidence for an unprecedented combination of potency and selectivity. *J Pharmacol Exp Ther* **311**, 441-448 (2004).

143. Zhang, D., *et al.* Fatty acid amide hydrolase inhibitors display broad selectivity and inhibit multiple carboxylesterases as off-targets. *Neuropharmacology* **52**, 1095-1105 (2007).

144. Clapper, J.R., *et al.* A Second Generation of Carbamate-Based Fatty Acid Amide Hydrolase Inhibitors with Improved Activity in vivo. *Chemmedchem* **4**, 1505-1513 (2009).

145. Ahn, K., *et al.* Novel mechanistic class of fatty acid amide hydrolase inhibitors with remarkable selectivity. *Biochemistry* **46**, 13019-13030 (2007).

146. Ahn, K., *et al.* Discovery and Characterization of a Highly Selective FAAH Inhibitor that Reduces Inflammatory Pain. *Chem Biol* **16**, 411-420 (2009).

147. Meyers, M.J., *et al.* Discovery of novel spirocyclic inhibitors of fatty acid amide hydrolase (FAAH). Part 2. Discovery of 7-azaspiro[3.5]nonane urea PF-04862853, an orally efficacious inhibitor of fatty acid amide hydrolase (FAAH) for pain. *Bioorg Med Chem Lett* **21**, 6545-6553 (2011).

148. Ahn, K., *et al.* Mechanistic and Pharmacological Characterization of PF-04457845: A Highly Potent and Selective Fatty Acid Amide Hydrolase Inhibitor That Reduces Inflammatory and Noninflammatory Pain. *J Pharmacol Exp Ther* **338**, 114-124 (2011).

149. Johnson, D.S*., et al.* Discovery of PF-04457845: A Highly Potent, Orally Bioavailable, and Selective Urea FAAH Inhibitor. *Acs Med Chem Lett* **2**, 91-96 (2011).
150. Li, G.L*., et al.* Assessment of the pharmacology and tolerability of PF-04457845, an irreversible inhibitor of fatty acid amide hydrolase-1, in healthy subjects. *Brit J Clin Pharmaco* **73**, 706-716 (2012).
151. Huggins, J.P., Smart, T.S., Langman, S., Taylor, L. & Young, T. An efficient randomised, placebo-controlled clinical trial with the irreversible fatty acid amide hydrolase-1 inhibitor PF-04457845, which modulates endocannabinoids but fails to induce effective analgesia in patients with pain due to osteoarthritis of the knee. *Pain* **153**, 1837-1846 (2012).
152. Blankman, J.L., Simon, G.M. & Cravatt, B.F. A comprehensive profile of brain enzymes that hydrolyze the endocannabinoid 2-arachidonoylglycerol. *Chem Biol* **14**, 1347-1356 (2007).
153. Karlsson, M., Contreras, J.A., Hellman, U., Tornqvist, H. & Holm, C. cDNA cloning, tissue distribution, and identification of the catalytic triad of monoglyceride lipase. Evolutionary relationship to esterases, lysophospholipases, and haloperoxidases. *The Journal of biological chemistry* **272**, 27218-27223 (1997).
154. Dinh, T.P*., et al.* Brain monoglyceride lipase participating in endocannabinoid inactivation. *Proceedings of the National Academy of Sciences of the United States of America* **99**, 10819-10824 (2002).
155. Dinh, T.P., Freund, T.F. & Piomelli, D. A role for monoglyceride lipase in 2-arachidonoylglycerol inactivation. *Chem Phys Lipids* **121**, 149-158 (2002).
156. Tornqvist, H. & Belfrage, P. Purification and some properties of a monoacylglycerol-hydrolyzing enzyme of rat adipose tissue. *The Journal of biological chemistry* **251**, 813-819 (1976).
157. Long, J.Z*., et al.* Selective blockade of 2-arachidonoylglycerol hydrolysis produces cannabinoid behavioral effects. *Nat Chem Biol* **5**, 37-44 (2009).
158. Long, J.Z., Nomura, D.K. & Cravatt, B.F. Characterization of monoacylglycerol lipase inhibition reveals differences in central and peripheral endocannabinoid metabolism. *Chem Biol* **16**, 744-753 (2009).
159. Kinsey, S.G*., et al.* Blockade of endocannabinoid-degrading enzymes attenuates neuropathic pain. *J Pharmacol Exp Ther* **330**, 902-910 (2009).
160. Pan, B*., et al.* Blockade of 2-arachidonoylglycerol hydrolysis by selective monoacylglycerol lipase inhibitor 4-nitrophenyl 4-(dibenzo[d][1,3]dioxol-5-yl(hydroxy)methyl)piperidine-1-carboxylate (JZL184) Enhances retrograde endocannabinoid signaling. *J Pharmacol Exp Ther* **331**, 591-597 (2009).
161. Sciolino, N.R., Zhou, W. & Hohmann, A.G. Enhancement of endocannabinoid signaling with JZL184, an inhibitor of the 2-arachidonoylglycerol hydrolyzing enzyme monoacylglycerol lipase, produces anxiolytic effects under conditions of high environmental aversiveness in rats. *Pharmacological research : the official journal of the Italian Pharmacological Society* **64**, 226-234 (2011).
162. Crow, J.A., Bittles, V., Borazjani, A., Potter, P.M. & Ross, M.K. Covalent inhibition of recombinant human carboxylesterase 1 and 2 and monoacylglycerol lipase by the carbamates JZL184 and URB597. *Biochem Pharmacol* **84**, 1215-1222 (2012).
163. Chang, J.W*., et al.* Highly selective inhibitors of monoacylglycerol lipase bearing a reactive group that is bioisosteric with endocannabinoid substrates. *Chem Biol* **19**, 579-588 (2012).
164. Muccioli, G.G*., et al.* Identification of a novel endocannabinoid-hydrolyzing enzyme expressed by microglial cells. *J Neurosci* **27**, 2883-2889 (2007).
165. Su, A.I*., et al.* Large-scale analysis of the human and mouse transcriptomes. *Proceedings of the National Academy of Sciences of the United States of America* **99**, 4465-4470 (2002).
166. Bachovchin, D.A*., et al.* Superfamily-wide portrait of serine hydrolase inhibition achieved by library-versus-library screening. *Proceedings of the National Academy of Sciences of the United States of America* **107**, 20941-20946 (2010).
167. Tchantchou, F. & Zhang, Y. Selective inhibition of alpha/beta-hydrolase domain 6 attenuates neurodegeneration, alleviates blood brain barrier breakdown, and improves functional recovery in a mouse model of traumatic brain injury. *Journal of neurotrauma* **30**, 565-579 (2013).
168. Hsu, K.L*., et al.* Discovery and optimization of piperidyl-1,2,3-triazole ureas as potent, selective, and in vivo-active inhibitors of alpha/beta-hydrolase domain containing 6 (ABHD6). *Journal of medicinal chemistry* **56**, 8270-8279 (2013).

169. Schlosburg, J.E., Kinsey, S.G. & Lichtman, A.H. Targeting fatty acid amide hydrolase (FAAH) to treat pain and inflammation. *The AAPS journal* **11**, 39-44 (2009).
170. Kinsey, S.G., Long, J.Z., Cravatt, B.F. & Lichtman, A.H. Fatty acid amide hydrolase and monoacylglycerol lipase inhibitors produce anti-allodynic effects in mice through distinct cannabinoid receptor mechanisms. *The journal of pain : official journal of the American Pain Society* **11**, 1420-1428 (2010).
171. Hohmann, A.G.*, et al.* An endocannabinoid mechanism for stress-induced analgesia. *Nature* **435**, 1108-1112 (2005).
172. Guindon, J., Guijarro, A., Piomelli, D. & Hohmann, A.G. Peripheral antinociceptive effects of inhibitors of monoacylglycerol lipase in a rat model of inflammatory pain. *British journal of pharmacology* **163**, 1464-1478 (2011).
173. Guindon, J., Lai, Y., Takacs, S.M., Bradshaw, H.B. & Hohmann, A.G. Alterations in endocannabinoid tone following chemotherapy-induced peripheral neuropathy: effects of endocannabinoid deactivation inhibitors targeting fatty-acid amide hydrolase and monoacylglycerol lipase in comparison to reference analgesics following cisplatin treatment. *Pharmacological research : the official journal of the Italian Pharmacological Society* **67**, 94-109 (2013).
174. Khasabova, I.A., Chandiramani, A., Harding-Rose, C., Simone, D.A. & Seybold, V.S. Increasing 2-arachidonoyl glycerol signaling in the periphery attenuates mechanical hyperalgesia in a model of bone cancer pain. *Pharmacological research : the official journal of the Italian Pharmacological Society* **64**, 60-67 (2011).
175. Ghosh, S.*, et al.* The monoacylglycerol lipase inhibitor JZL184 suppresses inflammatory pain in the mouse carrageenan model. *Life sciences* **92**, 498-505 (2013).
176. Gaetani, S.*, et al.* The endocannabinoid system as a target for novel anxiolytic and antidepressant drugs. *International review of neurobiology* **85**, 57-72 (2009).
177. Moreira, F.A., Kaiser, N., Monory, K. & Lutz, B. Reduced anxiety-like behaviour induced by genetic and pharmacological inhibition of the endocannabinoid-degrading enzyme fatty acid amide hydrolase (FAAH) is mediated by CB1 receptors. *Neuropharmacology* **54**, 141-150 (2008).
178. Busquets-Garcia, A.*, et al.* Differential role of anandamide and 2-arachidonoylglycerol in memory and anxiety-like responses. *Biological psychiatry* **70**, 479-486 (2011).
179. Gomes, F.V., Casarotto, P.C., Resstel, L.B. & Guimaraes, F.S. Facilitation of CB1 receptor-mediated neurotransmission decreases marble burying behavior in mice. *Progress in neuro-psychopharmacology & biological psychiatry* **35**, 434-438 (2011).
180. Kinsey, S.G., O'Neal, S.T., Long, J.Z., Cravatt, B.F. & Lichtman, A.H. Inhibition of endocannabinoid catabolic enzymes elicits anxiolytic-like effects in the marble burying assay. *Pharmacology, biochemistry, and behavior* **98**, 21-27 (2011).
181. Yu, M., Ives, D. & Ramesha, C.S. Synthesis of prostaglandin E-2 ethanolamide from anandamide by cyclooxygenase-2. *Journal of Biological Chemistry* **272**, 21181-21186 (1997).
182. Kozak, K.R., Rowlinson, S.W. & Marnett, L.J. Oxygenation of the endocannabinoid, 2-arachidonylglycerol, to glyceryl prostaglandins by cyclooxygenase-2. *Journal of Biological Chemistry* **275**, 33744-33749 (2000).
183. So, O.Y., Scarafia, L.E., Mak, A.Y., Callan, O.H. & Swinney, D.C. The dynamics of prostaglandin H synthases. Studies with prostaglandin h synthase 2 Y355F unmask mechanisms of time-dependent inhibition and allosteric activation. *The Journal of biological chemistry* **273**, 5801-5807 (1998).
184. Kozak, K.R., Prusakiewicz, J.J., Rowlinson, S.W., Prudhomme, D.R. & Marnett, L.J. Amino acid determinants in cyclooxygenase-2 oxygenation of the endocannabinoid anandamide. *Biochemistry* **42**, 9041-9049 (2003).
185. Kozak, K.R., Prusakiewicz, J.J., Rowlinson, S.W., Schneider, C. & Marnett, L.J. Amino acid determinants in cyclooxygenase-2 oxygenation of the endocannabinoid 2-arachidonylglycerol. *The Journal of biological chemistry* **276**, 30072-30077 (2001).
186. Vecchio, A.J. & Malkowski, M.G. The structural basis of endocannabinoid oxygenation by cyclooxygenase-2. *The Journal of biological chemistry* **286**, 20736-20745 (2011).

187. Kozak, K.R., *et al.* Metabolism of the endocannabinoids, 2-arachidonylglycerol and anandamide, into prostaglandin, thromboxane, and prostacyclin glycerol esters and ethanolamides. *The Journal of biological chemistry* **277**, 44877-44885 (2002).

188. Weber, A., *et al.* Formation of prostamides from anandamide in FAAH knockout mice analyzed by HPLC with tandem mass spectrometry. *J Lipid Res* **45**, 757-763 (2004).

189. Duggan, K.C., *et al.* (R)-Profens are substrate-selective inhibitors of endocannabinoid oxygenation by COX-2. *Nat Chem Biol* **7**, 803-809 (2011).

190. Ritter, J.K., *et al.* Production and actions of the anandamide metabolite prostamide E2 in the renal medulla. *J Pharmacol Exp Ther* **342**, 770-779 (2012).

191. Gatta, L., *et al.* Discovery of prostamide F2alpha and its role in inflammatory pain and dorsal horn nociceptive neuron hyperexcitability. *PloS one* **7**, e31111 (2012).

192. Silvestri, C., *et al.* Anandamide-derived prostamide F2alpha negatively regulates adipogenesis. *The Journal of biological chemistry* **288**, 23307-23321 (2013).

193. Hu, S.S., Bradshaw, H.B., Chen, J.S., Tan, B. & Walker, J.M. Prostaglandin E2 glycerol ester, an endogenous COX-2 metabolite of 2-arachidonoylglycerol, induces hyperalgesia and modulates NFkappaB activity. *British journal of pharmacology* **153**, 1538-1549 (2008).

194. Kingsley, P.J., Rouzer, C.A., Saleh, S. & Marnett, L.J. Simultaneous analysis of prostaglandin glyceryl esters and prostaglandins by electrospray tandem mass spectrometry. *Analytical biochemistry* **343**, 203-211 (2005).

195. Rouzer, C.A., *et al.* Zymosan-induced glycerylprostaglandin and prostaglandin synthesis in resident peritoneal macrophages: roles of cyclo-oxygenase-1 and -2. *Biochem J* **399**, 91-99 (2006).

196. Rouzer, C.A. & Marnett, L.J. Glycerylprostaglandin synthesis by resident peritoneal macrophages in response to a zymosan stimulus. *The Journal of biological chemistry* **280**, 26690-26700 (2005).

197. Alhouayek, M., Masquelier, J., Cani, P.D., Lambert, D.M. & Muccioli, G.G. Implication of the anti-inflammatory bioactive lipid prostaglandin D2-glycerol ester in the control of macrophage activation and inflammation by ABHD6. *Proceedings of the National Academy of Sciences of the United States of America* **110**, 17558-17563 (2013).

198. Kozak, K.R., *et al.* Metabolism of prostaglandin glycerol esters and prostaglandin ethanolamides in vitro and in vivo. *The Journal of biological chemistry* **276**, 36993-36998 (2001).

199. Correa, F., *et al.* Anandamide inhibits IL-12p40 production by acting on the promoter repressor element GA-12: possible involvement of the COX-2 metabolite prostamide E(2). *Biochem J* **409**, 761-770 (2008).

200. Woodward, D.F., *et al.* Bimatoprost: a novel antiglaucoma agent. *Cardiovascular drug reviews* **22**, 103-120 (2004).

201. Krauss, A.H. & Woodward, D.F. Update on the mechanism of action of bimatoprost: a review and discussion of new evidence. *Surv Ophthalmol* **49 Suppl 1**, S5-11 (2004).

202. Liang, Y., *et al.* Identification and pharmacological characterization of the prostaglandin FP receptor and FP receptor variant complexes. *British journal of pharmacology* **154**, 1079-1093 (2008).

203. Nirodi, C.S., Crews, B.C., Kozak, K.R., Morrow, J.D. & Marnett, L.J. The glyceryl ester of prostaglandin E2 mobilizes calcium and activates signal transduction in RAW264.7 cells. *Proceedings of the National Academy of Sciences of the United States of America* **101**, 1840-1845 (2004).

204. Sang, N., Zhang, J. & Chen, C. PGE2 glycerol ester, a COX-2 oxidative metabolite of 2-arachidonoyl glycerol, modulates inhibitory synaptic transmission in mouse hippocampal neurons. *J Physiol* **572**, 735-745 (2006).

205. Sang, N., Zhang, J. & Chen, C. COX-2 oxidative metabolite of endocannabinoid 2-AG enhances excitatory glutamatergic synaptic transmission and induces neurotoxicity. *J Neurochem* **102**, 1966-1977 (2007).

206. Ghosh, M., *et al.* COX-2 suppresses tissue factor expression via endocannabinoid-directed PPARdelta activation. *J Exp Med* **204**, 2053-2061 (2007).

207. Jack, D.B. One hundred years of aspirin. *Lancet* **350**, 437-439 (1997).

208. Vane, J.R. Inhibition of prostaglandin synthesis as a mechanism of action for aspirin-like drugs. *Nat New Biol* **231**, 232-235 (1971).

209. Smith, J.B. & Willis, A.L. Aspirin selectively inhibits prostaglandin production in human platelets. *Nat New Biol* **231**, 235-237 (1971).

210. Rome, L.H. & Lands, W.E. Structural requirements for time-dependent inhibition of prostaglandin biosynthesis by anti-inflammatory drugs. *Proceedings of the National Academy of Sciences of the United States of America* **72**, 4863-4865 (1975).

211. Van Der Ouderaa, F.J., Buytenhek, M., Nugteren, D.H. & Van Dorp, D.A. Acetylation of prostaglandin endoperoxide synthetase with acetylsalicylic acid. *European journal of biochemistry / FEBS* **109**, 1-8 (1980).

212. Roth, G.J., Machuga, E.T. & Ozols, J. Isolation and covalent structure of the aspirin-modified, active-site region of prostaglandin synthetase. *Biochemistry* **22**, 4672-4675 (1983).

213. Rome, L.H., Lands, W.E., Roth, G.J. & Majerus, P.W. Aspirin as a quantitative acetylating reagent for the fatty acid oxygenase that forms prostaglandins. *Prostaglandins* **11**, 23-30 (1976).

214. Loll, P.J., Picot, D. & Garavito, R.M. The structural basis of aspirin activity inferred from the crystal structure of inactivated prostaglandin H2 synthase. *Nature structural biology* **2**, 637-643 (1995).

215. FitzGerald, G.A.*, et al.* Endogenous biosynthesis of prostacyclin and thromboxane and platelet function during chronic administration of aspirin in man. *The Journal of clinical investigation* **71**, 676-688 (1983).

216. Selinsky, B.S., Gupta, K., Sharkey, C.T. & Loll, P.J. Structural analysis of NSAID binding by prostaglandin H2 synthase: time-dependent and time-independent inhibitors elicit identical enzyme conformations. *Biochemistry* **40**, 5172-5180 (2001).

217. Bhattacharyya, D.K., Lecomte, M., Rieke, C.J., Garavito, M. & Smith, W.L. Involvement of arginine 120, glutamate 524, and tyrosine 355 in the binding of arachidonate and 2-phenylpropionic acid inhibitors to the cyclooxygenase active site of ovine prostaglandin endoperoxide H synthase-1. *The Journal of biological chemistry* **271**, 2179-2184 (1996).

218. Rieke, C.J., Mulichak, A.M., Garavito, R.M. & Smith, W.L. The role of arginine 120 of human prostaglandin endoperoxide H synthase-2 in the interaction with fatty acid substrates and inhibitors. *The Journal of biological chemistry* **274**, 17109-17114 (1999).

219. Kulmacz, R.J. & Lands, W.E. Stoichiometry and kinetics of the interaction of prostaglandin H synthase with anti-inflammatory agents. *The Journal of biological chemistry* **260**, 12572-12578 (1985).

220. Mancini, J.A., Riendeau, D., Falgueyret, J.P., Vickers, P.J. & O'Neill, G.P. Arginine 120 of prostaglandin G/H synthase-1 is required for the inhibition by nonsteroidal anti-inflammatory drugs containing a carboxylic acid moiety. *The Journal of biological chemistry* **270**, 29372-29377 (1995).

221. Kalgutkar, A.S.*, et al.* Biochemically based design of cyclooxygenase-2 (COX-2) inhibitors: facile conversion of nonsteroidal antiinflammatory drugs to potent and highly selective COX-2 inhibitors. *Proceedings of the National Academy of Sciences of the United States of America* **97**, 925-930 (2000).

222. Kalgutkar, A.S., Marnett, A.B., Crews, B.C., Remmel, R.P. & Marnett, L.J. Ester and amide derivatives of the nonsteroidal antiinflammatory drug, indomethacin, as selective cyclooxygenase-2 inhibitors. *Journal of medicinal chemistry* **43**, 2860-2870 (2000).

223. Prusakiewicz, J.J., Felts, A.S., Mackenzie, B.S. & Marnett, L.J. Molecular basis of the time-dependent inhibition of cyclooxygenases by indomethacin. *Biochemistry* **43**, 15439-15445 (2004).

224. Felts, A.S.*, et al.* Desmethyl derivatives of indomethacin and sulindac as probes for cyclooxygenase-dependent biology. *Acs Chem Biol* **2**, 479-483 (2007).

225. Rowlinson, S.W.*, et al.* A novel mechanism of cyclooxygenase-2 inhibition involving interactions with Ser-530 and Tyr-385. *The Journal of biological chemistry* **278**, 45763-45769 (2003).

226. Mancini, J.A.*, et al.* Altered sensitivity of aspirin-acetylated prostaglandin G/H synthase-2 to inhibition by nonsteroidal anti-inflammatory drugs. *Mol Pharmacol* **51**, 52-60 (1997).

227. Masferrer, J.L.*, et al.* Selective inhibition of inducible cyclooxygenase 2 in vivo is antiinflammatory and nonulcerogenic. *Proceedings of the National Academy of Sciences of the United States of America* **91**, 3228-3232 (1994).

228.	Bombardier, C.*, et al.* Comparison of upper gastrointestinal toxicity of rofecoxib and naproxen in patients with rheumatoid arthritis. VIGOR Study Group. *The New England journal of medicine* **343**, 1520-1528, 1522 p following 1528 (2000).

229.	Silverstein, F.E.*, et al.* Gastrointestinal toxicity with celecoxib vs nonsteroidal anti-inflammatory drugs for osteoarthritis and rheumatoid arthritis: the CLASS study: A randomized controlled trial. Celecoxib Long-term Arthritis Safety Study. *Jama* **284**, 1247-1255 (2000).

230.	Gans, K.R.*, et al.* Anti-inflammatory and safety profile of DuP 697, a novel orally effective prostaglandin synthesis inhibitor. *J Pharmacol Exp Ther* **254**, 180-187 (1990).

231.	Lee, S.H.*, et al.* Selective expression of mitogen-inducible cyclooxygenase in macrophages stimulated with lipopolysaccharide. *The Journal of biological chemistry* **267**, 25934-25938 (1992).

232.	Copeland, R.A.*, et al.* Mechanism of selective inhibition of the inducible isoform of prostaglandin G/H synthase. *Proceedings of the National Academy of Sciences of the United States of America* **91**, 11202-11206 (1994).

233.	Lanzo, C.A., Beechem, J.M., Talley, J. & Marnett, L.J. Investigation of the binding of isoform-selective inhibitors to prostaglandin endoperoxide synthases using fluorescence spectroscopy. *Biochemistry* **37**, 217-226 (1998).

234.	Lanzo, C.A., Sutin, J., Rowlinson, S., Talley, J. & Marnett, L.J. Fluorescence quenching analysis of the association and dissociation of a diarylheterocycle to cyclooxygenase-1 and cyclooxygenase-2: dynamic basis of cyclooxygenase-2 selectivity. *Biochemistry* **39**, 6228-6234 (2000).

235.	Walker, M.C.*, et al.* A three-step kinetic mechanism for selective inhibition of cyclo-oxygenase-2 by diarylheterocyclic inhibitors. *Biochem J* **357**, 709-718 (2001).

236.	Leblanc, Y.*, et al.* Synthesis and biological evaluation of 2,3-diarylthiophenenes as selective Cox-2 and Cox-1 inhibitors. *Biorganic & Medicinal Chemistry Letters* **5**, 2123-2128 (1995).

237.	Guo, Q., Wang, L.H., Ruan, K.H. & Kulmacz, R.J. Role of Val509 in time-dependent inhibition of human prostaglandin H synthase-2 cyclooxygenase activity by isoform-selective agents. *The Journal of biological chemistry* **271**, 19134-19139 (1996).

238.	Gierse, J.K.*, et al.* A single amino acid difference between cyclooxygenase-1 (COX-1) and -2 (COX-2) reverses the selectivity of COX-2 specific inhibitors. *The Journal of biological chemistry* **271**, 15810-15814 (1996).

239.	Wong, E., Bayly, C., Waterman, H.L., Riendeau, D. & Mancini, J.A. Conversion of prostaglandin G/H synthase-1 into an enzyme sensitive to PGHS-2-selective inhibitors by a double His513 --> Arg and Ile523 --> val mutation. *The Journal of biological chemistry* **272**, 9280-9286 (1997).

240.	Windsor, M.A., Valk, P.L., Xu, S., Banerjee, S. & Marnett, L.J. Exploring the molecular determinants of substrate-selective inhibition of cyclooxygenase-2 by lumiracoxib. *Bioorg Med Chem Lett* **23**, 5860-5864 (2013).

241.	Blobaum, A.L. & Marnett, L.J. Molecular determinants for the selective inhibition of cyclooxygenase-2 by lumiracoxib. *The Journal of biological chemistry* **282**, 16379-16390 (2007).

242.	Capone, M.L.*, et al.* Human pharmacology of naproxen sodium. *J Pharmacol Exp Ther* **322**, 453-460 (2007).

243.	Juni, P., Rutjes, A.W. & Dieppe, P.A. Are selective COX 2 inhibitors superior to traditional non steroidal anti-inflammatory drugs? *BMJ* **324**, 1287-1288 (2002).

244.	Warner, T.D.*, et al.* Nonsteroid drug selectivities for cyclo-oxygenase-1 rather than cyclo-oxygenase-2 are associated with human gastrointestinal toxicity: a full in vitro analysis. *Proceedings of the National Academy of Sciences of the United States of America* **96**, 7563-7568 (1999).

245.	Bresalier, R.S.*, et al.* Cardiovascular events associated with rofecoxib in a colorectal adenoma chemoprevention trial. *The New England journal of medicine* **352**, 1092-1102 (2005).

246.	Solomon, S.D.*, et al.* Cardiovascular risk associated with celecoxib in a clinical trial for colorectal adenoma prevention. *The New England journal of medicine* **352**, 1071-1080 (2005).

247.	McAdam, B.F.*, et al.* Systemic biosynthesis of prostacyclin by cyclooxygenase (COX)-2: the human pharmacology of a selective inhibitor of COX-2. *Proceedings of the National Academy of Sciences of the United States of America* **96**, 272-277 (1999).

248. Graham, D.J*., et al.* Risk of acute myocardial infarction and sudden cardiac death in patients treated with cyclo-oxygenase 2 selective and non-selective non-steroidal anti-inflammatory drugs: nested case-control study. *Lancet* **365**, 475-481 (2005).

249. Kearney, P.M*., et al.* Do selective cyclo-oxygenase-2 inhibitors and traditional non-steroidal anti-inflammatory drugs increase the risk of atherothrombosis? Meta-analysis of randomised trials. *BMJ* **332**, 1302-1308 (2006).

250. McGettigan, P. & Henry, D. Cardiovascular risk and inhibition of cyclooxygenase: a systematic review of the observational studies of selective and nonselective inhibitors of cyclooxygenase 2. *JAMA* **296**, 1633-1644 (2006).

251. Grosser, T., Fries, S. & FitzGerald, G.A. Biological basis for the cardiovascular consequences of COX-2 inhibition: therapeutic challenges and opportunities. *The Journal of clinical investigation* **116**, 4-15 (2006).

252. Yuan, C., Rieke, C.J., Rimon, G., Wingerd, B.A. & Smith, W.L. Partnering between monomers of cyclooxygenase-2 homodimers. *Proceedings of the National Academy of Sciences of the United States of America* **103**, 6142-6147 (2006).

253. Rowlinson, S.W., Crews, B.C., Lanzo, C.A. & Marnett, L.J. The binding of arachidonic acid in the cyclooxygenase active site of mouse prostaglandin endoperoxide synthase-2 (COX-2). A putative L-shaped binding conformation utilizing the top channel region. *The Journal of biological chemistry* **274**, 23305-23310 (1999).

254. Kulmacz, R.J. & Lands, W.E. Prostaglandin H synthase. Stoichiometry of heme cofactor. *The Journal of biological chemistry* **259**, 6358-6363 (1984).

255. Dong, L*., et al.* Human Cyclooxygenase-2 Is a Sequence Homodimer That Functions as a Conformational Heterodimer. *Journal of Biological Chemistry* **286**, 19035-19046 (2011).

256. Kulmacz, R.J. & Lands, W.E.M. Prostaglandin-H Synthase - Stoichiometry of Heme Cofactor. *Journal of Biological Chemistry* **259**, 6358-6363 (1984).

257. Yuan, C*., et al.* Cyclooxygenase Allosterism, Fatty Acid-mediated Cross-talk between Monomers of Cyclooxygenase Homodimers. *The Journal of biological chemistry* **284**, 10046-10055 (2009).

258. Rimon, G*., et al.* Coxibs interfere with the action of aspirin by binding tightly to one monomer of cyclooxygenase-1. *Proceedings of the National Academy of Sciences of the United States of America* **107**, 28-33 (2010).

259. Sidhu, R.S., Lee, J.Y., Yuan, C. & Smith, W.L. Comparison of cyclooxygenase-1 crystal structures: cross-talk between monomers comprising cyclooxygenase-1 homodimers. *Biochemistry* **49**, 7069-7079 (2010).

260. Kozak, K.R., Rowlinson, S.W. & Marnett, L.J. Oxygenation of the endocannabinoid, 2-arachidonylglycerol, to glyceryl prostaglandins by cyclooxygenase-2. *The Journal of biological chemistry* **275**, 33744-33749 (2000).

261. Prusakiewicz, J.J., Duggan, K.C., Rouzer, C.A. & Marnett, L.J. Differential sensitivity and mechanism of inhibition of COX-2 oxygenation of arachidonic acid and 2-arachidonoylglycerol by ibuprofen and mefenamic acid. *Biochemistry* **48**, 7353-7355 (2009).

CHAPTER II

THE BASIS OF SUBSTRATE-SELECTIVE CYCLOOXYGENASE-2 INHIBITION

Introduction

Cyclooxygenase-2 (COX-2) catalyzes the committed step in the production of prostaglandins (PGs). In addition to oxygenating arachidonic acid (AA), it can also oxygenate 2-arachidonoylglycerol (2-AG) and arachidonoylethanolamide (AEA) to form prostaglandin glycerols (PG-Gs) and prostaglandin ethanolamides (PG-EAs), respectively.[1,2] While 2-AG and AA are oxygenated by human COX-2 at comparable k_{cat}/K_M's, AEA is oxygenated at approximately 30% of the rate of 2-AG and AA.

Investigations into the inhibition of COX-2 revealed that 2-AG oxygenation is inhibited at much lower concentrations of (*S*)-ibuprofen or mefenamic acid than AA oxygenation.[3] The finding that (*S*)-ibuprofen and mefenamic acid are non-competitive inhibitors of 2-AG oxygenation, but competitive inhibitors of AA oxygenation lead to a mechanistic hypothesis. Binding of one molecule of (*S*)-ibuprofen or mefenamic acid to the first monomer of COX-2 results in inhibition of 2-AG oxygenation in the second monomer, but does not block AA oxygenation. Inhibition of AA oxygenation requires a second molecule of (*S*)-ibuprofen or mefenamic acid to bind to the second monomer (Figure 1). These studies reveal that (*S*)-ibuprofen and mefenamic acid inhibit the oxygenation of AA and 2-AG by different mechanisms and with different potencies, a phenomenon that has been termed "substrate-selective" inhibition.
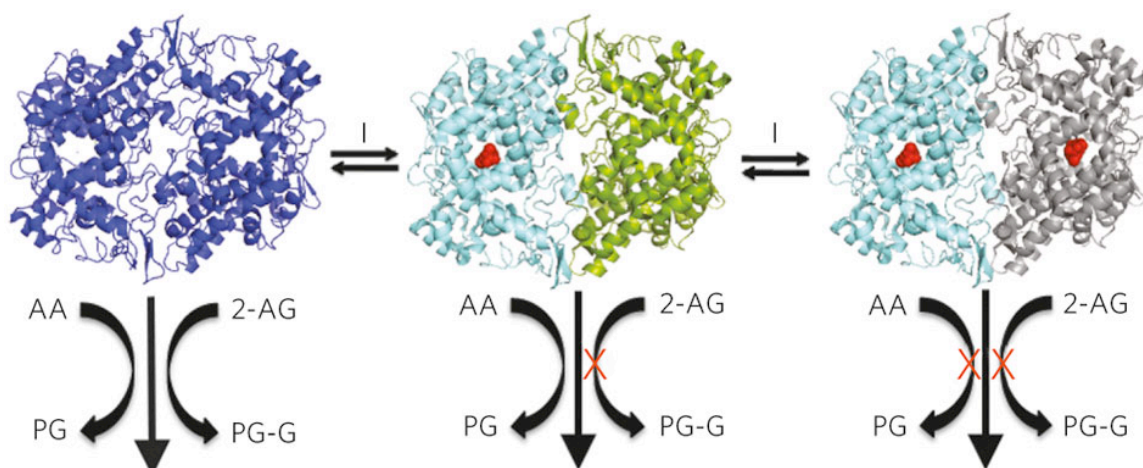
Figure 1: Model for differential inhibition of 2-AG and AA oxygenation by COX-2. The uninhibited COX-2 homodimer (blue) is able to oxygenate both AA and 2-AG. Binding of an inhibitor (red) to a single monomer (teal) precludes the productive binding of 2-AG in the partner monomer (green) but still allows for AA oxygenation. Metabolism of AA is inhibited only when an inhibitor occupies both active sites of COX-2.

A growing body of evidence that the COX-2 monomers are sequence homodimers but functional heterodimers suggests that binding of a substrate, an inhibitor, or an activator to one monomer causes a change in the second monomer.[4] In the case of substrate-selective inhibition, binding of a single molecule of (S)-ibuprofen or mefenamic acid to one monomer causes a change in the second monomer of COX-2 such that 2-AG cannot be oxygenated, but AA can still be utilized as a substrate. While multiple reports have identified some residues that mediate monomer cross talk, the basis of substrate-selective inhibition has not been studied. In addition, the scope of compounds that exhibit substrate-selective inhibition has not been established.

We sought to determine the generalizability of substrate-selective inhibition by studying the inhibition of COX-2 mediated oxygenation of 2-AG and AA by several different classes of non-steroidal anti-inflammatory drugs (NSAIDs). These studies identified that compounds that are weak, reversible inhibitors of AA oxygenation are potent, substrate-selective inhibitors of 2-AG oxygenation. In contrast, COX-2 inhibitors that are slow, tight-binding inhibitors potently inhibit 2-AG and AA oxygenation with comparable IC_{50} values for the two substrates. Additionally, we identified and characterized substrate-selective inhibition by (R)-arylpropionic acids. Further studies were undertaken to determine the structural basis and enzymatic mechanism of substrate-selective inhibition utilizing a combination of site-directed mutagenesis and X-ray crystallography. These studies identified rotation of Leu-351, which lies adjacent to the binding pocket of the glycerol moiety of 2-AG, as a critical mediator of substrate-selective inhibition.

<div align="center">Experimental Procedures</div>

Materials

Wild-type and mutant murine COX-2s were expressed and purified as previously described.[5] AA was purchased from Nu-Check Prep, Inc. (Elysian, MN). Diclofenac, (S)-ibuprofen, (S)-flurbiprofen, (S)-naproxen, indomethacin, mefenamic acid, (R)-naproxen, PGE_2, and glycerol-d_5 were purchased from Sigma-Aldrich (Milwaukee, WI). (R)-ibuprofen was purchased from Santa Cruz Biotechnology (Santa Cruz, CA). (R)-flurbiprofen, 2-AG, AEA, PGE_2-d_4, and 5-phenyl-4-pentenyl hydroperoxide (PPHP) were purchased from Cayman Chemical Company (Ann Arbor, MI). Lumiracoxib was purchased from LKT Laboratories, Inc. (St.

Paul, MN). 2′-*des*-methylindomethacin (DM-indomethacin), celecoxib, and rofecoxib were synthesized according to published methods.[6-8] All substrates and inhibitors were dissolved in dimethyl sulfoxide (DMSO) for use. Reagents used in the crystallization of murine COX-2 were purchased from Hampton Research (Aliso Viejo, CA).

Inhibition of AA and 2-AG oxygenation as measured by oxygen uptake

For AA experiments, 440 nM mCOX-2 was pre-incubated with inhibitor for 2 minutes at 37°C prior to the addition of 50 μM AA. For experiments in which 2-AG was used as the substrate, the concentration of mCOX-2 was increased to 890 nM to allow for a similar extent of oxygenation of 2-AG compared to AA. Initial reaction velocity was determined from the linear portion of the oxygen uptake curves as measured by an Instech 210 Fiber Optic oxygen monitor (Plymouth Meeting, PA) and normalized to the DMSO control. Each condition was performed in triplicate.

Inhibition of AA, 2-AG, and AEA oxygenation by murine COX-2 by mass spectrometry

A fixed concentration of murine COX-2 (50 nM for 5 μM substrate or 250 nM for 50 μM substrate) was suspended in a 100 mM Tris-HCl, pH = 8, 500 μM phenol buffer. 2 equivalents of heme were added, the solution was vigorously mixed, and then aliquoted out at 190 μl per tube. To each tube 5 μl of DMSO or inhibitor solution was added and the tube was vigorously mixed and capped for pre-incubation for five or fifteen minutes at 37 °C before the addition of substrate; pre-incubation times were determined based on previous reports of the time necessary to achieve maximal inhibition. After pre-incubation, 5 μM or 50 μM of AA or 2-AG was added in 5 μl of DMSO to the tube, vigorously mixed, and allowed to react for 30 seconds. After 30 seconds the reaction was quenched by adding 200 μl of ethyl acetate containing 0.1% glacial acetic acid, 300 pmol of PGE_2-d_4, and 300 pmol of PGE_2-G-d_5. Tubes were then frozen and the organic layer was separated and evaporated to dryness under nitrogen gas. The samples were then reconstituted in 200 μl of 1:1 MeOH:water and analyzed using liquid chromatography-tandem mass spectrometry (LC-MS/MS) analysis. For

kinetic inhibition assays, 100 nM of murine COX-2 was incubated with different concentrations of substrate

from 2.5 to 40 μM. LC-MS/MS analysis was performed using mobile phases consisting of 5 mM ammonium

acetate in water at pH 3.5 with glacial acetic acid (buffer A) and acetonitrile with 6% buffer A (Buffer B).

Samples were separated on an Ascentis® C18 column (5 cm x 2.1 mm, 3 μm pore size) using a gradient starting

at 20% buffer B for 1 minute, then to 95% buffer B over 4 minutes, then 1 minute at 95% buffer B, and re-

equilibration to 20% buffer B over 30 seconds for a total time of 6.5 minutes. The PGs and PG-Gs were

monitored using selected reaction monitoring (SRM) with the transitions m/z 370 → 317 (PGE$_2$/D$_2$), m/z 374 →

321 (PGE$_2$-d$_4$), m/z 444 → 391 (PGE$_2$-G/D$_2$-G), m/z 449→ 396 (PGE$_2$-G-d$_5$). Analytes were quantitated using

the ratio of the area of the analyte peak to its corresponding internal standard peak area. Percent activity was

calculated by normalizing samples to the average of the DMSO control samples.

Peroxidase activity assay

Assays were performed as described with slight modifications.[9] Hematin-reconstituted murine COX-2 (100 nM)

in 100 mM Tris-HCl buffer was incubated with inhibitor (100 μM – 5 μM) in the presence of 200 μM phenol at

37°C for 5 min. The reaction was initiated by the addition of PPHP (100 μM) and terminated after 5 min by the

addition of ice cold quench solution (ethyl acetate + 0.5% acetic acid) followed by vigorous mixing and

centrifugation at 4°C. The organic layer was removed, evaporated to dryness under nitrogen gas, and

reconstituted in 300 μL of a 1:1 solution of methanol and water. Samples were separated by reverse phase high-

performance liquid chromatography (HPLC) using a UV detector set at 254 nm. Samples were

chromatographed with a C8 reverse-phase column (150 x 2.00 mm Luna C$_8$ HPLC column, 3 μm particle size)

with a gradient beginning at 50% (v/v) methanol/water, increasing to 90% methanol over 9 minutes, and held at

90% methanol for 10 additional minutes at a flow rate of 0.20 mL/min. The area of the peak was used to

determine the concentrations of the analytes. Peroxidase activity was measured by the percent conversion of

PPHP to 5-phenyl-4-pentenyl alcohol (PPA) using the equation: [PPA]/([PPA]+[PPHP]).

Crystallography

COX-2 was expressed and purified as previously described.[10] Purified protein was prepared for crystallization and hanging-drop crystallization experiments were set up according to published methods.[11] All diffraction data were collected at 100 K at beamline 24ID-E located at the Advanced Photon Source using an ADSC Quantum 315 charge-coupled-device-based detector. Diffraction data were processed with HKL2000.[12] Initial phases were determined by molecular replacement using a search model (PDB 3NT1) with MOLREP.[13] A solution having two molecules in the asymmetric unit was obtained. The model was improved with iterative rounds of model building in Coot and refinement in PHENIX.[14,15] Molecular graphics were generated using PyMOL.[16]

<div align="center">Results</div>

Differential inhibition of COX-2

To determine the generalizability of substrate-selective inhibition we assayed a series of inhibitors from multiple structural classes against both AA and 2-AG. We first analyzed several arylcarboxylic acids and diarylheterocycles, which are classified as slow, tight-binding inhibitors of COX-2 (Table 1).[17] These compounds have low K_d values for binding and exhibit time-dependent inhibition of COX-1 and COX-2. For example, indomethacin, an indole acetic acid derivative, is a potent inhibitor of both COX-1 and COX-2, but requires up to 15 minutes of preincubation with the enzymes for full inhibition.[18] Indomethacin acted as a potent inhibitor of both substrates with IC_{50} values of 180 nM for AA and of 10 nM for 2-AG. As discussed previously, it has been shown that binding of a single molecule of indomethacin to the COX homodimer is sufficient to achieve full inhibition of AA oxygenation by the enzyme.[19] Additional studies found that the COX-2 selective inhibitors rofecoxib and celecoxib are also potent inhibitors of both AA and 2-AG oxygenation. These studies suggest that a single binding event of indomethacin or a diarylheterocycle to one monomer inhibits the oxygenation of both AA and 2-AG in the second monomer.

Previous studies have determined that the primary determinant of the slow, tight binding of indomethacin to COX-2 is the insertion of the 2'-methyl group of the indole ring into a hydrophobic pocket in the COX active site.[7] Removal of the 2'-methyl group to generate 2'-*des*methyl indomethacin (DM-indo) results in a rapid reversible inhibitor of AA oxygenation with a significantly increased IC_{50}.[20] To probe the importance

<div align="center">49</div>

of this methyl group for inhibition of 2-AG, DM-indo was assayed for inhibition of both AA and 2-AG. DM-indo did not display potent inhibition of AA oxygenation, with maximal inhibition of 30% at 25 μM inhibitor concentration. In sharp contrast, DM-indo was a potent inhibitor of 2-AG oxygenation by COX-2, with an IC_{50} of 110 nM. Thus, as with the rapid-reversible inhibitors (S)-ibuprofen and mefenamic acid, DM-indo exhibits little inhibition of AA oxygenation by COX-2, but acts as an extremely potent inhibitor of 2-AG oxygenation.[3]

As both (S)-ibuprofen and DM-indo bind to the constriction site of COX-2, we sought to determine if different binding poses could also display substrate-selectivity. Thus, we also compared the inhibition of AA and 2-AG by diclofenac and its analog lumiracoxib. Diclofenac is a slow-tight binding inhibitor that binds in an inverted pose relative to (S)-ibuprofen and DM-indo, with its carboxylate hydrogen bonded to Tyr-385 and Ser-530.[5] Lumiracoxib is a diclofenac analog that contains a single substitution of fluorine for chlorine on its lower ring and a meta-methyl group on its upper ring. Notably, lumiracoxib is the most selective COX-2-selective inhibitor in the *ex vivo* human whole blood assay.[21] Despite its clinical use as a selective COX-2 inhibitor, lumiracoxib is a poor inhibitor of AA oxygenation and acts as a rapid-reversible inhibitor.[22] Diclofenac inhibits AA with an IC_{50} of 60 nM and 2-AG with an IC_{50} of 50 nM. In sharp contrast, lumiracoxib exhibits little to no inhibition of AA, but inhibits 2-AG with an IC_{50} of 40 nM.

Thus, compounds classified as rapid, reversible inhibitors are potent inhibitors of 2-AG oxidation, but weak inhibitors of AA oxidation. In contrast, compounds that are classified as slow, tight-binding inhibitors exhibit potent inhibition of both 2-AG and AA oxidation by COX-2, with similar IC_{50} values for both substrates. Multiple inhibitor classes and binding modes exhibit these distinct kinetic inhibition modes and within the inhibitor classes no differences are apparent, including between COX-2-selective inhibitors or non-selective inhibitors of COX-1 and COX-2.

Table 1: IC$_{50}$ values for various COX inhibitors against AA and 2-AG oxygenation by COX-2. Enzyme and inhibitor were pre-incubated for 15 minutes prior to the addition of 50 μM substrate for 30 seconds. Reactions were quenched with organic solvent containing deuterated internal standards. Product formation was analyzed by LC-MS/MS using SRM and normalized to DMSO control. *AA oxygenation was measured using an oxygen electrode. Values for ibuprofen and mefenamic acid reproduced from.[3]

	Inhibitor	50 μM AA IC$_{50}$	50 μM 2-AG IC$_{50}$
Rapid, reversible inhibitors	(*S*)-Ibuprofen*	7 μM	20 nM
	Mefenamic acid*	180 μM	210 nM
	DM-Indo	> 25 μM	110 nM
	Lumiracoxib	No inhibition	40 nM
Slow, tight inhibitors	Diclofenac	60 nM	50 nM
	(*S*)-Flurbiprofen	130 nM	30 nM
	Indomethacin	180 nM	10 nM
	Celecoxib	80 nM	95 nM
	Rofecoxib	520 nM	85 nM

Substrate-selective inhibition by (R)-profens

The arylpropionic acid class of NSAIDs, also known as the profens, contains a methyl group α to their carboxylic acid moieties. The stereochemistry of this methyl group has an enormous impact of the ability of arylpropionic acid inhibitors to inhibit the oxygenation of AA by COX enzymes, with the (*S*)-enantiomers being inhibitors and the (*R*)-enantiomers displaying no inhibition (Figure 2).[23] As discussed above, the rapid, reversible inhibitor (*S*)-ibuprofen acts as a substrate-selective inhibitor with potent inhibition of 2-AG, but weak inhibition of AA oxygenation by COX-2. In contrast, (*S*)-flurbiprofen is a slow, tight binding inhibitor and inhibits AA and 2-AG with similar IC$_{50}$ values.
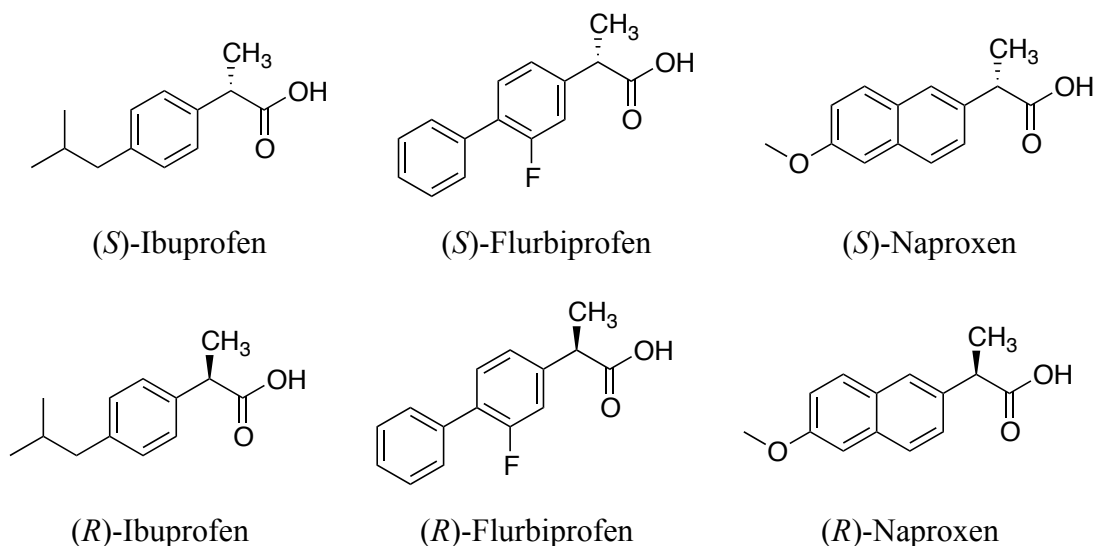
Figure 2: Chemical structures of (*S*)- and (*R*)-arylpropionic acid NSAIDs.

A third widely used member of the arylpropionic acid class of inhibitors is (*S*)-naproxen, which is a non-selective COX-1 and COX-2 inhibitor and is the only arylpropionic acid marketed exclusively as the (*S*)-enantiomer. (*S*)-naproxen exhibits a "mixed" inhibition mode, as it does not associate with COX in a single-step mechanism as a rapid-reversible inhibitor does, but also does not form an irreversible enzyme-inhibitor complex as a slow, tight binder does.[24] With substrate concentrations of 5 μM, (*S*)-naproxen inhibits AA oxygenation with an IC_{50} of 340 nM and 2-AG oxygenation with an IC_{50} of 30 nM. Thus, it acts as a slightly substrate-selective inhibitor under these conditions.

Given our findings with other weak inhibitors of AA oxygenation by COX-2, we hypothesized that the (*R*)-enantiomers of flurbiprofen, ibuprofen, and naproxen may inhibit 2-AG oxygenation despite the fact that they had previously been shown to not inhibit AA oxygenation. As previously demonstrated, (*R*)-flurbiprofen, (*R*)-ibuprofen, and (*R*)-naproxen did not inhibit AA oxygenation by COX-2 (Figure 3). However, all three inhibitors blocked the oxygenation of 2-AG by COX-2 with IC_{50} values of 80 nM for (*R*)-flurbiprofen, 10 μM for (*R*)-ibuprofen, and 3 μM for (*R*)-naproxen when 5 μM substrate was used. The ability of the (*R*)-profens to inhibit 2-AG is quite striking as previous reports suggested that (*R*)-profens do not bind in the COX active site due to steric clashes with the constriction site.[25]
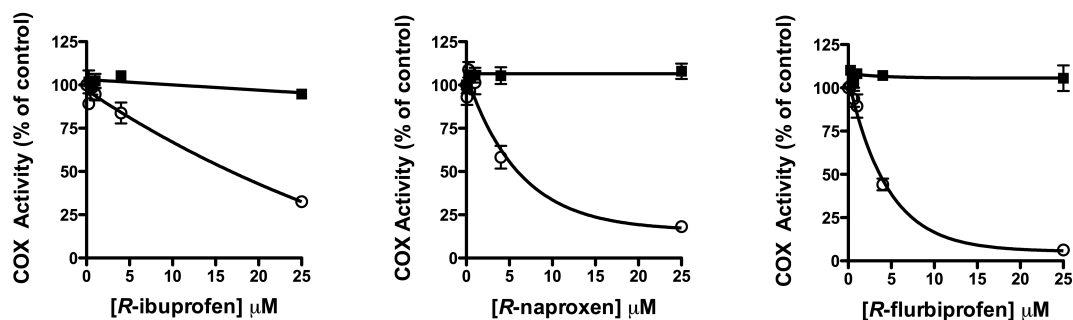
Figure 3: Inhibition of COX-2-mediated AA and 2-AG oxygenation by (*R*)-profens. COX-2 was pre-incubated with 62.5 nM–25 µM (*R*)-ibuprofen, (*R*)-naproxen, or (*R*)-flurbiprofen for 15 minutes followed by the addition of 50 µM AA (■) or 2-AG (○) for 30 seconds. PG and PG-G production were measured by LC-MS/MS as described under Experimental Procedures.

Previous reports have demonstrated that COX-2-mediated oxygenation of 2-AG is much more sensitive to peroxide tone than the oxygenation of AA.[26] To determine if the (*R*)-profens inhibit 2-AG oxygenation by either binding to the peroxidase active site or interfering with the peroxide tone of the enzyme mixture, Kelsey Duggan analyzed the ability of (*R*)-flurbiprofen and (*R*)-naproxen to inhibit the peroxidase (POX) activity of COX-2. POX activity was determined by HPLC monitoring of the conversion of PPHP to its corresponding alcohol, PPA. No significant inhibition of POX activity was evident with concentrations of either (*R*)-flurbiprofen or (*R*)-naproxen up to 500 µM (Figure 4).
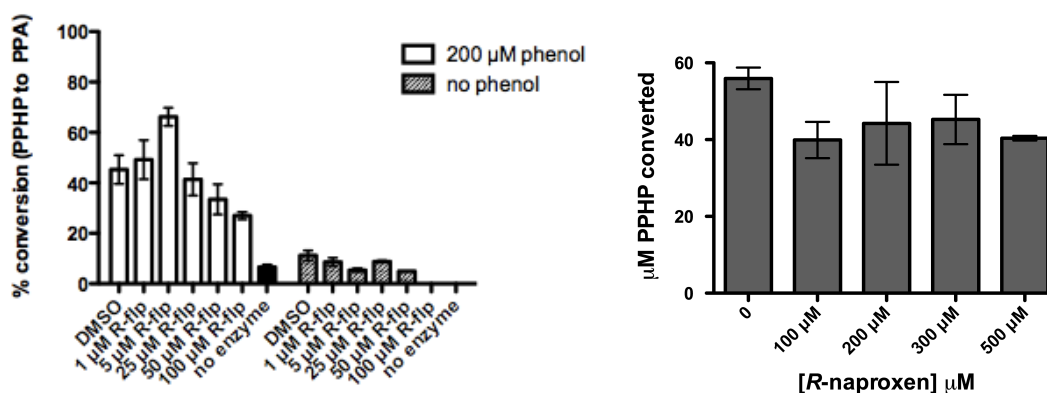
Figure 4: Lack of inhibition of POX activity by (*R*)-flurbiprofen and (*R*)-naproxen. (*R*)-flurbiprofen or (*R*)-naproxen (100-500 µM) were pre-incubated with murine COX-2 for 5 minutes at 37 °C prior to the addition of 100 µM PPHP. The reaction was quenched after 5 minutes by the addition of ethyl acetate with 0.5% acetic acid. Conversion of PPHP to PPA was monitored by HPLC as described under experimental procedures.

Structural basis of (R)-profen substrate-selective inhibition

To determine the basis of (R)-profen substrate-selective inhibition of 2-AG we utilized a combination of site-directed mutagenesis and X-ray crystallography. Previous reports have identified residues that mediate the ability of NSAIDs to inhibit AA oxygenation by using site-directed mutagenesis to modulate the ability of residues to interact with inhibitors. We employed this strategy to identify the residues critical for (R)-flurbiprofen inhibition of 2-AG. Mutation of Tyr-355 to Phe, Glu-524 to Leu, or Ser-530 to Ala did not have significant effects on the IC_{50} value of (R)-flurbiprofen inhibition of 2-AG oxygenation relative to wild-type murine COX-2 (Figure 5). In contrast, mutation of Arg-120 to Gln resulted in no inhibition of 2-AG oxygenation by (R)-flurbiprofen, revealing that the ion-pairing interaction between (R)-flurbiprofen and the constriction site is a critical mediator of substrate-selective inhibition. These studies suggest that (R)-profens bind to the COX active site in a similar manner to the (S)-profens, with their carboxylate moieties ion-paired to Arg-120.
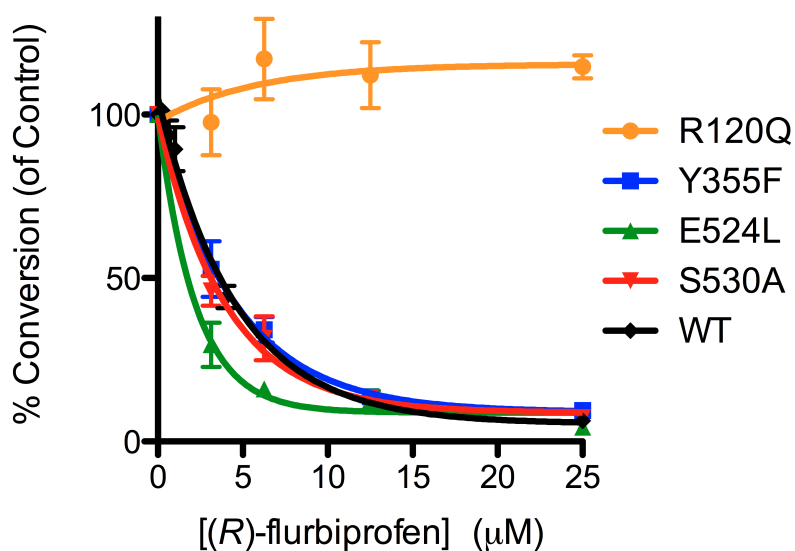
Figure 5: Inhibition of wild-type and mutant murine COX-2 oxygenation of 2-AG by (R)-flurbiprofen. While (R)-flurbiprofen inhibited the oxygenation of 2-AG by wild-type, Y355F, E524L, and S530A COX-2 with similar IC_{50} values. In contrast, mutation of Arg-120 to Gln resulted in no inhibition of 2-AG oxygenation by (R)-flurbiprofen.

In agreement with the site-directed mutagenesis studies, crystal structures of (R)-flurbiprofen and (R)-naproxen bound to murine COX-2 generated by Kelsey Duggan, Joel Musee, and Surajit Banerjee revealed that

they bind in a nearly identical fashion to the COX active site as previously determined for (*S*)-ibuprofen bound to COX-1, (*S*)-naproxen bound to COX-2, and (*S*)-flurbiprofen bound to COX-1 and COX-2.[11,27-29] Both (*R*)-flurbiprofen and (*R*)-naproxen bind with their carboxylates coordinated to Arg-120 at the constriction site and their aryl rings projecting up into the COX active site (Figure 6). This is in sharp contrast to a previous report that the α-methyl groups of (*R*)-profens abrogate binding to the COX active site through a steric clash with Tyr-355.[25] In fact, the α-methyl groups of both (*R*)-flurbiprofen and (*R*)-naproxen bind adjacent to Tyr-355.
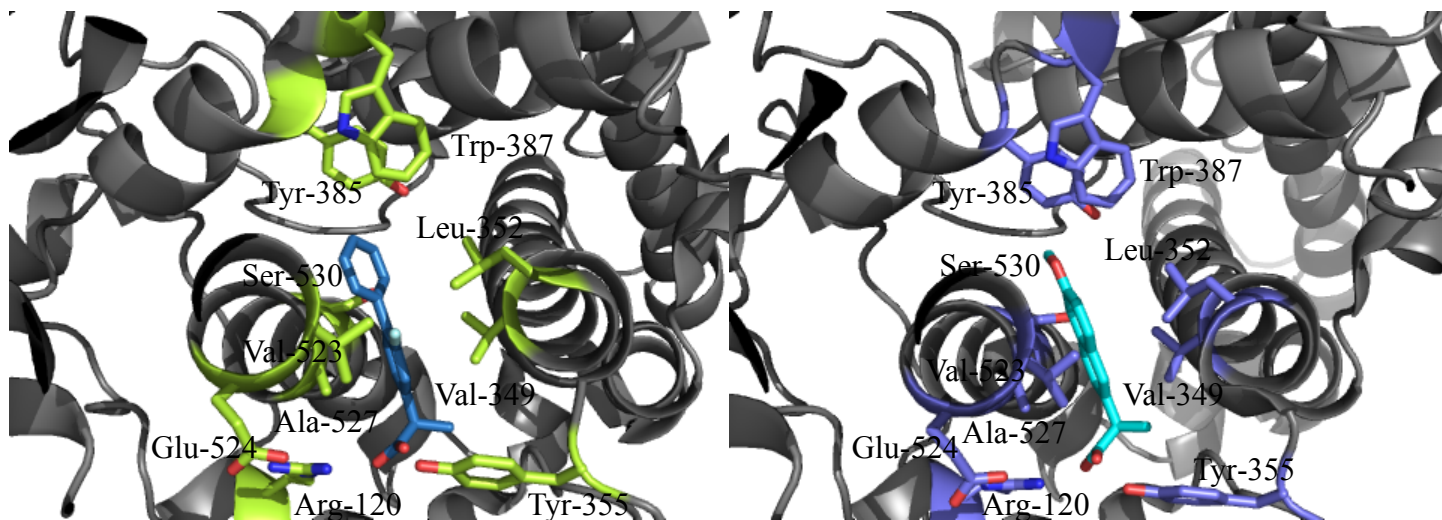
Figure 6: Crystal structures of (*R*)-flurbiprofen and (*R*)-naproxen bound to murine COX-2. Both (*R*)-flurbiprofen (left, blue, PDB ID: 3RR3) and (*R*)-naproxen (right, teal, PDB ID: 3Q7D) bind with their carboxylates coordinated to Arg-120 at the constriction site and their aryl rings projecting up into the COX active site.

Overlaying the 1.7 Å resolution crystal structure of (*S*)-naproxen with the (*R*)-naproxen structure allows for direct comparison of the binding of (*S*)-naproxen to (*R*)-naproxen.[30] This overlay reveals the near superimposition of the two naphthyl rings and the difference in chirality of the two α-methyl groups (Figure 7). Both (*S*)-naproxen and (*R*)-naproxen ion-pair and hydrogen bond with Arg-120 and Tyr-355 and form hydrophobic interactions with Ala-527, Val-349, Gly-526, Trp-387, Tyr-385, and Leu-352. However, there is a repositioning of Arg-120 and Tyr-355 (r.m.s. deviations of 0.47 Å and 0.45 Å, respectively) to accommodate the α-methyl group of (*R*)-naproxen, which increases the hydrogen bond distance between Tyr-355 and the carboxylate of (*R*)-naproxen to 3.05 Å compared to 2.44 Å for the same interaction in the (*S*)-naproxen complex.
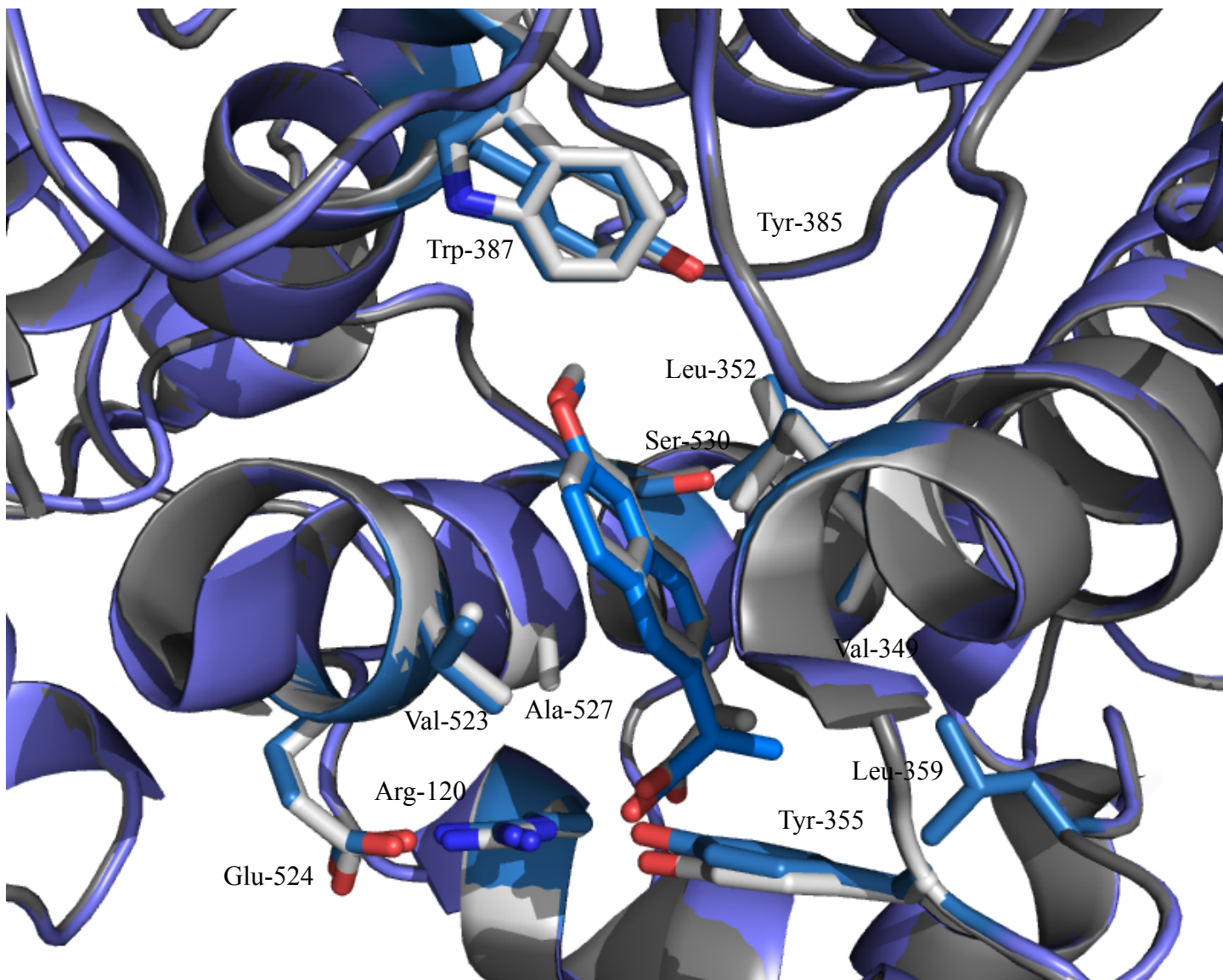
Figure 7: Overlay of (*S*)- and (*R*)-naproxen crystal structures. (*S*)-naproxen (blue, PDB ID: 3NT1) and (*R*)-naproxen (grey, PDB ID: 3Q7D) display nearly identical binding modes to the COX active site. The primary difference in binding is a repositioning of Arg-120 and Tyr-355 to accommodate the (*R*)-methyl group of (*R*)-naproxen.

As with the naproxen enantiomers, (*R*)-flurbiprofen and (*S*)-flurbiprofen bind in a similar fashion within the COX-2 active site (Figure 8). Both form an ion-pair and hydrogen bonds with Arg-120 and Tyr-355 at the base of the active site and hydrophobic interactions with Ala-527, Val-349, Gly-526, Tyr-385, Leu-359, and Ser-530. The comparison of the crystal structures of the flurbiprofen and naproxen enantiomers identifies substrate-selective inhibition is imparted through very subtle differences in binding and not overt changes in either binding mode or inhibitor-enzyme interactions. Thus, the primary determinant of substrate-selective inhibition appears to be the kinetic mode of inhibition.
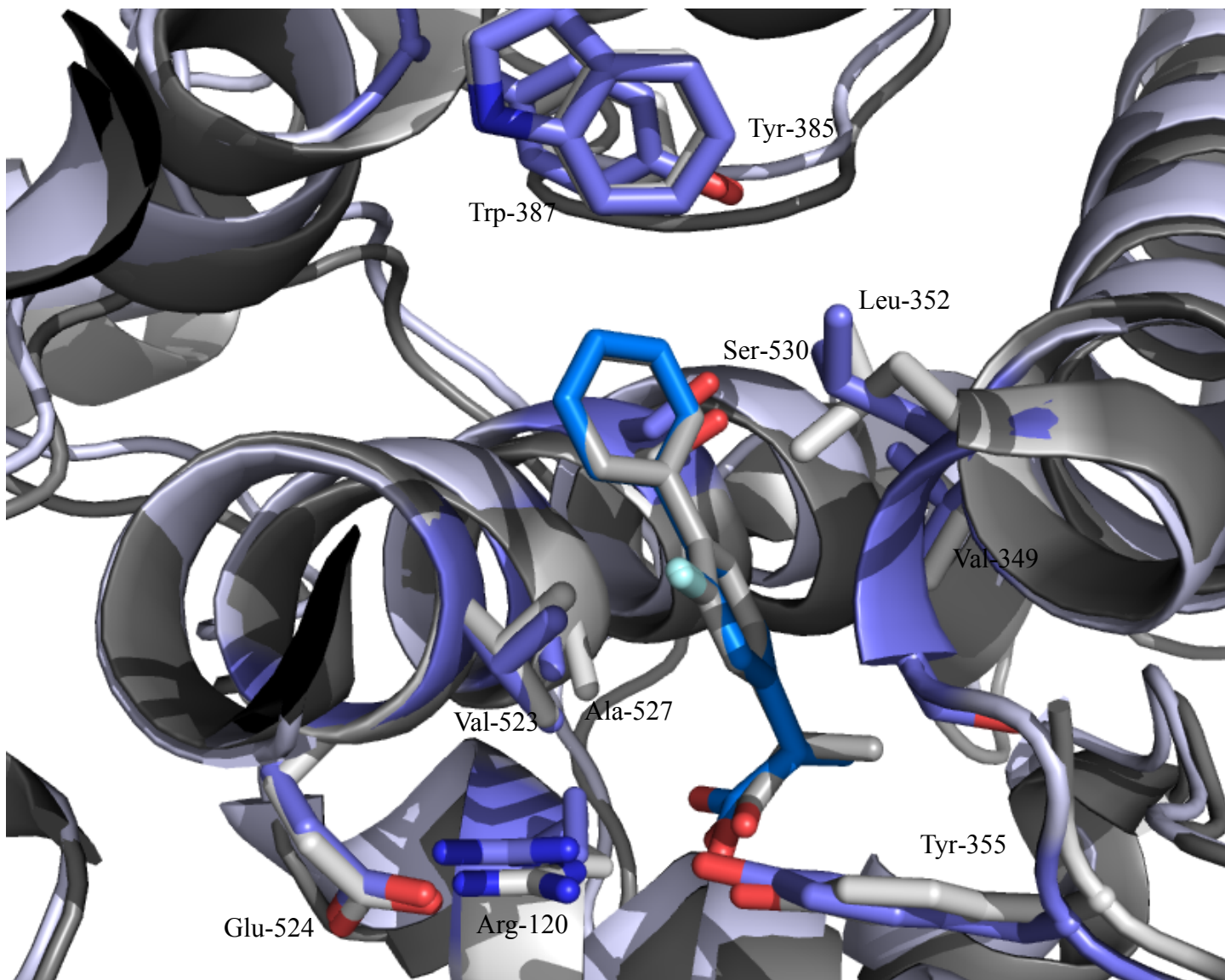
Figure 8: Overlay of (*S*)- and (*R*)-flurbiprofen crystal structures. (*S*)-naproxen (blue, PDB ID: 3PGH) and (*R*)-naproxen (grey, PDB ID: 3RR3) display nearly identical binding modes to the COX active site. As with naproxen, the primary difference in binding is a repositioning of Arg-120 and Tyr-355 to accommodate the (*R*)-methyl group of (*R*)-flurbiprofen.

Investigations into the mechanism of substrate-selective inhibition

Although multiple substrate-selective inhibitors from multiple NSAID classes had been identified, the mechanism by which substrate-selective inhibition occurs remained elusive. The elucidation of the binding mode of 1-AG to COX-2 and novel insights into COX dimer crosstalk assisted in the identification of the residues that mediate substrate-selective inhibition. The crystal structure of 1-AG bound to the active site of COX-2 identified that the 2,3-dihydroxypropyl moiety binds above the side chain of Arg-120 in a pocket formed by rotation of Leu-531 (Figure 9).[31] This movement of Leu-531 is identical to that observed when AA binds to COX-2 in the non-productive conformation.[32] However, when AA binds in the productive

57

conformation, Leu-531 is rotated in toward the active site. Thus, rotation of Leu-531 prevents the oxygenation of 2-AG but not AA.
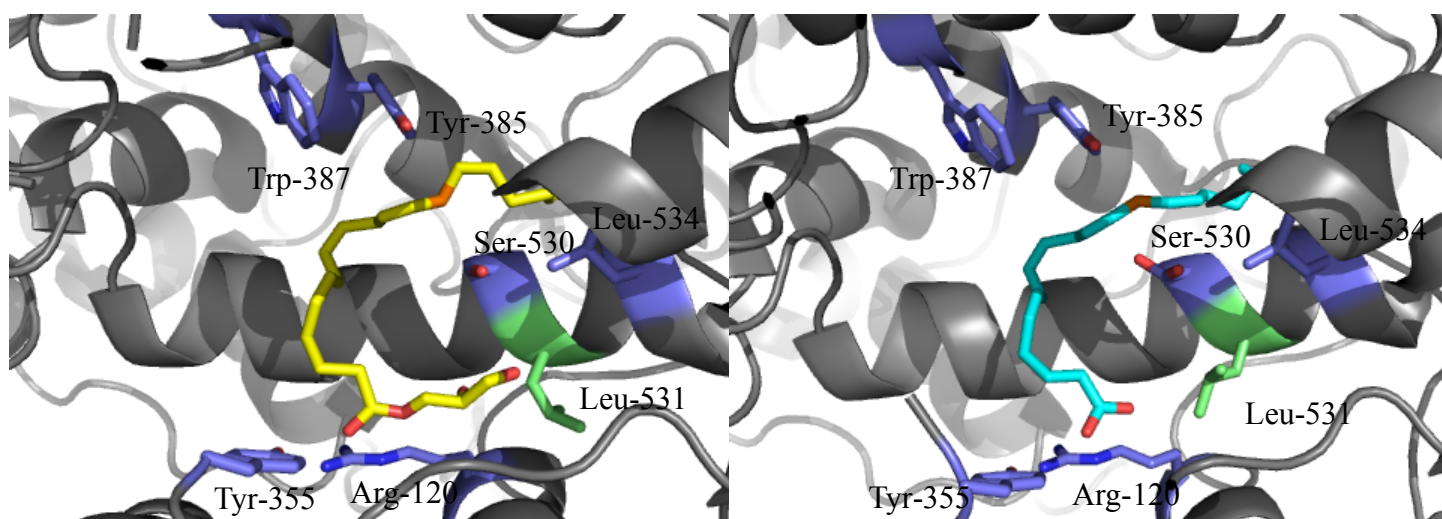
Figure 9: Comparison of the productive binding modes of 1-AG and AA with murine COX-2. 1-AG (yellow) bound in the productive mode positions C-13 (orange) adjacent to Tyr-385 for abstraction of the 13-pro-(*S*)-hydrogen. This binding requires the rotation of Leu-531 (green) to accommodate the binding of the 2,3-dihydroxypropyl moiety of 1-AG (left, PDB ID: 3MDL). Similarly, the productive conformation of AA (teal) positions its C-13 (orange) adjacent to Tyr-385 for abstraction of the 13-pro-(*S*)-hydrogen. However, the binding of AA does not require the rotation of Leu-531 (green) out of the active site (right, PDB ID: 3HS5).

In depth studies on communication between the two COX monomers have identified that the two monomers are functionally interdependent and that binding of a substrate, inhibitor, or activator at one active site alters the properties of the active site of the second monomer.[4] This subunit communication occurs through the repositioning of residues and translation through the dimer interface.[33] A crystal structure of the COX-2-selective inhibitor celecoxib bound to one monomer of COX-1 identified a conformational change in the loop consisting of residues 121 to 127 that may be the basis for dimer communication.[34]

We hypothesized that substrate-selective inhibition could arise from binding of an inhibitor to the first monomer and a subsequent conformational change in the second monomer such that 2-AG could not be oxygenated but AA could still be utilized as a substrate. The identification of the rotation of Leu-531 as a critical mediator of 1-AG binding suggested that this rotation could be a key determinant of substrate-selective inhibition, as Leu-531 rotation into the COX active site would not impair AA oxygenation but would prevent 2-AG oxygenation due to a steric clash with the glycerol moiety.

Previous studies have identified that mutation of Leu-531 has minor effects on the oxygenation of AA, 2-AG, and 1-AG by COX-2.[31,32] While mutation of Leu-531 has some impact on the oxygenation of substrates by COX-2, we hypothesized that decreasing the steric bulk of Leu-531 could reduce substrate-selective inhibition by reducing the steric impact of the rotation of residue 531 on the ability of 2-AG to bind and be oxygenated in the catalytic monomer. To determine the impact of Leu-531 on substrate-selective inhibition we screened the ability of (R)-flurbiprofen to inhibit a series of Leu-531 mutants with decreased steric bulk. Mutation of Leu-531 to Ile had no impact on (R)-flurbiprofen inhibition of 2-AG, however, mutation of Leu-531 to Val increased the IC_{50} and mutation of Leu-531 to Ala resulted in an abrogation of 2-AG inhibition altogether (Figure 10). To further assess this finding we also analyzed the ability of lumiracoxib, which binds in an inverted mode compared to (R)-flurbiprofen, to inhibit 2-AG oxygenation by COX-2. As with (R)-flurbiprofen, lumiracoxib exhibited a loss of potency with substitution of Leu-531 for either valine or alanine. Thus, decreasing the steric bulk of residue 531 results in decreased inhibition of 2-AG oxygenation by multiple substrate-selective inhibitors.
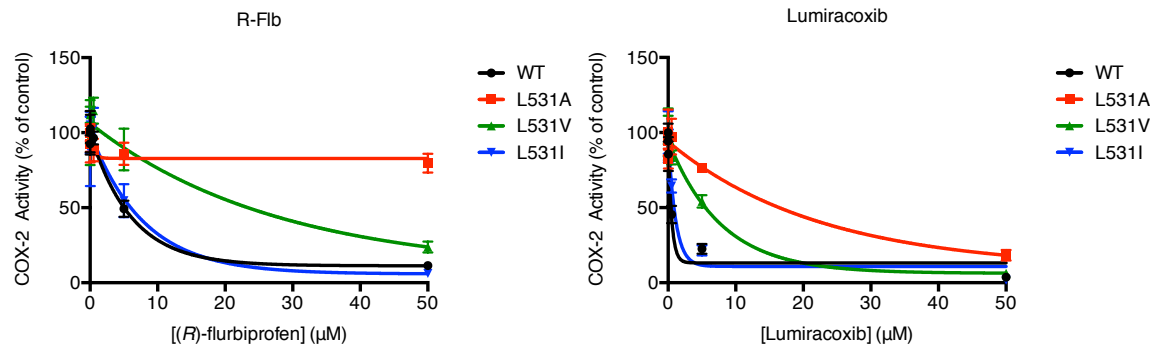
Figure 10: Impact of mutation of Leu-531 on inhibition of 2-AG oxygenation by (R)-flurbiprofen and lumiracoxib. Both (R)-flurbiprofen (left) and lumiracoxib (right) have decreased inhibition of 2-AG oxygenation against L531V and L531A mutants compared to wild-type or L531I murine COX-2.

To further explore the impact of Leu-531 mutation to Ala we performed kinetic experiments to determine the kinetic mode of inhibition of (R)-flurbiprofen against wild-type and L531A murine COX-2. Previous studies demonstrated that the substrate-selective inhibitors (S)-ibuprofen and mefenamic acid acted as competitive inhibitors of AA oxygenation but non-competitive inhibitors of 2-AG oxygenation.[3] Consistent with these data, (R)-flurbiprofen acted as a non-competitive inhibitor of 2-AG oxygenation in wild type COX-2 (Figure 11). However, mutation of Leu-531 to Ala converted (R)-flurbiprofen into a competitive inhibitor of 2-

AG oxygenation. Thus, mutation of Leu-531 to Ala abolishes the ability of a substrate-selective inhibitor to act as a non-competitive inhibitor of 2-AG oxygenation.
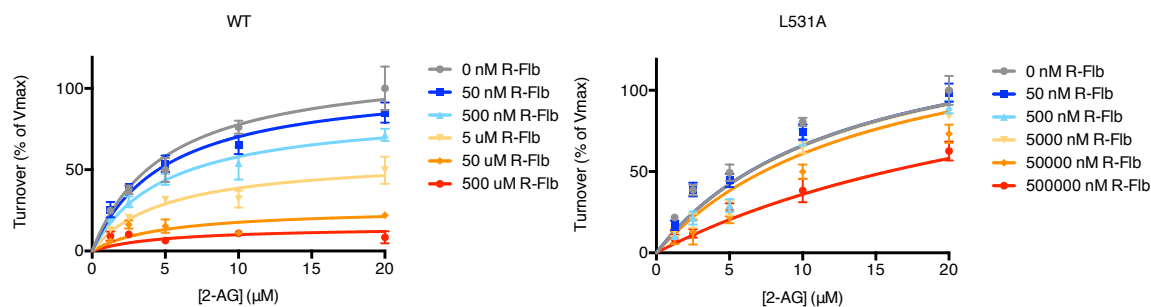
Figure 11: Inhibition kinetics of (*R*)-flurbiprofen against wild-type and L531A COX-2. While (*R*)-flurbiprofen acts as a non-competitive inhibitor of 2-AG oxygenation with wild-type COX-2 (left), it acts as a competitive inhibitor of 2-AG oxygenation with L531A COX-2 (right).

To determine if mutation of Leu-531 to Ala modifies the binding of substrate-selective inhibitors we attempted to crystalize (*R*)-flurbiprofen and lumiracoxib with L531A COX-2. A crystal structure solved by Shu Xu revealed that lumiracoxib binds in a nearly identical fashion to L531A COX-2 as wild type COX-2 (Figure 12).[35] Lumiracoxib forms hydrogen bonds between its carboxylate and Tyr-385 and Ser-530 in both wild-type and L531A COX-2. In addition, the *ortho*-chlorine atom lies adjacent to Ser-530 and inserts into a hydrophobic pocket comprised of Val-349, Ala-527, and Leu-531 (or Ala-531 in L531A). Thus, the binding of substrate-selective inhibitors to wild type and L531A COX-2 appears to be analogous.
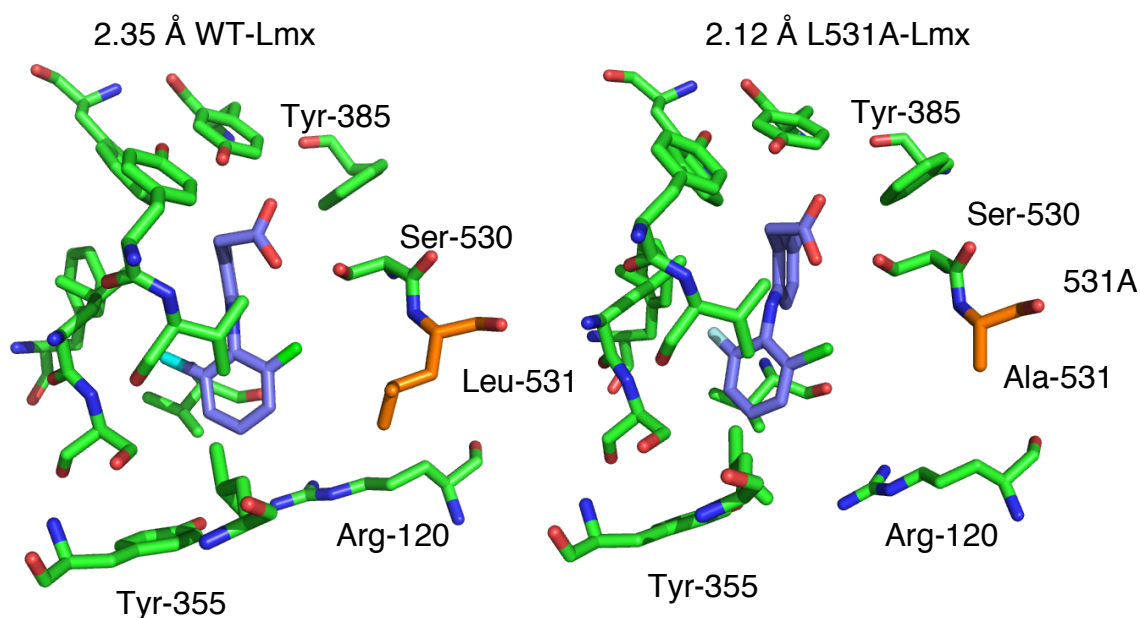
Figure 12: Comparison of the binding of lumiracoxib to wild-type and L531A COX-2. Lumiracoxib (blue) exhibits nearly identical binding in wild-type (left, PDB ID: 4OTY) and L531A COX-2 (right). Mutation of L531A results in a larger pocket between Ser-530 and Arg-120 relative to wild-type enzyme.

60

COX inhibitors exhibit multiple kinetic modes of inhibition. The two primary modes are rapid, reversible inhibition and slow, tight-binding inhibition.[18] Previous reports have identified that rapid, reversible inhibitors are weak inhibitors of AA oxygenation and slow, tight-binders are potent inhibitors of AA oxygenation.[3] Consistent with previous studies in our laboratory, we have found that rapid, reversible inhibitors are potent inhibitors of 2-AG oxygenation while slow, tight-binders are potent inhibitors of AA oxygenation and 2-AG oxygenation.[3] Taken together, these studies identify that rapid, reversible inhibitors of COX-2 exhibit substrate-selective inhibition while slow, tight binding inhibitors inhibit AA and 2-AG oxygenation with comparable IC_{50} values.

Slow, tight-binding inhibitors have very low dissociation rates due to a two-step mechanism of inhibition. After binding to the enzyme they exhibit a slow, time-dependent second step that leads to a functionally irreversible interaction with the enzyme.[36-38] Inhibition of both AA and 2-AG can occur with the binding of a single slow, tight-binding inhibitor to one subunit in the case of indomethacin and (*S*)-flurbiprofen (Figure 13).[19] Thus, slow, tight-binding inhibitors have similar IC_{50} values toward both AA and 2-AG.
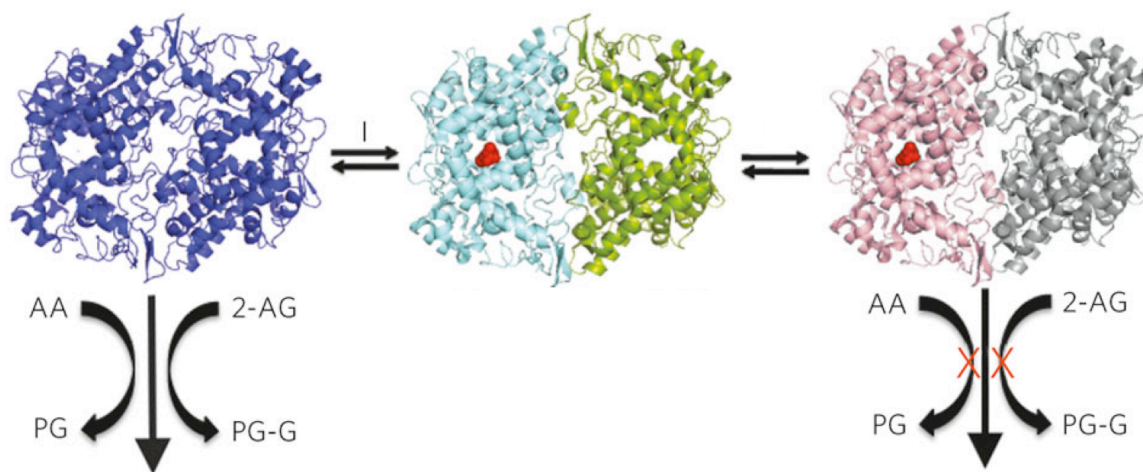
Figure 13: Mechanism of inhibition of AA and 2-AG by slow, tight-binding inhibitors. Binding of one molecule of a slow, tight-binding inhibitor to the first monomer results in a time-dependent conformational change in the second monomer such that the oxygenation of both AA and 2-AG by COX-2 is inhibited.

In contrast, rapid, reversible inhibitors have different kinetic modes of inhibition for AA and 2-AG. While they are competitive inhibitors of AA oxygenation, they exhibit non-competitive inhibition of 2-AG oxygenation.[3] Studies on the communication between the two subunits of COX-2 suggest that this non-

competitive inhibition occurs through the dimer interface.[4] Our data are consistent with the hypothesis that binding of a single molecule of a rapid, reversible inhibitor to the first monomer is sufficient to inhibit 2-AG oxygenation, but not AA oxygenation, in the second monomer. Thus, although both slow, tight-binding inhibitors and rapid, reversible inhibitors induce conformational changes in the second subunit after binding to the first subunit, the changes are not identical given the lack of AA inhibition by rapid, reversible inhibitors.

In addition to previously characterized rapid, reversible inhibitors, we have identified the (R)-profens, which were previously classified as inactive with respect to inhibition of AA oxygenation by COX-2, as substrate-selective inhibitors. The (R)-profens display a remarkable selectivity for 2-AG inhibition as they do not have any observable inhibition of AA oxygenation *in vitro*. This discovery suggests that molecules previously classified as non-inhibitors of AA oxygenation by COX-2 could be exceptional substrate-selective inhibitors. Understanding the scope of scaffolds that exhibit substrate-selective inhibition will assist in the design and development of novel substrate-selective inhibitors.

Investigations into the binding mode of 1-AG to COX-2 suggested that substrate-selective inhibition could be mediated by the rotation of Leu-531 into the COX channel. While the 2,3-dihydroxypropyl moiety of 1-AG requires rotation of Leu-531 out of the channel for productive binding, the productive binding of AA does not.[31,32] Consistent with the hypothesis that substrate-selective inhibition is imparted by binding of an inhibitor to the first subunit causing a rotation of Leu-531 in the second subunit, mutation of Leu-531 to Ala abrogates substrate-selective inhibition by both (R)-flurbiprofen and lumiracoxib. This is notable because (R)-flurbiprofen and lumiracoxib bind in a complimentary fashion to the COX active site, suggesting that regardless of binding pose Leu-531 mediates substrate-selective inhibition. In addition, a crystal structure of lumiracoxib bound to L531A COX-2 revealed that it has the same binding interactions with L531A COX-2 as it does with wild-type COX-2. Notably, lumiracoxib did inhibit the oxygenation of 2-AG by L531A COX-2, however it was at a significantly increased IC_{50} value relative to WT COX-2. This suggests that mutation of L531A does not necessarily completely abolish inhibition of 2-AG oxygenation by some substrate-selective inhibitors.

References

1. Yu, M., Ives, D. & Ramesha, C.S. Synthesis of prostaglandin E-2 ethanolamide from anandamide by cyclooxygenase-2. *Journal of Biological Chemistry* **272**, 21181-21186 (1997).
2. Kozak, K.R., Rowlinson, S.W. & Marnett, L.J. Oxygenation of the endocannabinoid, 2-arachidonylglycerol, to glyceryl prostaglandins by cyclooxygenase-2. *The Journal of biological chemistry* **275**, 33744-33749 (2000).
3. Prusakiewicz, J.J., Duggan, K.C., Rouzer, C.A. & Marnett, L.J. Differential Sensitivity and Mechanism of Inhibition of COX-2 Oxygenation of Arachidonic Acid and 2-Arachidonoylglycerol by Ibuprofen and Mefenamic Acid. *Biochemistry* **48**, 7353-7355 (2009).
4. Yuan, C., Rieke, C.J., Rimon, G., Wingerd, B.A. & Smith, W.L. Partnering between monomers of cyclooxygenase-2 homodimers. *Proc Natl Acad Sci U S A* **103**, 6142-6147 (2006).
5. Rowlinson, S.W.*, et al.* A novel mechanism of cyclooxygenase-2 inhibition involving interactions with Ser-530 and Tyr-385. *Journal of Biological Chemistry* **278**, 45763-45769 (2003).
6. Blobaum, A.L. & Marnett, L.J. Molecular determinants for the selective inhibition of cyclooxygenase-2 by lumiracoxib. *The Journal of biological chemistry* **282**, 16379-16390 (2007).
7. Prusakiewicz, J.J., Felts, A.S., Mackenzie, B.S. & Marnett, L.J. Molecular basis of the time-dependent inhibition of cyclooxygenases by indomethacin. *Biochemistry* **43**, 15439-15445 (2004).
8. Prasit, P.*, et al.* The discovery of rofecoxib, [MK 966, Vioxx, 4-(4'-methylsulfonylphenyl)-3-phenyl-2(5H)-furanone], an orally active cyclooxygenase-2-inhibitor. *Bioorg Med Chem Lett* **9**, 1773-1778 (1999).
9. Markey, C.M., Alward, A., Weller, P.E. & Marnett, L.J. Quantitative studies of hydroperoxide reduction by prostaglandin H synthase. Reducing substrate specificity and the relationship of peroxidase to cyclooxygenase activities. *The Journal of biological chemistry* **262**, 6266-6279 (1987).
10. Rowlinson, S.W., Crews, B.C., Lanzo, C.A. & Marnett, L.J. The binding of arachidonic acid in the cyclooxygenase active site of mouse prostaglandin endoperoxide synthase-2 (COX-2). A putative L-shaped binding conformation utilizing the top channel region. *The Journal of biological chemistry* **274**, 23305-23310 (1999).
11. Duggan, K.C.*, et al.* Molecular basis for cyclooxygenase inhibition by the non-steroidal anti-inflammatory drug, naproxen. *The Journal of biological chemistry* (2010).
12. Otwinowski, Z. & Minor, M. Processing of X-ray diffraction data collected in oscillation mode. *Methods Enzymol* **276**, 307-326 (1997).
13. Vagin, A. & Teplyakov, A. An approach to multi-copy search in molecular replacement. *Acta Crystallogr D Biol Crystallogr* **56**, 1622-1624 (2000).
14. Emsley, P. & Cowtan, K. Coot: model-building tools for molecular graphics. *Acta Crystallogr D Biol Crystallogr* **60**, 2126-2132 (2004).
15. Adams, P.D.*, et al.* PHENIX: building new software for automated crystallographic structure determination. *Acta Crystallogr D Biol Crystallogr* **58**, 1948-1954 (2002).
16. DeLano, W.L. *The PyMol Molecular Graphics System.*, (DeLano Scientific LLC, Palo Alto, CA, 2009).
17. Blobaum, A.L. & Marnett, L.J. Structural and functional basis of cyclooxygenase inhibition. *J Med Chem* **50**, 1425-1441 (2007).
18. Rome, L.H. & Lands, W.E. Structural requirements for time-dependent inhibition of prostaglandin biosynthesis by anti-inflammatory drugs. *Proc Natl Acad Sci U S A* **72**, 4863-4865 (1975).
19. Kulmacz, R.J. & Lands, W.E. Stoichiometry and kinetics of the interaction of prostaglandin H synthase with anti-inflammatory agents. *The Journal of biological chemistry* **260**, 12572-12578 (1985).
20. Felts, A.S.*, et al.* Desmethyl derivatives of indomethacin and sulindac as probes for cyclooxygenase-dependent biology. *Acs Chem Biol* **2**, 479-483 (2007).
21. Esser, R.*, et al.* Preclinical pharmacology of lumiracoxib: a novel selective inhibitor of cyclooxygenase-2. *Brit J Pharmacol* **144**, 538-550 (2005).
22. Blobaum, A.L. & Marnett, L.J. Molecular determinants for the selective inhibition of cyclooxygenase-2 by lumiracoxib. *Journal of Biological Chemistry* **282**, 16379-16390 (2007).

23. Bhattacharyya, D.K., Lecomte, M., Rieke, C.J., Garavito, R.M. & Smith, W.L. Involvement of arginine 120, glutamate 524, and tyrosine 355 in the binding of arachidonate and 2-phenylpropionic acid inhibitors to the cyclooxygenase active site of ovine prostaglandin endoperoxide H synthase-1. *Journal of Biological Chemistry* **271**, 2179-2184 (1996).

24. Gierse, J.K., Koboldt, C.M., Walker, M.C., Seibert, K. & Isakson, P.C. Kinetic basis for selective inhibition of cyclo-oxygenases. *The Biochemical journal* **339 (Pt 3)**, 607-614 (1999).

25. Bhattacharyya, D.K., Lecomte, M., Rieke, C.J., Garavito, M. & Smith, W.L. Involvement of arginine 120, glutamate 524, and tyrosine 355 in the binding of arachidonate and 2-phenylpropionic acid inhibitors to the cyclooxygenase active site of ovine prostaglandin endoperoxide H synthase-1. *The Journal of biological chemistry* **271**, 2179-2184 (1996).

26. Musee, J. & Marnett, L.J. Prostaglandin H Synthase-2-catalyzed Oxygenation of 2-Arachidonoylglycerol Is More Sensitive to Peroxide Tone than Oxygenation of Arachidonic Acid. *Journal of Biological Chemistry* **287**, 37383-37394 (2012).

27. Selinsky, B.S., Gupta, K., Sharkey, C.T. & Loll, P.J. Structural analysis of NSAID binding by prostaglandin H2 synthase: time-dependent and time-independent inhibitors elicit identical enzyme conformations. *Biochemistry* **40**, 5172-5180 (2001).

28. Gupta, K., Selinsky, B.S. & Loll, P.J. 2.0 angstroms structure of prostaglandin H2 synthase-1 reconstituted with a manganese porphyrin cofactor. *Acta Crystallogr D Biol Crystallogr* **62**, 151-156 (2006).

29. Kurumbail, R.G., *et al.* Structural basis for selective inhibition of cyclooxygenase-2 by anti-inflammatory agents. *Nature* **384**, 644-648 (1996).

30. Duggan, K.C., *et al.* Molecular Basis for Cyclooxygenase Inhibition by the Non-steroidal Anti-inflammatory Drug Naproxen. *Journal of Biological Chemistry* **285**, 34950-34959 (2010).

31. Vecchio, A.J. & Malkowski, M.G. The Structural Basis of Endocannabinoid Oxygenation by Cyclooxygenase-2. *Journal of Biological Chemistry* **286**, 20736-20745 (2011).

32. Vecchio, A.J., Simmons, D.M. & Malkowski, M.G. Structural Basis of Fatty Acid Substrate Binding to Cyclooxygenase-2. *Journal of Biological Chemistry* **285**, 22152-22163 (2010).

33. Yuan, C., *et al.* Cyclooxygenase Allosterism, Fatty Acid-mediated Cross-talk between Monomers of Cyclooxygenase Homodimers. *The Journal of biological chemistry* **284**, 10046-10055 (2009).

34. Rimon, G., *et al.* Coxibs interfere with the action of aspirin by binding tightly to one monomer of cyclooxygenase-1. *Proc Natl Acad Sci U S A* **107**, 28-33 (2010).

35. Windsor, M.A., Valk, P.L., Xu, S., Banerjee, S. & Marnett, L.J. Exploring the molecular determinants of substrate-selective inhibition of cyclooxygenase-2 by lumiracoxib. *Bioorganic & Medicinal Chemistry Letters* **23**, 5860-5864 (2013).

36. Lanzo, C.A., Sutin, J., Rowlinson, S., Talley, J. & Marnett, L.J. Fluorescence quenching analysis of the association and dissociation of a diarylheterocycle to cyclooxygenase-1 and cyclooxygenase-2: dynamic basis of cyclooxygenase-2 selectivity. *Biochemistry* **39**, 6228-6234 (2000).

37. Walker, M.C., *et al.* A three-step kinetic mechanism for selective inhibition of cyclo-oxygenase-2 by diarylheterocyclic inhibitors. *The Biochemical journal* **357**, 709-718 (2001).

38. Copeland, R.A., *et al.* Mechanism of selective inhibition of the inducible isoform of prostaglandin G/H synthase. *Proc Natl Acad Sci U S A* **91**, 11202-11206 (1994).

CHAPTER III

SUBSTRATE-SELECTIVE INHIBITION IN CELLULAR SYSTEMS

Introduction

The endocannabinoids anandamide (AEA) and 2-arachidonoyl glycerol (2-AG) are the endogenous ligands of the G-protein coupled cannabinoid 1 and 2 receptors (CB$_1$ and CB$_2$).[1,2] Both AEA and 2-AG activate the CB receptors to produce some of their manifold biological effects.[3] The CB receptors inhibit adenylyl cyclase through their G$_{i/o}$ subunits and couple to the mitogen-activated protein kinase-extracellular-signal-regulated kinase pathway through their G$_{\beta\gamma}$ subunits.[4-6] The CB$_1$ receptor is highly expressed through the central nervous system including in the hippocampus, basal ganglia, cerebellum, brain stem, spinal cord, and dorsal root ganglia.[7,8] In contrast, the CB$_2$ receptor is highly expressed in the spleen and on immune cells including monocytes, macrophages, B-cells, and T-cells.[9,10]

A primary therapeutic effect of endocannabinoids is analgesia. Activation of CB$_1$ receptors by endocannabinoids regulates analgesia through the modulation of neuronal transmission in the rostral ventral medulla, the periaqueductal grey, and the spinal trigeminal nucleus.[11-13] Treatment of these areas with CB$_1$ antagonists leads to hyperalgesia in an opiod receptor-independent manner.[14,15] Pain is generated by noxious stimuli from peripheral insults, which activate glutamatergic signaling and cause neuronal hyperexcitability in the dorsal horn of the spinal cord. Glutamatergic activation in the dorsal horn can further induce excitotoxicity and the production of inflammatory cytokines, such as IL-1β, which cause expression of cyclooxygenase-2 (COX-2).[14-18] Importantly, CB$_2$ signaling is a critical mediator of cytokine release in immune cells.[6] Thus, the cannabinoid receptors modulate the central response to peripheral pain and can mediate the generation of cytokines, which amplify of painful stimuli. The signaling cascade of pain demonstrates a connection between cannabinoid receptor signaling, analgesia, inflammation, and COX-2.

In addition to its production of prostaglandins (PGs) from arachidonic acid (AA), COX-2 also oxygenates and inactivates 2-AG to form prostaglandin glyceryl esters (PG-Gs) and AEA to form prostaglandin ethanolamides (PG-EAs).[19,20] PGE$_2$-G has been shown to cause potent Ca^{2+} mobilization in RAW264.7 macrophages and H1819 non-small cell lung carcinoma cells.[21,22] PGE$_2$-G also induces hyperalgesia and

mechanical allodynia in rats.[23] Therefore, the oxygenation of 2-AG by COX-2 not only terminates analgesic endocannabinoid signaling, but also generates a series of nociceptive metabolites.

Although COX-2 oxygenates AEA and 2-AG, under physiological conditions both AEA and 2-AG are primarily regulated through their hydrolysis to AA. AEA is primarily degraded by the enzyme fatty acid amide hydrolase (FAAH) to form AA and ethanolamine.[24-26] 2-AG is hydrolyzed to AA and glycerol by several enzymes including monoacylglycerol lipase (MAGL), α/β-hydrolase domain 6 (ABHD6), α/β-hydrolase domain 12 (ABHD12), carboxylesterases 1 and 2 (CES1 and CES2), and palmitoylprotein thioesterase 1 (PPT1).[27-31] While inhibition of these hydrolytic enzymes augments the levels of AEA or 2-AG in multiple settings, the impact of COX-2 inhibition on endocannabinoid levels in cellular systems has not been studied.

Two macrophage cell lines that synthesize PG-Gs have been identified, RAW 264.7 macrophages and resident peritoneal macrophages (RPMs).[20,32-35] Interestingly, RPMs synthesize PG-Gs through the action of COX-1 despite previous studies identifying 2-AG as a poor substrate for COX-1 *in vitro*.[34] To develop cellular assays for substrate-selective inhibition we focused first on RAW 264.7 macrophages due to their relative ease of use and extensive metabolomic profiling.

RAW 264.7 macrophages produce PG-Gs in response to overnight treatment with granulocyte macrophage colony-stimulating factor (GM-CSF) followed by lipopolysaccharide (LPS), interferon-γ (IFNγ), and ionomycin treatment the following day.[32,33] Upon binding to its receptor on stem cells, GM-CSF induces differentiation into granulocytes (neutrophils, eosinophils, and basophils) and monocytes.[36] LPS is a component of the outer membrane of gram-negative bacteria and consists of a lipid head group, a core oligosaccharide, and an *O*-antigen.[37] LPS elicits a strong immune response in cells and animals through its binding and activation of toll-like receptor 4 (TLR4).[38] IFNγ binds to a heterodimeric receptor consisting of two subunits, interferon gamma receptor 1 and 2, and activates the Janus kinase (JAK)-signal transducer and activator of transcription (STAT) pathway.[39] Ionomycin is a calcium ionophore produced by *Streptomyces conglobatus* that robustly increases intracellular calcium and stimulates the production of IFN, perforin, interleukin-2, and interleukin-4.[40,41] Treatment of cells with these stimuli results in robust expression of COX-2 and the release of AA and 2-AG, which are then converted to PGs and PG-Gs.

In addition to characterizing RAW 264.7 macrophages, we sought to develop a model cell culture system containing neurons. To do this we utilized primary cultures of murine dorsal root ganglia (DRG). DRGs translate sensory information from the periphery into the dorsal horn of the spinal cord and consist of a mixture of both neurons and glia.[42] We selected these cells because previous studies have determined that inflammatory stimuli induce COX-2 in DRGs, leading to hyperexcitability, hyperalgesia, and allodynia.[14] Thus, DRGs may offer insights into the role of COX-2 in pain and inflammatory *in vivo*.

Experimental Procedures

Materials

RAW 264.7 cells were obtained from American type culture collection (Rockville, MD). Cell culture reagents were purchased from Life Technologies (Gaithersburg, MD). PGE$_2$-G, PGF$_{2\alpha}$-G, PGE$_2$-d$_4$, AA-d$_8$, AEA-d$_8$, and 2-AG-d$_8$ were purchased from Cayman Chemical (Ann Arbor, MI). LPS, ionomycin, and IFNγ were purchased from Sigma Aldrich (Milwaukee, WI). PGE$_2$-G-d$_5$ was synthesized as described previously using chemicals from Sigma Aldrich.[20] Inhibitors were purchased from Sigma Aldrich and Cayman Chemical or synthesized as previously outlined.[43,44] GM-CSF was purchased from R&D Systems (Minneapolis, MN).

Inhibition of PG-G formation in RAW 264.7 macrophages

Low passage (< 15) RAW 264.7 macrophages were plated onto 100 mM dishes at 3 x 10^6 cells per dish in 6 mL of DMEM containing 10% fetal bovine serum and 20 ng/mL GM-CSF. After a 22-hour incubation the media was removed and replaced with 6 mL of serum-free DMEM containing 1 µg/mL LPS and 20 units/mL IFNγ. At this point vehicle (DMSO) or inhibitors were added to the media. After 6 hours of stimulation the cells were treated with 2 µM ionomycin for 1 additional hour. After 7 total hours of stimulation the media was removed and extracted in 2 volumes of ethyl acetate containing 0.1% glacial acetic acid, PGE$_2$-G-d$_5$, and PGE$_2$-d$_4$. The cells were then scraped into 2 mL of methanol containing AA-d$_8$ and 2-AG-d$_8$ and added to the ethyl acetate solution. The extraction mixture was then vigorously mixed and placed in a -20°C refrigerator overnight. The next day the organic layer was removed and dried under a stream of nitrogen gas. The resulting film was reconstituted in 200 µL of 1:1 water:methanol and subjected to liquid chromatography/mass spectrometry (LC/MS) analysis.

Isolation of embryonic dorsal root ganglia

DRGs were harvested as previously described.[45] Briefly, pregnant (E14-15) mice were euthanized by CO_2 asyphyxiation. Embryos were then removed and the entire spinal column and DRGs were collected. The DRGs were washed in PBS and dissociated by incubation in 0.001% collagenase/DNase and 0.15% trypsin at 37°C for one hour. 80,000 cells were then plated onto acid-treated, collagen-coated coverslips in 35 mm dishes and incubated in 3 mL of UltraCulture Media (10% Hyclone fetal bovine serum, 1 mM L-glutamine, 1% penicillin-streptomycin, and 50 ng/mL of nerve growth factor). Cells were cultured at 37°C and 5% CO_2.

Generation of pure neuronal dorsal root ganglia cultures

Following the isolation of DRGs described above, cultures were allowed to acclimatize for 48 hours at 37°C and 5% CO_2. Cells were then treated with 5 μM arabinoside (AraC) for 7 days. After 7 days the media was removed, the cells were washed once with PBS, and incubated with fresh media.

DRG culture stimulation and inhibition

After culturing the DRGs for 3-5 days the media was removed and replaced with media containing 20 ng/mL GM-CSF. Following a 22-hour incubation the media was then removed and replaced with fresh serum-free media containing LPS (1 μg/mL), IFNγ (20 units/mL), and 10 μM 15(*S*)-hydroxy-5,8,11,13-eicosatetraenoic acid for 6 hours. Inhibitors or vehicle (DMSO) were added concurrently with the media replacement. Following the 6-hour incubation, 2 μM ionomycin was added for 1 hour, after which the media and cells were harvested and extracted as described above for RAW 264.7 macrophages.

Immunoblotting analysis of COX-2 in DRGs

Unstimulated or stimulated cells were scraped into lysis buffer and immunoblotted for COX-2 expression as previously described with minor modifications.[46] Cells were lysed in 200 μl M-PER lysis buffer containing mammalian protease inhibitors and phosphatase inhibitor mixtures I and II. Cell lysates were mixed by vortexing and placed on ice for 30 min. Cellular debris were then removed by centrifugation for 10 min at 16,000 g. Samples were stored at -80°C until analyses. Equal quantities of protein (~20 μg) were resolved by gradient (2-12%) SDS-Polyacrylamide gel electrophoresis (SDS-PAGE) and transferred onto a polyvinylidene

difluoride membrane. Membranes were blocked (20 mM Tris, pH 7.6, 140 mM NaCl, 0.05% Tween 20, 5% nonfat dry milk) prior to incubation with antibodies. Primary antibodies were used at a 1:1000 dilution and the secondary antibody at a 1:5000 dilution.

Staining for COX-2 in stimulated DRGs

DRGs were stimulated as described above and imaged for COX-2 using Fluorocoxib A as described previously.[47]

Mass spectrometry analysis

Samples were analyzed for eicosanoids and endocannabinoids as previously described.[48-51]

Results

Inhibition of PG-G formation in RAW 264.7 macrophages

We sought to develop a cellular system in which we could analyze substrate-selective inhibitors in a biological setting after *in vitro* analyses. To do this we first utilized stimulated RAW 264.7 macrophages, which produce both PGs and PG-Gs under the stimulation conditions outlined in the experimental methods. RAW 264.7 macrophages are easily cultured and the effects of inflammatory stimuli treatments on PG and PG-G production have been extensively characterized on a metabolic level.[52-55]

We analyzed the effects of substrate-selective inhibitors on PG and PG-G levels in stimulated RAW 264.7 macrophages. As with *in vitro* experiments, we found that substrate-selective inhibitors decreased the production of PG-Gs without having significant inhibition of PGs. For example, the non-substrate-selective inhibitor (*S*)-flurbiprofen inhibits the production of both PGs and PG-Gs with comparable IC_{50} values, while the substrate-selective inhibitor (*R*)-flurbiprofen retains inhibition of PG-Gs but does not inhibit PG production (Figure 1). These data reveal that substrate-selective inhibition occurs not only *in vitro*, but also in cellular systems with endogenous substrate pools and stimulated COX-2 expression.
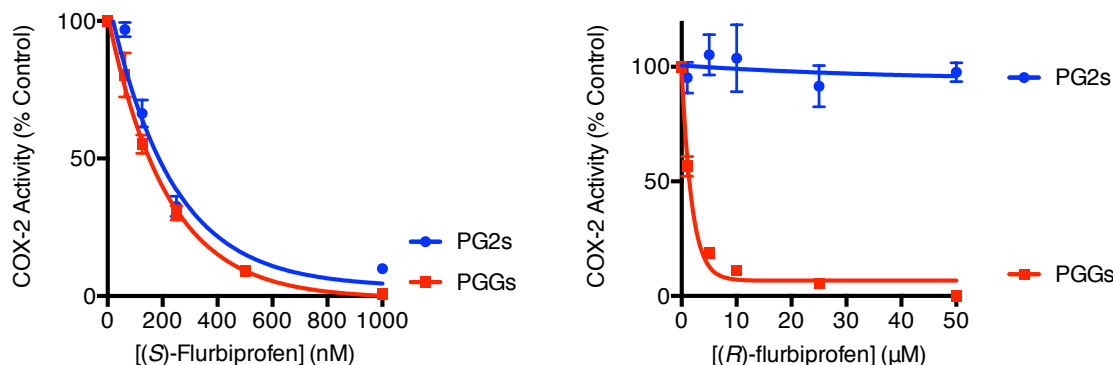
Figure 1: Inhibition of PGs and PG-Gs in stimulated RAW 264.7 cells by (*S*)- and (*R*)-flurbiprofen. (*S*)-flurbiprofen inhibits the production of both PGs and PG-Gs with comparable IC_{50} values, while (*R*)-flurbiprofen acts as a substrate-selective inhibitor with minimal inhibition of PGs and full inhibition of PG-G production. Data shown are mean $\pm$ s.e.m., n = 6.

In addition to monitoring PG and PG-G production, we also sought to determine if inhibition of COX-2 modulates the levels of AA and 2-AG in stimulated RAW 264.7 cells. Both (*S*)-flurbiprofen and (*R*)-flurbiprofen increased 2-AG in a concentration-dependent manner, with similar values for both PG-G inhibition and increasing 2-AG (Figure 2). While (*S*)-flurbiprofen also increased AA levels, (*R*)-flurbiprofen did not. These results demonstrate that inhibition of COX-2 not only decreases PGs and PG-Gs, it also increases the levels of AA and 2-AG. This is an important discovery because 2-AG counteracts the deleterious effects of PG-Gs through its activation of the cannabinoid receptors. Thus, as oxygenation of 2-AG to PG-Gs results in hyperalgesia and the production of potent calcium mobilizers, substrate-selective inhibition of COX-2 represents a potential therapeutic treatment for neuropathic pain and inflammation.
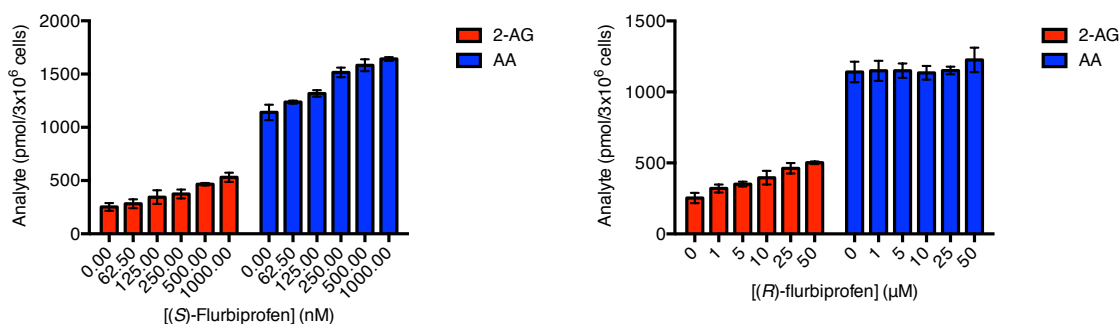
Figure 2: Effects of (*S*)- and (*R*)-flurbiprofen on the levels of 2-AG and AA in RAW 264.7 cells. (*S*)-flurbiprofen increases both 2-AG and AA, while (*R*)-flurbiprofen selectively increases 2-AG levels. Data shown are mean $\pm$ s.e.m., n = 6.

Although (*R*)-flurbiprofen is a valuable substrate-selective inhibitor *in vitro* and *ex vivo*, it undergoes a unidirectional isomerization in mice (but to a lesser extent in rats, humans, or monkeys) to the non-substrate-selective inhibitor (*S*)-flurbiprofen, rendering it unsuitable for preclinical studies in mice.[56] To surmount this chiral inversion, Matt Windsor synthesized a series of achiral profen analogs and assessed them for *in vitro* substrate-selective inhibition (Figure 3).[43] These studies identified a series of achiral profens that displayed substrate-selective inhibition against purified COX-2.

compd	2-AG IC$_{50}$ (μM)[b]	AA % inhibition[c]
3a	0.11 ± 0.02	7 ± 11
3b	1.4 ± 0.4	16 ± 12
3c	5.5 ± 0.8	14 ± 13
3d	6.1 ± 0.5 (68%)	24 ± 10
3e	0.5 ± 0.1	10 ± 16
4a	1.1 ± 0.4	5 ± 11
4b	− (12%)	7 ± 11
4c	− (5%)	5 ± 14
4d	7.3 ± 0.5 (65%)	17 ± 14
4e	3.0 ± 1.2	32 ± 6
5a	2.3 ± 1.2 (87%)	0 ± 18
5b	3.4 ± 1.2 (77%)	6 ± 12
5c	− (45%)	10 ± 9
5d	5.0 ± 0.8	15 ± 10
5e	4.1 ± 1.4 (75%)	10 ± 20

Figure 3: Inhibition of COX-2-mediated 2-AG and AA oxygenation by achiral profen derivatives. The IC$_{50}$ values were determined by incubating five concentrations of inhibitor and a DMSO control with purified murine COX-2 (40 nM) for 3 minutes followed by addition of 2-AG or AA (5 μM) at 37°C for 30 seconds. Dashes indicate <50% inhibition of 2-AG oxygenation at 10 μM inhibitor. Numbers in parentheses indicate maximal inhibition at 10 μM inhibitor. Percent inhibition of AA oxygenation reported as measured at 10 μM inhibitor. Values are mean ± s.d. (n = 6). Reproduced from.[43]

To further assess the potential of these achiral profen derivatives to serve as substrate-selective inhibitors we analyzed the effects of *des*-methyl-flurbiprofen, dimethyl-flurbiprofen, and cyclopropyl-flurbiprofen in stimulated RAW 264.7 cells. While each inhibitor displayed substrate-selective inhibition *in vitro*, in the RAW 264.7 cells they had significantly reduced potency and were less selective for 2-AG inhibition than the *in vitro* assay and (*R*)-flurbiprofen (Figure 4). These studies suggest that achiral analogs of

the profens could serve as substrate-selective inhibitors, although their performance in cellular systems is not as robust as (R)-flurbiprofen.
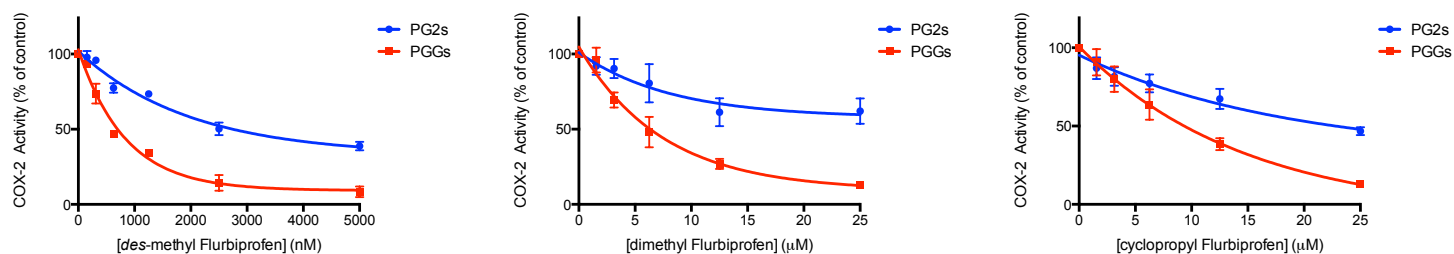
Figure 4: Inhibition of PG and PG-G production in stimulated RAW 264.7 cells by achiral profen analogs. All three inhibitors display substrate-selective inhibition, albeit with some inhibition of PG production and reduced potency relative to *in vitro* assays. Data shown are mean ± s.e.m., n = 6.

Optimization of DRG cultures for PG-G and PG-EA production

Although RAW 264.7 cells are a robust model system for studying substrate-selective inhibition of 2-AG, they have very little AEA and do not produce detectable amounts of PG-EAs. As an alternative cell culture system, we utilized primary embryonic murine DRGs. This culture system consists of a combination of neurons and glia and initial studies revealed that treatment of DRG cultures with IFNγ and Il-1β, two cytokines that upregulate COX-2 expression physiologically, caused robust stimulation of COX-2 expression (Figure 5).[57,58] Thus, these primary DRG cultures respond to physiological inflammatory stimuli by expressing COX-2.
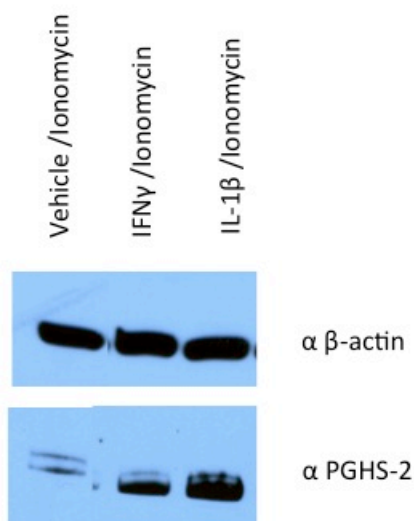
Figure 5: Stimulation of COX-2 expression in DRG cultures treated with IFNγ and IL-1β. Western blot analyses identify a robust stimulation of COX-2 expression upon treatment of DRGs with either IFNγ or IL-1β. Experiment performed by Joel Musee.

To optimize the production of PGs and PG-Gs in DRGs we surveyed a series of stimulation paradigms. Treatment of cultures with GM-CSF overnight followed by LPS stimulation the following morning for 6 hours resulted in a robust production of PGs, but PG-Gs were not detected (Figure 6). Treatment of cultures with a combination of LPS and IFNγ resulted in a small amount of PG-G production. Treatment with 12-*O*-tetradecanoylphorbol-13-acetate (TPA), an activator of protein kinase c, did not result in the production of PG-Gs. However, treatment of cultures with a combination of LPS, IFNγ, and the calcium ionophore ionomycin resulted in robust production of PG-Gs. These studies were in agreement with studies by Joel Musee, which demonstrated that while PGs were produced by IFNγ or Il-1β treatment, the production of PG-Gs only occurred when stimulation was followed by ionomycin treatment. Although ionomycin was required to stimulate PG-G production, it did not produce PG-Gs without prior stimulation by IFNγ or Il-1β. This suggests that PG-G production in DRGs requires the stimulation of COX-2 expression by LPS and IFNγ and the levels of PG-Gs can be increased by subsequent stimulation of 2-AG production by ionomycin-mediated calcium influx.
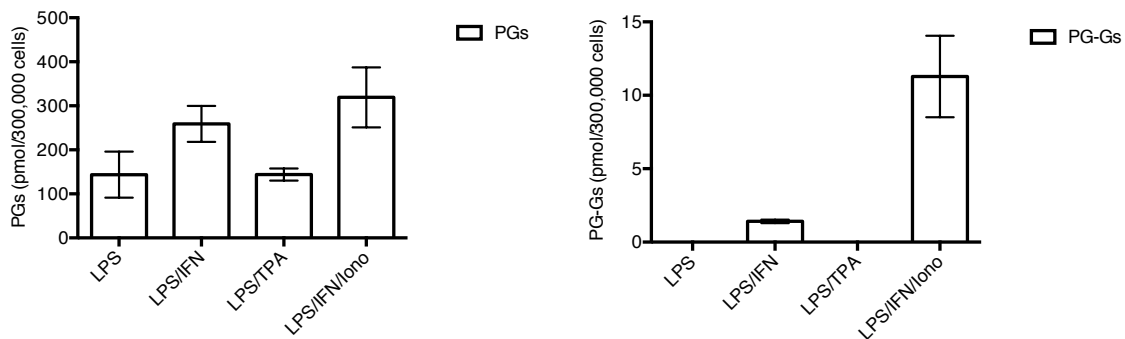
Figure 6: Production of PGs and PG-Gs in stimulated DRGs. While DRGs produce PGs in response to multiple stimulation conditions, PG-Gs are produced only by a combination of LPS and IFNγ. Treatment of cells stimulated by LPS and IFNγ with ionomycin results in a robust production of PG-Gs. Data shown are mean ± s.e.m., n = 6.

Further optimization of the stimulation conditions identified 15(*S*)-hydroxy-5,8,11,13-eicosatetraenoic acid (15(*S*)-HETE) as a potent inducer of not only PG-G, but also PG-EA production in DRGs. Treatment of DRGs with LPS, IFNγ, and 15(*S*)-HETE followed by ionomycin lead to a strong induction of COX-2 but did not alter the expression of COX-1, MAGL, ABHD6, or FAAH (Figure 7). Additionally, these stimulation conditions lead to the production of PGs, PG-Gs, and PG-EAs (Figure 8). To validate the identification of PG-G and PG-EA production we utilized MS/MS fragmentation to compare the fragmentation spectra from stimulated

DRGs to synthetic standards (Figure 9). The production of PG-Gs and PG-EAs in DRGs is notable as this is the first example of these products being produced in neuronal cells in response to endogenously generated 2-AG and AEA. Thus, we identified stimulation conditions that lead to the production of PGs, PG-Gs, and PG-EAs in DRGs.
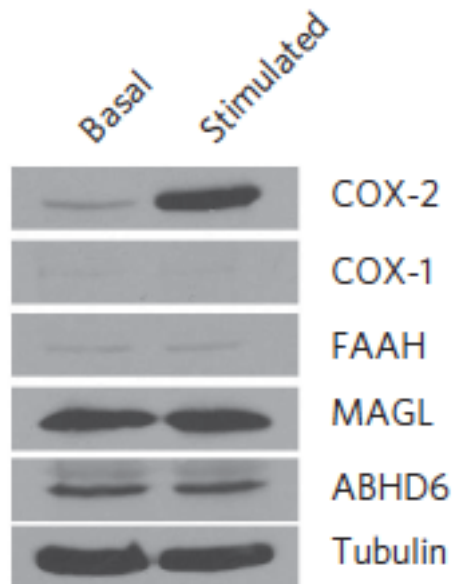
Figure 7: Expression of endocannabinoid metabolizing enzymes in basal and stimulated DRGs. While COX-2 expression is increased in stimulated cells, the expression of COX-1, FAAH, MAGL, and ABHD6 are unchanged. Reproduced from.[59]
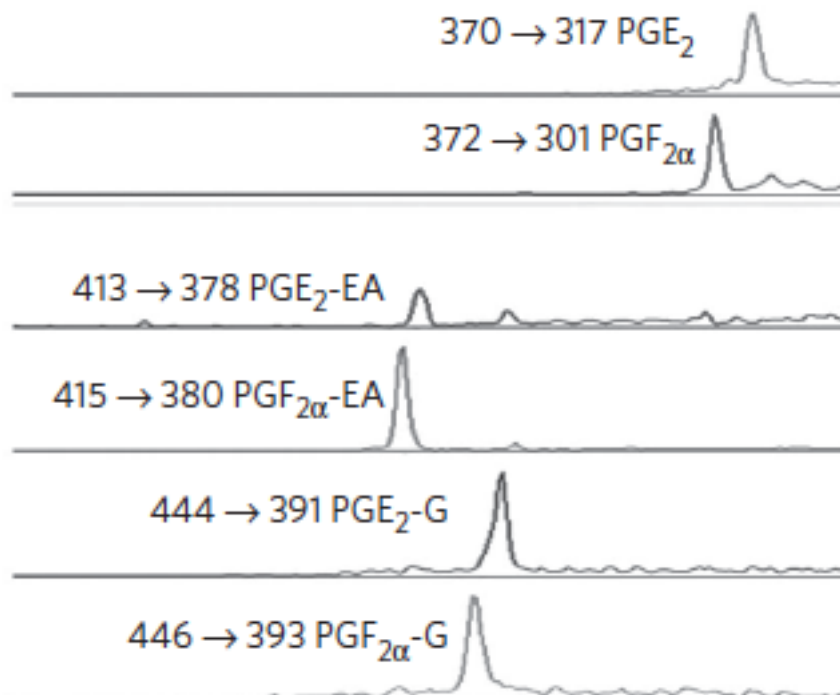
Figure 8: Representative LC-MS/MS chromatogram from stimulated DRGs detecting PGs, PG-EAs, and PG-Gs. Stimulation of DRGs with GM-CSF, LPS, IFNγ, 15(S)-HETE, and ionomycin leads to the production of PGs, PG-EAs, and PG-Gs. Reproduced from.[59]
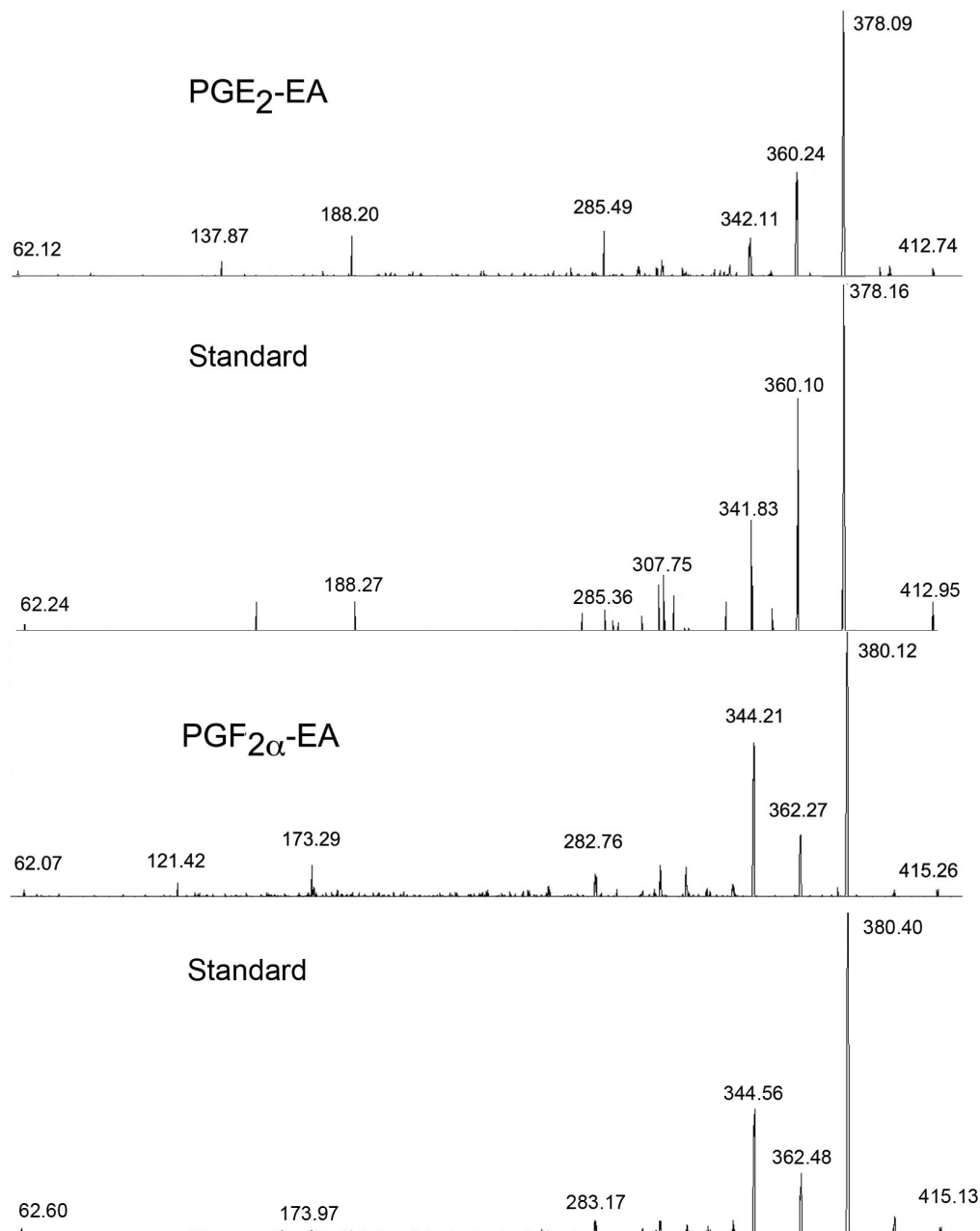
Figure 9: MS/MS spectra of PGE$_2$-EA and PGF$_{2\alpha}$-EA. Validation of the identification of PGE$_2$-EA and PGF$_{2\alpha}$-EA generated by DRGs by matching MS/MS fragmentation patterns with synthetic standards of PGE$_2$-EA and PGF$_{2\alpha}$-EA. Reproduced from.[59]

We next analyzed the ability of pure neuronal DRG cultures and pure glial DRG cultures to produce PGs, PG-Gs, and PG-EAs in response to stimulation. Pure neuronal DRG cultures were generated by treating DRG cultures with 5 μM arabinoside for 7 days and pure glial DRG cultures were generated by culturing the DRGs in media lacking NGF. Stimulation of DRG cultures containing both neurons and glia resulted in the production of PGs, PG-Gs, and PG-EAs (Figure 10). However, stimulation of DRG cultures containing only glia or only neurons resulting in a significant blunting of the production of PGs, PG-Gs, and PG-EAs. This

suggests that the stimulation of COX-2 expression, release of substrates, and production of PG products

requires both neurons and glia.
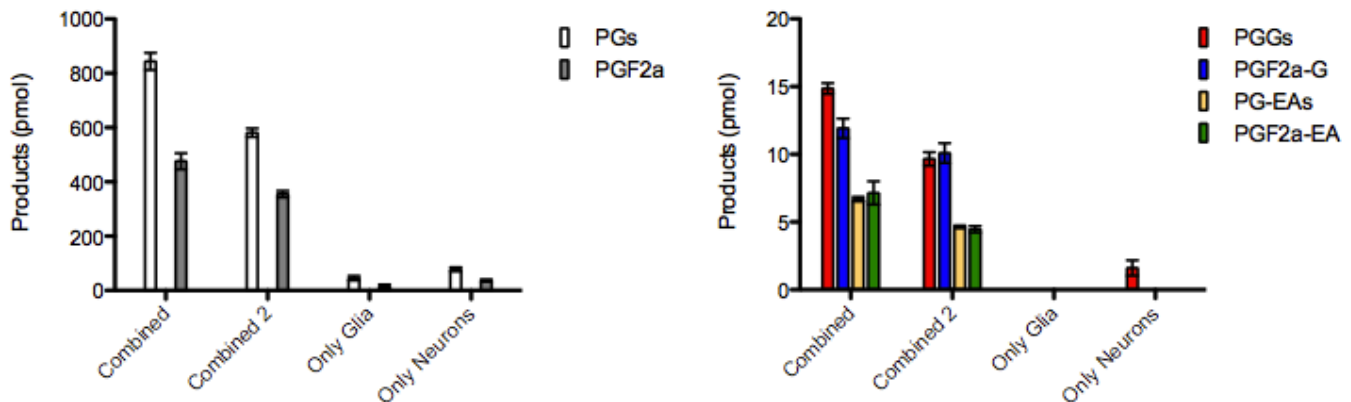
Figure 10: Production of PGs, PG-Gs, and PG-EAs in DRG cultures containing neurons and glia, only glia, and only neurons. While cultures containing both neurons and glia produced PGs, PG-Gs, and PG-EAs, cultures containing only glia or only neurons did not display robust production after stimulation. Values shown are mean ± s.e.m., n = 3.

To further explore the roles of glia and neurons in the production of PGs, PG-Gs, and PG-EAs we

sought to determine the localization of COX-2 after stimulation. To do this we utilized Fluorocoxib A, a COX-2

selective inhibitor conjugated to a fluorescent tag.[47] We stimulated DRG cultures and then incubated them with

Fluruocoxib A to visualize COX-2, TuJ1 to visualize neurons, and DAPI to visualize cell nuclei (Figure 11).

Surprisingly, COX-2 was localized mainly in neurons as evidenced by a co-localization of Fluorocoxib A

staining with TuJ1 fluorescence. This suggests that although both neurons and glia are required for the

production of PGs, PG-Gs, and PG-EAs, the site of biosynthesis by COX-2 is in neurons. The role that glia play

in the production of PGs, PG-Gs, and PG-EAs is essential, but COX-2 is clearly not expressed in glial cells to

the extent that it is expressed in neurons.
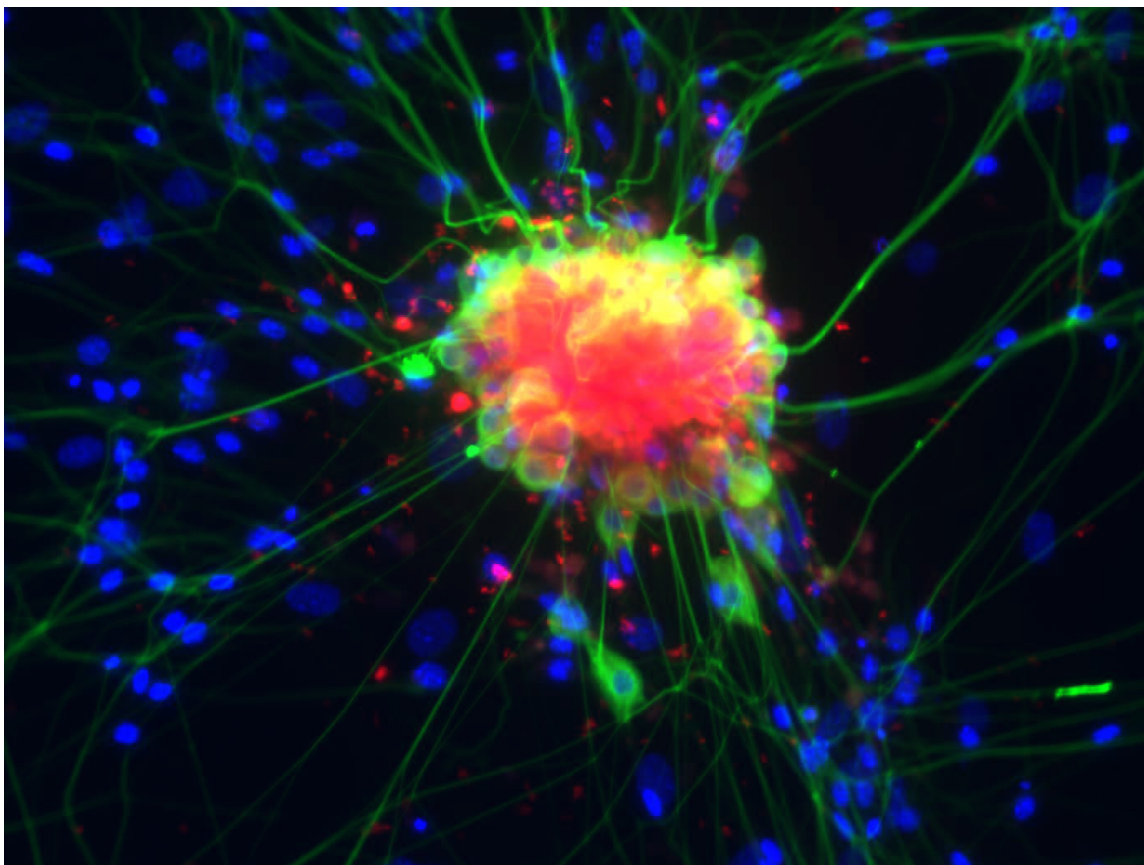
Figure 11: Fluorescent labeling of neurons, glia, and COX-2 in stimulated DRG cultures. COX-2 expression was labeled using Fluorocoxib A (red), neurons were labeled with TuJ1 (green), and cell nuclei were labeled with DAPI (blue).

Assessment of substrate-selective inhibitors in DRG cultures

After optimizing the stimulation conditions that produce PGs, PG-Gs, and PG-EAs in DRGs we sought to determine the effects of the (*R*)-profens on DRGs. As discussed in chapter II and above, the (*R*)-profens are substrate-selective inhibitors of COX-2 *in vitro*. In agreement with the *in vitro* data, (*R*)-flurbiprofen, (*R*)-naproxen, and (*R*)-ibuprofen all display a concentration-dependent decrease in the production of PG-Gs and PG-EAs in DRGs while not inhibiting PG production (Figure 12). Thus, the (*R*)-profens retain substrate-selective inhibition in a cellular setting.
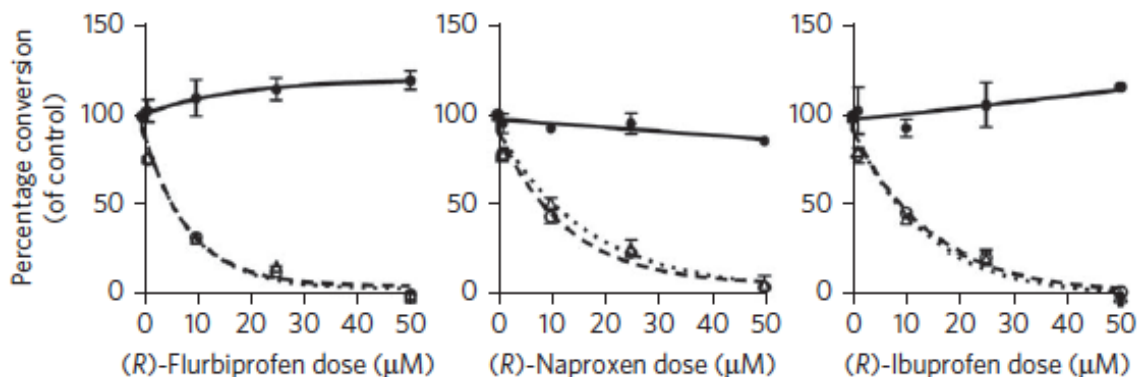
Figure 12: Substrate-selective inhibition by (*R*)-profens in stimulated DRGs. The (*R*)-profens decrease the production of PG-Gs (dashed lines) and PG-EAs (dotted lines) but do not inhibit PG formation (solid lines) in DRGs. Data shown are mean ± s.e.m., n = 6. Reproduced from.[59]

To determine if substrate-selective COX-2 inhibition also modulates endocannabinoid levels in DRGs, as it modulates 2-AG levels in RAW 264.7 cells, we also measured the levels of AA, AEA, and 2-AG upon treatment of basal and stimulated DRGs with the (*R*)-profens. The (*R*)-profens had no significant effect on AA, AEA, or 2-AG in basal DRGs (Figure 13). However, in stimulated DRGs all three (*R*)-profens increased the levels of AEA and 2-AG in a concentration-dependent manner while having no significant effect on AA. Thus, the (*R*)-profens modulate the levels of not only PG-EAs and PG-Gs through substrate-selective COX-2 inhibition, but also the levels of the endocannabinoids AEA and 2-AG. The effects of the (*R*)-profens on AEA and 2-AG are dependent upon the stimulation of COX-2 expression in DRGs, implicating COX-2 as a mediator of endocannabinoid tone under inflammatory settings in primary neuronal cultures. These studies identify DRGs as a novel cellular model for studying substrate-selective inhibition and elucidate a novel function of COX-2.
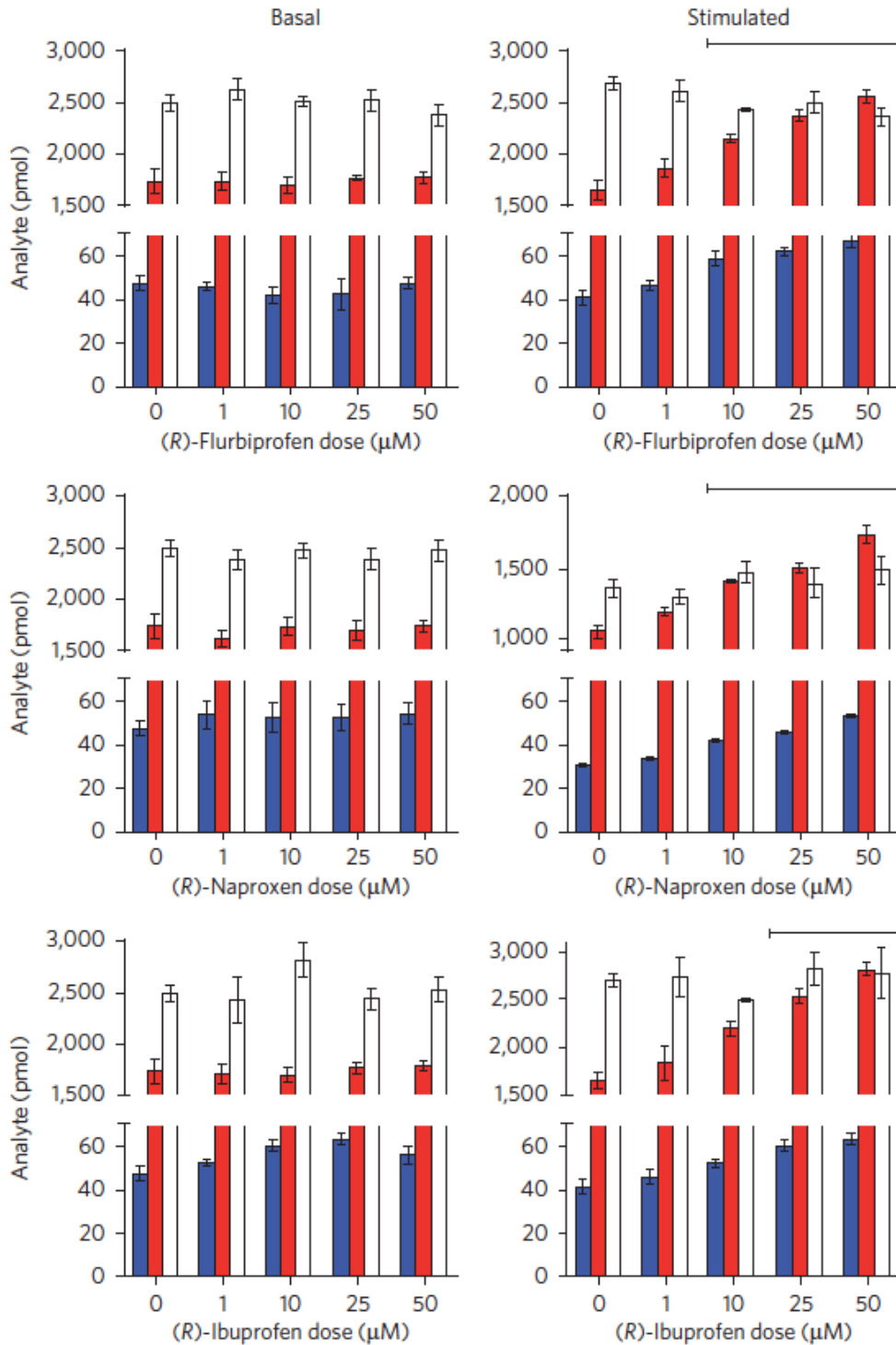
Figure 13: Comparison of the effects of the (R)-profens on AEA, 2-AG, and AA concentrations in basal and stimulated DRGs. The (R)-profens significantly increase the levels of AEA (blue) and 2-AG (red), but not AA (white), in stimulated DRGs in a concentration-dependent manner. In contrast, the (R)-profens have no significant effect on any of the analytes in basal DRGs. Data shown are mean ± s.e.m., n = 6.

<center>Discussion</center>

COX-2 oxygenation of 2-AG and AEA leads to the degradation of analgesic and anti-inflammatory lipids. The oxidative products of 2-AG and AEA, PG-Gs and PG-EAs, have a range of biological activities including calcium mobilization, hyperalgesia, and regulation of synaptic signaling, among others.[21,23,60,61] While the receptors that mediate these effects have not been identified, they are distinct from classical PG and cannabinoid receptors.[21,62] Thus, oxygenation of endocannabinoids by COX-2 degrades a series of antinociceptive lipids and generates a series of nociceptive lipid signaling molecules. This implicates COX-2 oxygenation of AEA and 2-AG in the pathology of neuropathic pain and suggests that inhibition of COX-2 could have therapeutic effects.

While NSAIDs have already been extensively validated as analgesic and anti-inflammatory in multiple settings, including neuropathic pain, substrate-selective inhibition represents a novel approach to COX-2 inhibition. While under normal conditions the levels of AEA are regulated by FAAH and the levels of 2-AG are regulated by MAGL, the stimulation-dependent effects of the (R)-profens on endocannabinoid levels suggests that COX-2 regulates endocannabinoids in a state-dependent manner. The augmentation of AEA and 2-AG and inhibition of PG-G and PG-EA synthesis produced by the (R)-profens in stimulated DRGs suggests that they may also have analgesic and anti-inflammatory effects in neuropathic pain. These effects may be mediated by multiple mechanisms including increased cannabinoid receptor signaling mediated by an increase endocannabinoid levels or a reduction in pro-inflammatory and nociceptive PG-Gs and/or PG-EAs. Indeed, previous reports have already identified (R)-flurbiprofen as having endocannabinoid-mediated therapeutic effects in neuropathic pain models.[63-65]

Substrate-selective COX-2 inhibitors are also important tools to test the biological functions of PG-Gs and PG-EAs without confounding PG inhibition. These studies identify the (R)-profens as robust substrate-selective inhibitors not only *in vitro*, but also in cellular systems. The complete lack of PG inhibition exhibited by the (R)-profens makes them valuable probes for identifying the contributions of COX-2 to cellular physiology or pathophysiology by uncoupling COX-2-mediated endocannabinoid oxygenation from AA oxygenation.

<center>80</center>

Many studies have identified increases in COX-2 in the peripheral and central nervous system after injury and inflammation.[14,57,66] These studies suggest that elevation of COX-2 in the peripheral or central nervous system may lead to the depletion of AEA and 2-AG and contribute to the development and progression of neuropathic pain. Thus, substrate-selective inhibition of COX-2 by (R)-profens could reverse this depletion of endocannabinoids and produce analgesic effects not only from removing hyperalgesic products such as PGE_2-G, but also augmenting the pro-analgesic endocannabinoids. The hypothesis that substrate-selective inhibition of COX-2 can increase endocannabinoid tone and produce therapeutic effects is supported by the blockade of the analgesic effects of (R)-flurbiprofen by CB_1 receptor antagonists.[63]

References

1. Devane, W.A.*, et al.* Isolation and structure of a brain constituent that binds to the cannabinoid receptor. *Science* **258**, 1946-1949 (1992).
2. Sugiura, T.*, et al.* 2-Arachidonoylglycerol: a possible endogenous cannabinoid receptor ligand in brain. *Biochem Biophys Res Commun* **215**, 89-97 (1995).
3. Piomelli, D. The molecular logic of endocannabinoid signalling. *Nat Rev Neurosci* **4**, 873-884 (2003).
4. Shoemaker, J.L., Ruckle, M.B., Mayeux, P.R. & Prather, P.L. Agonist-directed trafficking of response by endocannabinoids acting at CB2 receptors. *Journal of Pharmacology and Experimental Therapeutics* **315**, 828-838 (2005).
5. Bouaboula, M.*, et al.* Signaling pathway associated with stimulation of CB2 peripheral cannabinoid receptor - Involvement of both mitogen-activated protein kinase and induction of Krox-24 expression. *Eur J Biochem* **237**, 704-711 (1996).
6. Pertwee, R.G. The pharmacology of cannabinoid receptors and their ligands: an overview. *Int J Obesity* **30**, S13-S18 (2006).
7. Herkenham, M.*, et al.* Cannabinoid receptor localization in brain. *Proc Natl Acad Sci U S A* **87**, 1932-1936 (1990).
8. Caulfield, M.P. & Brown, D.A. Cannabinoid Receptor Agonists Inhibit Ca Current in Ng108-15 Neuroblastoma-Cells Via a Pertussis Toxin-Sensitive Mechanism. *British journal of pharmacology* **106**, 231-232 (1992).
9. Galiegue, S.*, et al.* Expression of Central and Peripheral Cannabinoid Receptors in Human Immune Tissues and Leukocyte Subpopulations. *Eur J Biochem* **232**, 54-61 (1995).
10. Basu, S., Ray, A. & Dittel, B.N. Cannabinoid Receptor 2 Is Critical for the Homing and Retention of Marginal Zone B Lineage Cells and for Efficient T-Independent Immune Responses. *J Immunol* **187**, 5720-5732 (2011).
11. Jennings, E.A., Vaughan, C.W. & Christie, M.J. Cannabinoid actions on rat superficial medullary dorsal horn neurons in vitro. *J Physiol* **534**, 805-812 (2001).
12. Meng, I.D., Manning, B.H., Martin, W.J. & Fields, H.L. An analgesia circuit activated by cannabinoids. *Nature* **395**, 381-383 (1998).
13. Lichtman, A.H., Cook, S.A. & Martin, B.R. Investigation of brain sites mediating cannabinoid-induced antinociception in rats: evidence supporting periaqueductal gray involvement. *J Pharmacol Exp Ther* **276**, 585-593 (1996).
14. Amaya, F., Samad, T.A., Barrett, L., Broom, D.C. & Woolf, C.J. Periganglionic inflammation elicits a distally radiating pain hypersensitivity by promoting COX-2 induction in the dorsal root ganglion. *Pain* **142**, 59-67 (2009).
15. Zhang, J. & Chen, C. Endocannabinoid 2-arachidonoylglycerol protects neurons by limiting COX-2 elevation. *J Biol Chem* **283**, 22601-22611 (2008).
16. Tegeder, I., Niederberger, E., Vetter, G., Brautigam, L. & Geisslinger, G. Effects of selective COX-1 and -2 inhibition on formalin-evoked nociceptive behaviour and prostaglandin E(2) release in the spinal cord. *J Neurochem* **79**, 777-786 (2001).
17. Yaksh, T.L.*, et al.* The acute antihyperalgesic action of nonsteroidal, anti-inflammatory drugs and release of spinal prostaglandin E2 is mediated by the inhibition of constitutive spinal cyclooxygenase-2 (COX-2) but not COX-1. *J Neurosci* **21**, 5847-5853 (2001).
18. Samad, T.A.*, et al.* Interleukin-1beta-mediated induction of Cox-2 in the CNS contributes to inflammatory pain hypersensitivity. *Nature* **410**, 471-475 (2001).
19. Yu, M., Ives, D. & Ramesha, C.S. Synthesis of prostaglandin E-2 ethanolamide from anandamide by cyclooxygenase-2. *Journal of Biological Chemistry* **272**, 21181-21186 (1997).
20. Kozak, K.R., Rowlinson, S.W. & Marnett, L.J. Oxygenation of the endocannabinoid, 2-arachidonylglycerol, to glyceryl prostaglandins by cyclooxygenase-2. *Journal of Biological Chemistry* **275**, 33744-33749 (2000).

21.   Nirodi, C.S., Crews, B.C., Kozak, K.R., Morrow, J.D. & Marnett, L.J. The glyceryl ester of prostaglandin E2 mobilizes calcium and activates signal transduction in RAW264.7 cells. *Proc Natl Acad Sci U S A* **101**, 1840-1845 (2004).

22.   Richie-Jannetta, R.*, et al.* Structural determinants for calcium mobilization by prostaglandin E2 and prostaglandin F2alpha glyceryl esters in RAW 264.7 cells and H1819 cells. *Prostaglandins Other Lipid Mediat* **92**, 19-24 (2010).

23.   Hu, S.S., Bradshaw, H.B., Chen, J.S., Tan, B. & Walker, J.M. Prostaglandin E(2) glycerol ester, an endogenous COX-2 metabolite of 2-arachidonoylglycerol, induces hyperalgesia and modulates NFkappaB activity. *British journal of pharmacology* (2008).

24.   Cravatt, B.F.*, et al.* Molecular characterization of an enzyme that degrades neuromodulatory fatty-acid amides. *Nature* **384**, 83-87 (1996).

25.   Kurahashi, Y., Ueda, N., Suzuki, H., Suzuki, M. & Yamamoto, S. Reversible hydrolysis and synthesis of anandamide demonstrated by recombinant rat fatty-acid amide hydrolase. *Biochem Bioph Res Co* **237**, 512-515 (1997).

26.   Thomas, E.A., Cravatt, B.F., Danielson, P.E., Gilula, N.B. & Sutcliffe, J.G. Fatty acid amide hydrolase, the degradative enzyme for anandamide and oleamide, has selective distribution in neurons within the rat central nervous system. *J Neurosci Res* **50**, 1047-1052 (1997).

27.   Kano, M., Ohno-Shosaku, T., Hashimotodani, Y., Uchigashima, M. & Watanabe, M. Endocannabinoid-Mediated Control of Synaptic Transmission. *Physiol Rev* **89**, 309-380 (2009).

28.   Marrs, W.R.*, et al.* The serine hydrolase ABHD6 controls the accumulation and efficacy of 2-AG at cannabinoid receptors. *Nature neuroscience* **13**, 951-957 (2010).

29.   Savinainen, J.R., Saario, S.M. & Laitinen, J.T. The serine hydrolases MAGL, ABHD6 and ABHD12 as guardians of 2-arachidonoylglycerol signalling through cannabinoid receptors. *Acta physiologica* **204**, 267-276 (2012).

30.   Xie, S.*, et al.* Inactivation of lipid glyceryl ester metabolism in human THP1 monocytes/macrophages by activated organophosphorus insecticides: role of carboxylesterases 1 and 2. *Chemical research in toxicology* **23**, 1890-1904 (2010).

31.   Wang, R.*, et al.* Identification of Palmitoyl Protein Thioesterase 1 in Human THP1 Monocytes and Macrophages and Characterization of Unique Biochemical Activities for This Enzyme. *Biochemistry* **52**, 7559-7574 (2013).

32.   Kozak, K.R.*, et al.* Metabolism of the endocannabinoids, 2-arachidonylglycerol and anandamide, into prostaglandin, thromboxane, and prostacyclin glycerol esters and ethanolamides. *Journal of Biological Chemistry* **277**, 44877-44885 (2002).

33.   Kozak, K.R.*, et al.* Metabolism of prostaglandin glycerol esters and prostaglandin ethanolamides in vitro and in vivo. *Journal of Biological Chemistry* **276**, 36993-36998 (2001).

34.   Rouzer, C.A.*, et al.* Zymosan-induced glycerylprostaglandin and prostaglandin synthesis in resident peritoneal macrophages: roles of cyclo-oxygenase-1 and-2. *Biochem J* **399**, 91-99 (2006).

35.   Rouzer, C.A. & Marnett, L.J. Glycerylprostaglandin synthesis by resident peritoneal macrophages in response to a zymosan stimulus. *Journal of Biological Chemistry* **280**, 26690-26700 (2005).

36.   van Nieuwenhuijze, A.*, et al.* GM-CSF as a therapeutic target in inflammatory diseases. *Mol Immunol* **56**, 675-682 (2013).

37.   Raetz, C.R.*, et al.* Kdo2-Lipid A of Escherichia coli, a defined endotoxin that activates macrophages via TLR-4. *Journal of lipid research* **47**, 1097-1111 (2006).

38.   Netea, M.G., van Deuren, M., Kullberg, B.J., Cavaillon, J.M. & Van der Meer, J.W.M. Does the shape of lipid A determine the interaction of LPS with Toll-like receptors? *Trends Immunol* **23**, 135-139 (2002).

39.   Schroder, K., Hertzog, P.J., Ravasi, T. & Hume, D.A. Interferon-gamma: an overview of signals, mechanisms and functions. *Journal of leukocyte biology* **75**, 163-189 (2004).

40.   Liu, C.M. & Hermann, T.E. Characterization of Ionomycin as a Calcium Ionophore. *Journal of Biological Chemistry* **253**, 5892-5894 (1978).

41. Zaki, A.M., Galatowicz, G. & Calder, V.L. Differential cytokine profiles in response to Fc epsilon RI cross-linking, or PMA +/- ionomycin stimulation of mast cells. *Immunology* **140**, 209-209 (2013).

42. Howe, J.F., Loeser, J.D. & Calvin, W.H. Mechanosensitivity of Dorsal Root-Ganglia and Chronically Injured Axons - Physiological Basis for Radicular Pain of Nerve Root Compression. *Pain* **3**, 25-41 (1977).

43. Windsor, M.A., *et al.* Substrate-Selective Inhibition of Cyclooxygenase-2: Development and Evaluation of Achiral Profen Probes. *Acs Med Chem Lett* **3**, 759-763 (2012).

44. Blobaum, A.L. & Marnett, L.J. Molecular determinants for the selective inhibition of cyclooxygenase-2 by lumiracoxib. *Journal of Biological Chemistry* **282**, 16379-16390 (2007).

45. Wu, H.H., *et al.* Glial precursors clear sensory neuron corpses during development via Jedi-1, an engulfment receptor. *Nature neuroscience* **12**, 1534-U1579 (2009).

46. Rouzer, C.A., *et al.* Cyclooxygenase-1-dependent prostaglandin synthesis modulates tumor necrosis factor-alpha secretion in lipopolysaccharide-challenged murine resident peritoneal macrophages. *J Biol Chem* **279**, 34256-34268 (2004).

47. Uddin, M.J., *et al.* Selective Visualization of Cyclooxygenase-2 in Inflammation and Cancer by Targeted Fluorescent Imaging Agents. *Cancer Res* **70**, 3618-3627 (2010).

48. Kingsley, P.J. & Marnett, L.J. Analysis of endocannabinoids, their congeners and COX-2 metabolites. *J Chromatogr B* **877**, 2746-2754 (2009).

49. Kingsley, P.J. & Marnett, L.J. LC-MS-MS analysis of neutral eicosanoids. *Method Enzymol* **433**, 91-+ (2007).

50. Kingsley, P.J., Rouzer, C.A., Saleh, S. & Marnett, L.J. Simultaneous analysis of prostaglandin glyceryl esters and prostaglandins by electrospray tandem mass spectrometry. *Anal Biochem* **343**, 203-211 (2005).

51. Kingsley, P.J. & Marnett, L.J. Analysis of endocannabinoids by Ag+ coordination tandem mass spectrometry. *Anal Biochem* **314**, 8-15 (2003).

52. Rouzer, C.A., Ivanova, P.T., Byrne, M.O., Brown, H.A. & Marnett, L.J. Lipid profiling reveals glycerophospholipid remodeling in zymosan-stimulated macrophages. *Biochemistry* **46**, 6026-6042 (2007).

53. Rouzer, C.A., *et al.* Lipid profiling reveals arachidonate deficiency in RAW264.7 cells: Structural and functional implications. *Biochemistry* **45**, 14795-14808 (2006).

54. Rouzer, C.A., *et al.* RAW264.7 cells lack prostaglandin-dependent autoregulation of tumor necrosis factor-alpha secretion. *Journal of lipid research* **46**, 1027-1037 (2005).

55. Rouzer, C.A., Ghebreselasie, K. & Marnett, L.J. Chemical stability of 2-arachidonylglycerol under biological conditions. *Chemistry and physics of lipids* **119**, 69-82 (2002).

56. Leipold, D.D., Kantoci, D., Murray, E.D., Jr., Quiggle, D.D. & Wechter, W.J. Bioinversion of R-flurbiprofen to S-flurbiprofen at various dose levels in rat, mouse, and monkey. *Chirality* **16**, 379-387 (2004).

57. Fehrenbacher, J.C., Burkey, T.H., Nicol, G.D. & Vasko, M.R. Tumor necrosis factor alpha and interleukin-1beta stimulate the expression of cyclooxygenase II but do not alter prostaglandin E2 receptor mRNA levels in cultured dorsal root ganglia cells. *Pain* **113**, 113-122 (2005).

58. Vikman, K.S., Hill, R.H., Backstrom, E., Robertson, B. & Kristensson, K. Interferon-gamma induces characteristics of central sensitization in spinal dorsal horn neurons in vitro. *Pain* **106**, 241-251 (2003).

59. Duggan, K.C., *et al.* (R)-Profens are substrate-selective inhibitors of endocannabinoid oxygenation by COX-2. *Nat Chem Biol* **7**, 803-809 (2011).

60. Yang, H. & Chen, C. Cyclooxygenase-2 in synaptic signaling. *Current pharmaceutical design* **14**, 1443-1451 (2008).

61. Woodward, D.F., *et al.* The pharmacology and therapeutic relevance of endocannabinoid derived cyclo-oxygenase (COX)-2 products. *Pharmacol Ther* **120**, 71-80 (2008).

62. Liang, Y., *et al.* Identification and pharmacological characterization of the prostaglandin FP receptor and FP receptor variant complexes. *British journal of pharmacology* **154**, 1079-1093 (2008).

63.   Bishay, P*., et al.* R-flurbiprofen reduces neuropathic pain in rodents by restoring endogenous cannabinoids. *PloS one* **5**, e10628 (2010).

64.   Geisslinger, G*., et al.* Inhibition of noxious stimulus-induced spinal prostaglandin E2 release by flurbiprofen enantiomers: a microdialysis study. *J Neurochem* **74**, 2094-2100 (2000).

65.   Tegeder, I*., et al.* Inhibition of NF-kappaB and AP-1 activation by R- and S-flurbiprofen. *FASEB journal : official publication of the Federation of American Societies for Experimental Biology* **15**, 595-597 (2001).

66.   Guay, J., Bateman, K., Gordon, R., Mancini, J. & Riendeau, D. Carrageenan-induced paw edema in rat elicits a predominant prostaglandin E2 (PGE2) response in the central nervous system associated with the induction of microsomal PGE2 synthase-1. *J Biol Chem* **279**, 24866-24872 (2004).

CHAPTER IV

DEVELOPMENT AND CHARACTERIZATION OF *IN VIVO*
SUBSTRATE-SELECTIVE INHIBITORS

Introduction

Two decades of intense scientific inquiry have defined a prominent role for central endogenous

cannabinoid (eCB) signaling in a variety of physiological and pathophysiological processes.[1,2] eCBs are

arachidonate-containing lipid signaling molecules that exert biological actions via activation of cannabinoid

type 1 and 2 receptors (CB_1 and CB_2), in addition to other targets including vanilloid receptor 1 (TRPV1),

peroxisome proliferator-activated receptor (PPAR), and some ion channels.[1] The two most well studied eCBs,

anandamide (AEA) and 2-arachidonoylglycerol (2-AG), are synthesized and degraded by discrete sets of

enzymes.[3-5] Elucidation of the molecular regulation of eCB metabolism has led to the development of

pharmacological tools to enhance eCB signaling and probe the therapeutic utility of eCB augmentation for a

variety of pathological conditions.[6-8]

In the brain AEA is primarily degraded by fatty acid amide hydrolase (FAAH) to ethanolamine and

arachidonic acid (AA), and pharmacological inhibition of FAAH causes robust increases in brain AEA

levels.[9,10] However, FAAH also degrades a number of non-cannabinoid N-acylethanolamides (NAEs), which

are elevated upon FAAH inhibition and active at molecular targets such as PPARs.[11-13] Similarly, 2-AG is

primarily degraded to AA and glycerol by monoacylglycerol lipase (MAGL), which also metabolizes a series of

monoacylglycerols (MAGs).[14] Inhibition of FAAH or MAGL has demonstrated preclinical efficacy in models

of neuropathic pain, neurodegeneration, anxiety and depression, pain, hyperemesis, and drug withdrawal

syndromes, many of which are mediated by CB receptor-dependent mechanisms.[6,8,15-18] These studies

demonstrate the pleiotropic therapeutic potential of eCB augmentation via FAAH and MAGL inhibition and the

resulting modulation of cannabinoid receptor signaling.

In addition to FAAH and MAGL, a connection between COX-2 action and eCB inactivation has been

suggested by a series of converging data. Inhibition of COX-2 potentiates retrograde eCB synaptic signaling in

the hippocampus and decreases excitatory responses in a CB_1-dependent manner, revealing a functional tie

between COX-2 activity and eCB tone at central synapses.[19,20] NSAIDs inhibit the metabolism of AEA by rat cerebellar membrane preparations and extend the stability of exogenous AEA in mouse brain, suggesting that COX-2 directly metabolizes AEA *in vivo*.[21,22] COX-2 is constitutively expressed in the spinal cord and mediates tissue injury-induced hyperalgesia.[23] The NSAIDs indomethacin and nimesulide produce eCB-mediated spinal antinociception as evidenced by blockade of antinociceptive effects by the CB_1 receptor antagonist AM251.[24,25] The peripheral antinociceptive effects of AEA and NSAIDs are synergistic and ibuprofen interacts with AEA in both acute and inflammatory pain models.[26,27] COX-2 selective inhibitors, but not COX-1 selective inhibitors, also reverse spinal hyperexcitability in a CB_1 receptor-dependent manner and reduce the breakdown of 2-AG.[28] These studies indicate that COX-2 plays a fundamental role as an eCB-inactivating enzyme in multiple settings and across a series of tissues.

Direct evidence of COX-2 as an eCB metabolizing enzyme has also been published. In addition to the oxygenation of AA, COX-2 also catalyzes the oxygenation of AEA and 2-AG to form prostaglandin ethanolamides (PG-EAs) and prostaglandin glyceryl esters (PG-Gs), respectively.[29,30] While PGH_2 is converted to PGE_2, PGD_2, $PGF_{2\alpha}$, PGI_2, and TxA_2 by downstream synthases, PGH_2-EA and PGH_2-G are not good substrates for thromboxane synthase; thus, they each only form four of the five downstream products.[31] The production of PG-EAs has been demonstrated in several settings including in FAAH knockout mice treated with AEA, lipopolysaccharide-stimulated mouse dorsal root ganglia cultures, mouse renal medulla, rat spinal cord, and in mouse adipocytes.[32-36] PG-Gs have been detected in rat paws and multiple stimulated macrophage cell lines including RAW 264.7 cells, resident peritoneal macrophages, and J774 macrophages.[37-39] Several studies have demonstrated that PG-Gs are unstable due to enzymatic hydrolysis to PGs, which may account for the fewer reports of their formation *in vivo* compared to PG-EAs.[40-42]

While the two subunits of COX-2 are sequence homodimers, the heme prosthetic group binds to only a single monomer, creating functional heterodimers. The heme-containing subunit is the catalytic subunit, whereas the non-heme-containing subunit is the allosteric subunit.[43,44] Binding of substrates, activators, and inhibitors to the allosteric subunit alters binding in the catalytic subunit through subunit communication via the dimer interface.[45] COX-2 inhibitors bind in one of two kinetic modes, rapid-reversible or slow-tight binding.

Compounds that are rapid-reversible inhibitors of COX-2 inhibit eCB oxygenation at concentrations that are orders of magnitude lower than the concentrations required for inhibition of AA oxygenation, a phenomenon termed substrate-selective COX-2 inhibition.[46] Substrate-selective inhibitors bind in the allosteric subunit and induce a conformational change that blocks eCB oxidation in the catalytic subunit. Binding of a second inhibitor molecule in the catalytic subunit blocks AA oxygenation, but this typically occurs at inhibitor concentrations orders of magnitude higher than the concentrations that block eCB oxygenation.[46] Slow, tight-binding inhibitors bind in the catalytic subunit and block the oxygenation of all substrates at similar concentrations.[47,48]

Substrate-selective COX-2 inhibition represents a novel pharmacological approach to COX-2 inhibition by inhibiting the oxygenation of 2-AG and AEA but not AA.[33,46,49] Substrate-selective inhibition has been utilized to identify novel functions of eCB-derived prostanoids including that PGD_2-G exhibits anti-inflammatory activity in isolated macrophages and *in vivo* and $PGF_{2\alpha}$-EA negatively regulates adipogenesis.[36,39] Here we sought to determine the effects of different modes of COX inhibition, including substrate-selective COX-2 inhibition, *in vivo*.

Experimental Procedures

Materials

Indomethacin and (*S*)-flurbiprofen were purchased from Sigma Aldrich Chemical (St. Louis, MO). (*R*)-flurbiprofen, NS-398, SC-560, JZL-184, PF-3845, URB597, PGE_2–d_4, AA-d_8, 2-AG-d_8, and AEA-d_8 were purchased from Cayman Chemical (Ann Arbor, MI). Indomethacin analogs, including LM-4131, were synthesized as previously described.[50]

In vitro enzyme purification and activity assays

Wild-type, R120Q, and Y355F COX-2 were expressed in insect cells and purified as described previously.[51] *In vitro* COX-2 inhibition assays were performed as previously described.[33] The RAW 264.7 macrophage inhibition assay was performed as previously described.[52] MAGL was purified using BL21(DE3) pLysS E. coli transformed with pET-45b(+) plasmid containing human MGL-His. Cells were grown at 37ºC to a density of 0.7 OD and then protein expression induced with IPTG (1 mM). Cells were harvested 4 hr later and proteins

purified using Ni-NTA Agarose (Qiagen) as previously described.[53] After purification, the protein was dialyzed overnight at 4ºC into buffer containing 10 mM HEPES and 0.01% TritonX-100. MAGL inhibition was assessed as previously described.[53] Humanized rat FAAH was a generous gift of R. Stevens and B. Cravatt (The Scripps Research Institute). FAAH inhibition was assessed as previously described.[54] Human DAGLα in pcDNA3.1D was expressed in HEK293T cells for 24 hours then harvested and membranes prepared as described previously.[55] DAGLα activity was assessed using 5μg of membrane protein in a 50 ul reaction of assay buffer containing 50 mM MES (pH 6.5) and 2.5 mM $CaCl_2$. 1-steroyl-2-arachidonoyl glycerol (SAG) was added directly from a 100% methanol stock for a final concentration of 250 μM (5% final concentration of methanol in reaction). The reaction was terminated after 15 min by the addition of 200 μl methanol containing 125 pmol 2-AG-d_8. The samples were spun down at 2000 xg and the soluble material injected directly for LC/MS/MS analysis.

Animals

5-7 week old male ICR mice were used for all experiments with the exception of knockout animals (Harlan, Indianapolis, IN). Mice were housed 5 per cage. All behavioral tests were conducted during the light cycle between 0900 and 1700. Knockout and wild-type littermate controls for $FAAH^{-/-}$ and $COX-2^{-/-}$ mice were derived from heterozygote breeding pairs, bred and genotyped as previously described.[32,56] $CB_1^{-/-}$ mice were bred from homozygote breeding pairs and genotyped as previously described.[57] Mice were group-housed on a 12:12 light-dark cycle (lights on at 06:00), with food and water available *ad libitum*. All animal studies were approved by the Vanderbilt Institutional Animal Care and Use Committee and conducted in accordance with the NIH Guide for the Care and Use of Laboratory animals.

Tissue preparation and lipid extraction

Mice were sacrificed by cervical dislocation and decapitation. The brain, lungs, liver, stomach, small intestines, heart, and kidneys were then rapidly removed and frozen on a metal block in dry ice. The tissue was then placed in a tube and stored at -80ºC until extraction, usually one day after harvesting. For PG and eCB analysis, lipid extraction from tissue was carried out as described previously.[58]

Open field test

Animals were tested for open-field activity in a novel environment one hour after i.p. injection of compound as previously described.[59] Briefly, one-hour sessions were performed using automated experimental chambers (27.9×27.9 cm; MED-OFA-510; MED Associates, Georgia, VT) under constant illumination within a sound-attenuated room. Analysis of open field activity was performed using Activity Monitor v5.10 (MED Associates).

Light-dark box

Anxiety responses were assessed in a plastic light-dark chamber measuring 20 x 20 cm. Half of the chamber is opaque with a black Plexiglas insert; the other half remains transparent. Photocells recorded the movement of the mice between compartments. Mice were placed individually into the dark compartment at the beginning of the session. Total time spent in the light and dark compartments, the number of light to dark transitions, and total distance travelled during the 20-minute session were measured.

Elevated plus-maze

EPM analyses were conducted using Any Maze tracking software as described previously.[59]

Rectal temperature, catalepsy, and antinociception

Mice were treated with either LM 4131 (10 mg/kg) or WIN-55,212-2 (10 mg/kg), or vehicle (DMSO) by i.p. injection. Every 15 minutes, the rectal temperature of the mice was taken using a lubricated rectal thermometer for a total of 1 hour post drug injection. To test catalepsy the hindpaws of the mice were rested on a table and the front paws of the mouse were placed on a metal ring attached to a stand elevated 16 cm above the table every 15 minutes. The time for the mouse to place its front paws on the table was recorded. For the hot plate antinociception test, mice were placed on a flat surface that was electrically-heated to 55°C within an open Plexiglas tube, which was cleaned in between testing each mouse with Vimoba, a chlorine dioxide solution. The latency of the mouse to respond by shaking, hindpaw licking, jumping, or tucking of the forepaws or hindpaws after placement on the hot plate apparatus was recorded.

Novel object recognition

Mice were handled 4 days prior to training for at least 1 min per day. During pre-training, mice were placed in an open Plexiglas rectangular chamber for 10 minutes to sensitize the mice to the testing environment. Twenty-four hours later, the mice were placed into the same rectangular chamber with two identical sample objects, yellow rubber ducks, for 10 minutes in order for the mice to become familiar with the objects. During training, the sample objects were placed in opposite corners in the back of the chamber 5 cm from each wall and secured by weight to the floor of the chamber. Twenty-four hours later, the mice were placed into the chamber again with one sample or familiar object and a novel object, a white leaf statue, for 5 min. During testing, the objects were placed in opposite corners in the back of the chamber 5 cm from each wall and secured by weight to the floor of the chamber. Two hours prior to testing, the mice were treated either with vehicle (DMSO) or LM-4131 (10 mg/kg) by i.p. injection. To determine exploration time with the sample and novel objects, each mouse was timed when interacting, defined as when the nose of the mouse was in contact with the object or directed toward the object, within a 2 cm distance of the object of the sample or novel object. The time the mouse spent on top of the objects was not included in the exploration time analyses. In addition, a discrimination ratio (e.g., ratio of a mouse's interaction with a novel object to that mouse's total interaction with both sample and novel objects) was determined. If the discrimination ratio was above 0.5, it was considered that the mouse interacted more with the novel object than with the sample or familiar object.

Mass spectrometry analysis

Analytes were quantified using LC-MS/MS on a Quantum triple-quadrupole mass spectrometer in positive-ion mode using selected reaction monitoring. Detection of eicosanoids was performed as previously described.[60] For fatty acid analysis the mobile phases used were 80 µM AgOAc with 0.1% (v/v) acetic acid in H_2O (solvent A) and 120 µM AgOAc with 0.1% (v/v) acetic acid in MeOH (solvent B). The analytes were eluted using a gradient from 20% A to 99% B over 5 minutes. The transitions used were m/z 300→282 for PEA, m/z 328→310 for SEA, m/z 434→416 for OEA, m/z 456→438 for AEA, m/z 464→446 for AEA-d$_8$, m/z 331→257 for 2-PG, m/z 359→285 for 2-SG, m/z 463→389 for 2-OG, m/z 485→411 for 2-AG, m/z 493→419 for 2-AG-

d$_8$, *m/z* 519→409 for AA, and *m/z* 527→417 for AA-d$_8$. Peak areas for the analytes were normalized to the appropriate internal standard and then normalized to tissue mass for *in vivo* samples.

Statistical analysis

Statistical analysis was performed using GraphPad Prism® Version 6.0c. For determining statistical significance between groups a two-tailed t-test, one-way ANOVA, or two-way ANOVA with a Sidak's post-test analysis, or multiple t-tests with Holm-Sidak α correction for multiple comparisons was used throughout. F and P values shown correspond to the value obtained from the test used. Error bars represent S.E.M. throughout. N for each group represents number of mice, i.e. independent biological replicate. Mice were arbitrarily assigned to treatment group in a manner that resulted in approximately equal sample sizes per treatment group. Each treatment group was represented at least once per cage of mice.

<div align="center">Results</div>

In vivo effects of (R)- and (S)-flurbiprofen

We first sought to determine the effects of (*R*)- and (*S*)-flurbiprofen on brain eCBs by injecting mice with 10 mg/kg i.p. of compound or vehicle (DMSO) and harvesting the brain 4 hours later. We also treated mice with 10 mg/kg of URB-597, a FAAH inhibitor, as a comparator.[61] The brains were harvested and extracted and then analyzed for AA, 2-AG, AEA, and PGs. As expected, URB-597 significantly increased the levels of AEA while having no effect on 2-AG, AA, and PGs (Figure 1). Somewhat surprisingly, (*R*)-flurbiprofen and (*S*)-flurbiprofen also significantly increased the levels of AEA. While (*R*)-flurbiprofen and (*S*)-flurbiprofen had no significant effect on 2-AG or AA, both molecules caused significant inhibition of PG production. These results suggest that while (*R*)-flurbiprofen acts as a substrate-selective inhibitor *in vitro* and in cellular settings, in mice it does not. A likely mechanism for this lack of substrate-selective inhibition in the brain is that previous reports have found that (*R*)-flurbiprofen undergoes a one-way isomerization to (*S*)-flurbiprofen in mice.[62] Thus, (*R*)-flurbiprofen is not a suitable substrate-selective inhibitor in mice despite its utility *in vitro* and in cellular studies.
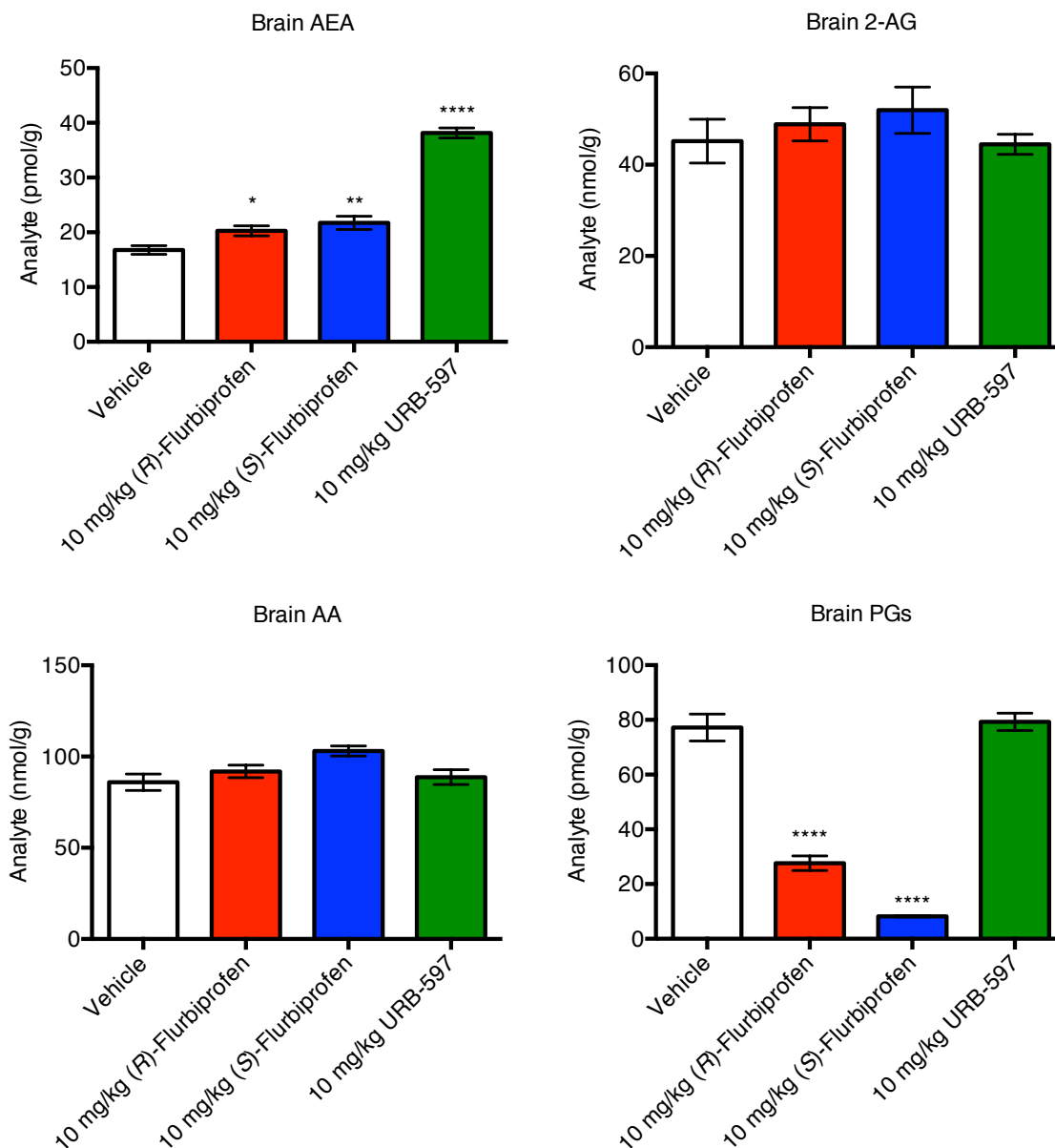
Figure 1: Effects of (*R*)-flurbiprofen, (*S*)-flurbiprofen, and URB597 on brain eCBs and PGs. Mice were treated with compounds via i.p. injection and sacrificed 4 hours later. Brain levels of eCBs and PGs were then analyzed by mass spectrometry. Data shown are mean ± s.e.m., n = 16 for vehicle, (*R*)-flurbiprofen, URB597, and n = 8 for (*S*)-flurbiprofen.

Development of novel in vivo substrate-selective inhibitors

Initial efforts to develop achiral profen analogs did not result in probes suitable for *in vivo* use, so we sought to develop substrate-selective inhibitors from alternative inhibitor scaffolds.[63] To do this, we sought to understand the key molecular interactions required for substrate-selective inhibition. Based on the studies outlined in chapter II, we hypothesized that while ion pairing and hydrogen bonding with COX-2 are required for slow, tight binding inhibition, they may be less important for rapid, reversible inhibition.

To test this hypothesis, we utilized the slow, tight binding inhibitor indomethacin, which binds to the constriction site of COX-2 via ion pairing and hydrogen bonding interactions with Arg-120 and Tyr-355.[64] In accordance with previous reports, mutation of Arg-120 to Gln or Tyr-355 to Phe resulted in abrogation of AA inhibition by indomethacin (Figure 2). Surprisingly, indomethacin still potently inhibited eCB oxygenation by the mutant proteins. Thus, removal of an interaction between indomethacin and the COX-2 active site converts it from a slow, tight-binding inhibitor to a rapid, reversible inhibitor.
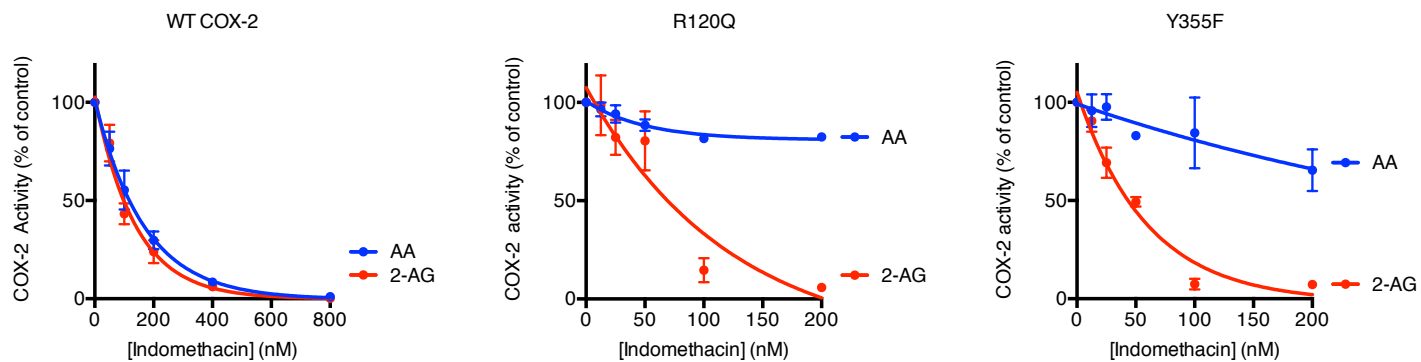
Figure 2: Indomethacin inhibition of AA and 2-AG oxygenation by wild-type, R120Q, and Y355F COX-2. Indomethacin acts as a slow, tight binding inhibitor and inhibits AA and 2-AG oxygenation with comparable IC_{50} values with wild-type COX-2. However, R120Q and Y355F mutant COX-2 causes indomethacin to become a substrate-selective inhibitor. Data shown are mean ± s.e.m., n = 3. Reproduced from.[49]

To explore the generalizability of this phenomenon, we also analyzed the ability of the slow, tight binding inhibitor diclofenac to inhibit a series of COX-2 mutants. Diclofenac binds in an inverted conformation relative to indomethacin, forming hydrogen bonds between its carboxylate and Tyr-385 and Ser-530.[65] While diclofenac inhibits the oxygenation of AA and 2-AG with comparable IC_{50} values in wild-type and R120Q COX-2, it acts as a substrate-selective inhibitor against S530A COX-2 (Figure 3). This suggests that, as with indomethacin, removal of an interaction between a slow, tight binding inhibitor and the enzyme converts it to a substrate-selective inhibitor. These studies indicate that substrate-selective inhibitors can be rationally designed by modifying the ability of slow, tight binders to interact with the active site of COX-2.
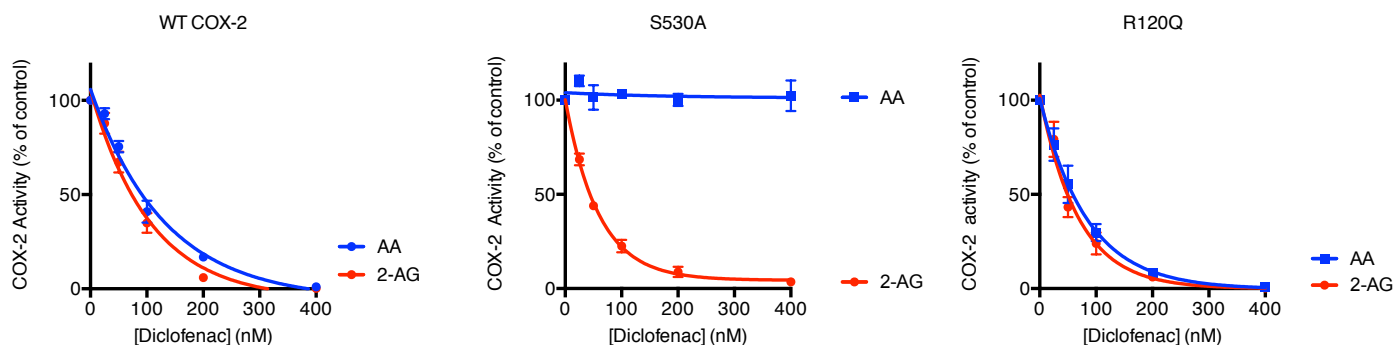
Figure 3: Inhibition of AA and 2-AG oxygenation by wild-type, S530A, and Y355F COX-2 by diclofenac. Diclofenac acts as a slow, tight binding inhibitor and inhibits AA and 2-AG oxygenation with comparable IC_{50} values with wild-type and R120Q COX-2. However, in mutant S530A COX-2 diclofenac acts as a substrate-selective inhibitor. Data shown are mean ± s.e.m., n = 3.

We sought to leverage the finding that removal of an interaction between a slow, tight binding inhibitor and COX-2 results in substrate-selective inhibition by synthesizing and screening a small library of tertiary amide derivatives of indomethacin. Modification of indomethacin to a tertiary amide results in molecules with a reduced capacity to ion-pair and hydrogen bond with Arg-120 and Tyr-355 at the constriction site. We screened the ability of these inhibitors to inhibit AA and 2-AG oxygenation by COX-2 and found that all of the tertiary amides of indomethacin exhibit substrate-selective inhibition (Table 1). In contrast, indomethacin, primary, and secondary amides of indomethacin are potent inhibitors of COX-2 oxygenation of both AA and 2-AG. This is in agreement with previous studies identifying primary and secondary amides of indomethacin as potent selective inhibitors of COX-2.[50,64] These studies identify a facile method for developing substrate-selective inhibitors from slow, tight binding inhibitors by modulation of their ability to bind to the COX-2 active site.

Table 1: Inhibition of COX-2-mediated AA and 2-AG oxygenation by indomethacin and derivatives.
While indomethacin and primary or secondary amides of indomethacin inhibit AA and 2-AG oxygenation, tertiary amides exhibit substrate-selective inhibition. Reproduced from.[49]
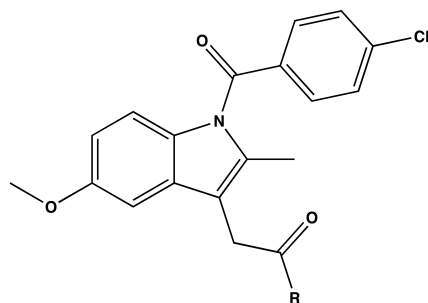
Compound	R	AA IC_{50}	2-AG IC_{50}
Indomethacin	(OH)	180 nM	30 nM
LM-4132	(NH_2)	610 nM	590 nM
LM-4101	(NH–CH₂CH₂–OH)	262 nM	237 nM
LM-4127	(N(CH₃)₂)	19 μM	524 nM
LM-4128	(N(Et)₂)	23 μM	583 nM
LM-4129	(piperidine)	>25 μM	653 nM
LM-4130	(N-methyl-phenethylamine)	>25 μM	715 nM
LM-4131	(morpholine)	>25 μM	622 nM

We selected LM-4131, the morpholino amide of indomethacin, as a candidate for further investigation. While indomethacin potently inhibits the COX-2-mediated oxygenation of AA, 2-AG, and AEA with similar potencies *in vitro*, LM-4131 selectively inhibited AEA and 2-AG oxygenation by COX-2 while displaying no inhibition of AA oxygenation (Figure 4). To further characterize LM-4131 we also analyzed its effects in stimulated RAW 264.7 cells. In stimulated RAW 264.7 cells LM-4131 selectively inhibited the production of PG-Gs with no apparent inhibition of PG production. As with (*R*)-flurbiprofen, LM-4131 also increased the levels of 2-AG but had no significant effect on AA levels in stimulated RAW 264.7 cells. These studies validate

LM-4131 as a substrate-selective inhibitor *in vitro* and in stimulated RAW 264.7 cells.
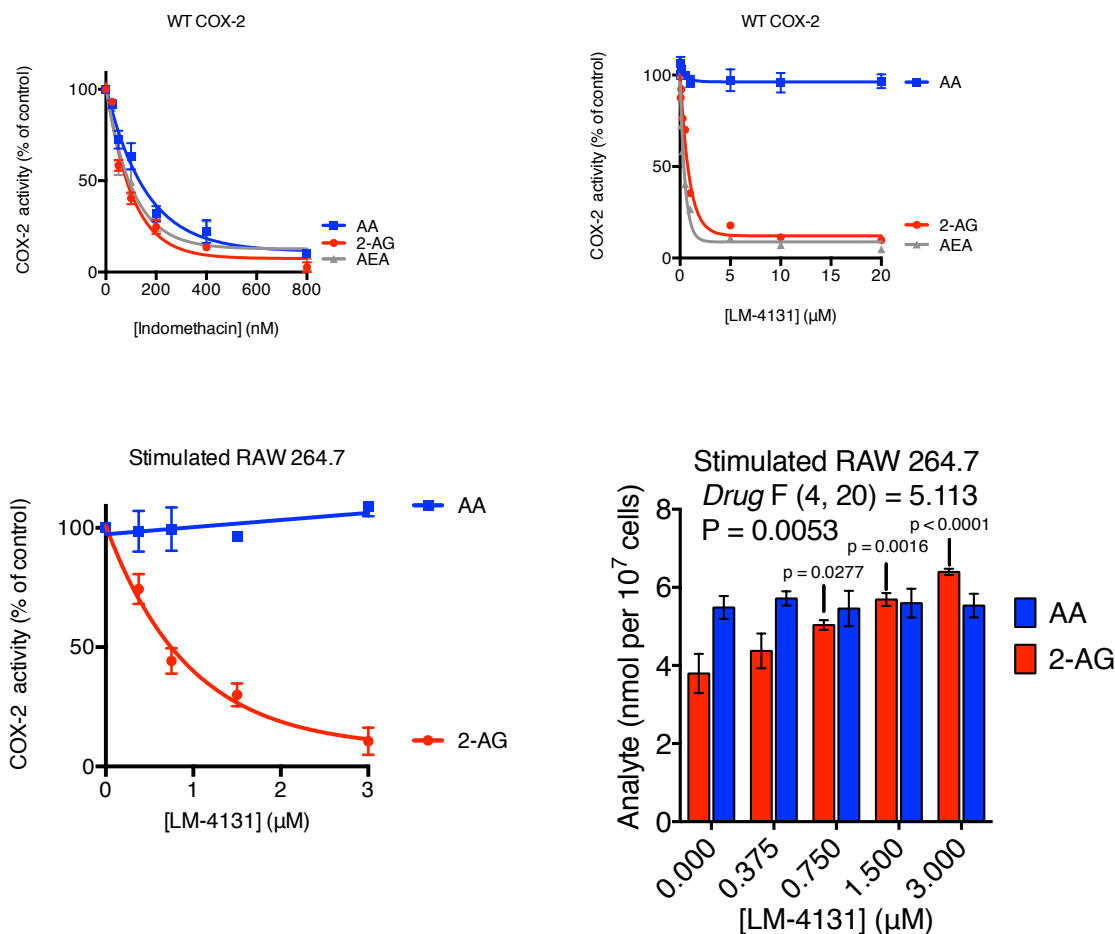
Figure 4: *In vitro* and cellular validation of substrate-selective COX-2 inhibition by LM-4131. While indomethacin potently inhibits the oxygenation of AA, 2-AG, and AEA, LM-4131 selectively inhibits the oxygenation of 2-AG and AEA. LM-4131 inhibits the production of PG-Gs and increases the levels of 2-AG in stimulated RAW 264.7 macrophages. Data shown are mean ± s.e.m., n = 3. Reproduced from.[49]

To further assess the viability of LM-4131 to serve as an *in vivo* substrate-selective inhibitor we analyzed its ability to inhibit the eCB metabolizing enzymes FAAH and MAGL *in vitro*. LM-4131 did not display inhibition of FAAH, while the previously characterized FAAH inhibitors URB597 and PF-3845 did in parallel (Figure 5). Similarly, LM-4131 did not inhibit MAGL hydrolysis of 2-AG to AA, while the previously characterized MAGL inhibitor JZL-184 displayed potent inhibition. Additionally, LM-4131 did not inhibit DAGLα, the primary synthetic source of 2-AG in the brain, while the DAGL inhibitor THL displayed robust inhibition.[66] Taken together, these *in vitro* and cellular studies validate LM-4131 as a substrate-selective COX-2 inhibitor that is selective for COX-2 inhibition over other eCB-metabolizing enzymes.
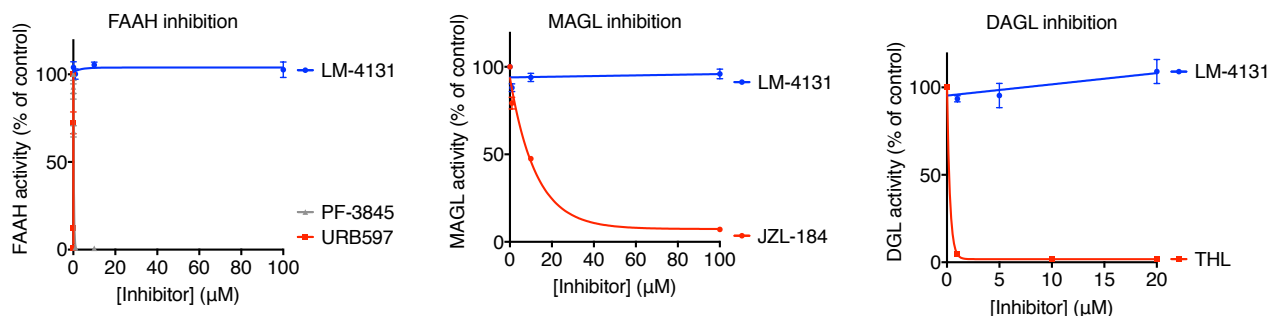
Figure 5: Inhibition of eCB metabolizing and synthetic enzymes by LM-4131. LM-4131 does not display inhibition of FAAH, MAGL, or DAGL *in vitro*. In contrast, previously identified inhibitors display robust inhibition in parallel. Data shown are mean ± s.e.m., n = 3. Reproduced from.[49]

Biochemical effects of COX inhibitors in vivo

Based on our preliminary finding that (*R*)- and (*S*)-flurbiprofen increase the levels of AEA in the brain we sought to assess the ability of LM-4131 to modulate eCB levels in the brain. LM-4131 was administered to male ICR mice via intraperitoneal injection and the mice were then sacrificed 2 hours after treatment. The brains were harvested and flash frozen on a metal block in dry ice then extracted and analyzed for eCBs, PGs, and AA levels by mass spectrometry. We first sought to determine the optimal dosing of LM-4131, by treating mice with vehicle, 0.3, 1, 3, and 10 mg/kg. LM-4131 significantly increased AEA levels at the 3 and 10 mg/kg doses with a non-significant trend to increase 2-AG at 10 mg/kg (Figure 6). Importantly, LM-4131 did not affect AA or PG levels at any of the doses tested. Thus, unlike (*R*)-flurbiprofen, LM-4131 appears to retain substrate-selective inhibition *in vivo* as it increases AEA but does not inhibit PG production in the brain.
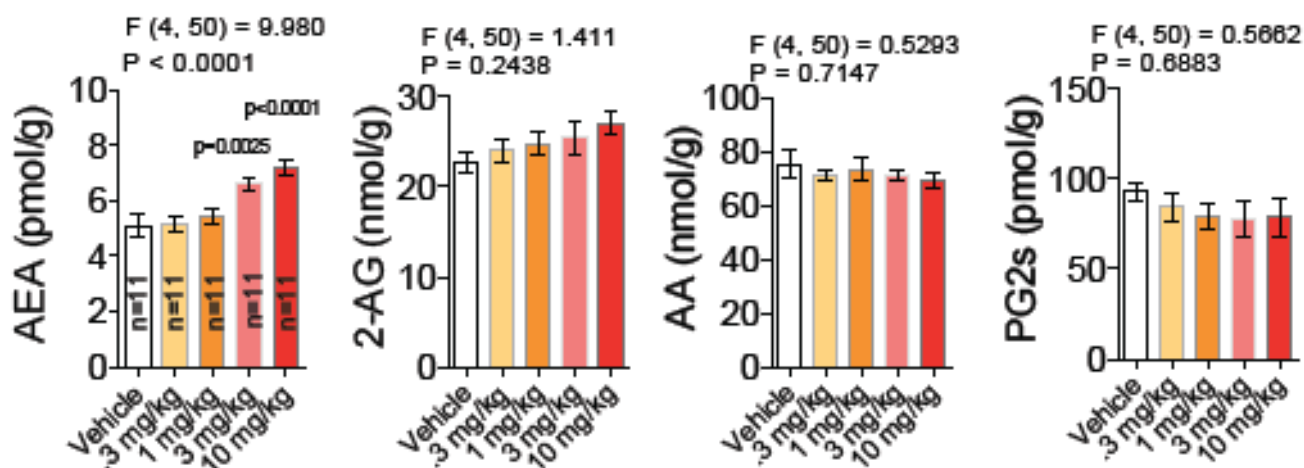
Figure 6: Dose-response of LM-4131 on brain eCBs, AA, and PGs. LM-4131 significantly increases AEA levels with a trending increase in 2-AG at higher doses. LM-4131 appears to retain substrate-selectivity as it does not modulate AA or PGs in the brain 2 hours after intraperitoneal injection. *F* and *P* values are shown for one-way ANOVA and *P* values for Dunnett's *post hoc* analysis. Data shown are mean ± s.e.m., n = 11. Reproduced from.[49]

To quantify the effects of LM-4131 treatment on brain eCBs, we conducted a meta-analysis of data obtained from 12 cohorts of mice, normalizing eCB levels in each mouse to mean eCB levels in the respective vehicle control group. This meta-analysis revealed that, on average, treatment with 10 mg/kg LM-4131 significantly increased AEA levels to 139% of those observed when treated with vehicle and increased 2-AG levels to 109% of those observed when treated with vehicle (Figure 7). Thus, LM-4131 increases the levels of AEA and 2-AG, but appears to modulate AEA levels to a greater extent than 2-AG levels based on percent change.
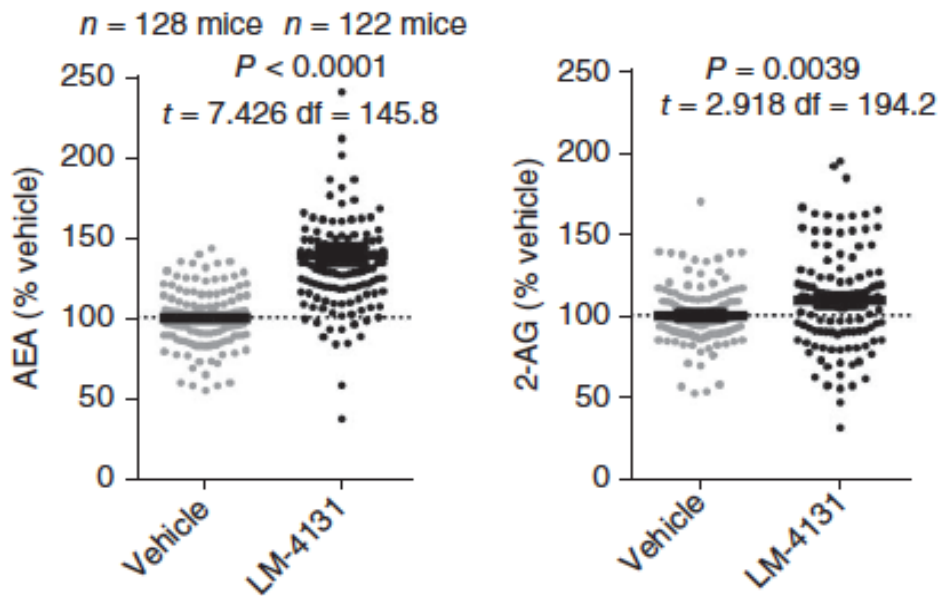
Figure 7: Meta-analysis of brain AEA and 2-AG levels after vehicle and LM-4131 treatment. LM-4131 significantly increases the levels of both AEA and 2-AG relative to vehicle treatment. Data shown are mean ± s.e.m., vehicle n = 128 and LM-4131 n = 122. Reproduced from.[49]

We also analyzed brain extracts to determine if LM-4131 was present after treatment. We found that LM-4131 was present in the brain 2 hours after treatment (Figure 8). Importantly, LM-4131 was not converted to indomethacin during this 2 hour treatment. Thus, LM-4131 selectively increases eCB levels without affecting AA or PGs in the brain 2 hours after intraperitoneal injection and is not metabolized to indomethacin within this timeframe. Therefore, LM-4131 acts as an *in vivo* substrate-selective inhibitor at 2 hours after intraperitoneal injection.
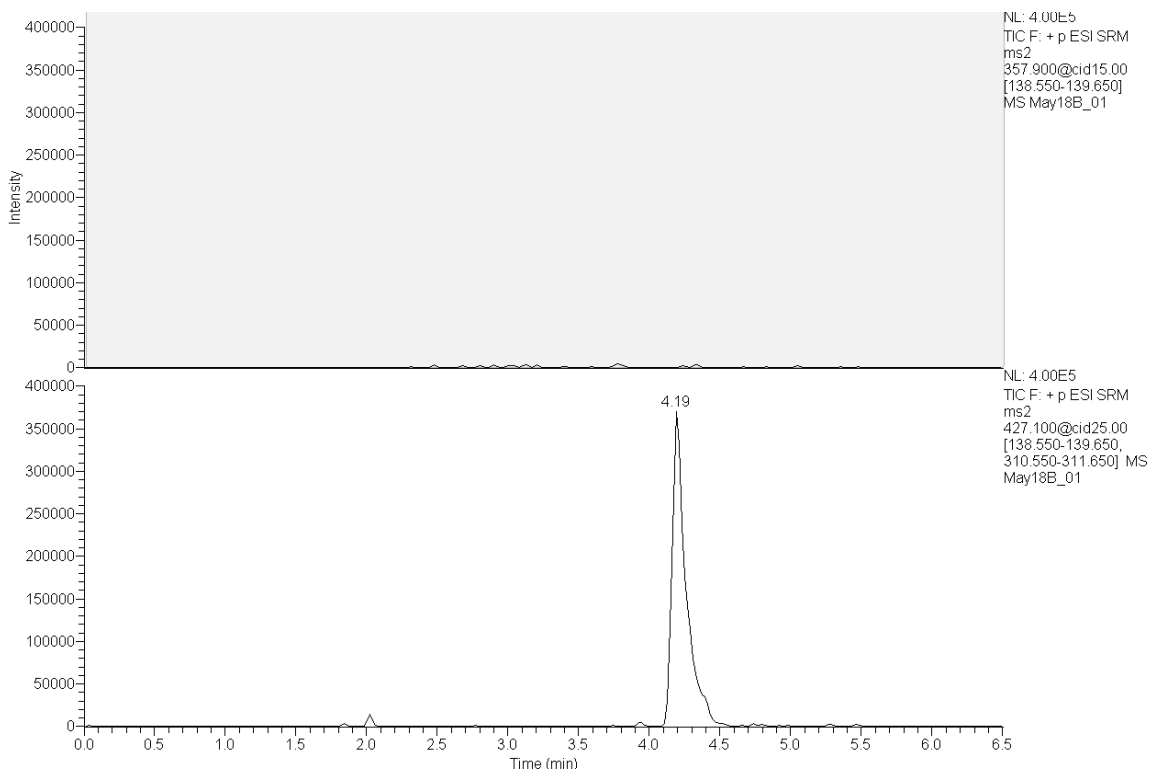
Figure 8: Detection of LM-4131 in brain 2 hours after intraperitoneal injection. Representative detection of LM-4131 in brain extract by mass spectrometry. LM-4131 (bottom) was detected using SRM LC-MS/MS with a parent ion of 427.1 and a fragment ion of 139.1 at a CID of 25. Indomethacin (top) was not detected as measured by a parent ion of 357.9 and a fragment ion of 139.1 at a CID of 15. Reproduced from.[49]

To compare the *in vivo* profile of LM-4131 to other COX inhibition modes we determined the ability of indomethacin (10 mg/kg, a nonselective COX-1/COX-2 inhibitor and the parent compound of LM-4131), the COX-2 selective inhibitor NS-398 (10 mg/kg), and the COX-1 selective inhibitor SC-560 (10 mg/kg) to modulate eCB, AA, and PG levels *in vivo*. LM-4131, indomethacin, NS-398, and SC-560 all significantly increased AEA levels, whereas only LM-4131 and indomethacin significantly increased 2-AG levels (Figure 9). Importantly, while LM-4131 had no effect on AA levels, indomethacin, NS-398, and SC-560 all significantly increased AA levels. In addition, indomethacin, NS-398, and SC-560, but not LM-4131, decreased brain PG levels. These data indicate that the *in vivo* substrate-selective pharmacological profile of LM-4131 is unique and is not shared by traditional modes of COX inhibition.
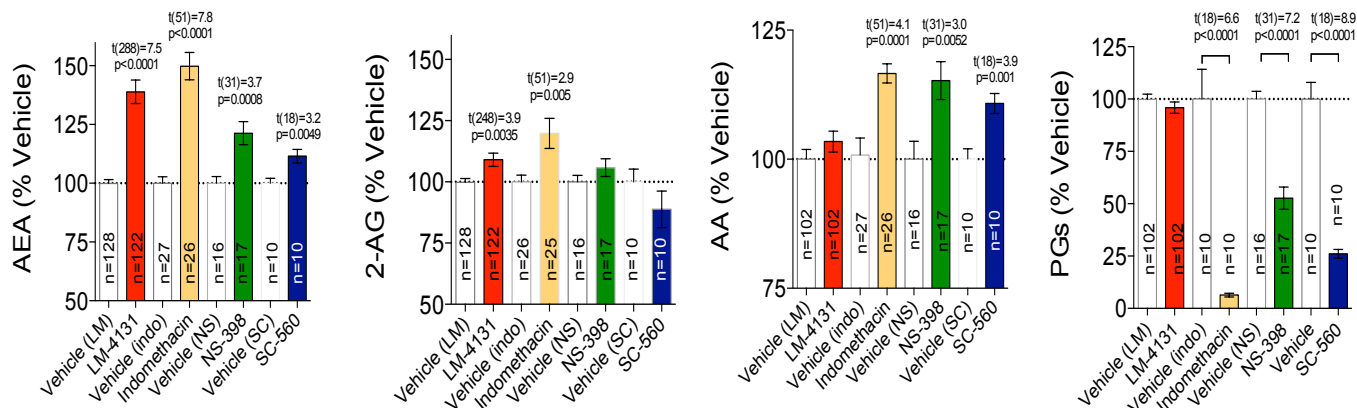
Figure 9: Differential effects of COX inhibitors on eCB, AA, and PG levels. Substrate-selective inhibition by LM-4131 has a unique biochemical profile relative to other classes of COX inhibitors. While LM-4131 significantly increases AEA and 2-AG, indomethacin, NS-398, and SC-560 significantly increase not only AEA, but also AA and significantly decrease PGs. Data shown are mean ± s.e.m., n values are shown on the bars. Reproduced from.[49]

We then sought to validate COX-2 as the *in vivo* molecular target of LM-4131. To do this we utilized

Ptgs2$^{-/-}$ mice treated with vehicle or LM-4131 (10 mg/kg) compared to wild-type littermates treated with

vehicle or LM-4131 (10 mg/kg). LM-4131 treatment significantly increased AEA and 2-AG levels in wild-type

but not *Ptgs2$^{-/-}$* littermates (Figure 10). Intriguingly, *Ptgs2$^{-/-}$* mice had significantly higher brain AEA levels

than their wild-type littermates in vehicle treated mice. LM-4131 retained the profile demonstrated in figures 6

and 9, as it increased brain AEA and 2-AG but had no effect on AA or PG levels in either wild type or *Ptgs2$^{-/-}$*

mice. Thus, LM-4131 increases brain eCB levels via a COX-2-dependent mechanism. Additionally, COX-2

regulates basal brain AEA levels *in vivo*.
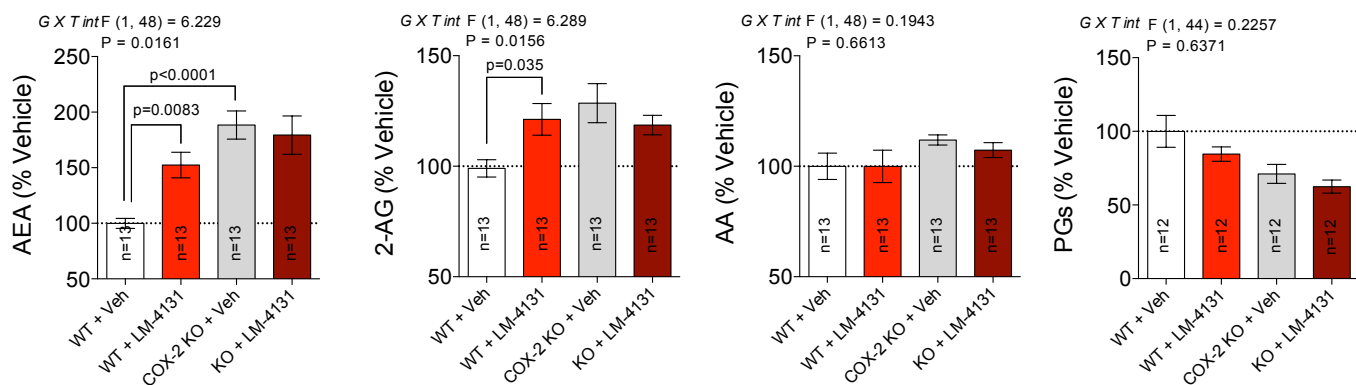
Figure 10: Effects of LM-4131 in COX-2 knockout and wild-type littermates. While LM-4131 significantly increases AEA and 2-AG in wild-type mice, it has no significant effect in COX-2 knockout littermates. Data shown are mean ± s.e.m., n values are shown on the bars. Reproduced from.[49]

Although LM-4131 increases both AEA and 2-AG, the magnitude of effect is smaller than that elicited by either FAAH or MAGL inhibition, respectively. However, a major limitation of FAAH and MAGL inhibitors is their lack of selectivity to increase eCBs over related non-eCB lipids. FAAH inhibition increases AEA levels, but also increases N-acylethanolamides (NAEs; oleoylethanolamide (OEA), palmitoylethanolamide (PEA), and stearoylethanolamide (SEA)). Similarly, MAGL inhibition increases 2-AG levels, but also increases the levels of related monoacylglcyerols (MAGs; 2-oleoylglycerol (2-OG), 2-palmitoylglycerol (2-PG), and 2-stearoylglycerol (2-SG)). Since COX-2 selectively oxygenates AA-containing lipids, we hypothesized that LM-4131 could be selective for increasing AEA and 2-AG levels over those of other NAEs and MAGs. We conducted targeted lipid profiling of NAEs and MAGs after LM-4131 treatment, and while LM-4131 significantly increased brain AEA levels, it did not increase the levels of other NAEs (Figure 11). In contrast, the FAAH inhibitor PF-3845 (10 m/kg) increases the levels of all NAEs, including AEA.[67,68] Thus, LM-4131 selectively increases brain AEA levels over those of other NAEs. In addition to the lack of effect of LM-4131 on AEA in $Ptgs2^{-/-}$ mice, these studies further suggest that its mechanism of action is not via FAAH inhibition, as one would expect to see increases in the levels of other NAEs if this were the case.
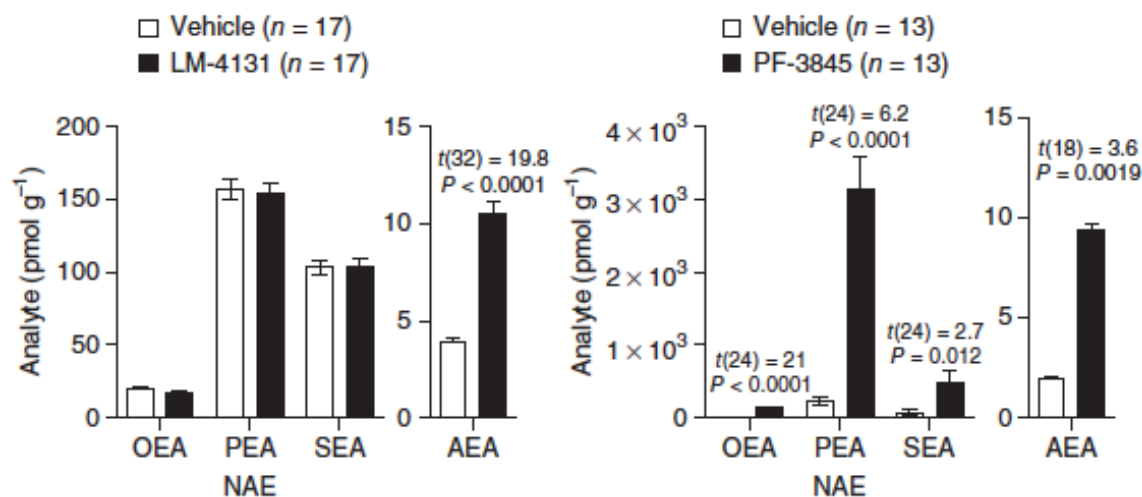
Figure 11: Effects of LM-4131 and the FAAH inhibitor PF-3845 on brain NAEs. LM-4131 significantly increases AEA but not other NAEs in the brain. In contrast, PF-3845 increases all NAEs in the brain. Data shown are mean ± s.e.m., n values are shown above the graphs. Reproduced from.[49]

To further exclude FAAH inhibition as contributing to the AEA-elevating effect of LM-4131, we analyzed the effects of LM-4131 co-treatment with PF-3845 compared to PF-3845 alone. Co-treatment of LM-4131 and PF-3845 caused a significant additional increase in AEA levels compared to PF-3845 alone (Figure

12). We also analyzed the effects of LM-4131 in the liver, which has very high FAAH expression, compared to the effects of PF-3845. While LM-4131 had no significant effects on any NAE in the liver, PF-3845 caused substantial increases in the levels of all NAEs. We also analyzed the effects of LM-4131 on brain AEA levels in wild-type and *Faah*$^{-/-}$ littermates. LM-4131 caused similar increases in brain AEA levels in wild-type and *Faah*$^{-/-}$ mice. Finally, we also analyzed the effects of LM-4131 on NAEs in *Ptgs2*$^{-/-}$ mice. While both LM-4131 and *Ptgs2*$^{-/-}$ mice had increased AEA levels relative to vehicle treated wild type mice, neither LM-4131 nor *Ptgs2*$^{-/-}$ mice had increased levels of other NAEs. Taken together with the lack of *in vitro* FAAH inhibition by LM-4131, these converging *in vivo* studies identify a unique COX-2-mediated mechanism of action for the increase in AEA levels elicited by LM-4131.
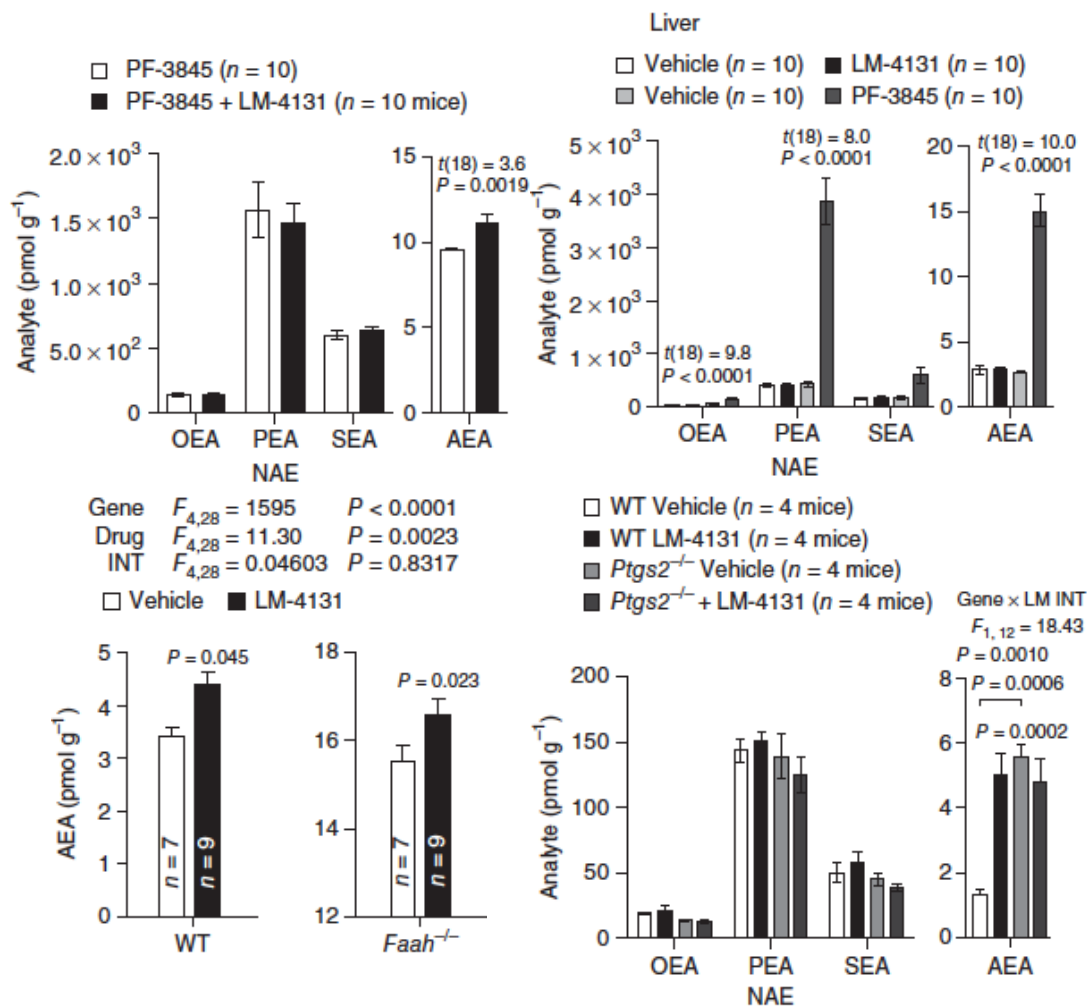
Figure 12: Effects of LM-4131 on NAEs. LM-4131 increases the levels of AEA, but not other NAEs, in the brain when co-treated with the FAAH inhibitor PF-3845. LM-4131 has no effect in the liver, while PF-3845 increases a series of NAEs. LM-4131 also increases the levels of AEA to a similar extent in both wild-type and *Faah*$^{-/-}$ mice. *Ptgs2*$^{-/-}$ mice have increased levels of AEA but not other NAEs in the brain. Data shown are mean ± s.e.m., n values are shown on the bars or above the graphs. Reproduced from.[49]

We also sought to determine the differences between MAGL inhibition and substrate-selective COX-2 inhibition by comparing the MAGL inhibitor JZL-184 to LM-4131. LM-4131 significantly increased brain 2-AG levels but did not increase the levels of any other MAG (Figure 13). In contrast, the MAGL inhibitor JZL-184 (40 mg/kg) increased the levels of 2-AG and three other MAGs. We further analyzed the effects of LM-4131 by treating mice with JZL-184 alone or a combination of LM-4131 and JZL-184. Co-treatment of LM-4131 and JZL-184 produced an additional significant increase in 2-AG levels over JZL-184 treatment alone. As with the FAAH experiments, these *in vivo* data combined with the fact that LM-4131 did not inhibit MAGL *in vitro* suggest that the ability of LM-4131 to increase 2-AG levels in the brain is not mediated via MAGL inhibition.
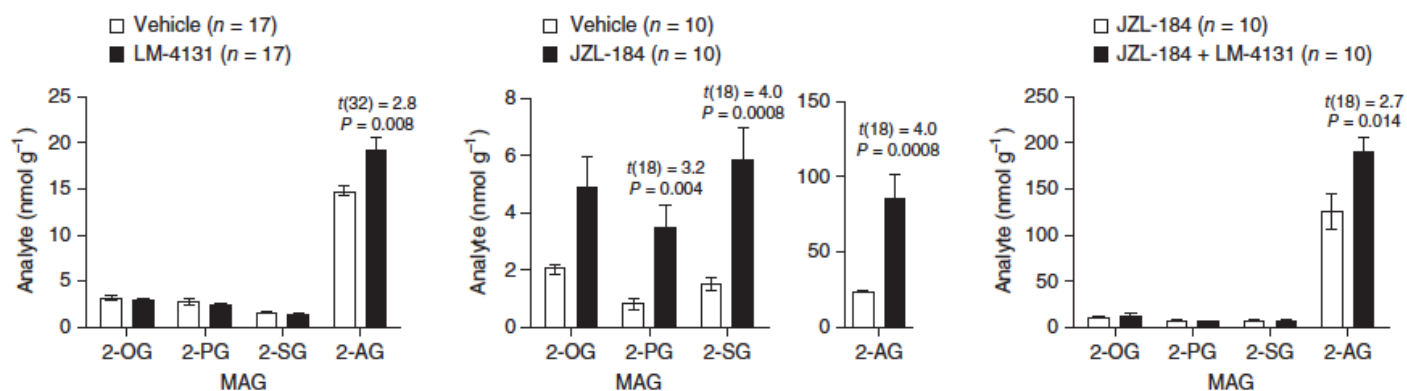
Figure 13: Effects of LM-4131 and JZL-184 on brain MAGs. LM-4131 significantly increases 2-AG but not other MAGs, while JZL-184 increases a series of MAGs in the brain. Co-treatment of LM-4131 and JZL-184 results in an increase in 2-AG relative to JZL-184 treatment alone. Data shown are mean ± s.e.m., n values are shown above the graphs. Reproduced from.[49]

As with FAAH and MAGL, COX-2 is expressed not only in the brain but several other tissues. We tested the effects of LM-4131 on eCB, NAE, MAG, and PG levels in a variety of peripheral tissues to determine if COX-2 modulates eCB levels in tissues other than the brain. LM-4131 (10 mg/kg) significantly increased AEA levels in the stomach, small intestine, kidney, and lung, but not in the heart or liver (Figure 14). As with the brain, LM-4131 did not affect the levels of any other NAE in any tissue. Although LM-4131 increased 2-AG in the brain, it had no effect on 2-AG or any other MAG in any of the peripheral tissues examined. We also treated mice with vehicle, LM-4131, or indomethacin to compare the effects on PG levels in the same tissues. Indomethacin robustly decreased PG levels in all of the tissues examined, whereas LM-4131 had no significant

PG inhibition in any of the tissues analyzed. Thus, LM-4131 can augment AEA levels in both central and

peripheral tissues and retains *in vivo* substrate-selectivity in peripheral tissues.
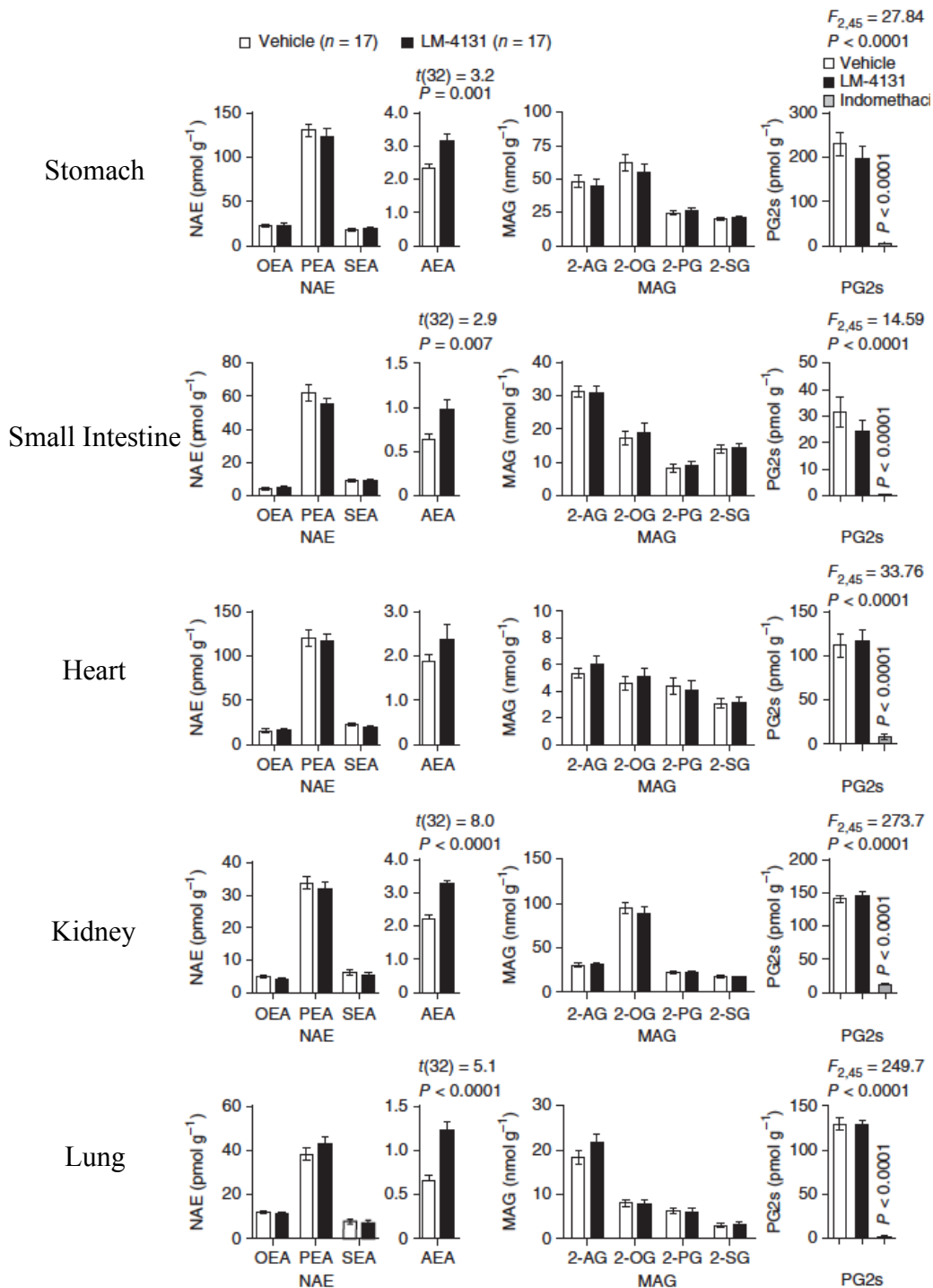
Figure 14: Effects of LM-4131 in peripheral tissues. LM-4131 selectively increases AEA in the stomach, small intestine, kidney, and lung. LM-4131 had no significant effect on other NAEs or MAGs in any of the peripheral tissues analyzed. While indomethacin significantly decreased PG levels in all of the tissues analyzed, LM-4131 did not. Data shown are mean ± s.e.m., n = 17. Reproduced from.[49]

Behavioral effects of LM-4131

Previous studies have identified pharmacological inhibition of FAAH as a potential therapeutic approach to the treatment of mood and anxiety disorders.[7,10] Preliminary work has shown that FAAH inhibitors are anxiolytic in the novel open-field arena.[69] Consistent with this, we found that the FAAH inhibitor PF-3845 (10 mg/kg) increased center distance travelled and center time in the open-field arena (Figure 15). The increase in brain AEA produced by LM-4131 suggests that it may also display behavioral effects in pre-clinical models of anxiety. Indeed, LM-4131 (10 mg/kg) also increased center distance traveled and center time in a parallel fashion to PF-3845. Thus, LM-4131 exhibits anxiolytic-like effects in a similar fashion to a FAAH inhibitor.
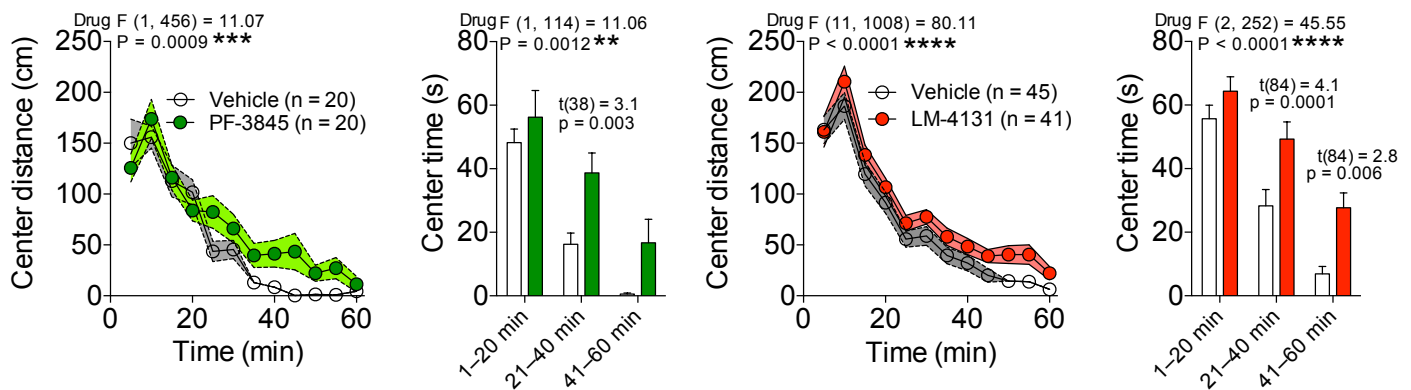
Figure 15: Behavioral effects of PF-3845 and LM-4131 in the novel open-field arena. Both PF-3845 and LM-4131 increase center distance and center time compared to vehicle treated mice. Data shown are mean ± s.e.m., n values are shown in the graphs. Reproduced from.[49]

Based on the effects of LM-4131, we hypothesized that all COX inhibitors that increase brain AEA can act as anxiolytics. To examine this hypothesis, we tested the effects of indomethacin (10 mg/kg), NS-398 (10 mg/kg), and SC-560 (10 mg/kg) in the open-field arena. Indomethacin and NS-398, which both significantly increased brain AEA levels, increased center distance and center time in the open-field arena, suggestive of an anxiolytic behavioral effect (Figure 16). However, SC-560, which increased AEA levels to a lesser extent than the other COX inhibitors, did not have any behavioral effects in the open-field arena. Thus, COX-2 inhibitors that increase brain AEA levels produce anxiolytic-like effects in a pre-clinical test of anxiety in a parallel fashion to FAAH inhibitors.
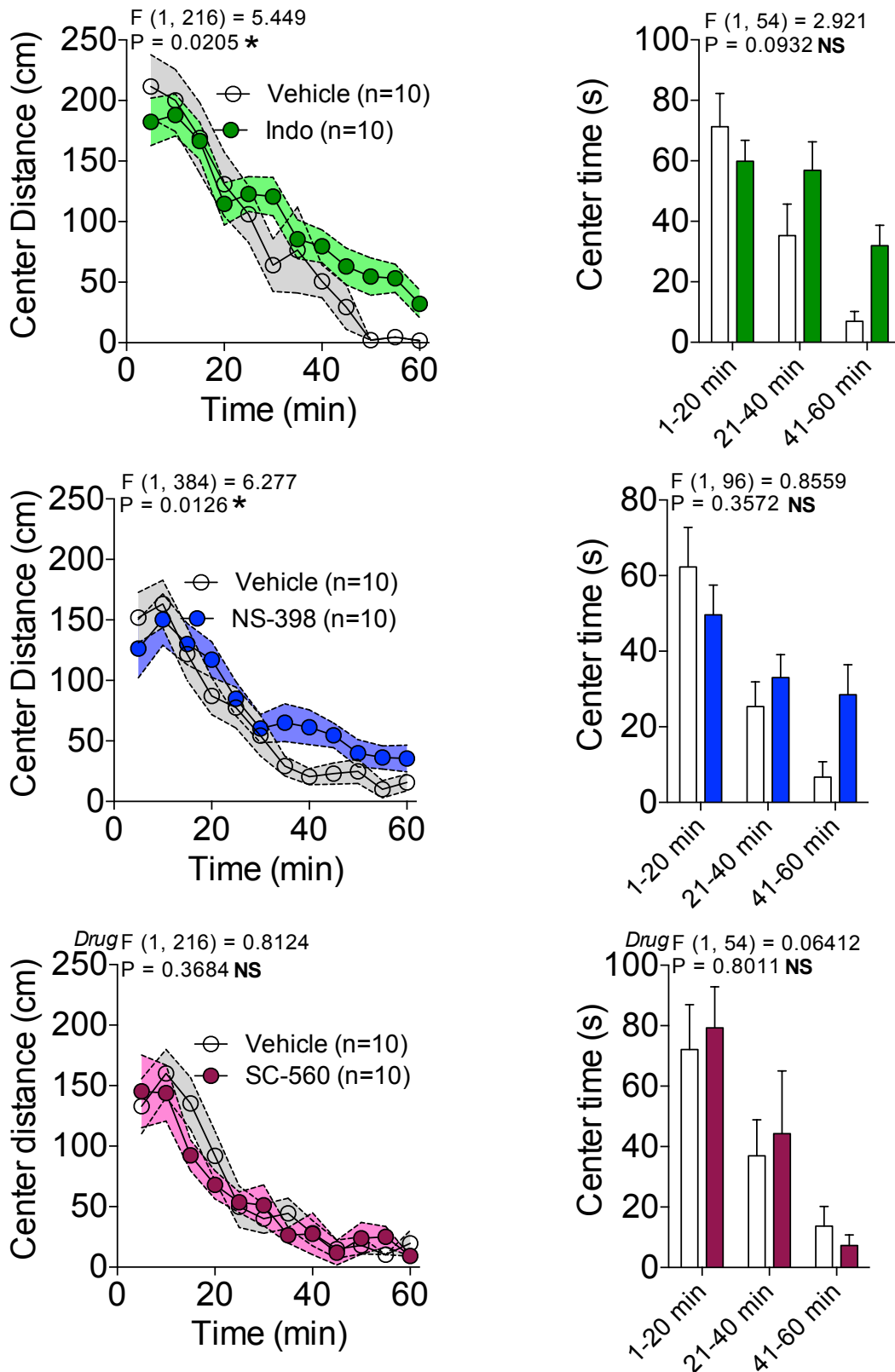
Figure 16: Effects of COX inhibitors in the open-field arena. While indomethacin and NS-398 increased center distance, indicative of anxiolytic-like effects, the COX-1 selective inhibitor SC-560 had no effect on either center distance or center time. Data shown are mean ± s.e.m., n = 10. Reproduced from.[49]

To determine if the behavioral effects of LM-4131 are mediated by substrate-selective COX-2 inhibition, we tested the behavioral effects of LM-4131 in $Ptgs2^{-/-}$ mice and their wild-type littermates. While LM-4131 produced anxiolytic-like effects in wild-type littermates, LM-4131 did not produce behavioral effects in $Ptgs2^{-/-}$ mice (Figure 17). This is consistent with the lack of AEA augmentation after LM-4131 administration in $Ptgs2^{-/-}$ mice. Intriguingly, $Ptgs2^{-/-}$ mice also showed a slight anxiolytic phenotype relative to wild-type littermates based on an increased center time. Thus, the biochemical and behavioral effects of LM-4131 are mediated by COX-2.
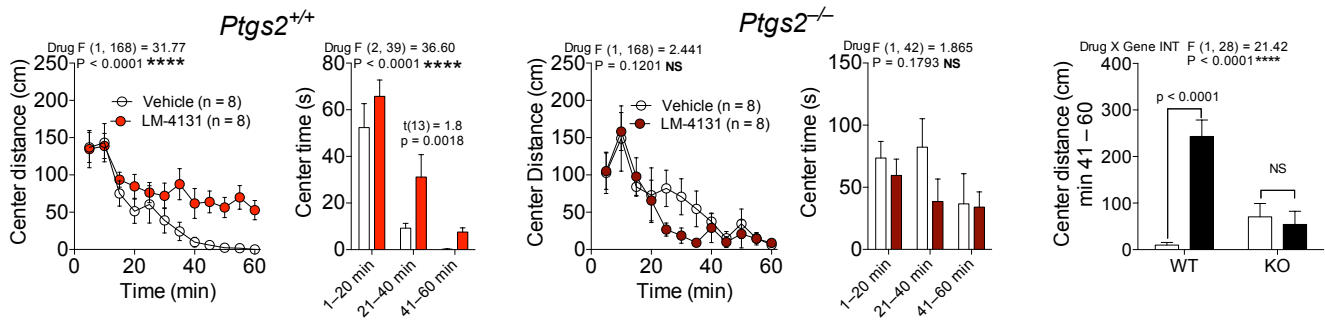
Figure 17: Behavioral effects of LM-4131 in $Ptgs2^{+/+}$ and $Ptgs2^{-/-}$ mice in the open-field arena. LM-4131 increases center distance and time in wild-type littermates, but not $Ptgs2^{-/-}$ mice. Data shown are mean ± s.e.m., n = 8. Reproduced from.[49]

Previous studies have identified that the anxiolytic effects of FAAH inhibition are mediated via AEA activation of CB_1 receptors.[10,70] We sought to determine if the anxiolytic-like effects of LM-4131 in the open-field arena are also mediated by increasing CB_1 receptor activation through AEA augmentation. While exerting anxiolytic effect in vehicle-pretreated mice, LM-4131 had no significant behavioral effects in mice co-treated with the CB_1 antagonist Rimonabant (3 mg/kg) (Figure 18). Furthermore, LM-4131 did not produce behavioral effects in CB_1 receptor knockout mice ($Cnr1^{-/-}$), despite increasing the levels of AEA and 2-AG in the knockout mice (Figure 19). Thus, the behavioral effects of LM-4131 are mediated via substrate-selective inhibition of COX-2, which selectively increases brain eCB levels, leading to increased activation of central CB_1 receptors and anxiolytic behavioral effects.
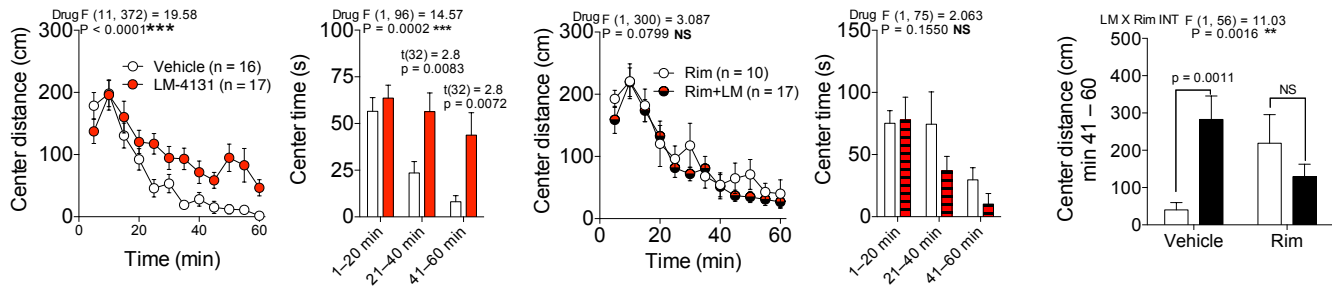
Figure 18: Abrogation of the anxiolytic behavioral effects of LM-4131 in the open-field arena by Rimonabant. While LM-4131 increases center distance and time in the open-field arena, co-treatment with the CB$_1$ antagonist Rimonabant abolishes these effects. Data shown are mean ± s.e.m., n values are shown in the graphs. Reproduced from.[49]
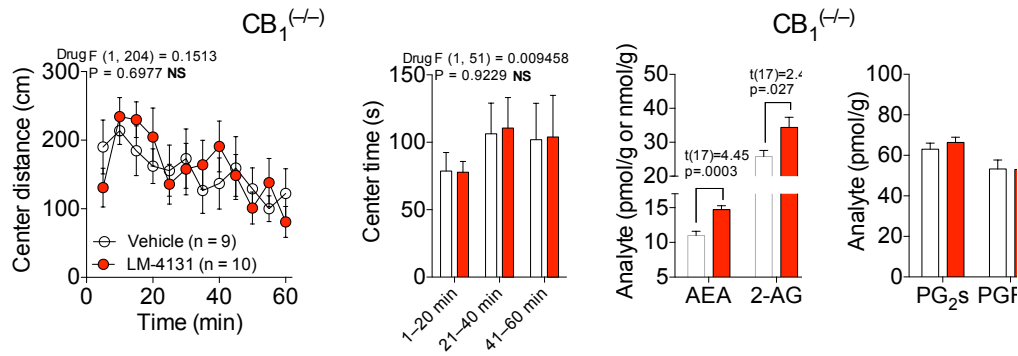
Figure 19: LM-4131 behavioral and biochemical effects in CB$_1$ knockout mice. LM-4131 does not produce behavioral effects in *Cnr1*$^{-/-}$ mice despite increasing the levels of AEA and 2-AG. Data shown are mean ± s.e.m., vehicle n = 9 and LM-4131 n = 10. Reproduced from.[49]

To further characterize the anxiolytic-like effects of LM-4131, we analyzed the effects of LM-4131 and the FAAH inhibitor PF-3845 in the light-dark box test. Both PF-3845 (10 mg/kg) and LM-4131 (10 mg/kg) significantly increased light-zone time and the number of light-zone entries without affecting overall locomotor activity (Figure 20). Again the anxiolytic effects of LM-4131 were blocked by pretreatment with the CB$_1$ receptor antagonist Rimonabant (3 mg/kg), suggesting that the anxiolytic effects of LM-4131 are mediated via CB$_1$ receptor activation in the light-dark box.
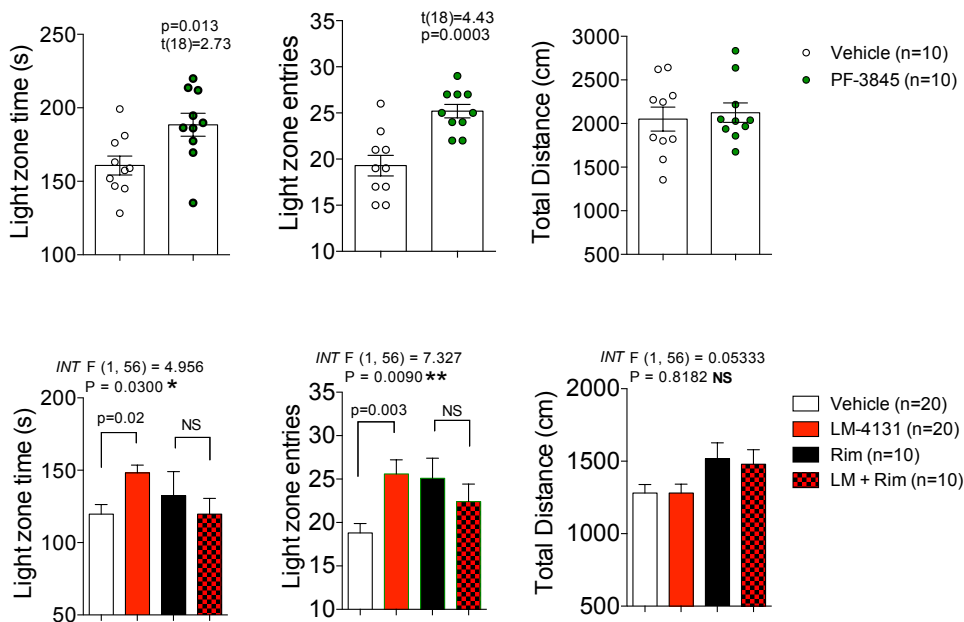
Figure 20: Effects of PF-3845 and LM-4131 in the light-dark box. Both PF-3845 and LM-4131 increase light zone time and entries but have no effect on total distance. The effects of LM-4131 are abolished by co-treatment with the CB$_1$ antagonist Rimonabant. Data shown are mean ± s.e.m., n values are listed on the graphs. Reproduced from.[49]

We also analyzed the anxiolytic potential of PF-3845 and LM-4131 in the elevated plus-maze. Both PF-3845 (10 mg/kg) and LM-4131 (10 mg/kg) significantly reduced open arm latency but did not affect other parameters, including total distance travelled (Figure 21). Taken together, these behavioral studies reveal that the anxiolytic effects of LM-4131 parallel the effects of PF-3845 in multiple pre-clinical tests of anxiety. Thus, substrate-selective COX-2 inhibition can exert anxiolytic effects via eCB augmentation in a similar manner to FAAH inhibition. These proof-of-concept studies suggest that substrate-selective COX-2 inhibitors could represent a class of COX-2-based eCB augmenting agents with therapeutic anxiolytic effects.
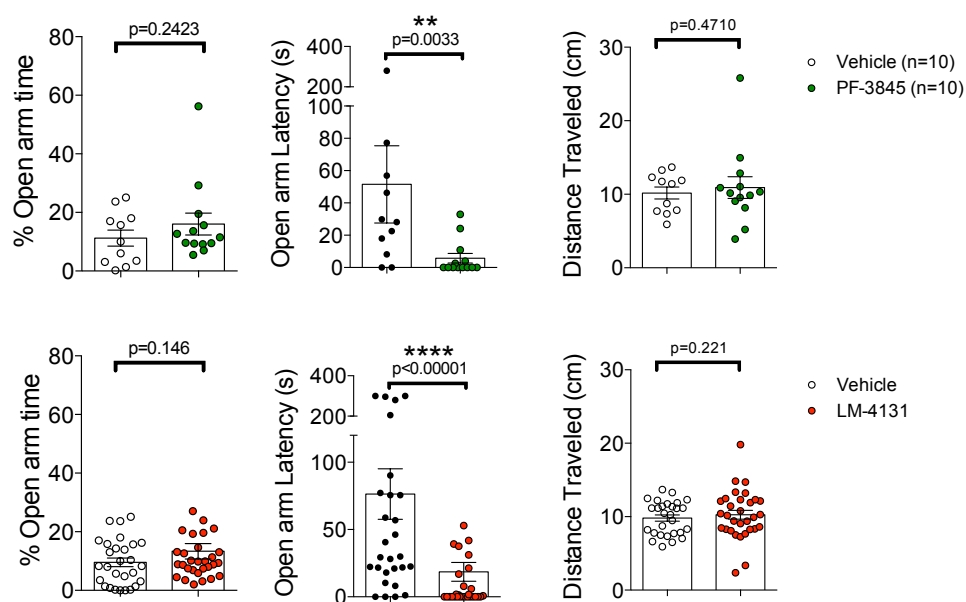
Figure 21: Effects of PF-3845 and LM-4131 in the elevated plus-maze. Both PF-3845 and LM-4131 significantly decrease open arm latency but have no effect on other measures including open arm time or total distance traveled. Data shown are mean ± s.e.m., PF-3845 vehicle n = 10, PF-3845 n = 10, LM-4131 vehicle n = 28, and LM-4131 n = 31. Reproduced from.[49]

Finally, we examined the potential cannabimimetic and gastrointestinal side effects of LM-4131. Direct agonists of CB_1 receptors produce a classical 'tetrad' of behavioral effects consisting of hypolocomotion, analgesia, catalepsy, and hypothermia.[71] The open-field assay, light-dark box, and elevated plus-maze data demonstrate that LM-4131 does not cause hypolocomotion. We also analyzed the effects of LM-4131 and the CB_1 agonist Win-55212-2 on rectal temperature, ring-stand catalepsy, and hot plate nociception (Figure 22). LM-4131 did not cause hypothermia, catalepsy, or analgesia in these tests. In contrast, Win-55212-2 induced hypothermia, catalepsy, and analgesia. We also assessed the effect of LM-4131 on memory using the novel object recognition assay. LM-4131 did not induce memory deficits when administered before object memory retrieval. Finally, LM-4131 did not cause overt gastrointestinal hemorrhage, a primary adverse effect of COX inhibitors, including indomethacin, the parent compound of LM-4131 (Figure 23). Taken together, these data indicate that LM-4131 induces a subset of behavioral effects that are mediated via eCB activation, but does not cause overt cannabimimetic effects or overt gastrointestinal toxicity observed with direct CB_1 agonists or traditional COX inhibitors, respectively.
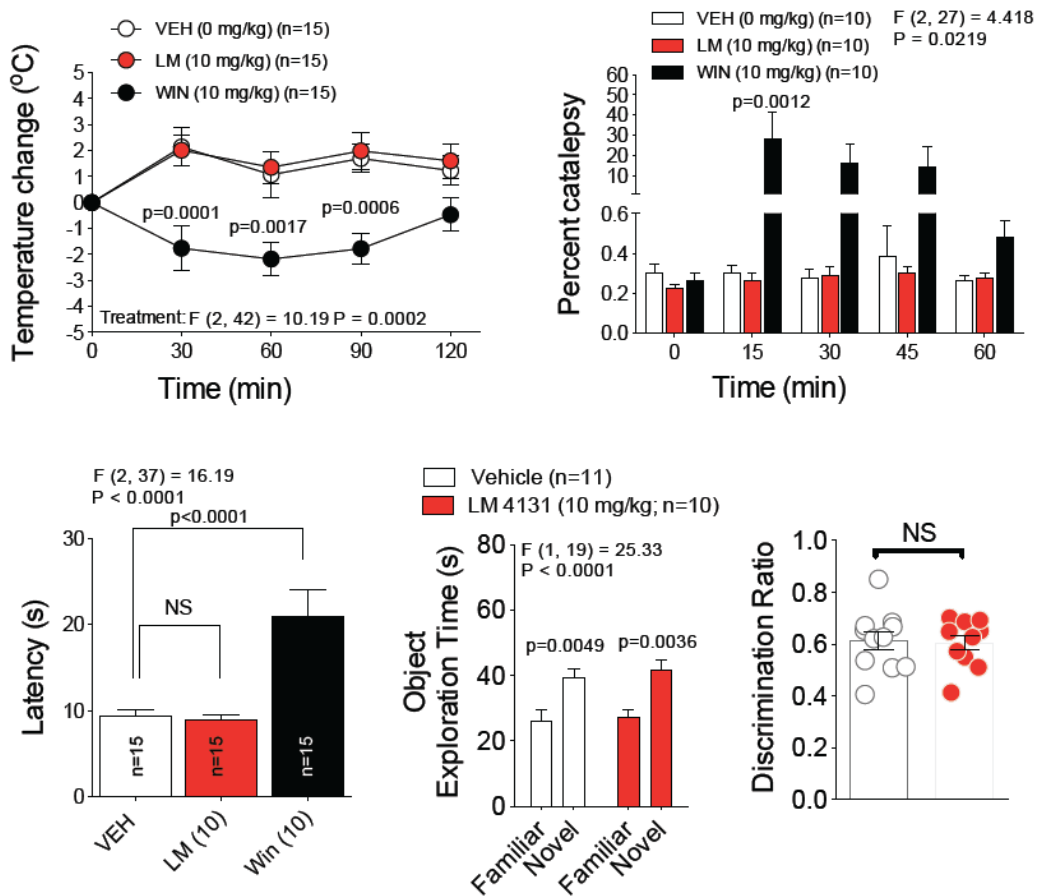
Figure 22: Effects of LM-4131 and Win-55212-2 on cannabinoid tetrad. LM-4131 does not cause hypothermia based on rectal temperature measurements, catalepsy as measured by the ring stand test, or antinociception as measured by hot plate paw withdrawal latency, while Win-55212-2 causes all three. LM-4131 also does not cause memory deficits in the novel object recognition assay. Data shown are mean ± s.e.m., n values are listed on the graphs. Reproduced from.[49]

Figure 23: Comparison of overt gastrointestinal bleeding caused by vehicle, LM-4131, and indomethacin. While vehicle and LM-4131 treated intestines do not display overt gastrointestinal bleeding, indomethacin treat intestines display significant blackening indicative of gastrointestinal hemorrhage.

<div align="center">Discussion</div>

Pharmacological inhibition of FAAH and MAGL have previously been validated to robustly augment eCB levels *in vivo* and exert preclinical therapeutic effects in a variety of pathological conditions.[10,72] However, both approaches also increase non-eCB lipids, NAEs for FAAH inhibition and MAGs for MAGL inhibition, that have biological actions at targets other than cannabinoid receptors.[73] Our studies demonstrate that, in addition to FAAH and MAGL, COX-2 is a key regulator of eCB levels *in vivo* and substrate-selective COX-2 inhibition represents a viable alternative approach to augment eCB levels with a high degree of selectivity for eCBs over related non-eCB lipids.

In contrast to traditional modes of COX inhibition, substrate-selective COX-2 inhibition augments eCB levels without inhibiting central or peripheral PG production. The development and validation of an *in vivo* substrate-selective COX-2 inhibitor, LM-4131, provides a new and effective pharmacological strategy to selectively augment AEA signaling via COX-2 inhibition. Although LM-4131 treatment significantly increased the levels of 2-AG, the effect was small and not recapitulated in every experiment; thus, the biological relevance of 2-AG augmentation remains to be determined. Consequently, our data suggest that COX-2 preferentially regulates AEA over 2-AG.

The larger relative effects of COX-2 inhibition on AEA over 2-AG may be a result of the closer proximity between COX-2 and the site of AEA biosynthesis and may explain its relative lack of overt cannabimimetic effects compared to dual FAAH and MAGL inhibition.[67] Interestingly, FAAH and COX-2 are localized to the same postsynaptic cellular compartment.[74] The co-localization of FAAH and COX-2 and similar effects of PF-3845 and LM-4131 suggests that they mutually regulate AEA with similar biological effects. However, as pharmacological inhibition or genetic deletion of COX-2 selectively increases AEA and 2-AG, but does not affect the levels of non-eCB NAEs or MAGs, targeting COX-2 provides enhanced eCB selectivity over FAAH or MAGL inhibition.

Consistent with previous findings that elevating AEA levels via FAAH inhibition exerts anxiolytic-like actions in pre-clinical models, we found that LM-4131 decreased anxiety-like behaviors in multiple validated pre-clinical assays.[10,69,70,75] Our studies suggest that substrate-selective COX-2 inhibitors could represent a

viable approach to the treatment of mood and anxiety disorders. Clinical support for this hypothesis has been put forth, as COX-2 inhibition has demonstrated clinical antidepressant efficacy as an adjunct to traditional antidepressants.[76] Our identification of COX-2 inhibitors as eCB augmenting agents provides a potential mechanism for the anxiolytic effects of COX-2 inhibitors.

In addition to having beneficial effects in the brain, the substrate-selectivity of LM-4131 could potentially reduce some of the common side effects mediated by the inhibition of PG synthesis by traditional NSAIDs. Gastrointestinal PG production is essential for the stimulation of mucosal bicarbonate and mucus secretion as well as increasing mucosal blood flow.[77] Thus, inhibition of gastrointestinal PG production by traditional NSAIDs leads to gastrointestinal complications such as ulcers. Our studies indicate that LM-4131 does not cause overt gastrointestinal hemorrhage, which is a major side effect of indomethacin.

A second major clinical concern for the chronic use of COX inhibitors is cardiovascular and cerebrovascular toxicity manifested by an increased incidence of heart attack and stroke. Cardiovascular side effects are exhibited by most NSAIDs, regardless of their selectivity for COX-2, due to a reduction in vascular PGI_2 biosynthesis.[78,79] As LM-4131 does not affect central or peripheral levels of PGs, including PGI_2, it is possible that this pharmacological class of inhibitors could be devoid of or exhibit significantly reduced cardio/cerebrovascular toxicity compared to NSAIDs. Indeed, clinical trials conducted with the substrate-selective COX-2 inhibitor (*R*)-flurbiprofen suggest that it does not increase cardiovascular events in humans.[80,81] Additional studies evaluating the side effects of substrate-selective COX-2 inhibitors relative to those of traditional COX inhibitors will be required to identify potential adverse effects of substrate-selective COX-2 inhibitors on a compound-by-compound basis.

These studies demonstrate that COX-2 is a key regulator of brain eCB signaling *in vivo* and that substrate-selective inhibition of COX-2 represents a novel pharmacological approach to augmenting eCBs. Given the numerous pathological processes in which dysregulation of eCB signaling has been demonstrated, coupled with the high degree of selectivity of substrate-selective COX-2 inhibitors for eCBs over related non-eCB lipids, this class of pharmaceutical agents could have broad therapeutic potential. Further research into the therapeutic effects of substrate-selective COX-2 inhibitors will identify their potential for use in diseases.

References

1. Kano, M., Ohno-Shosaku, T., Hashimotodani, Y., Uchigashima, M. & Watanabe, M. Endocannabinoid-mediated control of synaptic transmission. *Physiol Rev* **89**, 309-380 (2009).
2. Mechoulam, R. & Parker, L.A. The endocannabinoid system and the brain. *Annual review of psychology* **64**, 21-47 (2013).
3. Ahn, K., McKinney, M.K. & Cravatt, B.F. Enzymatic pathways that regulate endocannabinoid signaling in the nervous system. *Chem Rev* **108**, 1687-1707 (2008).
4. Piomelli, D. The molecular logic of endocannabinoid signalling. *Nat Rev Neurosci* **4**, 873-884 (2003).
5. Di Marzo, V. Endocannabinoids: synthesis and degradation. *Reviews of physiology, biochemistry and pharmacology* **160**, 1-24 (2008).
6. Petrosino, S. & Di Marzo, V. FAAH and MAGL inhibitors: therapeutic opportunities from regulating endocannabinoid levels. *Curr Opin Investig Drugs* **11**, 51-62 (2010).
7. Piomelli, D. The endocannabinoid system: a drug discovery perspective. *Curr Opin Investig Drugs* **6**, 672-679 (2005).
8. Blankman, J.L. & Cravatt, B.F. Chemical probes of endocannabinoid metabolism. *Pharmacological reviews* **65**, 849-871 (2013).
9. Cravatt, B.F.*, et al.* Supersensitivity to anandamide and enhanced endogenous cannabinoid signaling in mice lacking fatty acid amide hydrolase. *Proceedings of the National Academy of Sciences of the United States of America* **98**, 9371-9376 (2001).
10. Kathuria, S.*, et al.* Modulation of anxiety through blockade of anandamide hydrolysis. *Nature medicine* **9**, 76-81 (2003).
11. Khasabova, I.A., Xiong, Y., Coicou, L.G., Piomelli, D. & Seybold, V. Peroxisome proliferator-activated receptor alpha mediates acute effects of palmitoylethanolamide on sensory neurons. *The Journal of neuroscience : the official journal of the Society for Neuroscience* **32**, 12735-12743 (2012).
12. Fu, J.*, et al.* Oleylethanolamide regulates feeding and body weight through activation of the nuclear receptor PPAR-alpha. *Nature* **425**, 90-93 (2003).
13. O'Sullivan, S.E. & Kendall, D.A. Cannabinoid activation of peroxisome proliferator-activated receptors: potential for modulation of inflammatory disease. *Immunobiology* **215**, 611-616 (2010).
14. Dinh, T.P.*, et al.* Brain monoglyceride lipase participating in endocannabinoid inactivation. *Proceedings of the National Academy of Sciences of the United States of America* **99**, 10819-10824 (2002).
15. Hill, M.N.*, et al.* The therapeutic potential of the endocannabinoid system for the development of a novel class of antidepressants. *Trends Pharmacol Sci* **30**, 484-493 (2009).
16. Roques, B.P., Fournie-Zaluski, M.C. & Wurm, M. Inhibiting the breakdown of endogenous opioids and cannabinoids to alleviate pain. *Nature reviews. Drug discovery* **11**, 292-310 (2012).
17. Mulvihill, M.M. & Nomura, D.K. Therapeutic potential of monoacylglycerol lipase inhibitors. *Life sciences* **92**, 492-497 (2013).
18. Bari, M., Battista, N., Fezza, F., Gasperi, V. & Maccarrone, M. New insights into endocannabinoid degradation and its therapeutic potential. *Mini reviews in medicinal chemistry* **6**, 257-268 (2006).
19. Kim, J. & Alger, B.E. Inhibition of cyclooxygenase-2 potentiates retrograde endocannabinoid effects in hippocampus. *Nature neuroscience* **7**, 697-698 (2004).
20. Slanina, K.A. & Schweitzer, P. Inhibition of cyclooxygenase-2 elicits a CB1-mediated decrease of excitatory transmission in rat CA1 hippocampus. *Neuropharmacology* **49**, 653-659 (2005).
21. Fowler, C.J., Stenstrom, A. & Tiger, G. Ibuprofen inhibits the metabolism of the endogenous cannabimimetic agent anandamide. *Pharmacology & toxicology* **80**, 103-107 (1997).
22. Glaser, S.T. & Kaczocha, M. Cyclooxygenase-2 mediates anandamide metabolism in the mouse brain. *The Journal of pharmacology and experimental therapeutics* **335**, 380-388 (2010).
23. Ghilardi, J.R., Svensson, C.I., Rogers, S.D., Yaksh, T.L. & Mantyh, P.W. Constitutive spinal cyclooxygenase-2 participates in the initiation of tissue injury-induced hyperalgesia. *The Journal of neuroscience : the official journal of the Society for Neuroscience* **24**, 2727-2732 (2004).

24. Guhring, H., *et al.* A role for endocannabinoids in indomethacin-induced spinal antinociception. *European journal of pharmacology* **454**, 153-163 (2002).

25. Staniaszek, L.E., Norris, L.M., Kendall, D.A., Barrett, D.A. & Chapman, V. Effects of COX-2 inhibition on spinal nociception: the role of endocannabinoids. *British journal of pharmacology* **160**, 669-676 (2010).

26. Guindon, J., LoVerme, J., De Lean, A., Piomelli, D. & Beaulieu, P. Synergistic antinociceptive effects of anandamide, an endocannabinoid, and nonsteroidal anti-inflammatory drugs in peripheral tissue: a role for endogenous fatty-acid ethanolamides? *European journal of pharmacology* **550**, 68-77 (2006).

27. Guindon, J., De Lean, A. & Beaulieu, P. Local interactions between anandamide, an endocannabinoid, and ibuprofen, a nonsteroidal anti-inflammatory drug, in acute and inflammatory pain. *Pain* **121**, 85-93 (2006).

28. Telleria-Diaz, A., *et al.* Spinal antinociceptive effects of cyclooxygenase inhibition during inflammation: Involvement of prostaglandins and endocannabinoids. *Pain* **148**, 26-35 (2010).

29. Yu, M., Ives, D. & Ramesha, C.S. Synthesis of prostaglandin E2 ethanolamide from anandamide by cyclooxygenase-2. *The Journal of biological chemistry* **272**, 21181-21186 (1997).

30. Kozak, K.R., Rowlinson, S.W. & Marnett, L.J. Oxygenation of the endocannabinoid, 2-arachidonylglycerol, to glyceryl prostaglandins by cyclooxygenase-2. *The Journal of biological chemistry* **275**, 33744-33749 (2000).

31. Kozak, K.R., *et al.* Metabolism of the endocannabinoids, 2-arachidonylglycerol and anandamide, into prostaglandin, thromboxane, and prostacyclin glycerol esters and ethanolamides. *The Journal of biological chemistry* **277**, 44877-44885 (2002).

32. Weber, A., *et al.* Formation of prostamides from anandamide in FAAH knockout mice analyzed by HPLC with tandem mass spectrometry. *Journal of lipid research* **45**, 757-763 (2004).

33. Duggan, K.C., *et al.* (R)-Profens are substrate-selective inhibitors of endocannabinoid oxygenation by COX-2. *Nature chemical biology* **7**, 803-809 (2011).

34. Ritter, J.K., *et al.* Production and actions of the anandamide metabolite prostamide E2 in the renal medulla. *The Journal of pharmacology and experimental therapeutics* **342**, 770-779 (2012).

35. Gatta, L., *et al.* Discovery of prostamide F2alpha and its role in inflammatory pain and dorsal horn nociceptive neuron hyperexcitability. *PloS one* **7**, e31111 (2012).

36. Silvestri, C., *et al.* Anandamide-derived prostamide F2alpha negatively regulates adipogenesis. *The Journal of biological chemistry* **288**, 23307-23321 (2013).

37. Hu, S.S., Bradshaw, H.B., Chen, J.S., Tan, B. & Walker, J.M. Prostaglandin E2 glycerol ester, an endogenous COX-2 metabolite of 2-arachidonoylglycerol, induces hyperalgesia and modulates NFkappaB activity. *British journal of pharmacology* **153**, 1538-1549 (2008).

38. Kingsley, P.J., Rouzer, C.A., Saleh, S. & Marnett, L.J. Simultaneous analysis of prostaglandin glyceryl esters and prostaglandins by electrospray tandem mass spectrometry. *Analytical biochemistry* **343**, 203-211 (2005).

39. Alhouayek, M., Masquelier, J., Cani, P.D., Lambert, D.M. & Muccioli, G.G. Implication of the anti-inflammatory bioactive lipid prostaglandin D2-glycerol ester in the control of macrophage activation and inflammation by ABHD6. *Proceedings of the National Academy of Sciences of the United States of America* **110**, 17558-17563 (2013).

40. Kozak, K.R., *et al.* Metabolism of prostaglandin glycerol esters and prostaglandin ethanolamides in vitro and in vivo. *The Journal of biological chemistry* **276**, 36993-36998 (2001).

41. Xie, S., *et al.* Inactivation of lipid glyceryl ester metabolism in human THP1 monocytes/macrophages by activated organophosphorus insecticides: role of carboxylesterases 1 and 2. *Chemical research in toxicology* **23**, 1890-1904 (2010).

42. Wang, R., *et al.* Identification of Palmitoyl Protein Thioesterase 1 in Human THP1 Monocytes and Macrophages and Characterization of Unique Biochemical Activities for This Enzyme. *Biochemistry* **52**, 7559-7574 (2013).

43. Dong, L., *et al.* Human Cyclooxygenase-2 Is a Sequence Homodimer That Functions as a Conformational Heterodimer. *Journal of Biological Chemistry* **286**, 19035-19046 (2011).

44. Kulmacz, R.J. & Lands, W.E.M. Prostaglandin-H Synthase - Stoichiometry of Heme Cofactor. *Journal of Biological Chemistry* **259**, 6358-6363 (1984).

45. Yuan, C.*, et al.* Cyclooxygenase Allosterism, Fatty Acid-mediated Cross-talk between Monomers of Cyclooxygenase Homodimers. *The Journal of biological chemistry* **284**, 10046-10055 (2009).

46. Prusakiewicz, J.J., Duggan, K.C., Rouzer, C.A. & Marnett, L.J. Differential sensitivity and mechanism of inhibition of COX-2 oxygenation of arachidonic acid and 2-arachidonoylglycerol by ibuprofen and mefenamic acid. *Biochemistry* **48**, 7353-7355 (2009).

47. Duggan, K.C.*, et al.* Molecular basis for cyclooxygenase inhibition by the non-steroidal anti-inflammatory drug naproxen. *The Journal of biological chemistry* **285**, 34950-34959 (2010).

48. Kulmacz, R.J. & Lands, W.E. Stoichiometry and kinetics of the interaction of prostaglandin H synthase with anti-inflammatory agents. *The Journal of biological chemistry* **260**, 12572-12578 (1985).

49. Hermanson, D.J.*, et al.* Substrate-selective COX-2 inhibition decreases anxiety via endocannabinoid activation. *Nature neuroscience* **16**, 1291-1298 (2013).

50. Kalgutkar, A.S., Marnett, A.B., Crews, B.C., Remmel, R.P. & Marnett, L.J. Ester and amide derivatives of the nonsteroidal antiinflammatory drug, indomethacin, as selective cyclooxygenase-2 inhibitors. *J Med Chem* **43**, 2860-2870 (2000).

51. Rowlinson, S.W., Crews, B.C., Lanzo, C.A. & Marnett, L.J. The binding of arachidonic acid in the cyclooxygenase active site of mouse prostaglandin endoperoxide synthase-2 (COX-2) - A putative L-shaped binding conformation utilizing the top channel region. *Journal of Biological Chemistry* **274**, 23305-23310 (1999).

52. Rouzer, C.A. & Marnett, L.J. Glyceryl prostaglandin synthesis in lipopolysaccharide-treated RAW264.7 cells is augmented by interferon-gamma and granulocytemacrophage colony stimulating factor. *Prostag Oth Lipid M* **79**, 146-147 (2006).

53. Blankman, J.L., Simon, G.M. & Cravatt, B.F. A comprehensive profile of brain enzymes that hydrolyze the endocannabinoid 2-arachidonoylglycerol. *Chem Biol* **14**, 1347-1356 (2007).

54. Ahn, K.*, et al.* Discovery and Characterization of a Highly Selective FAAH Inhibitor that Reduces Inflammatory Pain. *Chem Biol* **16**, 411-420 (2009).

55. Pedicord, D.L.*, et al.* Molecular characterization and identification of surrogate substrates for diacylglycerol lipase alpha. *Biochem Bioph Res Co* **411**, 809-814 (2011).

56. Uddin, M.J.*, et al.* Fluorinated COX-2 Inhibitors as Agents in PET Imaging of Inflammation and Cancer. *Cancer Prev Res* **4**, 1536-1545 (2011).

57. Pan, B., Hillard, C.J. & Liu, Q.S. D-2 Dopamine Receptor Activation Facilitates Endocannabinoid-Mediated Long-Term Synaptic Depression of GABAergic Synaptic Transmission in Midbrain Dopamine Neurons via cAMP-Protein Kinase A Signaling. *Journal of Neuroscience* **28**, 14018-14030 (2008).

58. Patel, S., Kingsley, P.J., Mackie, K., Marnett, L.J. & Winder, D.G. Repeated Homotypic Stress Elevates 2-Arachidonoylglycerol Levels and Enhances Short-Term Endocannabinoid Signaling at Inhibitory Synapses in Basolateral Amygdala. *Neuropsychopharmacol* **34**, 2699-2709 (2009).

59. Sumislawski, J.J., Ramikie, T.S. & Patel, S. Reversible gating of endocannabinoid plasticity in the amygdala by chronic stress: a potential role for monoacylglycerol lipase inhibition in the prevention of stress-induced behavioral adaptation. *Neuropsychopharmacol* **36**, 2750-2761 (2011).

60. Kingsley, P.J. & Marnett, L.J. LC-MS-MS analysis of neutral eicosanoids. *Method Enzymol* **433**, 91-+ (2007).

61. Fegley, D.*, et al.* Characterization of the fatty acid amide hydrolase inhibitor cyclohexyl carbamic acid 3'-carbamoyl-biphenyl-3-yl ester (URB597): effects on anandamide and oleoylethanolamide deactivation. *The Journal of pharmacology and experimental therapeutics* **313**, 352-358 (2005).

62. Leipold, D.D., Kantoci, D., Murray, E.D., Jr., Quiggle, D.D. & Wechter, W.J. Bioinversion of R-flurbiprofen to S-flurbiprofen at various dose levels in rat, mouse, and monkey. *Chirality* **16**, 379-387 (2004).

63. Windsor, M.A.*, et al.* Substrate-Selective Inhibition of Cyclooxygenase-2: Development and Evaluation of Achiral Profen Probes. *ACS medicinal chemistry letters* **3**, 759-763 (2012).

64. Kalgutkar, A.S*., et al.* Biochemically based design of cyclooxygenase-2 (COX-2) inhibitors: facile conversion of nonsteroidal antiinflammatory drugs to potent and highly selective COX-2 inhibitors. *Proceedings of the National Academy of Sciences of the United States of America* **97**, 925-930 (2000).

65. Rowlinson, S.W*., et al.* A novel mechanism of cyclooxygenase-2 inhibition involving interactions with Ser-530 and Tyr-385. *The Journal of biological chemistry* **278**, 45763-45769 (2003).

66. Oudin, M.J., Hobbs, C. & Doherty, P. DAGL-dependent endocannabinoid signalling: roles in axonal pathfinding, synaptic plasticity and adult neurogenesis. *The European journal of neuroscience* **34**, 1634-1646 (2011).

67. Long, J.Z*., et al.* Dual blockade of FAAH and MAGL identifies behavioral processes regulated by endocannabinoid crosstalk in vivo. *Proceedings of the National Academy of Sciences of the United States of America* **106**, 20270-20275 (2009).

68. Kinsey, S.G., O'Neal, S.T., Long, J.Z., Cravatt, B.F. & Lichtman, A.H. Inhibition of endocannabinoid catabolic enzymes elicits anxiolytic-like effects in the marble burying assay. *Pharmacology, biochemistry, and behavior* **98**, 21-27 (2011).

69. Rossi, S*., et al.* Preservation of striatal cannabinoid CB1 receptor function correlates with the antianxiety effects of fatty acid amide hydrolase inhibition. *Molecular pharmacology* **78**, 260-268 (2010).

70. Moreira, F.A., Kaiser, N., Monory, K. & Lutz, B. Reduced anxiety-like behaviour induced by genetic and pharmacological inhibition of the endocannabinoid-degrading enzyme fatty acid amide hydrolase (FAAH) is mediated by CB1 receptors. *Neuropharmacology* **54**, 141-150 (2008).

71. Fride, E., Perchuk, A., Hall, F.S., Uhl, G.R. & Onaivi, E.S. Behavioral methods in cannabinoid research. *Methods in molecular medicine* **123**, 269-290 (2006).

72. Long, J.Z*., et al.* Selective blockade of 2-arachidonoylglycerol hydrolysis produces cannabinoid behavioral effects. *Nature chemical biology* **5**, 37-44 (2009).

73. O'Sullivan, S.E. Cannabinoids go nuclear: evidence for activation of peroxisome proliferator-activated receptors. *British journal of pharmacology* **152**, 576-582 (2007).

74. Cristino, L*., et al.* Immunohistochemical localization of anabolic and catabolic enzymes for anandamide and other putative endovanilloids in the hippocampus and cerebellar cortex of the mouse brain. *Neuroscience* **151**, 955-968 (2008).

75. Patel, S. & Hillard, C.J. Pharmacological evaluation of cannabinoid receptor ligands in a mouse model of anxiety: further evidence for an anxiolytic role for endogenous cannabinoid signaling. *The Journal of pharmacology and experimental therapeutics* **318**, 304-311 (2006).

76. Muller, N. & Schwarz, M.J. COX-2 inhibition in schizophrenia and major depression. *Current pharmaceutical design* **14**, 1452-1465 (2008).

77. Patrignani, P., Tacconelli, S., Bruno, A., Sostres, C. & Lanas, A. Managing the adverse effects of nonsteroidal anti-inflammatory drugs. *Expert review of clinical pharmacology* **4**, 605-621 (2011).

78. Yu, Y*., et al.* Vascular COX-2 modulates blood pressure and thrombosis in mice. *Science translational medicine* **4**, 132ra154 (2012).

79. Warner, T.D. & Mitchell, J.A. COX-2 selectivity alone does not define the cardiovascular risks associated with non-steroidal anti-inflammatory drugs. *Lancet* **371**, 270-273 (2008).

80. Wilcock, G.K. Disease-modifying treatments for Alzheimer's disease: a perspective based on experience with R-Flurbiprofen. *Alzheimer's & dementia : the journal of the Alzheimer's Association* **2**, 150-152 (2006).

81. Wilcock, G.K*., et al.* Efficacy and safety of tarenflurbil in mild to moderate Alzheimer's disease: a randomised phase II trial. *Lancet neurology* **7**, 483-493 (2008).

CHAPTER V

THE PHARMACOKINETICS AND PHARMACODYNAMICS OF LM-4131 IN MICE

<u>Introduction</u>

The endocannabinoids (eCBs), anandamide (AEA) and 2-arachidonoylglycerol (2-AG), are the endogenous ligands of the cannabinoid 1 and 2 receptors (CB_1 and CB_2).[1-3] eCBs are synthesized from phospholipids through distinct pathways in response to calcium influx or the activation of certain G-protein-coupled receptors.[4-6] After synthesis, eCB levels are mainly regulated through deactivation by hydrolysis. AEA is primarily hydrolyzed by fatty acid amide hydrolase to arachidonic acid (AA) and ethanolamine, whereas 2-AG is hydrolyzed to AA and glycerol by several enzymes including monoacylglycerol lipase, α/β-hydrolase domain 6, α/β-hydrolase domain 12, carboxylesterases 1 and 2, and palmitoylprotein thioesterase 1.[7-12]

In addition to hydrolysis, AEA and 2-AG can undergo oxygenation by a variety of enzymes including lipoxygenases, cyclooxygenases, and cytochromes P450.[13-17] Although the extent to which each oxygenation pathway is involved in the turnover of eCBs is uncertain, our work demonstrates that cyclooxygenase-2 (COX-2) can become a third pathway of eCB metabolism at sites of constitutive expression or at sites of inflammation, as discussed in chapters III and IV.[18,19] COX-1 and COX-2 catalyze the committed step in the biosynthesis of prostaglandins (PGs) from AA. In addition to metabolizing AA, COX-2 also oxygenates AEA to form prostaglandin ethanolamides (PG-EAs) and 2-AG to form prostaglandin glycerol esters (PG-Gs).[13,14] These prostaglandin products are not ligands for the cannabinoid receptors, so COX-2 activity inactivates eCBs while also synthesizing a series of bioactive eCB-derived prostanoids.

Non-steroidal anti-inflammatory drugs (NSAIDs) produce their effects by inhibiting COX-1 and/or COX-2. Most NSAIDs inhibit the oxygenation of AA, 2-AG, and AEA with similar potencies, but a subset of NSAIDs selectively inhibit the oxygenation of 2-AG and AEA by COX-2 without inhibiting AA oxygenation, a phenomenon termed substrate-selective inhibition of COX-2.[20] For example, indomethacin inhibits the oxygenation of AA, 2-AG, and AEA with similar potencies, but the morpholino analog of indomethacin, LM-4131, selectively inhibits endocannabinoid oxygenation *in vitro* and *in vivo*, as discussed in chapter IV.[18] Intraperitoneal (i.p.) administration of LM-4131 (10 mg/kg) elevates the levels of brain AEA and 2-AG without

120

affecting the levels of AA or PGs 2 hours after treatment.[18] The elevation of eCBs elicited by LM-4131 is COX-2 dependent and produces anxiolytic effects through CB_1 receptor activation in pre-clinical models of anxiety.[18]

Substrate-selective COX-2 inhibitors are important tools for dissecting the role of COX-2 oxygenation in eCB metabolism due to their lack of confounding PG inhibition. While LM-4131 has robust effects at 2 hours after i.p. injection, its effects have not been investigated over longer times *in vivo*. Previous studies have demonstrated that LM-4131 (also known as BML-190) is extensively metabolized by rat liver microsomes *in vitro*.[21] LM-4131 metabolism by rat liver microsomes parallels the metabolism of indomethacin, in that the *p*-chlorobenzoyl group is hydrolyzed and the indole methoxy group is oxidatively demethylated.[21,22] In addition, LM-4131 can be hydroxylated on either the indole or morpholine rings.[21] Following hydroxylation of the morpholino group, the ether of some of the metabolites can ring-open, leading to additional metabolites.[21]

The *in vivo* pharmacokinetics and pharmacodynamics of LM-4131 are critical to evaluating its usefulness as a COX-2-dependent eCB-augmenting probe in both acute and chronic settings. Thus, we investigated the time-course of LM-4131 accumulation in the brain and plasma after a single 10 mg/kg i.p. injection and compared it to the distribution of indomethacin after a single 10 mg/kg i.p. injection in mice. We also analyzed the tissue distribution of LM-4131 2 hours after a 10 mg/kg i.p. injection. The effects of LM-4131 or indomethacin on brain eCBs and PGs were determined over a 24-hour period to analyze the duration of action of the compounds. We found that LM-4131 is present in the brain up to 6 hours after dosing and that it loses substrate-selectivity at that time, apparently due to partial hydrolysis to indomethacin. Thus, these results define the parameters under which LM-4131 is a useful probe for studying substrate-selective COX-2 inhibition *in vivo*.

Reagents

Indomethacin was purchased from Sigma Aldrich (St. Louis, MO). LM-4131 was synthesized as described previously.[23] PGE_2-d_4, AEA-d_8, 2-AG-d_8, and AA-d_8 were purchased from Cayman Chemical (Ann Arbor, MI). Indomethacin-d_4 and morpholine-d_8 were purchased from C/D/N isotopes (Pointe-Claire, Quebec, Canada). LM-4131-d_8 was synthesized using morpholine-d_8 under the same conditions as the LM-4131 synthesis.

In vivo experiments

4-5 week old male ICR mice were used for all experiments (Harlan, Indianapolis, IN). Mice were group-housed on a 12:12 light-dark cycle (lights on at 06:00), with food and water available *ad libitum*. Mice received a single i.p. injection of either compound or vehicle (DMSO) and were sacrificed by cervical dislocation and decapitation at various times after injection as noted in the text. All animal studies were approved by the Vanderbilt Institutional Animal Care and Use Committee and conducted in accordance with the NIH Guide for the Care and Use of Laboratory animals.

Tissue preparation and lipid extraction

After mice were sacrificed by cervical dislocation and decapitation, the brain, lungs, heart, liver, stomach, small intestine, and kidneys were immediately removed and washed with ice-cold calcium and magnesium-free Dulbecco's phosphate-buffered saline (GIBCO, Carlsbad, CA) and flash frozen on a metal block in dry ice. The tissue was placed in a tube and stored at -80ºC until extraction, usually within 24 hours. For PG, eCB, LM-4131, and indomethacin analysis, lipid extraction from tissue was carried out as described previously.[24]

Plasma preparation and precipitation

After mice were sacrificed by cervical dislocation and decapitation, trunk blood was collected in a 50 mL conical tube coated with 200 μL of 1,000 ISP units/mL heparin (Hospira, Inc. Lake Forest, IL). The blood volume was then measured into a 2 mL tube and put on ice. The plasma was separated by centrifuging the tube at 3,000 RPM for 5 minutes and then removed. Protein was precipitated by addition of 2 mL of ice-cold acetonitrile spiked with LM-4131-d_8 and indomethacin-d_4. After vigorous mixing, 1.5 mL of acetonitirile was dried down under a stream of nitrogen and reconstituted in 200 μL of 1:1 methanol:water for analysis by mass

spectrometry. For analysis of *ex vivo* plasma hydrolysis, mouse trunk blood samples were collected as outlined above or were collected into tubes fortified with paraoxon (~50 μM).

In vitro plasma hydrolysis

CD-1 mouse plasma with K2 EDTA (Bioreclamation, Westbury, NY) was incubated with 1 μM LM-4131 or indomethacin for 0, 1, and 4 hours at 4°C, room temperature, 37°C, or at 37°C with 1 mM paraoxon in duplicate. The samples were then extracted with 2 volumes of acetonitrile containing 1 nM LM-4131-d_8 and 1 nM of indomethacin-d_4 and centrifuged at 3,000 RPM for 5 minutes and placed into a 96-well plate for liquid chromatography-mass spectrometry (LC-MS) analysis.

Mass spectrometry analysis

Analytes were quantified using LC-MS/MS on a Thermo Finnigan Quantum triple-quadrupole mass spectrometer in positive-ion mode using selected reaction monitoring. Detection of eicosanoids was performed as previously described.[25] Fatty acid and eCB analyses were performed as previously described.[18] Indomethacin and LM-4131 were analyzed using the same gradient and mobile phases as the eicosanoids. The transitions monitored were indomethacin *m/z* 358→139, indomethacin-d_4 *m/z* 362→143, LM-4131 *m/z* 427→139, and LM-4131-d_8 *m/z* 435→139. The transitions and retention times for indomethacin and LM-4131 were validated using standards prior to the analysis of tissues and plasma. *In vitro* plasma hydrolysis metabolites were identified using a Finnigan LCQ Deca XP[PLUS] ion trap mass spectrometer (Thermo Fisher Scientific, Waltham, MA) operated in positive ionization mode as described previously.[26] Peak areas for the analytes were normalized to the appropriate internal standard and then normalized to tissue mass or plasma volume.

Statistical Analysis

Statistical analyses were performed using GraphPad Prism® Version 6.0c as described in the text. For determining statistical significance between groups, a two-tailed t-test, multiple t-test with Holm-Sidak multiple comparisons post-hoc test, or one-way ANOVA with a Holm-Sidak multiple comparisons post-hoc test were used as indicated. Error bars represent mean ± s.e.m throughout.

<u>Results</u>

Distribution of LM-4131 in plasma and brain over time

We analyzed the time-concentration profiles of LM-4131 in the brain and plasma over 24-hours following a single 10 mg/kg i.p. injection. The 10 mg/kg dose was selected as it was previously shown to be maximally efficacious at increasing brain AEA levels 2 hours after i.p. injection, as discussed in chapter IV.[18] LM-4131 was detected in plasma at 30 minutes (770 ± 280 ng/mL), but its concentration declined rapidly and was below the limit of detection at 4 hours (Figure 1). The levels of LM-4131 in the brain displayed a similar pharmacokinetic profile as in plasma. LM-4131 was initially present in high levels in the brain (4240 ± 475 ng/g), but the levels declined over 6 hours.

Given the approximately 5:1 ratio between the detected brain and plasma levels of LM-4131, we hypothesized that LM-4131 may be hydrolyzed by plasma *ex vivo*. To test the possibility of *in vitro* plasma hydrolysis of LM-4131 we incubated mouse plasma with 1 µM LM-4131 or indomethacin for 0, 1, and 4 hours at 4°C, room temperature, 37°C, or 37°C with 1 mM paraoxon. Paraoxon is a broad-spectrum serine hydrolase inhibitor and has previously been shown to impair the *ex vivo* plasma hydrolysis of ester or amide containing compounds.[27] We found that LM-4131, but not indomethacin, was hydrolyzed in plasma *in vitro* and that this hydrolysis was both temperature and paraoxon sensitive. LC-MS/MS analyses of the plasma extracts indicated that the product of hydrolysis was the *N-des*-chlorobenzoyl metabolite. Interestingly, the analogous *p*-chlorobenzoyl group of indomethacin is stable in plasma and plasma extracts.

To substantiate the *ex vivo* hydrolysis of LM-4131 as the basis for its low apparent plasma levels, we administered a 10 mg/kg i.p. dose to mice and collected trunk blood at 30 minutes, 2 hours, and 4 hours post administration in tubes that had been fortified with ~50 µM paraoxon or no paraoxon in parallel. In agreement with the *in vitro* hydrolysis experiment, addition of paraoxon protected LM-4131 from *ex vivo* hydrolysis, as a significant increase in the plasma concentration of LM-4131 was observed. A corresponding reduction of the *N-des*-chlorobenzoyl metabolite of LM-4131 was observed in plasma samples collected in the paraoxon-fortified collection tubes. Thus, LM-4131 levels in plasma are lowered through hydrolysis by a paraoxon-sensitive

enzyme *ex vivo* to form *N-des*-chlorobenzoyl LM-4131. Upon addition of paraoxon in the collection process the plasma:brain ratio of LM-4131 is approximately 2:1.
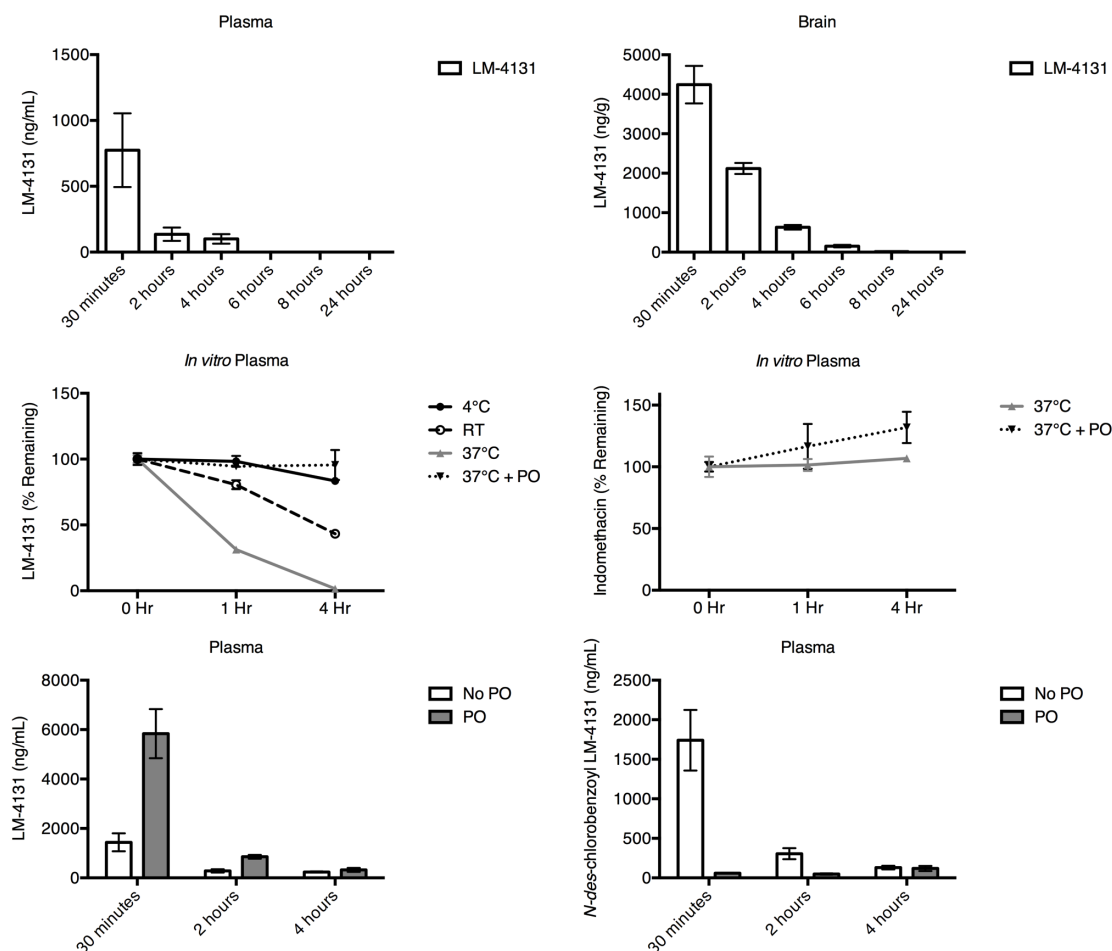
Figure 1: Detection of LM-4131 in plasma and brain after a single 10 mg/kg i.p. injection. LM-4131 is detected in both the brain and plasma, but is present at lower levels in plasma and disappears after 4 hours. While indomethacin is stable in plasma *ex vivo*, LM-4131 displays temperature and paraoxon-sensitive breakdown. Addition of paraoxon to the blood collection tubes resulted in a greater recovery of LM-4131 and a reduction in the *N-des*-chlorobenzoyl LM-4131 metabolite. Data shown are mean ± s.e.m., n = 5-12 for LM-4131 plasma and brain samples, n = 2 for in vitro plasma hydrolysis, and n = 5 for plasma paraoxon samples.

Hydrolysis of LM-4131 to indomethacin

LM-4131 is not hydrolyzed to indomethacin in the brain 2 hours after i.p. injection of 10 mg/kg LM-4131, as discussed in chapter IV.[18] To determine if LM-4131 is hydrolyzed to indomethacin at later time points in brain or plasma, we also measured the levels of indomethacin after 10 mg/kg LM-4131 i.p. injection in both the brain and plasma. Although indomethacin was not detected in the brain at any time point, low levels of indomethacin (2 ± 2 ng/mL) were detected in plasma at 4 hours post administration and peak concentrations of

indomethacin (48 ± 11 ng/mL) at 6 hours post administration, implicating amide hydrolysis as a minor pathway of biotransformation for LM-4131 *in vivo* (Figure 2). Indeed, representative chromatograms depicting plasma profiles at 2 and 6 hours following a 10 mg/kg i.p. administration of LM-4131 reveal the presence of indomethacin in plasma after 6 hours. This finding suggests that LM-4131 may act as a substrate-selective inhibitor for only 4 hours after treatment due to the hydrolytic biotransformation of LM-4131 to indomethacin.
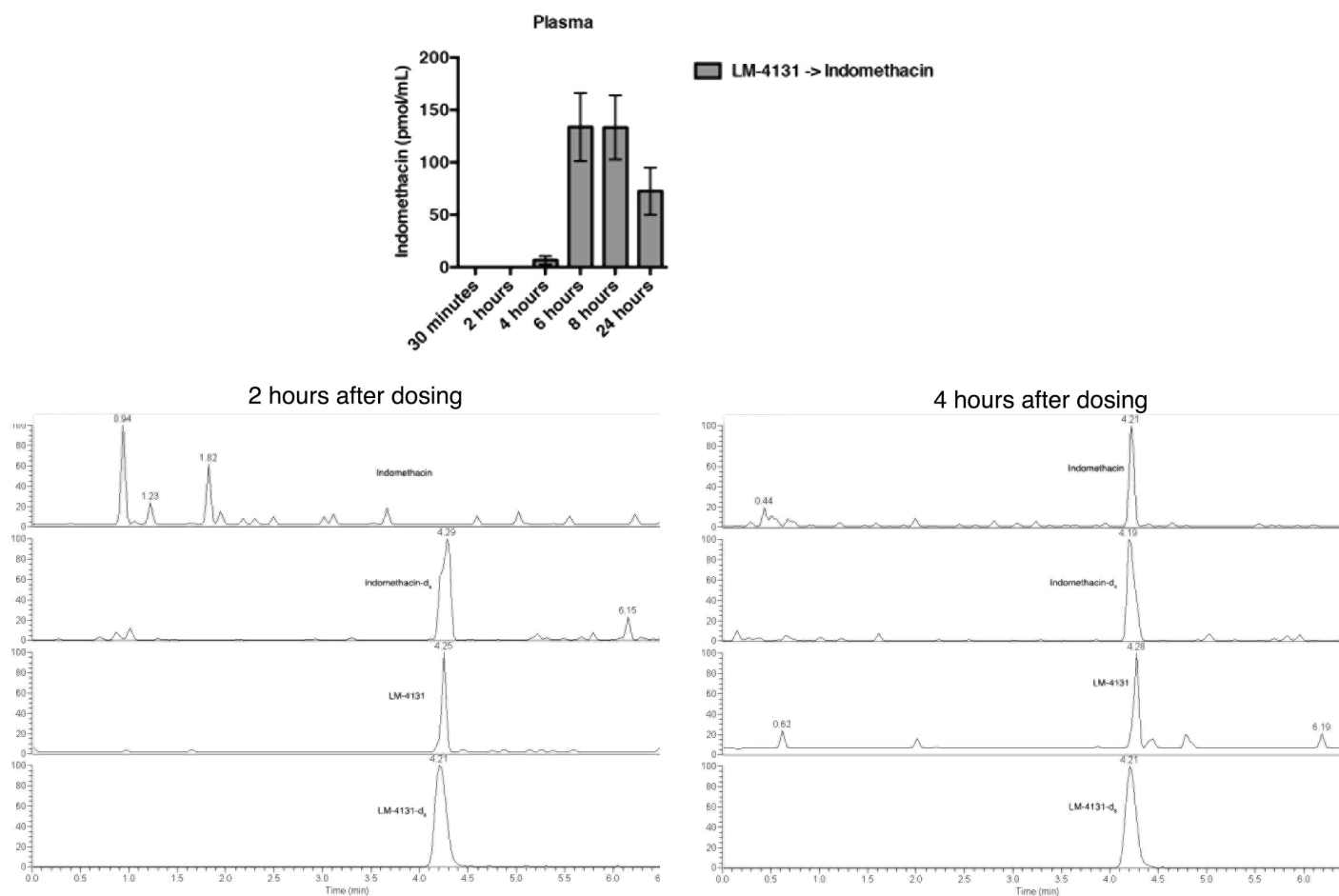
Figure 2: Hydrolysis of LM-4131 to indomethacin over time. Treatment of mice with LM-4131 (10 mg/kg) leads to the presence of indomethacin starting at 4 hours after dosing. Representative chromatograms depict the lack of indomethacin 2 hours after treatment and the presence of indomethacin 6 hours after treatment. Data shown are mean ± s.e.m., n = 5-12.

Time-dependent distribution of indomethacin in plasma and brain

To compare the time-course of LM-4131 to its parent compound, we measured the levels of indomethacin in plasma and brain over a 24-hour time period after a single 10 mg/kg i.p. injection of indomethacin. Indomethacin was initially present at high levels in the plasma and was detected over the entire

24-hour time period (Figure 3). Indomethacin displayed a characteristic long half-life in plasma after i.p. injection in mice, which has previously been shown in other species and using other routes of administration.[28-31] Indomethacin preferentially partitioned to the plasma, as in the brain it was present at approximately 20 percent of the level found in plasma. Despite it being present in reduced amounts relative to plasma, indomethacin was also detected in the brain over the entire 24-hour period. This is in agreement with previous studies showing that indomethacin is highly plasma bound and does not have high brain penetrance.[32] Thus, indomethacin has a similar pharmacokinetic profile in mice after i.p. injection as in other species and by different administration routes.
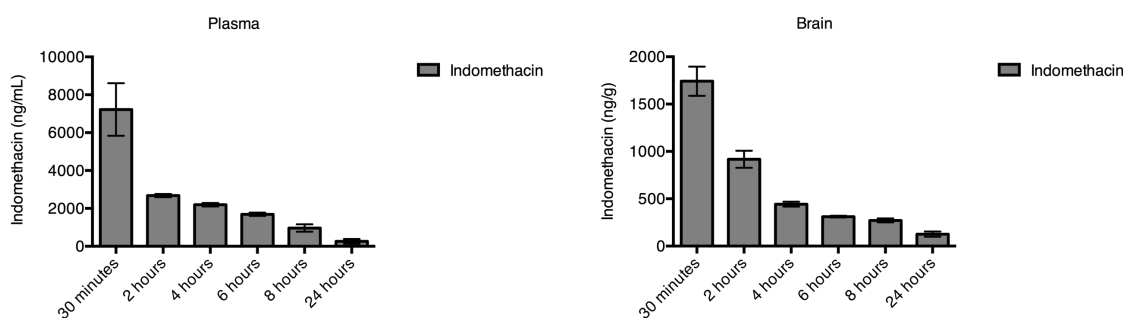
Figure 3: Time-course of indomethacin in plasma and brain. Indomethacin was detected in plasma and brain over the entire 24-hour period after a single 10 mg/kg i.p. injection. Data shown are mean ± s.e.m., n = 5-7.

Effects of indomethacin and LM-4131 on brain eCBs and PGs over time

To determine if the pharmacokinetic profiles of indomethacin and LM-4131 match their biochemical effects we measured the levels of brain eCBs and PGs over a 24-hour time course after 10 mg/kg i.p. injection of vehicle, indomethacin, or LM-4131. Both indomethacin and LM-4131 significantly increased brain AEA at the 2- and 4-hour time points, but not at later time points (Figure 4). The increase in AEA produced by LM-4131 correlates well with the detection of LM-4131 in the brain. In contrast, while indomethacin was present in the brain over the entire 24-hour period, it only significantly increased AEA for 4 hours. Neither indomethacin nor LM-4131 significantly increased 2-AG in the brain at any time point. Indomethacin significantly decreased brain PGs at all time points, whereas LM-4131 decreased brain PGs starting only 6 hours after treatment. The inhibition of PGs starting at 6 hours by LM-4131 is consistent with the time course for the hydrolysis of LM-4131 as estimated by the appearance of indomethacin in the plasma starting at 4 hours after LM-4131 dosing.
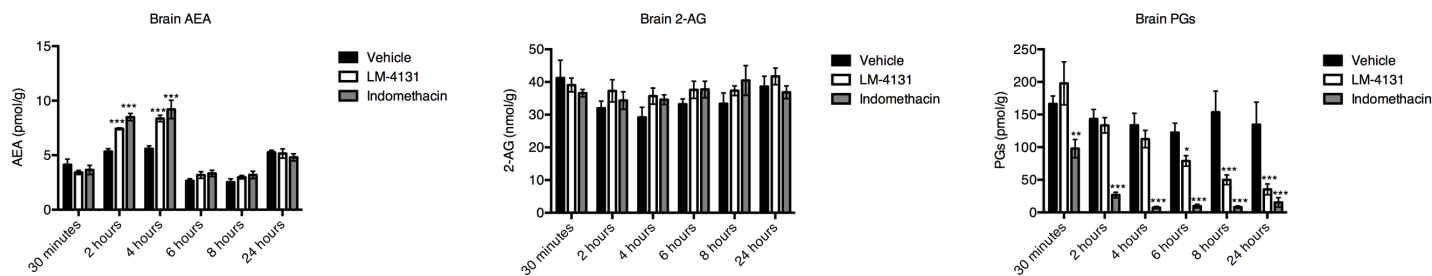
Figure 4: Effects of LM-4131 and indomethacin over time on brain eCBs and PGs. While LM-4131 and indomethacin significantly increase AEA at 2 and 4 hours after treatment, they had no significant effects on AEA at later time points or on 2-AG at any time points. Indomethacin significantly inhibited PG production at all time points, while LM-4131 significantly inhibited PG production starting at 6 hours after treatment. Data shown are mean ± s.e.m., n = 5-7.

Effects of low-dose indomethacin

Although no indomethacin was detected in the brain after LM-4131 administration, the small amount of hydrolysis to indomethacin detected in plasma and the PG inhibition after 6 hours prompted us to test the effects of low-dose indomethacin (0.5 mg/kg i.p.) on brain eCB and PG levels. Indomethacin injected at 0.5 mg/kg i.p. did not increase brain AEA 2 hours after treatment (Figure 5). Low-dose indomethacin also had no effect on 2-AG, but it did significantly decrease brain PG production. Thus, the biochemical effects of low-dose indomethacin do not mirror the effects of higher dose indomethacin or LM-4131 on brain AEA, but it does significantly inhibit PG production, suggesting that low doses of indomethacin inhibit COX-1 but not COX-2 in the brain. This further suggests that the PG inhibition observed starting at 6 hours after LM-4131 treatment could be due to the hydrolysis to indomethacin.
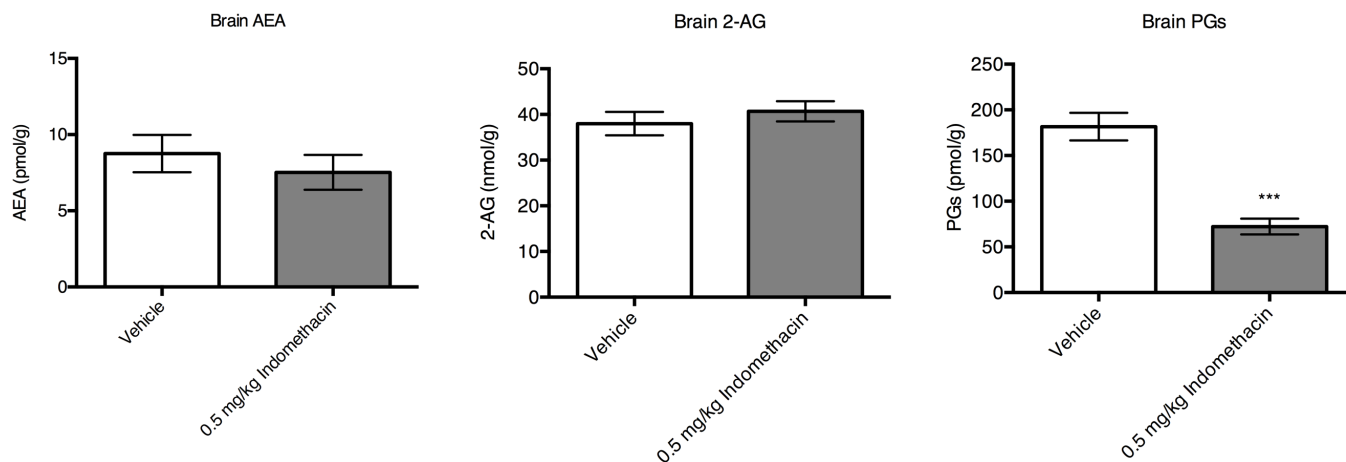
Figure 5: Effects of low-dose indomethacin on brain eCBs and PGs. Low-dose indomethacin (0.5 mg/kg) had no significant impact on AEA or 2-AG levels, but significantly decreased PG levels in the brain. Data shown are mean ± s.e.m., n = 10.

Tissue distribution of LM-4131 and indomethacin

To further examine the effects of tertiary amide substitution on tissue distribution we analyzed the levels of indomethacin and LM-4131 in the brain, lungs, kidneys, heart, intestine, stomach, liver, and plasma 2 hours after a single 10 mg/kg i.p. injection of either indomethacin or LM-4131. LM-4131 was detected in similar amounts throughout each of the tissues analyzed with the exception of the liver (Figure 6). Indomethacin was present in the largest amounts in the stomach and intestine, but in sharp contrast to LM-4131, was present in low amounts in the brain. Both compounds were detected in all of the tissues analyzed.
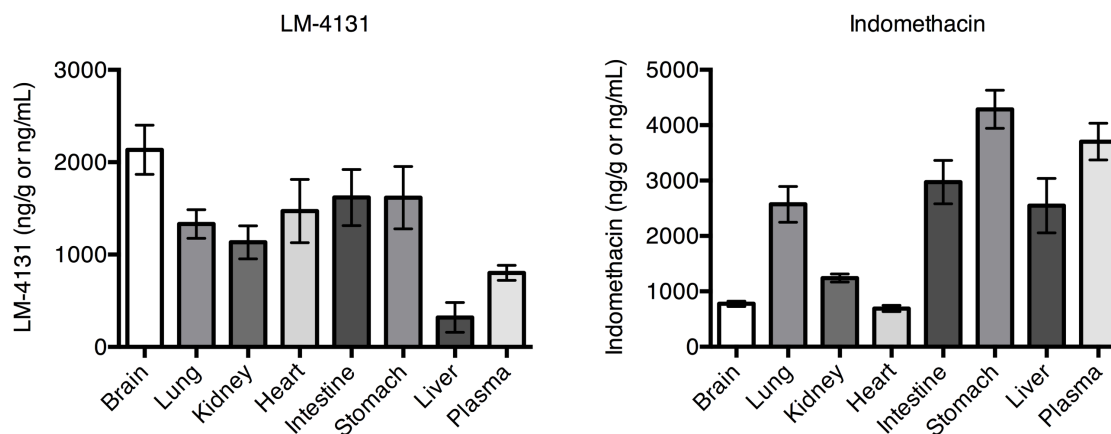
Figure 6: Tissue distribution of LM-4131 and indomethacin. LM-4131 and indomethacin were differentially distributed throughout the tissues analyzed. Data shown are mean ± s.e.m., n = 17.

Discussion

The addition of a morpholino amide functionality to indomethacin produces large changes in both activity and pharmacokinetics. Whereas indomethacin is a non-selective COX-1 and COX-2 inhibitor, LM-4131 is a substrate-selective inhibitor of COX-2.[18] This gives rise to a useful probe with the same core structure of indomethacin for studying the differential effects of COX inhibition *in vivo*. To understand the utility of these molecules, we characterized the pharmacokinetic and pharmacodynamic properties of LM-4131 and indomethacin and related them to eCB and PG modulation.

This is the first *in vivo* pharmacokinetic-pharmacodynamic profile of LM-4131, but the pharmacokinetics and pharmacodynamics of indomethacin have been extensively examined. Indomethacin is rapidly absorbed after dosing, although it is highly (>90%) bound to plasma proteins at therapeutic plasma concentrations.[28,29] Indomethacin displays a characteristic long half-life between 5 and 10 hours depending on the species and route of administration.[29,30,33] The long half-life of indomethacin is in part due to the glucuronidation of about 60 percent of indomethacin, which leads to extended entero-hepatic circulation.[28,31] In addition to glucuronidation, indomethacin is metabolized to *O-des*-methylindomethacin, *N-des*-chlorobenzoylindomethacin, and *O-des*-methylindomethacin-*N-des*-chlorobenzoylindomethacin, all of which can be detected in plasma following dosing (Figure 7).[22,34] The demethylation of indomethacin is catalyzed by both CYP2C9 and CYP2D6, whereas the cleavage of the chlorobenzoyl group is achieved by a liver carboxylesterase.[35,36]

Indomethacin   O-*des*-methyl indomethacin

CYP2C9 or CYP2D6

Carboxylesterase   Carboxylesterase

CYP2C9 or CYP2D6

N-des-chlorobenzoyl indomethacin   O-*des*-methyl-*N-des*-chlorobenzoyl indomethacin
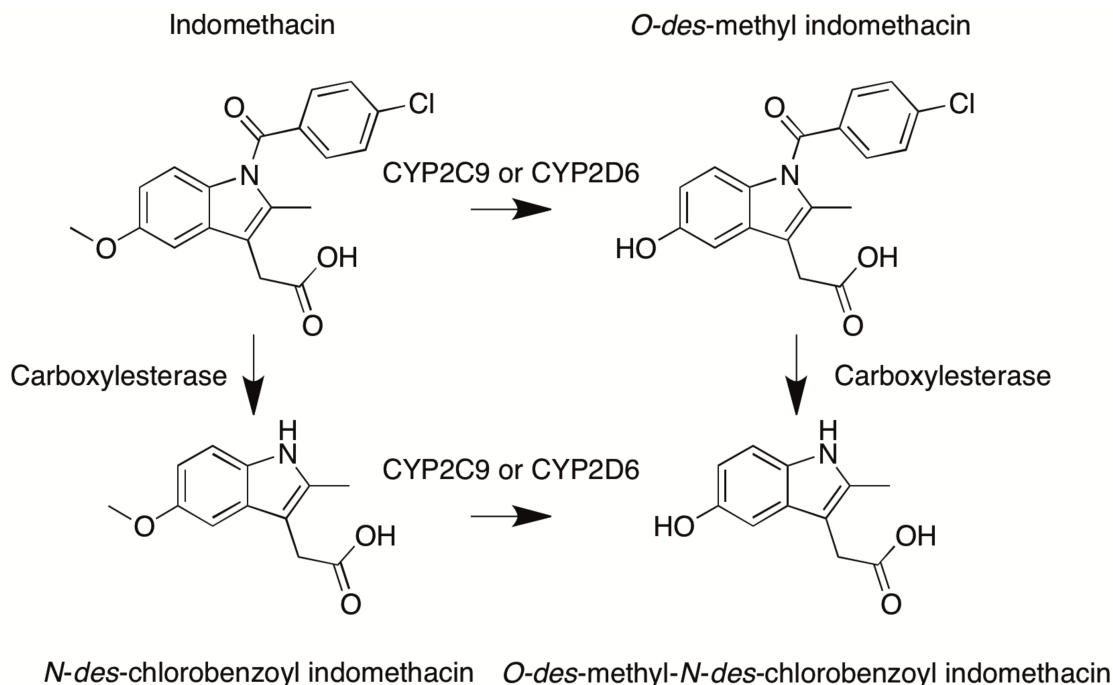
Figure 7: *In vivo* metabolism of indomethacin.

The modification of the carboxylate of indomethacin to a tertiary amide results in notable pharmacokinetic differences *in vivo*. The tissue distribution and half-life of LM-4131 are significantly different than indomethacin. LM-4131 has a much shorter half-life than indomethacin, suggesting that the morpholino ring contributes to metabolic instability. In particular, the morpholino ring of LM-4131 leads to paraoxon-sensitive *ex vivo* plasma hydrolysis to *N-des*-chlorobenzoyl LM-4131; the analogous plasma hydrolysis does not occur with indomethacin. In contrast to indomethacin and other acidic NSAIDs, LM-4131 is more centrally penetrant as evidenced by the higher levels relative to indomethacin in the brain. Numerous efforts have been made to improve the brain penetrance of indomethacin including creating more lipophilic pro-drugs, using alternative methods of administration, or conjugation of indomethacin with endogenous substrates that are transported across the blood-brain barrier such as glucose.[32,37,38]

Although the *in vivo* metabolism of LM-4131 has not been previously studied, the metabolism of LM-4131 by rat liver microsomes *in vitro* has been characterized. LM-4131 is extensively metabolized by rat liver microsomes, producing metabolites analogous to indomethacin metabolites including the loss of the chlorobenzoyl group and demethylation of the methoxy group of the indole ring (Figure 8).[21] In addition, LM-

4131 is converted to metabolites distinct from those formed from indomethacin. LM-4131 is hydroxylated on the morpholine ring and the morpholine ring can also be opened at the ether.[21]
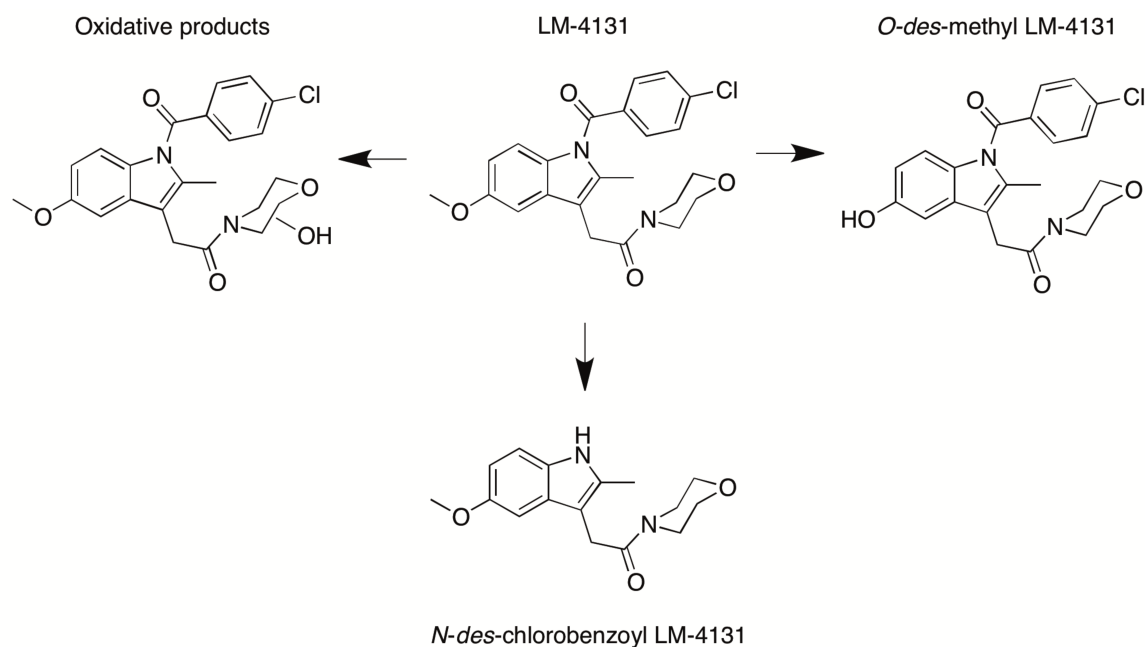
Figure 8: *In vivo* metabolism of LM-4131.

Of particular importance, LM-4131 is hydrolyzed in small amounts to indomethacin in a time-dependent manner *in vivo*. Indomethacin was detected in plasma starting at 4 hours after LM-4131 treatment and significant PG inhibition occurred in the brain starting at 6 hours after dosing. This reveals that LM-4131 acts as a substrate-selective inhibitor for 4 hours, but is then converted to a non-substrate-selective inhibitor at later time points. Whether this non-substrate-selective inhibition is due to the hydrolysis to indomethacin or conversion to a different active metabolite is unclear, however, we have found that a low dose of indomethacin is sufficient to cause PG inhibition but not AEA increases in the brain. The time course of LM-4131 action on AEA matches well with the presence of LM-4131 in the brain, as it increased AEA at 2 and 4 hours after treatment, and LM-4131 is present in the brain at these time points. In contrast, although indomethacin inhibits PG production over the entire 24-hour period after treatment, it only increased AEA levels at 2 and 4 hours after treatment.

Although LM-4131 is a useful probe for studying the acute effects of substrate-selective inhibition of COX-2, further drug discovery efforts focused on metabolically stable substrate-selective inhibitors are clearly

needed to fully investigate the *in vivo* effects of substrate-selective inhibition of COX-2 in both longer time-course settings and chronic dosage studies. Although other excellent substrate-selective inhibitors such as (*R*)-flurbiprofen are available for *in vitro* use in both purified protein and cellular systems, at this point, LM-4131 is the only substrate-selective inhibitor suitable for *in vivo* use.[18,19] Although these studies identify that it is only useful in a very limited, short-term setting, it is still a useful *in vivo* probe to determine the impact of COX-2 on eCB metabolism, particularly in the brain.

References

1. Di Marzo, V. Endocannabinoids: synthesis and degradation. *Reviews of physiology, biochemistry and pharmacology* **160**, 1-24 (2008).
2. Piomelli, D. The molecular logic of endocannabinoid signalling. *Nature reviews. Neuroscience* **4**, 873-884 (2003).
3. Ahn, K., McKinney, M.K. & Cravatt, B.F. Enzymatic pathways that regulate endocannabinoid signaling in the nervous system. *Chemical reviews* **108**, 1687-1707 (2008).
4. Matias, I. & Di Marzo, V. Endocannabinoid synthesis and degradation, and their regulation in the framework of energy balance. *Journal of endocrinological investigation* **29**, 15-26 (2006).
5. Wang, H.*, et al.* Differential regulation of endocannabinoid synthesis and degradation in the uterus during embryo implantation. *Prostaglandins & other lipid mediators* **83**, 62-74 (2007).
6. Wang, J. & Ueda, N. Biology of endocannabinoid synthesis system. *Prostaglandins & other lipid mediators* **89**, 112-119 (2009).
7. Cravatt, B.F.*, et al.* Molecular characterization of an enzyme that degrades neuromodulatory fatty-acid amides. *Nature* **384**, 83-87 (1996).
8. Long, J.Z.*, et al.* Selective blockade of 2-arachidonoylglycerol hydrolysis produces cannabinoid behavioral effects. *Nature chemical biology* **5**, 37-44 (2009).
9. Marrs, W.R.*, et al.* The serine hydrolase ABHD6 controls the accumulation and efficacy of 2-AG at cannabinoid receptors. *Nature neuroscience* **13**, 951-957 (2010).
10. Savinainen, J.R., Saario, S.M. & Laitinen, J.T. The serine hydrolases MAGL, ABHD6 and ABHD12 as guardians of 2-arachidonoylglycerol signalling through cannabinoid receptors. *Acta physiologica* **204**, 267-276 (2012).
11. Xie, S.*, et al.* Inactivation of lipid glyceryl ester metabolism in human THP1 monocytes/macrophages by activated organophosphorus insecticides: role of carboxylesterases 1 and 2. *Chemical research in toxicology* **23**, 1890-1904 (2010).
12. Wang, R.*, et al.* Identification of Palmitoyl Protein Thioesterase 1 in Human THP1 Monocytes and Macrophages and Characterization of Unique Biochemical Activities for This Enzyme. *Biochemistry* **52**, 7559-7574 (2013).
13. Yu, M., Ives, D. & Ramesha, C.S. Synthesis of prostaglandin E2 ethanolamide from anandamide by cyclooxygenase-2. *The Journal of biological chemistry* **272**, 21181-21186 (1997).
14. Kozak, K.R., Rowlinson, S.W. & Marnett, L.J. Oxygenation of the endocannabinoid, 2-arachidonylglycerol, to glyceryl prostaglandins by cyclooxygenase-2. *The Journal of biological chemistry* **275**, 33744-33749 (2000).
15. Chen, J.K.*, et al.* Identification of novel endogenous cytochrome p450 arachidonate metabolites with high affinity for cannabinoid receptors. *The Journal of biological chemistry* **283**, 24514-24524 (2008).
16. Snider, N.T., Walker, V.J. & Hollenberg, P.F. Oxidation of the endogenous cannabinoid arachidonoyl ethanolamide by the cytochrome P450 monooxygenases: physiological and pharmacological implications. *Pharmacological reviews* **62**, 136-154 (2010).
17. Ueda, N.*, et al.* Lipoxygenase-catalyzed oxygenation of arachidonylethanolamide, a cannabinoid receptor agonist. *Biochimica et biophysica acta* **1254**, 127-134 (1995).
18. Hermanson, D.J.*, et al.* Substrate-selective COX-2 inhibition decreases anxiety via endocannabinoid activation. *Nature neuroscience* **16**, 1291-1298 (2013).
19. Duggan, K.C.*, et al.* (R)-Profens are substrate-selective inhibitors of endocannabinoid oxygenation by COX-2. *Nature chemical biology* **7**, 803-809 (2011).
20. Prusakiewicz, J.J., Duggan, K.C., Rouzer, C.A. & Marnett, L.J. Differential sensitivity and mechanism of inhibition of COX-2 oxygenation of arachidonic acid and 2-arachidonoylglycerol by ibuprofen and mefenamic acid. *Biochemistry* **48**, 7353-7355 (2009).
21. Zhang, Q., Ma, P., Cole, R.B. & Wang, G. In vitro metabolism of indomethacin morpholinylamide (BML-190), an inverse agonist for the peripheral cannabinoid receptor (CB(2)) in rat liver microsomes.

European journal of pharmaceutical sciences : official journal of the European Federation for Pharmaceutical Sciences **41**, 163-172 (2010).

22. Harman, R.E., Meisinger, M.A., Davis, G.E. & Kuehl, F.A., Jr. The Metabolites of Indomethacin, a New Anti-Inflammatory Drug. *The Journal of pharmacology and experimental therapeutics* **143**, 215-220 (1964).

23. Kalgutkar, A.S., Marnett, A.B., Crews, B.C., Remmel, R.P. & Marnett, L.J. Ester and amide derivatives of the nonsteroidal antiinflammatory drug, indomethacin, as selective cyclooxygenase-2 inhibitors. *Journal of medicinal chemistry* **43**, 2860-2870 (2000).

24. Patel, S., Kingsley, P.J., Mackie, K., Marnett, L.J. & Winder, D.G. Repeated homotypic stress elevates 2-arachidonoylglycerol levels and enhances short-term endocannabinoid signaling at inhibitory synapses in basolateral amygdala. *Neuropsychopharmacology : official publication of the American College of Neuropsychopharmacology* **34**, 2699-2709 (2009).

25. Kingsley, P.J. & Marnett, L.J. LC-MS-MS analysis of neutral eicosanoids. *Methods in enzymology* **433**, 91-112 (2007).

26. Morrison, R.D., *et al.* The role of aldehyde oxidase and xanthine oxidase in the biotransformation of a novel negative allosteric modulator of metabotropic glutamate receptor subtype 5. *Drug metabolism and disposition: the biological fate of chemicals* **40**, 1834-1845 (2012).

27. Yoshigae, Y., Imai, T., Taketani, M. & Otagiri, M. Characterization of esterases involved in the stereoselective hydrolysis of ester-type prodrugs of propranolol in rat liver and plasma. *Chirality* **11**, 10-13 (1999).

28. Yesair, D.W., Callahan, M., Remington, L. & Kensler, C.J. Role of the entero-hepatic cycle of indomethacin on its metabolism, distribution in tissues and its excretion by rats, dogs and monkeys. *Biochemical pharmacology* **19**, 1579-1590 (1970).

29. Duggan, D.E., Hogans, A.F., Kwan, K.C. & McMahon, F.G. The metabolism of indomethacin in man. *The Journal of pharmacology and experimental therapeutics* **181**, 563-575 (1972).

30. Alvan, G., Orme, M., Bertilsson, L., Ekstrand, R. & Palmer, L. Pharmacokinetics of indomethacin. *Clinical pharmacology and therapeutics* **18**, 364-373 (1975).

31. Kwan, K.C., Breault, G.O., Umbenhauer, E.R., McMahon, F.G. & Duggan, D.E. Kinetics of indomethacin absorption, elimination, and enterohepatic circulation in man. *Journal of pharmacokinetics and biopharmaceutics* **4**, 255-280 (1976).

32. Dahan, A. & Hoffman, A. Mode of administration-dependent brain uptake of indomethacin: sustained systemic input increases brain influx. *Drug metabolism and disposition: the biological fate of chemicals* **35**, 321-324 (2007).

33. Emori, H.W., Paulus, H., Bluestone, R., Champion, G.D. & Pearson, C. Indomethacin serum concentrations in man. Effects of dosage, food, and antacid. *Annals of the rheumatic diseases* **35**, 333-338 (1976).

34. Bernstein, M.S. & Evans, M.A. High-performance liquid chromatography-fluorescence analysis for indomethacin and metabolites in biological fluids. *Journal of chromatography* **229**, 179-187 (1982).

35. Nakajima, M., *et al.* Cytochrome P450 2C9 catalyzes indomethacin O-demethylation in human liver microsomes. *Drug metabolism and disposition: the biological fate of chemicals* **26**, 261-266 (1998).

36. Terashima, K., *et al.* Purification and partial characterization of an indomethacin hydrolyzing enzyme from pig liver. *Pharmaceutical research* **13**, 1327-1335 (1996).

37. Dvir, E., *et al.* A novel phospholipid derivative of indomethacin, DP-155 [mixture of 1-steroyl and 1-palmitoyl-2-{6-[1-(p-chlorobenzoyl)-5-methoxy-2-methyl-3-indolyl acetamido]hexanoyl}-sn-glycero-3-phosophatidyl [corrected] choline], shows superior safety and similar efficacy in reducing brain amyloid beta in an Alzheimer's disease model. *The Journal of pharmacology and experimental therapeutics* **318**, 1248-1256 (2006).

38. Gynther, M., *et al.* Glucose promoiety enables glucose transporter mediated brain uptake of ketoprofen and indomethacin prodrugs in rats. *Journal of medicinal chemistry* **52**, 3348-3353 (2009).

IDENTIFICATION OF ALTERNATIVE *IN VIVO* SUBSTRATE-SELECTIVE COX-2 INHIBITORS

<u>Introduction</u>

The endocannabinoids (eCBs), anandamide (AEA) and 2-arachidonoylglycerol (2-AG), are the endogenous ligands of the cannabinoid 1 and 2 receptors (CB$_1$ and CB$_2$).[1-3] eCBs are synthesized from phospholipids through distinct pathways in response to calcium influx or the activation of certain G-protein-coupled receptors.[4-6] After synthesis, eCB levels are mainly regulated through deactivation by hydrolysis. AEA is primarily hydrolyzed by fatty acid amide hydrolase to arachidonic acid (AA) and ethanolamine, whereas 2-AG is hydrolyzed to AA and glycerol by several enzymes including monoacylglycerol lipase, α/β-hydrolase domain 6, α/β-hydrolase domain 12, carboxylesterases 1 and 2, and palmitoylprotein thioesterase 1.[7-12]

In addition to hydrolysis, AEA and 2-AG can undergo oxygenation by a variety of enzymes including lipoxygenases, cyclooxygenases, and cytochromes P450.[13-17] Although the extent to which each oxygenation pathway is involved in the turnover of eCBs is uncertain, our work demonstrates that cyclooxygenase-2 (COX-2) can become a third pathway of eCB metabolism at sites of constitutive expression or at sites of inflammation, as discussed in chapters III and IV.[18,19] COX-1 and COX-2 catalyze the committed step in the biosynthesis of prostaglandins (PGs) from AA. In addition to metabolizing AA, COX-2 oxygenates AEA to form prostaglandin ethanolamides and 2-AG to form prostaglandin glycerol esters (PG-Gs).[13,14] These prostaglandin products are not ligands for the cannabinoid receptors, so COX-2 activity inactivates eCBs while also synthesizing a series of bioactive eCB-derived prostanoids.

Non-steroidal anti-inflammatory drugs (NSAIDs) produce their effects by inhibiting COX-1 and/or COX-2. Most NSAIDs inhibit the oxygenation of AA, 2-AG, and AEA with similar potencies, but a subset of NSAIDs selectively inhibit the oxygenation of 2-AG and AEA by COX-2 without inhibiting AA oxygenation, a phenomenon termed substrate-selective inhibition of COX-2.[20] For example, indomethacin inhibits the oxygenation of AA, 2-AG, and AEA with similar potencies, but the morpholino analog of indomethacin, LM-4131, selectively inhibits endocannabinoid oxygenation *in vitro* and *in vivo*, as discussed in chapter IV.[18] Intraperitoneal (i.p.) administration of LM-4131 (10 mg/kg) elevates the levels of brain AEA and 2-AG without

affecting the levels of AA or PGs 2 hours after treatment.[18] The elevation of eCBs elicited by LM-4131 is COX-2 dependent and produces anxiolytic effects in pre-clinical models of anxiety through CB_1 receptor activation.[18]

Substrate-selective COX-2 inhibitors are important tools for dissecting the role of COX-2 oxygenation in eCB metabolism due to their lack of confounding PG inhibition. LM-4131 has robust effects at 2 hours after i.p. injection, but we found that while LM-4131 is present in the brain up to 6 hours after dosing, it loses substrate-selectivity at that time, apparently due to partial hydrolysis to indomethacin, as discussed in chapter V. Thus, LM-4131 is a not useful probe for studying substrate-selective COX-2 inhibition *in vivo* in acute settings beyond 4 hours or chronic settings.

To attempt to discover a more suitable *in vivo* probe, we explored alternative substrate-selective COX-2 inhibitors *in vivo*. Preliminary *in vitro* studies identified that lumiracoxib, an analog of diclofenac, was an extremely potent substrate-selective COX-2 inhibitor.[21] Lumiracoxib was originally classified as a COX-2-selective inhibitor, and in the human whole blood assay it has the highest selectivity for COX-2 inhibition over COX-1 inhibition of any NSAID.[22] Lumiracoxib is efficacious in multiple pre-clinical models of pain and inflammation.[23] Following a series of promising clinical trials, Novartis brought lumiracoxib to market in several countries under the trade name Prexige for the treatment of pain and inflammation in patients with osteoarthritis.[24-41]

Although lumiracoxib was efficacious in patient populations, it was withdrawn from most markets due to idiosyncratic liver toxicity stemming from the formation of reactive quinone imine lumiracoxib metabolites by peroxidases and cytochromes P450 in the liver.[42-45] These reactive quinone imine metabolites are formed by the oxidation of the 4' position by CYP2C9, which results in the formation of 4'-hydroxylumiracoxib (Figure 1). Further oxidation of the lower ring leads to the formation of reactive quinone imines, which are electrophilic species that can react to form glutathione and protein adducts. The hepatotoxicity of lumiracoxib is mirrored by diclofenac, which also can be metabolized to chemically reactive species by cytochrome P450-catalyzed hydroxylation at the 4' position, but also can be oxidized at the 5 position, unlike lumiracoxib which contains a methyl group to protect the 5 position from oxidation.[46,47] As with lumiracoxib, the hydroxylated diclofenac

metabolites can be further oxidized to reactive quinone imine intermediates, which have been characterized indirectly through the detection of glutathione and protein adducts.[48-50]
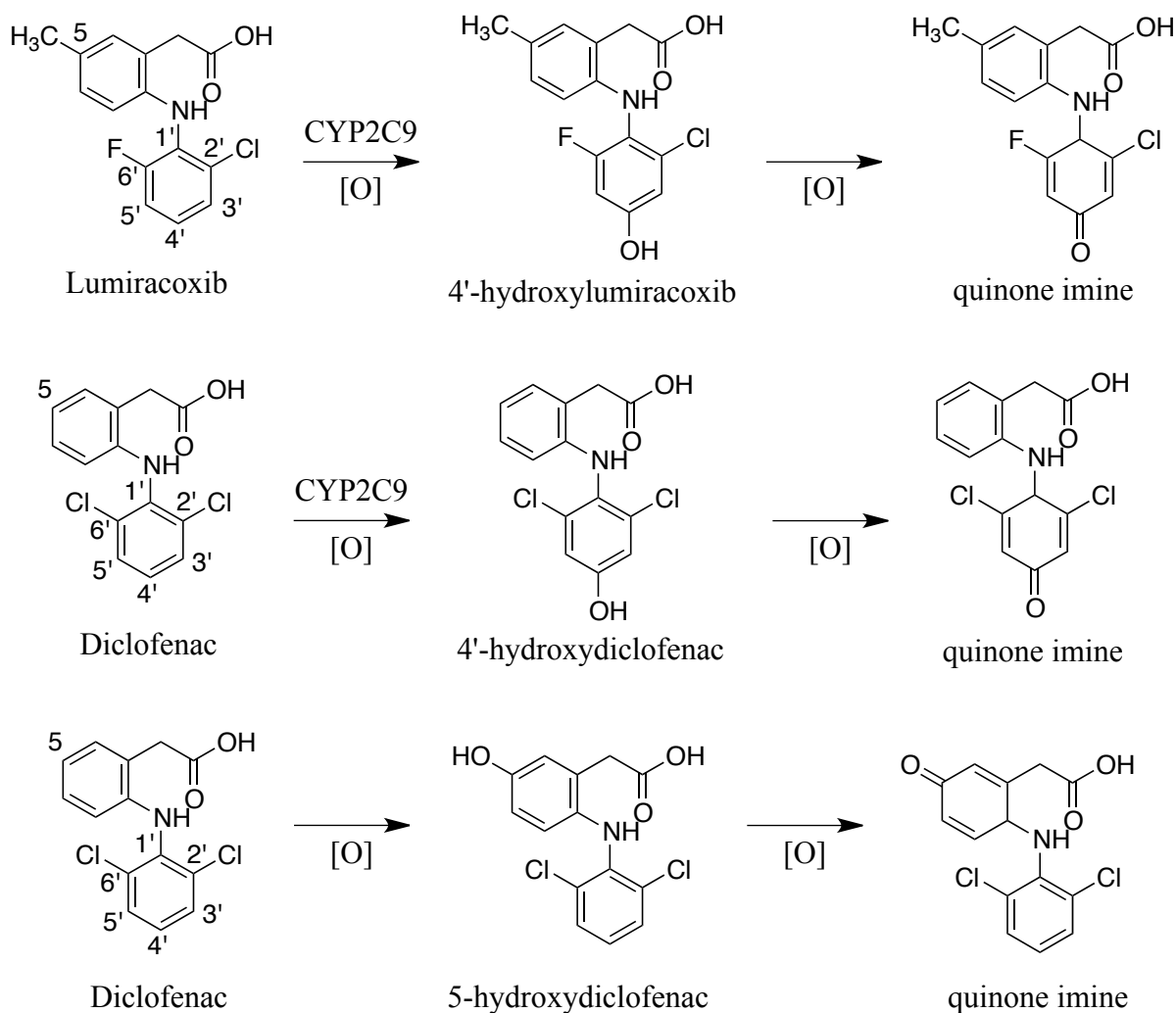
Figure 1: Oxidative metabolism of lumiracoxib and diclofenac in the liver.

Despite the clinical metabolic toxicity exhibited by lumiracoxib, some studies suggest that the liver toxicity of lumiracoxib could be avoided by giving lower doses or by genotyping patients, as a specific allele can identify at risk patients.[51,52] Lumiracoxib is an attractive possibility for an *in vivo* substrate-selective inhibitor due to the extensive studies identifying its therapeutic effects. In addition, lumiracoxib does not increase cardiovascular risk or cause increased gastrointestinal complications in patients, which are the two primary complications in individuals who take NSAIDs for prolonged periods.[53-56] Thus, management of the metabolic toxicity of lumiracoxib by using a lower dose or development of an analog that is not metabolized to reactive quinone imine metabolites could lead to a promising *in vivo* substrate-selective COX-2 inhibitor.

To assess the potential of lumiracoxib to act as a substrate-selective COX-2 inhibitor we analyzed its ability to modulate brain eCB and PG levels in both acute and chronic settings after intraperitoneal injection. We found that lumiracoxib exhibits substrate-selective COX-2 inhibition at a 1 mg/kg dose in mice but not at higher concentrations. Additionally, lumiracoxib retains substrate-selective inhibition in chronic dosing regiments when given at 1 mg/kg once per day. The *des*-fluoro derivative of lumiracoxib, which may have a reduced capacity to form reactive quinone imine intermediates *in vivo*, also displayed substrate-selective COX-2 inhibition in mice.

Experimental Procedures

Materials

Lumiracoxib was purchased from LKT Laboratories (St. Paul, MN). JZL-184, PGE_2–d_4, AA-d_8, 2-AG-d_8, and AEA-d_8 were purchased from Cayman Chemical (Ann Arbor, MI). LM-5703 was synthesized as previously described.[57]

Animals

5-7 week old male ICR mice were used for all experiments (Harlan, Indianapolis, IN). Mice were housed 5 per cage. Wild-type and knockout $Faah^{-/-}$ and $Ptgs2^{-/-}$ mice were derived from heterozygote breeding pairs, bred and genotyped as previously described.[58,59] Mice were group-housed on a 12:12 light-dark cycle (lights on at 06:00), with food and water available *ad libitum*. All animal studies were approved by the Vanderbilt Institutional Animal Care and Use Committee and conducted in accordance with the NIH Guide for the Care and Use of Laboratory animals.

Tissue preparation and lipid extraction

Mice were sacrificed by cervical dislocation and decapitation. The brain was then rapidly removed and frozen on a metal block in dry ice. The tissue was then placed in a tube and stored at -80ºC until extraction, usually one day after harvesting. For PG and eCB analysis, lipid extraction from tissue was carried out as described previously.[60]

In vitro enzyme purification and activity assays

MAGL was purified using BL21(DE3) pLysS E. coli transformed with pET-45b(+) plasmid containing human MGL-His. Cells were grown at 37ºC to a density of 0.7 OD and then protein expression induced with IPTG (1 mM). Cells were harvested 4 hr later and proteins purified using Ni-NTA Agarose (Qiagen) as previously described.[61] After purification, the protein was dialyzed overnight at 4ºC into buffer containing 0 mM HEPES and 0.01% TritonX-100. MAGL inhibition was assessed as previously described.[61] Humanized rat FAAH was a generous gift of R. Stevens and B. Cravatt (The Scripps Research Institute). FAAH inhibition was assessed as previously described.[62]

Mass spectrometry analysis

Analytes were quantified using LC-MS/MS on a Quantum triple-quadrupole mass spectrometer in positive-ion mode using selected reaction monitoring. Detection of eicosanoids was performed as previously described.[63] For fatty acid analysis the mobile phases used were 80 µM AgOAc with 0.1% (v/v) acetic acid in H_2O (solvent A) and 120 µM AgOAc with 0.1% (v/v) acetic acid in MeOH (solvent B). The analytes were eluted using a gradient from 20% A to 99% B over 5 minutes. The transitions used were m/z 434→416 for OEA, m/z 456→438 for AEA, m/z 464→446 for AEA-d_8, m/z 463→389 for 2-OG, m/z 485→411 for 2-AG, m/z 493→419 for 2-AG-d_8, m/z 519→409 for AA, and m/z 527→417 for AA-d_8. Peak areas for the analytes were normalized to the appropriate internal standard and then normalized to tissue mass for *in vivo* samples.

Statistical analysis

Statistical analyses were performed using GraphPad Prism® Version 6.0c. For determining statistical significance between groups a two-tailed t-test, one-way ANOVA, or two-way ANOVA with a Sidak's post-test analysis were used as indicated. Error bars represent S.E.M. throughout. N for each group represents number of mice, i.e. independent biological replicate. Mice were arbitrarily assigned to treatment group in a manner that resulted in approximately equal sample sized per treatment group. Each treatment group was represented at least once per cage of mice.

In vivo effects of lumiracoxib

An important consideration for using compounds in chronic studies is the ability to administer a drug in an aqueous solution. While LM-4131 is only soluble in DMSO, lumiracoxib can be dissolved in aqueous buffers. One commonly used solution for intraperitoneal injections of eCB augmenting agents is 18:1:1 saline:ethanol:emulphor.[8] This buffer solubilizes lipophilic drugs in a solution that is not toxic to mice in chronic settings, which is not the case for DMSO.[64-66] We first sought to determine the dose-response of lumiracoxib in the 18:1:1 saline:ethanol:emulphor vehicle to determine if lumiracoxib acts as a substrate-selective COX-2 inhibitor *in vivo*. Mice were treated with vehicle or various doses of lumiracoxib by intraperitoneal injection and sacrificed 2 hours after treatment. The brains were then harvested, extracted, and analyzed for eCBs, AA, and PGs. Lumiracoxib caused significant increases in AEA and AA at all doses, but only caused a significant increase in 2-AG at the 10 mg/kg dose (Figure 2). Lumiracoxib did not significantly inhibit PG production in the brain until 10 mg/kg, although there was a slight non-significant decrease in PG production at the 5 mg/kg dose. Thus, lumiracoxib exhibits dose-dependent substrate-selective inhibition in the brain with no effect on PGs at 1 mg/kg but a significant increase AEA. Surprisingly, lumiracoxib caused a robust increase in AA and 2-oleoyl glycerol (2-OG) at all doses, which was not seen with LM-4131. While indomethacin and NS-398 also increased AA, we had hypothesized that this was a direct result of inhibition PG production. As lumiracoxib had no effect on PGs at the lowest dose but increased AA, it is possible that the increase in AA is a mediated by a separate mechanism.
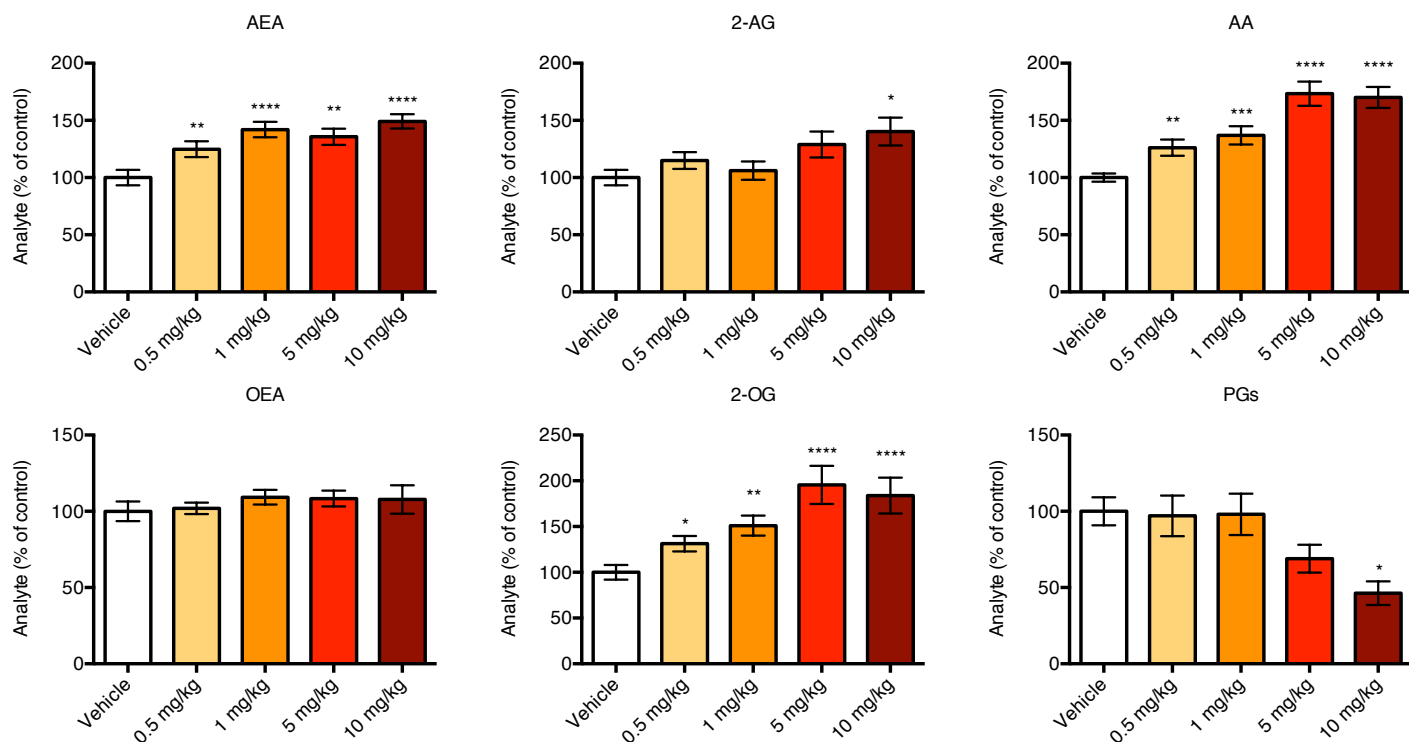
Figure 2: Dose-response of lumiracoxib on brain lipids and PGs. Lumiracoxib significantly increased AEA, AA, and 2-OG at all doses, but only increased 2-AG at the 10 mg/kg dose. Lumiracoxib significantly decreased PG levels at the 10 mg/kg dose. Lumiracoxib had no significant effect on OEA at any dose. Data shown are mean ± s.e.m., n = 6-15. Statistical significance calculated using one-way ANOVAs followed by Holm-Sidak post-tests.

The increase in 2-OG prompted us to probe the potential of lumiracoxib to inhibit MAGL. To do this we incubated various concentrations of lumiracoxib or the MAGL inhibitor JZL-184 with purified MAGL and assessed their ability to inhibit the hydrolysis of 2-AG to AA. While JZL-184 displayed potent inhibition of MAGL, lumiracoxib displayed approximately 20% inhibition with a 100 μM concentration (Figure 3). While lumiracoxib did not increase OEA, we also wanted to confirm that lumiracoxib is not a FAAH inhibitor *in vitro*. While the FAAH inhibitor PF-3845 displayed potent inhibition, lumiracoxib did not display any inhibition of FAAH activity up to a concentration of 100 μM.
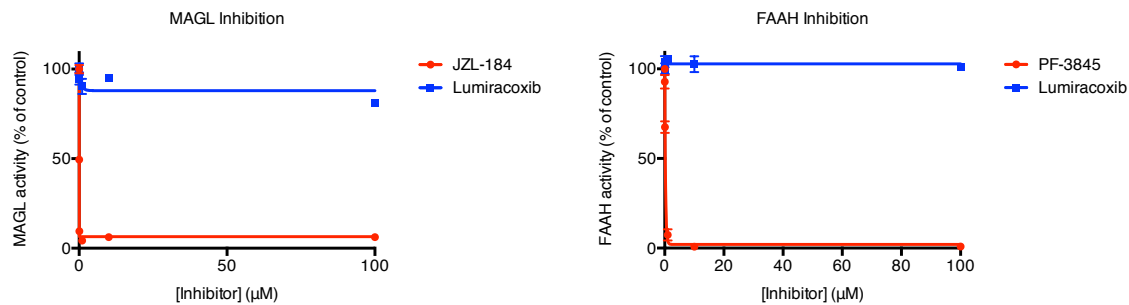
Figure 3: *In vitro* inhibition of MAGL and FAAH. While the MAGL inhibitor JZL-184 potently inhibits the hydrolysis of 2-AG to AA by MAGL, lumiracoxib only displayed approximately 20% inhibition at a concentration of 100 μM. Data shown are mean ± s.e.m., n = 3.

To determine if the increase in AA, 2-AG, and 2-OG produced by lumiracoxib *in vivo* was mediated by MAGL, we treated mice with vehicle (DMSO), the MAGL inhibitor JZL-184 (40 mg/kg), lumiracoxib (1 mg/kg), or a co-treatment of both JZL-184 and lumiracoxib. As seen previously, lumiracoxib caused a significant increase in AEA and AA (Figure 4). JZL-184 also caused a robust increase in 2-AG and 2-OG with a significant decrease in AA and PGs. Intriguingly, co-treatment of lumiracoxib with JZL-184 did not result in an additional increase in 2-AG or 2-OG over JZL-184 treatment alone. In addition, co-treatment of lumiracoxib with JZL-184 resulted in a decrease in AA, as seen with JZL-184 treatment alone. A potential explanation for these data is that lumiracoxib causes an increase in 2-AG through inhibition of COX-2, but the 2-AG is rapidly hydrolyzed to AA by MAGL. Taken together with the *in vitro* inhibition studies, lumiracoxib treatment does appear to have an impact on MAGL activity, but it could be through a secondary mechanism via its inhibition of 2-AG oxygenation by COX-2.

143
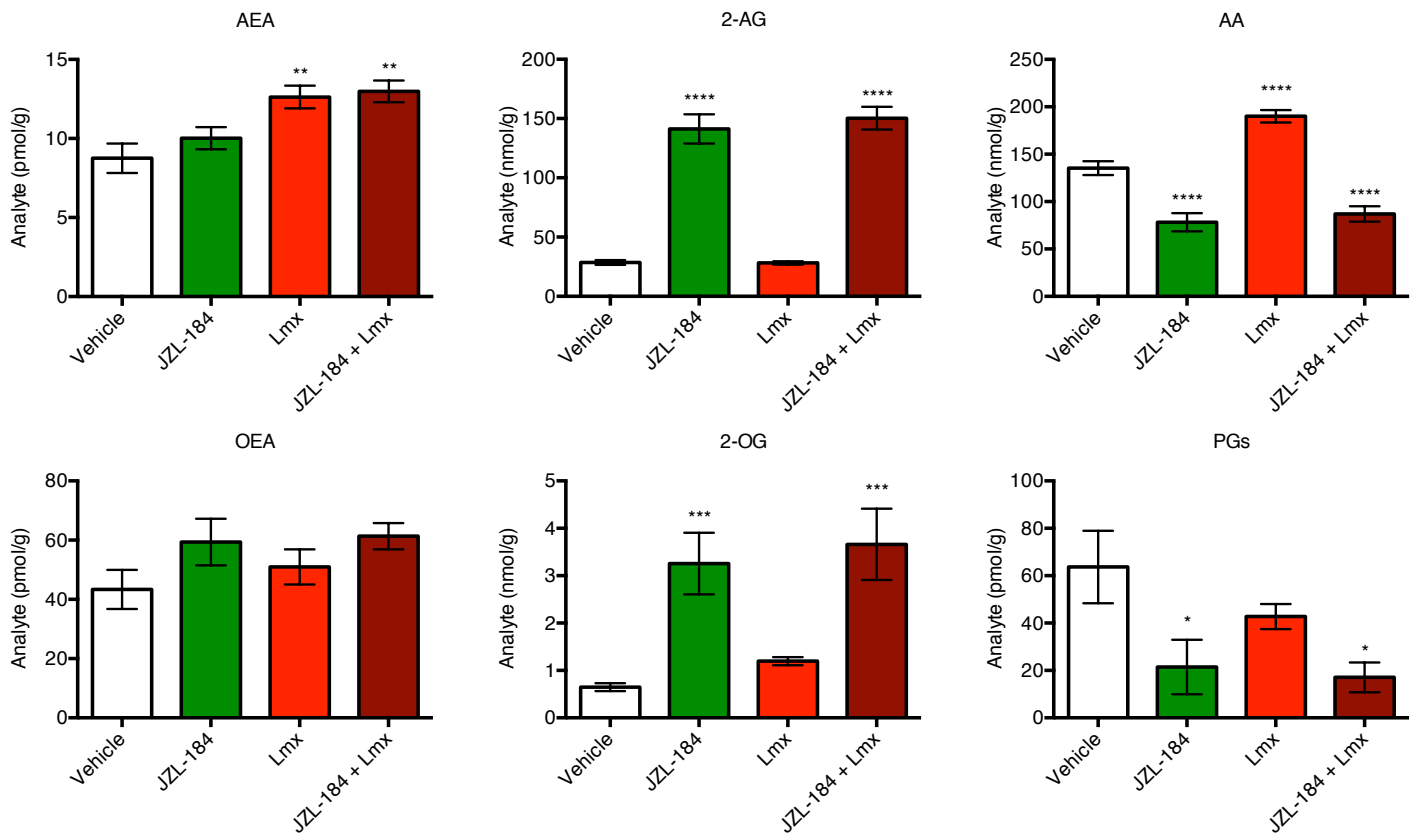
Figure 4: Effects of JZL-184, lumiracoxib, and co-treatment on brain lipids and PGs. Lumiracoxib caused a significant increase in AEA and AA, while JZL-184 caused an increase in 2-AG and 2-OG with a significant decrease in AA and PGs. Co-treatment of lumiracoxib with JZL-184 did not result in an additional increase in 2-AG or 2-OG over JZL-184 treatment alone. In addition, co-treatment of lumiracoxib with JZL-184 resulted in a decrease in AA, as seen with JZL-184 treatment alone. Data shown are mean ± s.e.m., vehicle and lumiracoxib n = 20, JZL-184 and JZL-184 + lumiracoxib n = 10. Statistical significance calculated using one-way ANOVAs followed by Holm-Sidak post-tests.

We next sought to determine the time-course of lumiracoxib's effects on brain lipids and PGs. We treated mice with vehicle (18:1:1 saline:ethanol:emulphor) or 1 mg/kg lumiracoxib and sacrificed the mice at the indicated time points after treatment. Lumiracoxib significantly increased AEA levels at 2, 4, 6, and 8 hours after treatment (Figure 5). Lumiracoxib treatment also significantly increased the levels of AA at all time points measured. Additionally, lumiracoxib caused a significant increase in 2-AG at 8 hours after treatment. There was no significant effect of lumiracoxib on either PGs or OEA at any time points. In contrast to earlier studies, lumiracoxib only significantly increased 2-OG 24 hours after treatment, but there was a strong trend toward increasing 2-OG at all time points. Thus, lumiracoxib displays a long duration of action after a single 1 mg/kg intraperitoneal injection with robust effects up to 8 hours after treatment.

144
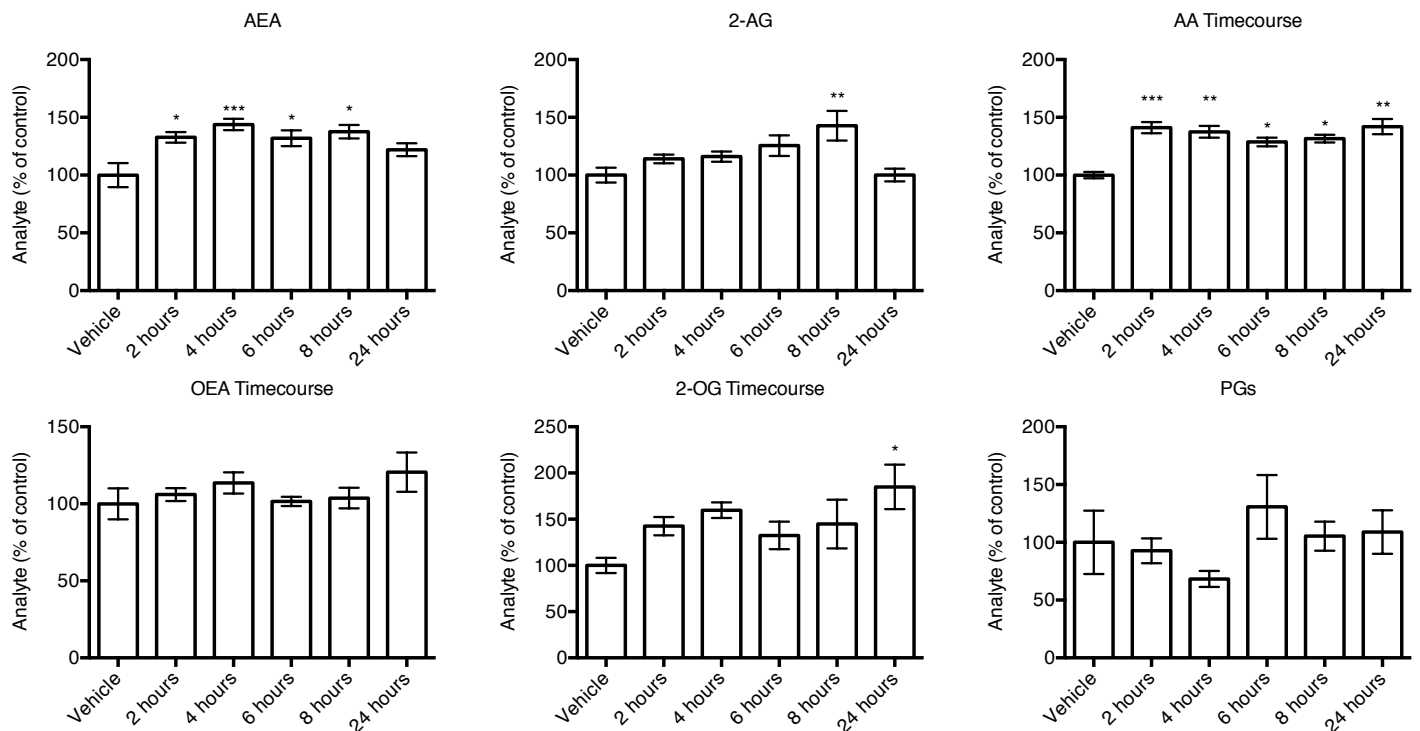
Figure 5: Time-course of lumiracoxib treatment. Lumiracoxib increases AEA up to 8 hours after treatment with no significant inhibition of PGs at any time point. Lumiracoxib also significantly increased 2-AG at 8 hours after treatment and 2-OG at 24 hours after treatment Lumiracoxib treatment significantly increased AA at all time points, but had no significant effect on OEA. Data shown are mean ± s.e.m., n = 5-26. Statistical significance calculated using one-way ANOVAs followed by Holm-Sidak post-tests.

Given the long duration of action of lumiracoxib and lack of PG inhibition, we next analyzed its effects after chronic treatment. Mice were treated with vehicle (18:1:1 saline:ethanol:emulphor) or lumiracoxib (1 mg/kg) by intraperitoneal injection once daily for 5 days. Mice were sacrificed 2 hours after the final treatment and their brains were analyzed by mass spectrometry. Chronic treatment with lumiracoxib increased AEA and AA levels but had no significant effect on the other analytes (Figure 6). Thus, chronic treatment with lumiracoxib results in an increase in AEA and does not result in PG inhibition.
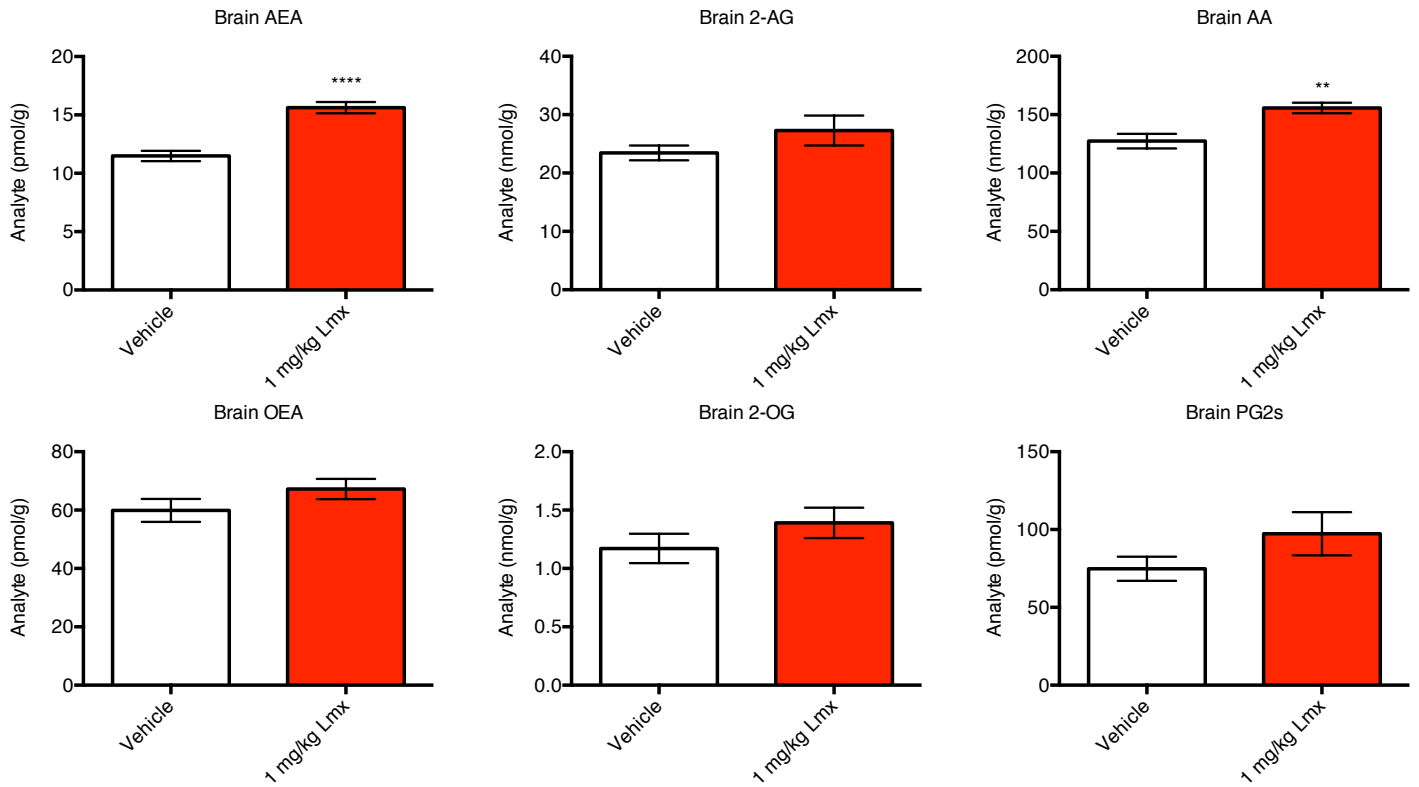
Figure 6: Effects of chronic lumiracoxib treatment on brain lipids and PGs. Chronic treatment with lumiracoxib significantly increases AEA and AA but has no significant effect on 2-AG, PGs, OEA, or 2-OG. Data shown are mean ± s.e.m., vehicle n = 10, LM-4131 n = 11. Statistical significance calculated using two-tailed t-tests.

To extend the chronic treatment data, we also treated mice with vehicle (18:1:1 saline:ethanol:emulphor) or lumiracoxib (1 mg/kg) by intraperitoneal injection once daily for 5 days and then sacrificed the mice 8 hours after the final treatment. After this treatment regimen, lumiracoxib significantly increased AEA, 2-AG, AA, and 2-OG levels but had no significant effect on PGs or OEA (Figure 7). Therefore, chronic treatment with lumiracoxib mirrors the time-course of acute treatment. These studies reveal that chronic lumiracoxib treatment does not result in a reduction of the effect of lumiracoxib on brain eCB or AA levels and does not cause PG inhibition. Taken together, these studies identify lumiracoxib as an *in vivo* substrate-selective COX-2 inhibitor in both acute and chronic settings with a long duration of action.
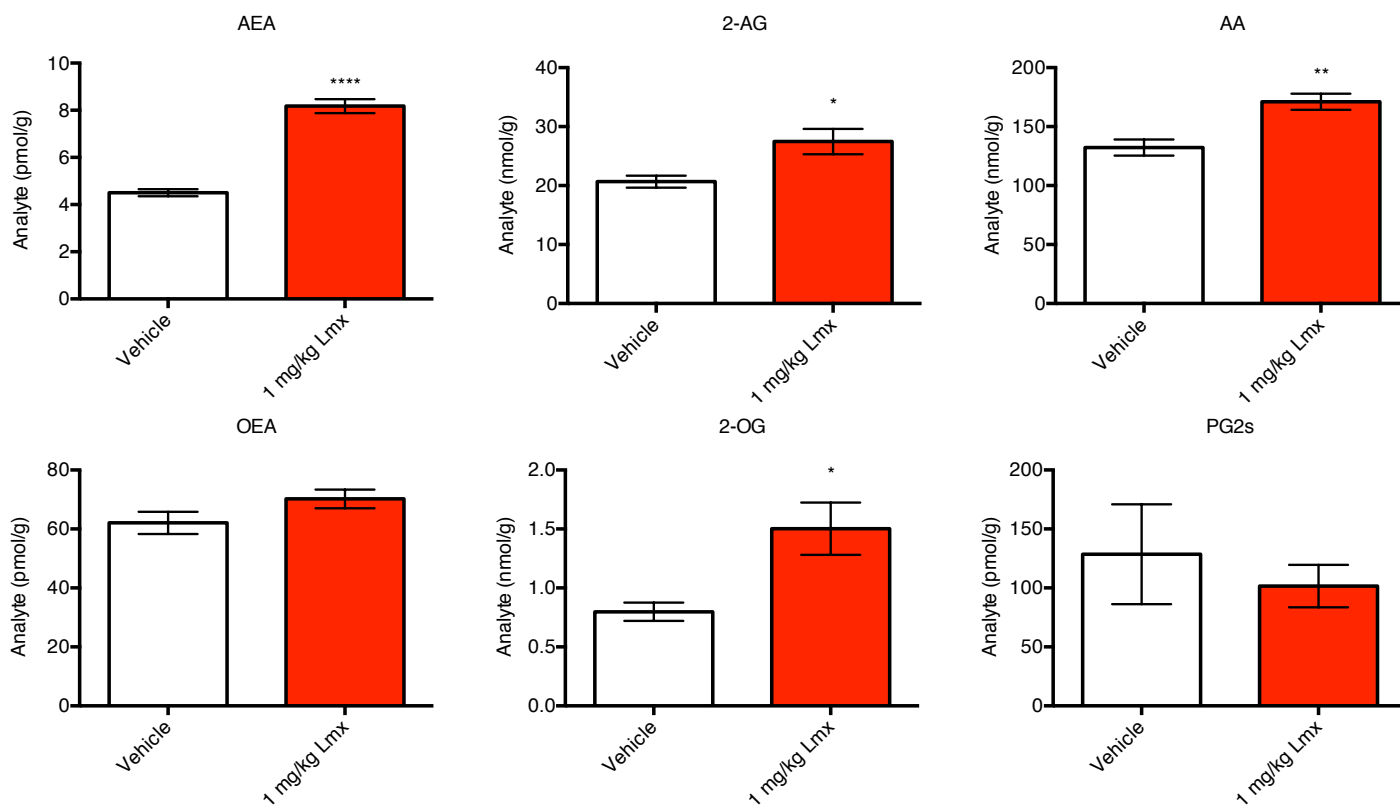
Figure 7: Effects of chronic lumiracoxib treatment on brain lipids and PGs 8 hours after last dosing.
Lumiracoxib significantly increases AEA, 2-AG, AA, and 2-OG levels 8 hours after the last treatment of 1 mg/kg once a day for 5 days. Under this treatment regimen lumiracoxib had no effect on either PGs or OEA. Data shown are mean ± s.e.m., n = 8. Statistical significance calculated using two-tailed t-tests.

Finally, we tested the effects of LM-5703, the *des*-fluoro analog of lumiracoxib. LM-5703 potentially is less likely to form reactive quinone imines than lumiracoxib or diclofenac due to the fact that its lower ring contains one less halogen and is thus less deactivated for enzymatic abstraction of its *para* hydrogen and subsequent oxidation. We treated mice by intraperitoneal injection with either vehicle (DMSO), 1 mg/kg LM-5703, or 10 mg/kg LM-5703 and harvested their brains 4 hours after treatment. Both the 1 and 10 mg/kg treatments significantly increased the levels of AEA, 2-AG, AA, and 2-OG (Figure 8). While the 10 mg/kg treatment did not significantly decrease PGs, there was a reduction in the average amount of PGs detected. Thus, LM-5703 displays a similar dose-response profile to lumiracoxib *in vivo*, identifying this probe as a potential alternative *in vivo* substrate-selective inhibitor to lumiracoxib.
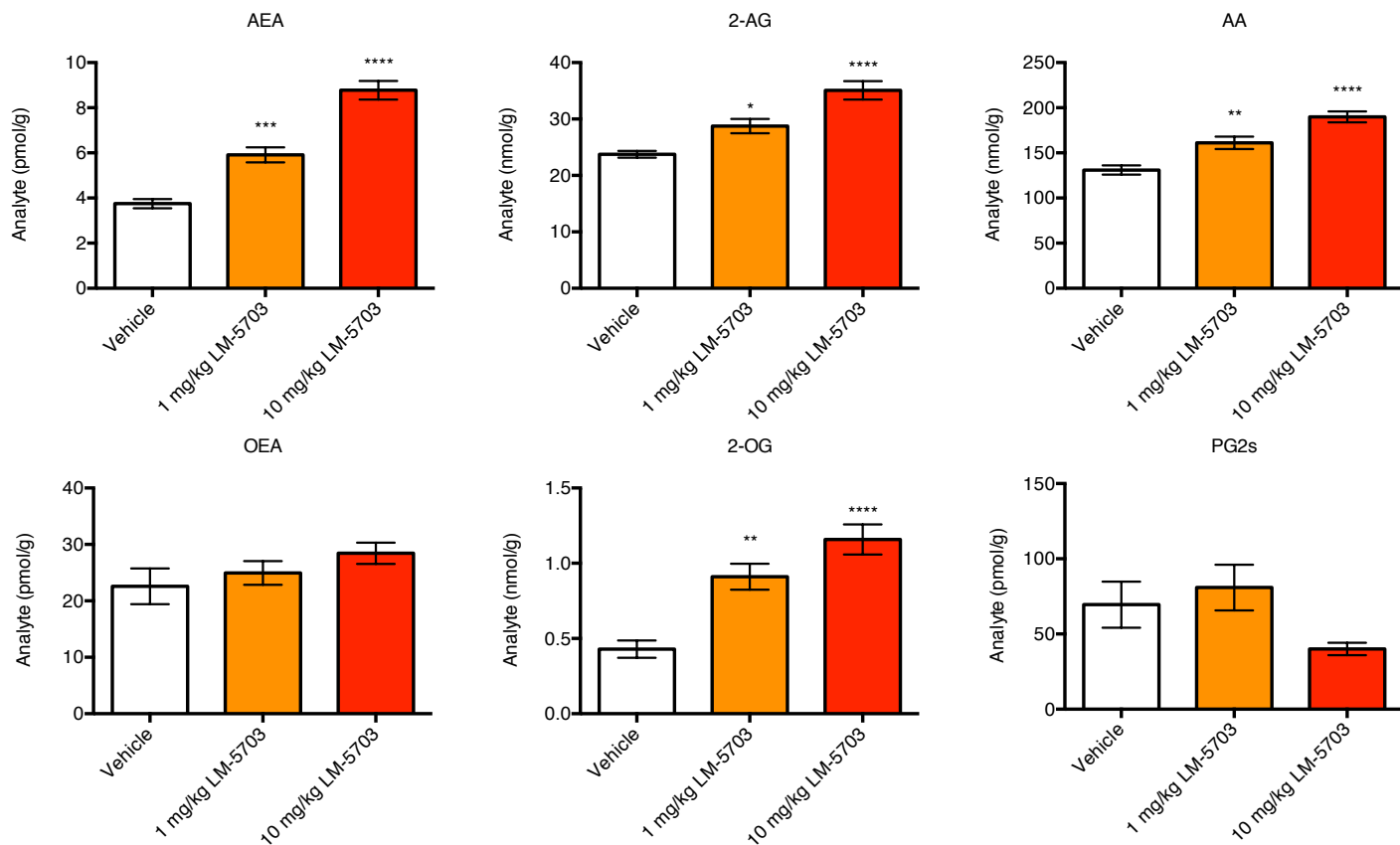
Figure 8: Dose-response of LM-5703. Treatment of mice with LM-5703 significantly increased the levels of AEA, 2-AG, AA, and 2-OG but had no significant effect on PGs or OEA. Data shown are mean ± s.e.m., n = 8. Statistical significance calculated using one-way ANOVAs followed by Holm-Sidak post-tests.

To further validate the biochemical effects of lumiracoxib as being mediated by substrate-selective COX-2 inhibition and not FAAH inhibition, we analyzed the effects of lumiracoxib compared to co-treatment of lumiracoxib with the FAAH inhibitor PF-3845 versus vehicle (DMSO) and PF-3845 treatment alone. After a 4 hour treatment, lumiracoxib (1 mg/kg) significantly increased brain AEA, AA, and 2-OG with a trending increase in 2-AG (Figure 9). While PF-3845 (10 mg/kg) significantly increased AEA and OEA, co-treatment of PF-3845 with lumiracoxib resulted in an additional significant increase in AEA but not OEA. Comparison of the vehicle versus lumiracoxib treated mice to PF-3845 treated mice versus lumiracoxib co-treatment with PF-3845 indicates that lumiracoxib treatment results in similar increases in AEA regardless of whether or not FAAH is inhibited.
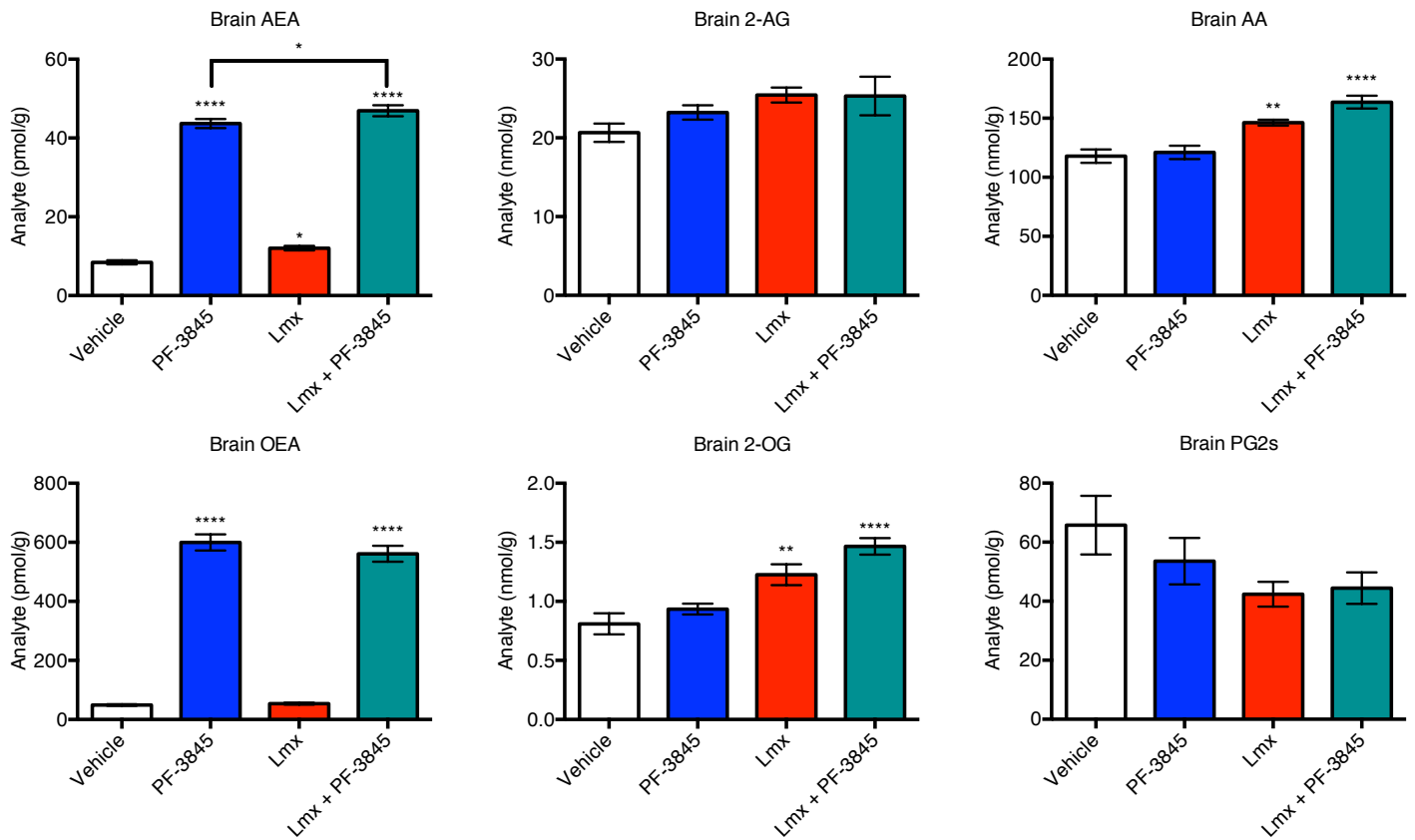
Figure 9: Effects of vehicle, PF-3845, lumiracoxib, and co-treatment on brain lipids and PGs. Both PF-3845 and lumiracoxib cause significant increases in AEA. While lumiracoxib has no significant effect on 2-AG, OEA, or PGs, it significantly increases AA and 2-OG 4 hours after treatment. PF-3845 also caused a significant increase in OEA, but co-treatment of lumiracoxib and PF-3845 resulted in additive increases in AEA but not OEA. Data shown are mean ± s.e.m., n = 10. Statistical significance calculated using one-way ANOVAs followed by Holm-Sidak post-tests.

We further analyzed the impact of FAAH on the effects of lumiracoxib by treating wild-type and *Faah⁻/⁻* littermates with vehicle (DMSO) or lumiracoxib for 4 hours. While lumiracoxib did not significantly increase AEA in wild-type littermates in this experiment, it did produce an additional significant increase compared to vehicle treated *Faah⁻/⁻* mice (Figure 10). Lumiracoxib significantly increased 2-AG levels in both wild-type and *Faah⁻/⁻* mice to a similar extent, but significantly increased AA and 2-OG in *Faah⁻/⁻* but not wild-type mice. Lumiracoxib treatment had no significant effect on OEA or PG levels in either wild-type or *Faah⁻/⁻* mice. As expected, *Faah⁻/⁻* mice had significantly increased levels of AEA and OEA, but not other lipids or PGs. Thus, lumiracoxib treatment produces additive increases in AEA when co-treated with the FAAH inhibitor PF-3845 and in *Faah⁻/⁻* mice. This suggests that the mechanism by which lumiracoxib increases AEA is independent of FAAH.
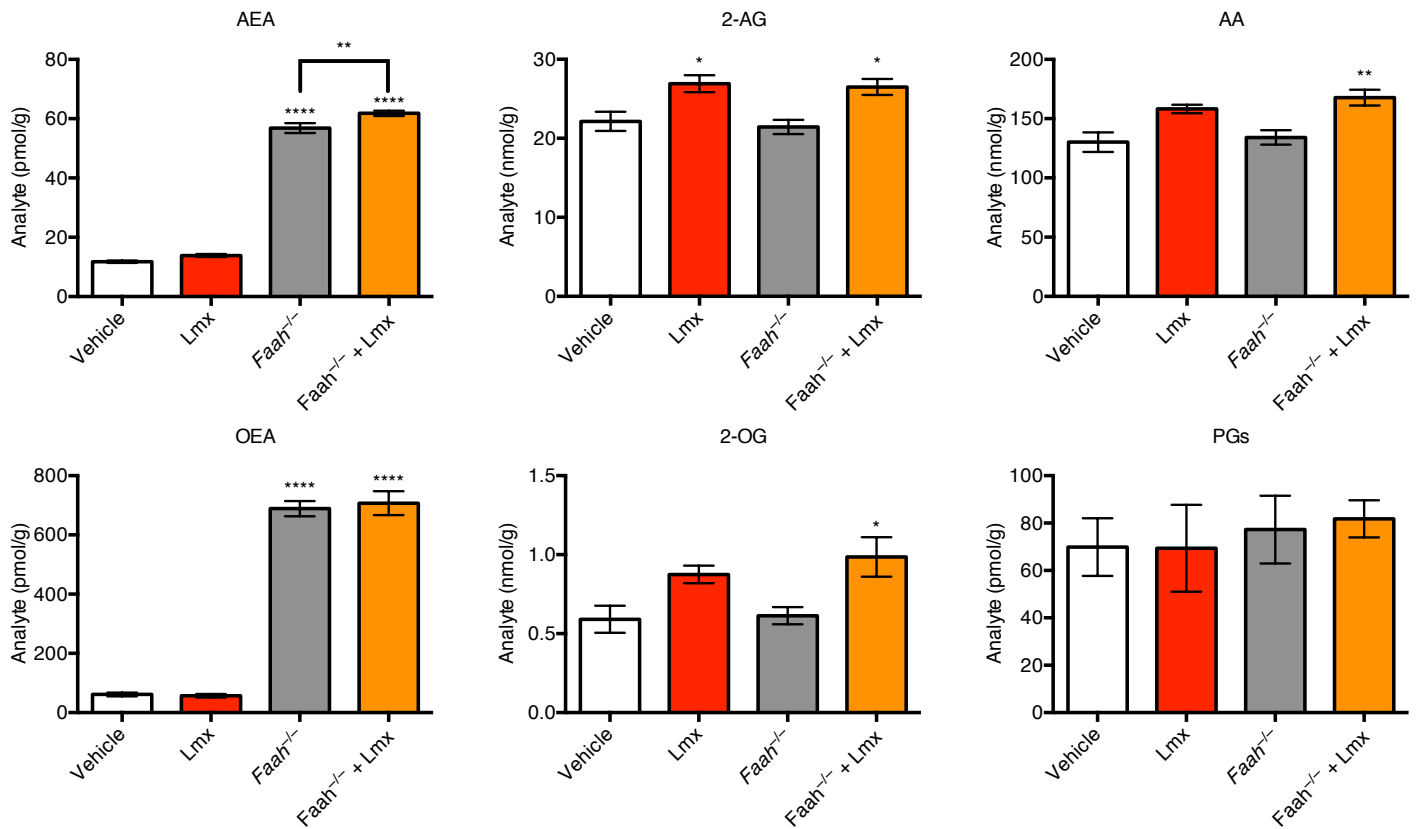
Figure 10: Effects of lumiracoxib on brain lipids and PGs in wild-type and *Faah*^{−/−} littermates.
Lumiracoxib had no significant increase of AEA in wild-type littermates, but produced an additional significant increase in AEA compared to vehicle treated *Faah*^{−/−} mice. Lumiracoxib significantly increased 2-AG levels in both wild-type and *Faah*^{−/−} mice, but significantly increased AA and 2-OG in *Faah*^{−/−} but not wild-type mice. Lumiracoxib treatment had no significant effect on OEA or PG levels in either wild-type or *Faah*^{−/−} mice. Data shown are mean ± s.e.m., vehicle n = 5, lumiracoxib n = 4, *Faah*^{−/−} n = 5, *Faah*^{−/−} + lumiracoxib n = 6. Statistical significance calculated using one-way ANOVAs followed by Holm-Sidak post-tests.

<center>Discussion</center>

These studies have identified lumiracoxib as an *in vivo* substrate-selective COX-2 inhibitor. While preliminary *in vitro* studies identified that lumiracoxib is an extremely potent substrate-selective COX-2 inhibitor, the present studies extend that finding to *in vivo* settings.[21] It is notable that lumiracoxib has the highest selectivity for COX-2 inhibition over COX-1 inhibition of any NSAID in the human whole blood assay.[22] Interestingly, this assay measures COX-2 inhibition by the inhibition of PGE_2 production elicited by lipopolysaccharide and COX-1 inhibition by the inhibition of thromboxane synthesis elicited by calcium ionophore treatment. The selective inhibition of PGE_2 but not thromboxane by lumiracoxib is intriguing because PGH_2-G is converted readily to PGE_2 but is not a good substrate for thromboxane synthase.[67] Thus, our studies suggest that the COX-2 selectivity of lumiracoxib may actually be due to substrate-selective inhibition of COX-2 and a reduction in PGE_2-G formation, which can be hydrolyzed to PGE_2.

Notably, lumiracoxib is efficacious in multiple pre-clinical models of pain and inflammation.[23] Despite the clinical metabolic toxicity exhibited by lumiracoxib, some studies suggest that the liver toxicity of lumiracoxib could be avoided by giving lower doses or by genotyping patients, as a specific allele can identify at risk patients.[51,52] Given our findings that lumiracoxib can increase brain eCBs at a dose of 1 mg/kg, it is possible that substrate-selective inhibition by lumiracoxib could be sufficient to provide therapeutic benefits without liver toxicity. In addition, as previous studies have identified that lumiracoxib does not increase cardiovascular risk or cause increased gastrointestinal complications in patients, the two primary complications in individuals who take NSAIDs for prolonged periods, it could be a promising therapeutic option.[53-56]

The aqueous solubility of lumiracoxib and efficacy in chronic settings make it a promising probe to study substrate-selective inhibition *in vivo*. Additionally, the *des*-fluoro derivative of lumiracoxib, which may have a reduced capacity to form reactive quinone imine metabolites *in vivo*, also displayed substrate-selective COX-2 inhibition in mice. These studies expand the probes available to study *in vivo* substrate-selective COX-2 inhibition and advance a probe with an improved pharmacological profile relative to LM-4131.

<center>151</center>

<div align="center">References</div>

1.   Di Marzo, V. Endocannabinoids: synthesis and degradation. *Reviews of physiology, biochemistry and pharmacology* **160**, 1-24 (2008).
2.   Piomelli, D. The molecular logic of endocannabinoid signalling. *Nature reviews. Neuroscience* **4**, 873-884 (2003).
3.   Ahn, K., McKinney, M.K. & Cravatt, B.F. Enzymatic pathways that regulate endocannabinoid signaling in the nervous system. *Chemical reviews* **108**, 1687-1707 (2008).
4.   Matias, I. & Di Marzo, V. Endocannabinoid synthesis and degradation, and their regulation in the framework of energy balance. *Journal of endocrinological investigation* **29**, 15-26 (2006).
5.   Wang, H.*, et al.* Differential regulation of endocannabinoid synthesis and degradation in the uterus during embryo implantation. *Prostaglandins & other lipid mediators* **83**, 62-74 (2007).
6.   Wang, J. & Ueda, N. Biology of endocannabinoid synthesis system. *Prostaglandins & other lipid mediators* **89**, 112-119 (2009).
7.   Cravatt, B.F.*, et al.* Molecular characterization of an enzyme that degrades neuromodulatory fatty-acid amides. *Nature* **384**, 83-87 (1996).
8.   Long, J.Z.*, et al.* Selective blockade of 2-arachidonoylglycerol hydrolysis produces cannabinoid behavioral effects. *Nature chemical biology* **5**, 37-44 (2009).
9.   Marrs, W.R.*, et al.* The serine hydrolase ABHD6 controls the accumulation and efficacy of 2-AG at cannabinoid receptors. *Nature neuroscience* **13**, 951-957 (2010).
10.   Savinainen, J.R., Saario, S.M. & Laitinen, J.T. The serine hydrolases MAGL, ABHD6 and ABHD12 as guardians of 2-arachidonoylglycerol signalling through cannabinoid receptors. *Acta physiologica* **204**, 267-276 (2012).
11.   Xie, S.*, et al.* Inactivation of lipid glyceryl ester metabolism in human THP1 monocytes/macrophages by activated organophosphorus insecticides: role of carboxylesterases 1 and 2. *Chemical research in toxicology* **23**, 1890-1904 (2010).
12.   Wang, R.*, et al.* Identification of Palmitoyl Protein Thioesterase 1 in Human THP1 Monocytes and Macrophages and Characterization of Unique Biochemical Activities for This Enzyme. *Biochemistry* **52**, 7559-7574 (2013).
13.   Yu, M., Ives, D. & Ramesha, C.S. Synthesis of prostaglandin E2 ethanolamide from anandamide by cyclooxygenase-2. *The Journal of biological chemistry* **272**, 21181-21186 (1997).
14.   Kozak, K.R., Rowlinson, S.W. & Marnett, L.J. Oxygenation of the endocannabinoid, 2-arachidonylglycerol, to glyceryl prostaglandins by cyclooxygenase-2. *The Journal of biological chemistry* **275**, 33744-33749 (2000).
15.   Chen, J.K.*, et al.* Identification of novel endogenous cytochrome p450 arachidonate metabolites with high affinity for cannabinoid receptors. *The Journal of biological chemistry* **283**, 24514-24524 (2008).
16.   Snider, N.T., Walker, V.J. & Hollenberg, P.F. Oxidation of the endogenous cannabinoid arachidonoyl ethanolamide by the cytochrome P450 monooxygenases: physiological and pharmacological implications. *Pharmacological reviews* **62**, 136-154 (2010).
17.   Ueda, N.*, et al.* Lipoxygenase-catalyzed oxygenation of arachidonylethanolamide, a cannabinoid receptor agonist. *Biochimica et biophysica acta* **1254**, 127-134 (1995).
18.   Hermanson, D.J.*, et al.* Substrate-selective COX-2 inhibition decreases anxiety via endocannabinoid activation. *Nature neuroscience* **16**, 1291-1298 (2013).
19.   Duggan, K.C.*, et al.* (R)-Profens are substrate-selective inhibitors of endocannabinoid oxygenation by COX-2. *Nature chemical biology* **7**, 803-809 (2011).
20.   Prusakiewicz, J.J., Duggan, K.C., Rouzer, C.A. & Marnett, L.J. Differential sensitivity and mechanism of inhibition of COX-2 oxygenation of arachidonic acid and 2-arachidonoylglycerol by ibuprofen and mefenamic acid. *Biochemistry* **48**, 7353-7355 (2009).
21.   Windsor, M.A., Valk, P.L., Xu, S., Banerjee, S. & Marnett, L.J. Exploring the molecular determinants of substrate-selective inhibition of cyclooxygenase-2 by lumiracoxib. *Bioorganic & medicinal chemistry letters* **23**, 5860-5864 (2013).

22. Tacconelli, S., Capone, M.L. & Patrignani, P. Clinical pharmacology of novel selective COX-2 inhibitors. *Current pharmaceutical design* **10**, 589-601 (2004).

23. Esser, R.*, et al.* Preclinical pharmacology of lumiracoxib: a novel selective inhibitor of cyclooxygenase-2. *British journal of pharmacology* **144**, 538-550 (2005).

24. Stam, W., Jansen, J. & Taylor, S. Efficacy of etoricoxib, celecoxib, lumiracoxib, non-selective NSAIDs, and acetaminophen in osteoarthritis: a mixed treatment comparison. *The open rheumatology journal* **6**, 6-20 (2012).

25. Schnitzer, T.J.*, et al.* A 13-week, multicenter, randomized, double-blind study of lumiracoxib in hip osteoarthritis. *Clinical rheumatology* **30**, 1433-1446 (2011).

26. Stricker, K., Yu, S. & Krammer, G. A 6-week, multicentre, randomised, double-blind, double-dummy, active-controlled, clinical safety study of lumiracoxib and rofecoxib in osteoarthritis patients. *BMC musculoskeletal disorders* **9**, 118 (2008).

27. Sheldon, E.A., Beaulieu, A., Paster, Z., Yu, S. & Rebuli, R. Long-term efficacy and safety of lumiracoxib 100 mg: an open-label extension of a 13-week randomized controlled trial in patients with primary osteoarthritis of the knee. *Clinical and experimental rheumatology* **26**, 611-619 (2008).

28. Geusens, P. & Lems, W. Efficacy and tolerability of lumiracoxib, a highly selective cyclo-oxygenase-2 (COX2) inhibitor, in the management of pain and osteoarthritis. *Therapeutics and clinical risk management* **4**, 337-344 (2008).

29. Chen, Y.F.*, et al.* Cyclooxygenase-2 selective non-steroidal anti-inflammatory drugs (etodolac, meloxicam, celecoxib, rofecoxib, etoricoxib, valdecoxib and lumiracoxib) for osteoarthritis and rheumatoid arthritis: a systematic review and economic evaluation. *Health technology assessment* **12**, 1-278, iii (2008).

30. Profit, L. & Chrisp, P. Lumiracoxib: the evidence of its clinical impact on the treatment of osteoarthritis. *Core evidence* **2**, 131-150 (2007).

31. Dougados, M., Moore, A., Yu, S. & Gitton, X. Evaluation of the patient acceptable symptom state in a pooled analysis of two multicentre, randomised, double-blind, placebo-controlled studies evaluating lumiracoxib and celecoxib in patients with osteoarthritis. *Arthritis research & therapy* **9**, R11 (2007).

32. Bannwarth, B. & Berenbaum, F. Lumiracoxib in the management of osteoarthritis and acute pain. *Expert opinion on pharmacotherapy* **8**, 1551-1564 (2007).

33. Wittenberg, R.H.*, et al.* First-dose analgesic effect of the cyclo-oxygenase-2 selective inhibitor lumiracoxib in osteoarthritis of the knee: a randomized, double-blind, placebo-controlled comparison with celecoxib [NCT00267215]. *Arthritis research & therapy* **8**, R35 (2006).

34. Fleischmann, R.*, et al.* Lumiracoxib is effective in the treatment of osteoarthritis of the knee: a prospective randomized 13-week study versus placebo and celecoxib. *Clinical rheumatology* **25**, 42-53 (2006).

35. Sheldon, E.*, et al.* Efficacy and tolerability of lumiracoxib in the treatment of osteoarthritis of the knee: a 13-week, randomized, double-blind comparison with celecoxib and placebo. *Clinical therapeutics* **27**, 64-77 (2005).

36. Schnitzer, T.J., Gitton, X., Jayawardene, S. & Sloan, V.S. Lumiracoxib in the treatment of osteoarthritis, rheumatoid arthritis and acute postoperative dental pain: results of three dose-response studies. *Current medical research and opinion* **21**, 151-161 (2005).

37. Lehmann, R.*, et al.* Efficacy and tolerability of lumiracoxib 100 mg once daily in knee osteoarthritis: a 13-week, randomized, double-blind study vs. placebo and celecoxib. *Current medical research and opinion* **21**, 517-526 (2005).

38. Berenbaum, F.*, et al.* Efficacy of lumiracoxib in osteoarthritis: a review of nine studies. *The Journal of international medical research* **33**, 21-41 (2005).

39. Tannenbaum, H.*, et al.* Lumiracoxib is effective in the treatment of osteoarthritis of the knee: a 13 week, randomised, double blind study versus placebo and celecoxib. *Annals of the rheumatic diseases* **63**, 1419-1426 (2004).

40. Schnitzer, T.J.*, et al.* Efficacy and safety of four doses of lumiracoxib versus diclofenac in patients with knee or hip primary osteoarthritis: a phase II, four-week, multicenter, randomized, double-blind, placebo-controlled trial. *Arthritis and rheumatism* **51**, 549-557 (2004).

41. Grifka, J.K.*, et al.* Efficacy and tolerability of lumiracoxib versus placebo in patients with osteoarthritis of the hand. *Clinical and experimental rheumatology* **22**, 589-596 (2004).

42. Fok, K.C., Bell, C.J., Read, R.B., Eckstein, R.P. & Jones, B.E. Lumiracoxib-induced cholestatic liver injury. *Internal medicine journal* **43**, 731-732 (2013).

43. Pillans, P.I.*, et al.* Severe acute liver injury associated with lumiracoxib. *Journal of gastroenterology and hepatology* **27**, 1102-1105 (2012).

44. Kang, P., Dalvie, D., Smith, E. & Renner, M. Bioactivation of lumiracoxib by peroxidases and human liver microsomes: identification of multiple quinone imine intermediates and GSH adducts. *Chemical research in toxicology* **22**, 106-117 (2009).

45. Li, Y.*, et al.* In vitro metabolic activation of lumiracoxib in rat and human liver preparations. *Drug metabolism and disposition: the biological fate of chemicals* **36**, 469-473 (2008).

46. Boelsterli, U.A. Diclofenac-induced liver injury: a paradigm of idiosyncratic drug toxicity. *Toxicology and applied pharmacology* **192**, 307-322 (2003).

47. Tang, W. The metabolism of diclofenac--enzymology and toxicology perspectives. *Current drug metabolism* **4**, 319-329 (2003).

48. Pumford, N.R., Myers, T.G., Davila, J.C., Highet, R.J. & Pohl, L.R. Immunochemical detection of liver protein adducts of the nonsteroidal antiinflammatory drug diclofenac. *Chemical research in toxicology* **6**, 147-150 (1993).

49. Leemann, T., Transon, C. & Dayer, P. Cytochrome P450TB (CYP2C): a major monooxygenase catalyzing diclofenac 4'-hydroxylation in human liver. *Life sciences* **52**, 29-34 (1993).

50. Yu, L.J., Chen, Y., Deninno, M.P., O'Connell, T.N. & Hop, C.E. Identification of a novel glutathione adduct of diclofenac, 4'-hydroxy-2'-glutathion-deschloro-diclofenac, upon incubation with human liver microsomes. *Drug metabolism and disposition: the biological fate of chemicals* **33**, 484-488 (2005).

51. Singer, J.B.*, et al.* A genome-wide study identifies HLA alleles associated with lumiracoxib-related liver injury. *Nature genetics* **42**, 711-714 (2010).

52. Hinz, B.*, et al.* Lumiracoxib inhibits cyclo-oxygenase 2 completely at the 50 mg dose: is liver toxicity avoidable by adequate dosing? *Annals of the rheumatic diseases* **68**, 289-291 (2009).

53. Mackenzie, I.S., Wei, L. & Macdonald, T.M. Cardiovascular safety of lumiracoxib: a meta-analysis of randomised controlled trials in patients with osteoarthritis. *European journal of clinical pharmacology* **69**, 133-141 (2013).

54. Matchaba, P.*, et al.* Cardiovascular safety of lumiracoxib: a meta-analysis of all randomized controlled trials > or =1 week and up to 1 year in duration of patients with osteoarthritis and rheumatoid arthritis. *Clinical therapeutics* **27**, 1196-1214 (2005).

55. Hart, L. Lumiracoxib reduced ulcer complications compared with ibuprofen and naproxen in osteoarthritis and did not increase cardiovascular outcomes. *ACP journal club* **142**, 46-47 (2005).

56. Farkouh, M.E.*, et al.* Comparison of lumiracoxib with naproxen and ibuprofen in the Therapeutic Arthritis Research and Gastrointestinal Event Trial (TARGET), cardiovascular outcomes: randomised controlled trial. *Lancet* **364**, 675-684 (2004).

57. Blobaum, A.L. & Marnett, L.J. Molecular determinants for the selective inhibition of cyclooxygenase-2 by lumiracoxib. *The Journal of biological chemistry* **282**, 16379-16390 (2007).

58. Uddin, M.J.*, et al.* Fluorinated COX-2 Inhibitors as Agents in PET Imaging of Inflammation and Cancer. *Cancer Prev Res* **4**, 1536-1545 (2011).

59. Weber, A.*, et al.* Formation of prostamides from anandamide in FAAH knockout mice analyzed by HPLC with tandem mass spectrometry. *Journal of lipid research* **45**, 757-763 (2004).

60. Patel, S., Kingsley, P.J., Mackie, K., Marnett, L.J. & Winder, D.G. Repeated Homotypic Stress Elevates 2-Arachidonoylglycerol Levels and Enhances Short-Term Endocannabinoid Signaling at Inhibitory Synapses in Basolateral Amygdala. *Neuropsychopharmacol* **34**, 2699-2709 (2009).

61. Blankman, J.L., Simon, G.M. & Cravatt, B.F. A comprehensive profile of brain enzymes that hydrolyze the endocannabinoid 2-arachidonoylglycerol. *Chem Biol* **14**, 1347-1356 (2007).

62. Ahn, K.*, et al.* Discovery and Characterization of a Highly Selective FAAH Inhibitor that Reduces Inflammatory Pain. *Chem Biol* **16**, 411-420 (2009).

63. Kingsley, P.J. & Marnett, L.J. LC-MS-MS analysis of neutral eicosanoids. *Method Enzymol* **433**, 91-+ (2007).

64. Colucci, M.*, et al.* New insights of dimethyl sulphoxide effects (DMSO) on experimental in vivo models of nociception and inflammation. *Pharmacological research : the official journal of the Italian Pharmacological Society* **57**, 419-425 (2008).

65. Walters, M.N., Papadimitriou, J.M. & Shilkin, K.B. Inflammation induced by dimethylsulfoxide (DMSO). 1. Ultrastructural investigation of preinflammatory phase. *Experimental and molecular pathology* **6**, 106-117 (1967).

66. Papadimitriou, J.M., Shilkin, K.B., Archer, J.M. & Walters, M.N. Inflammation induced by dimethylsulfoxide (DMSO). II. Ultrastructural investigation of the inflammatory phase. *Experimental and molecular pathology* **6**, 347-360 (1967).

67. Kozak, K.R.*, et al.* Metabolism of the endocannabinoids, 2-arachidonylglycerol and anandamide, into prostaglandin, thromboxane, and prostacyclin glycerol esters and ethanolamides. *The Journal of biological chemistry* **277**, 44877-44885 (2002).

CHAPTER VII

SUBSTRATE-DEPENDENT ENDOCANNABINOID OXYGENATION BY CYCLOOXYGENASE-2

Introduction

Since the discovery that 2-arachidonylglycerol (2-AG) is a substrate for cyclooxygenase-2 (COX-2) our laboratory has explored the synthesis and physiology of prostaglandin glycerol esters (PG-Gs).[1] Several studies have demonstrated that COX-2-mediated endocannabinoid metabolism is an important alternative pathway to hydrolysis at sites of COX-2 constitutive or induced expression.[2-4] Previous efforts have focused on the stimulatory conditions that produce PG-Gs, however, the biosynthetic pathway that is responsible for the synthesis of 2-AG for use by COX-2 has not been elucidated.[5-7]

The development and validation of several macrophage cell lines for the study of PG-G biosynthesis has provided a valuable set of model systems to define their full biosynthetic pathway. Although PG-G production has been demonstrated in several cell lines, the relative abundant levels of arachidonic acid (AA)-derived prostaglandins (PGs) compared to a dearth of 2-AG derived PG-Gs, even when correcting for the relative amounts of AA and 2-AG, suggests that the two substrates are not equally utilized by COX-2.[5,6] Previous studies in our laboratory have identified that one mediator of this large difference between substrate utilization is based on the requirement of higher peroxide tone for 2-AG oxygenation.[8]

While both AA and 2-AG are oxygenated by COX-2, they are synthesized through distinct pathways. A primary source of AA is the hydrolysis of phospholipids at the *sn*-2 position catalyzed by cytosolic phospholipase A_2 (cPLA$_2$). There are six identified isoforms of cPLA$_2$ in mice: α, β, γ, δ, ε, and ζ. These isoforms are expressed in different tissues and are activated in response to different stimuli. In activated macrophages, AA biosynthesis is primarily mediated by the action of cPLA$_2$α, an 85 kDa protein containing an N-terminal C2 domain and a C-terminal catalytic domain.[9] The activity of cPLA$_2$α is regulated by intracellular calcium levels through the binding of calcium to the C2 domain, which results in translocation of the enzyme to the phospholipid membrane.[10] In addition to calcium, cPLA$_2$α activity is also modulated by ceramide-1-phosphate, phosphatidylinositol 4,5-bis phosphate (PIP$_2$), and phosphorylation by mitogen-activated protein kinase.[11-13]

After translocation to the membrane, cPLA$_2$α utilizes an active site Ser-228/Asp-549 dyad within its α/β hydrolase domain to catalyze the hydrolysis of the *sn*-2 position of phospholipids including phosphatidylcholine (PC), phosphatidylethanolamine (PE), and phosphatidylinositol (PI).[14,15] Importantly, cPLA$_2$α hydrolysis of phospholipid substrate has high substrate specificity for phospholipids containing AA at the *sn*-2 position.[10] In addition to PLA$_2$ activity, cPLA$_2$α possesses calcium-independent lysophospholipase and transacylase activities.[16] Intriguingly, genetic deletion of cPLA$_2$α results in a robust reduction of AA and PG production in resident peritoneal macrophages (RPMs), but has no significant effect on 2-AG and PG-G levels.[7]

The identification of cPLA$_2$α as the major mediator of AA production in macrophages has led to considerable interest in the development of pharmacological inhibitors of cPLA$_2$α due to the potential to block AA production and metabolism along the COX or lipoxygenase pathways, which generate pro-inflammatory and nociceptive bioactive lipids including PGs, leukotrienes, and lipoxins. These eicosanoids are important in intracellular immunity and have been implicated in the pathogenesis of several diseases including thrombosis, cancer, atherosclerosis, asthma, arthritis, and rhinitis.[17-21] A variety of different classes of cPLA$_2$α inhibitors have been developed. The first series of inhibitors developed were AA analogs such as AA-trifluoromethyl ketone and methyl arachidonyl fluorophosphonate, although they also inhibit iPLA$_2$α.[22] These compounds prevent intraplantar carrageenan mediated thermal hyperalgesia and formalin-induced flinching.[23] These initial studies spurred pharmaceutical companies to develop compounds of their own. Bristol-Myers Squibb developed and patented a series of α- and β-substituted trifluoromethyl ketones.[24,25] Shionogi identified a series of pyrrolidines, including pyrrophenone, which inhibited PG and leukotriene formation in human whole blood and displayed anti-arthritic effects in a murine arthritis model.[26,27] Additional scaffolds including 2-oxoamides and 1,3-disubstituted propan-2-ones have been developed and validated by AstraZeneca.

The most concerted medicinal chemistry efforts have been advanced by Genetics Institute, which was later acquired by Wyeth, using an indole scaffold. These efforts lead to the development of ecopladib (Figure 1), which displayed oral efficacy in the rat carrageenan air pouch and rat carrageenan-induced paw edema models and advanced to phase I clinical trials.[28] Further efforts identified the optimal phenylmethane sulfonamide region substitution, giving rise to efipladib and WAY-196025, which both have shown efficacy

when dosed orally in multiple acute and chronic PG- and leukotriene-dependent *in vivo* pain and inflammation models.[29-31] Additional studies were performed on another analog, giripladib, which had efficacy in multiple mouse models of rheumatoid arthritis and was advanced into phase II clinical trails for osteoarthritis but failed to advance due to a lack of improvement over naproxen, a non-steroidal anti-inflammatory drug (NSAID) that inhibits both COX-1 and COX-2 and is the current standard of care.[32] Additional efforts have optimized the *in vitro* potency and rat pharmacokinetics for oral efficacy, and Wyeth has also identified 1,2,4-oxadiazolidin-3,5-diones and 1,3,5-triazin-2,4,6-triones as well as quinazoline-2,4(1H,3H)-dione cPLA$_2\alpha$ inhibitors with reduced lipophilicity and improved aqueous solubility.[31,33-35] These combined efforts have developed potent and selective cPLA$_2\alpha$ inhibitors that are active *in vivo*, although most are not commercially available and require lengthy syntheses.
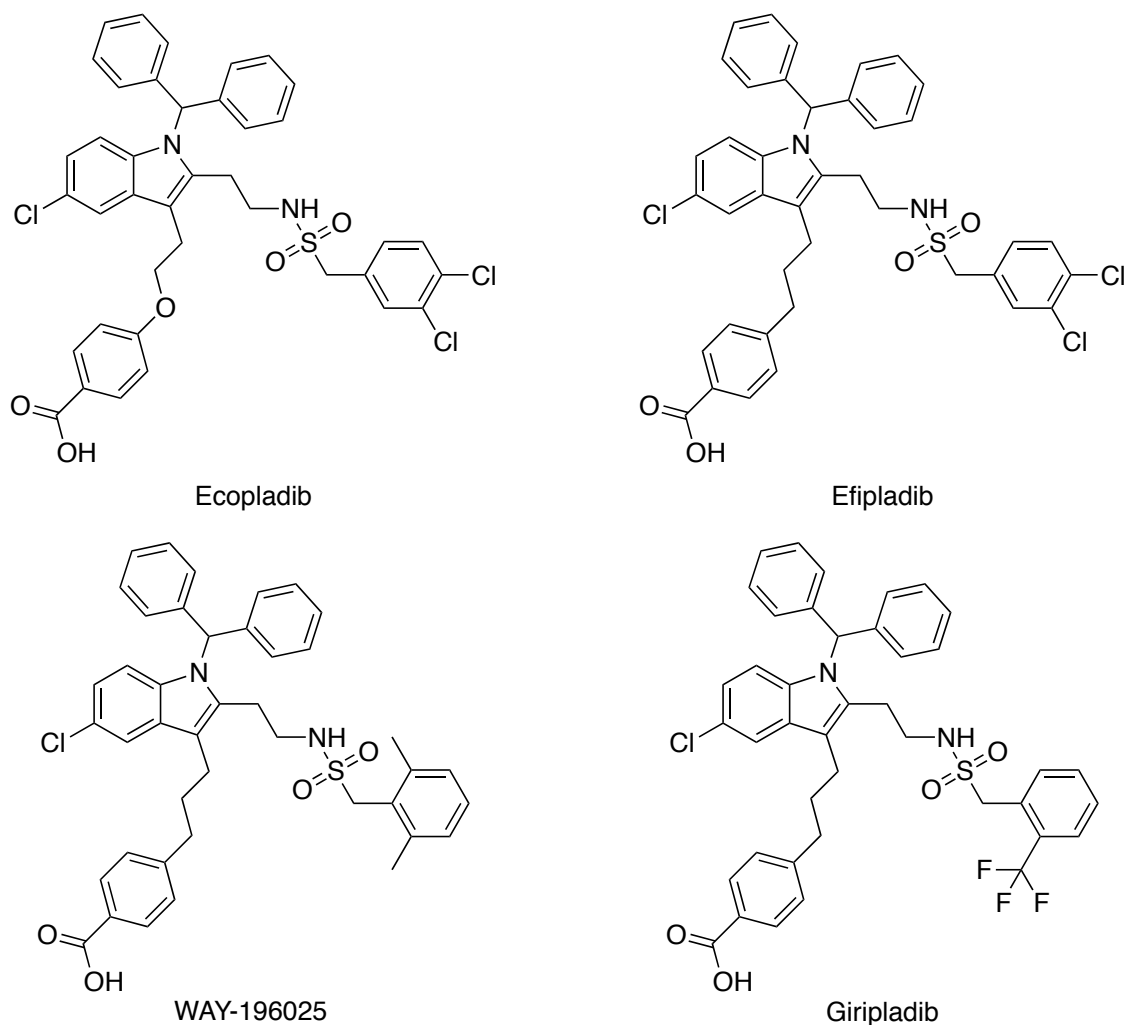
Figure 1: Structures of cPLA$_2\alpha$ inhibitors.

While the synthesis of AA by macrophages proceeds primarily through the action of $cPLA_2\alpha$ on phospholipids, it can also be formed by the hydrolysis of 2-AG in the brain and other settings.[36] The primary source of 2-AG in most cells and tissues is the phospholipase C (PLC)-diacylglycerol lipase (DAGL) pathway (Figure 2).[37] In this pathway, PLC hydrolyzes 2-arachidonoyl-PIP_2 to form AA-containing diacylglycerols (DAGs), which are then hydrolyzed to 2-AG by diaclyglycerol lipase (DAGL).[38,39] In neurons, PLCβ isoforms have been implicated in this pathway due to the formation of 2-AG in response to the stimulation of $G_{q/11}$-coupled receptors.[40] Interestingly, the 4 isoforms of PLCβ are expressed in a regiospecific manner throughout the brain and are stimulated by different $G_{q/11}$-coupled receptors including the group I metabotropic glutamate receptors (mGluRs) mGluR1 and mGluR5, as well as the muscarinic acetylcholine receptor M1.[41] Alternative pathways to synthesize 2-arachidonoyl-DAG have been identified including the hydrolysis of phosphatidic acid (PA) in ionomycin-stimulated neuroblastoma cells and PC in phorbol ester treated mouse ear tissue.[42,43] Additionally, PI can be hydrolyzed by PLA_1 to form lyso-PI (LPI), followed by LPI-PLC hydrolysis to form 2-AG.[44,45] 2-AG can also be formed from 2-arachidonoyl-lysophosphatidic acid (LPA).[46] While these lipases all have biological interest, very few selective inhibitors have been developed to probe the exact function of each of the enzymes. The only enzyme in the 2-AG biosynthetic pathways with a validated selective inhibitor is DAGLβ, however, that compound also inhibits the hydrolysis of 2-AG to AA by α/β-hydrolase domain 6 (ABHD6).[47]
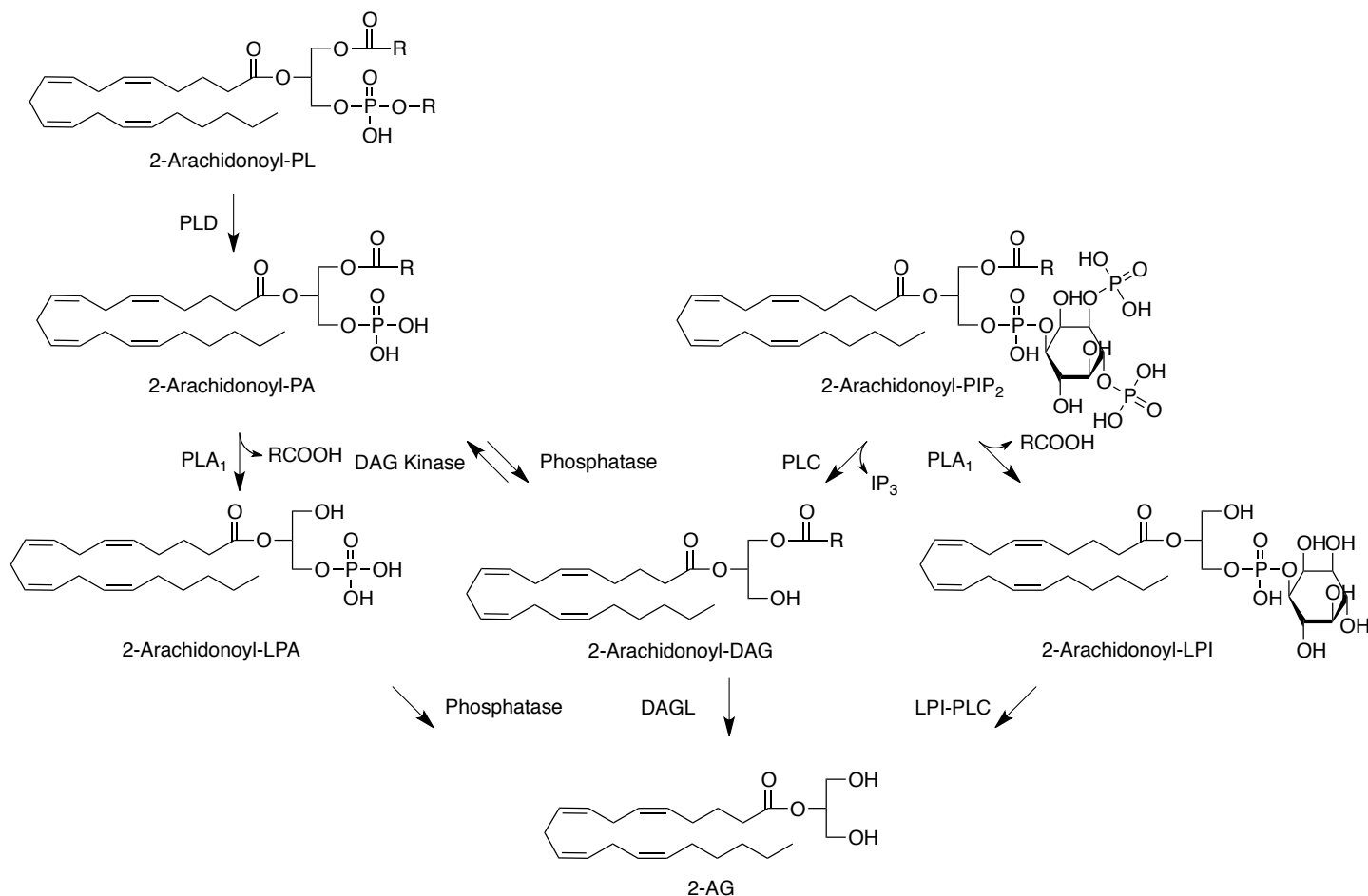
Figure 2: Biosynthetic pathways for 2-AG.

We sought to directly investigate the influence of AA on 2-AG oxygenation *in vitro* and in cellular

settings. Utilizing the previously established biosynthetic routes of 2-AG and AA, we also sought to identify the

biosynthetic source of 2-AG and AA in multiple macrophage cell lines using previously established stimulation

conditions through lipidomic analyses. We identified AA as a non-competitive inhibitor of COX-2-mediated 2-

AG oxygenation *in vitro*. With this finding in hand, we identified the effects of the inhibition or deletion of

cPLA$_2\alpha$ and, thus, a reduction of AA production on the production of PG-Gs. These studies identified 38:4 PI as

a major source of both 2-AG and AA in RAW 264.7 and bone-marrow-derived macrophages (BMDM).

Inhibition or genetic deletion of cPLA$_2\alpha$ led to decreased levels of AA and PGs, but increased levels of 38:4 PI,

38:4 DAG, and PG-Gs in stimulated RAW 264.7 cells and BMDMs. The selectivity and mechanism of

giripladib were validated using BMDMs harvested from cPLA$_2\alpha^{+/+}$ and cPLA$_2\alpha^{-/-}$ mice. Finally, we established

that the production of PG-Gs in BMDMs is mediated by COX-2.

Materials

RAW 264.7 cells were obtained from American type culture collection (Rockville, MD). Cell culture reagents were purchased from Life Technologies (Gaithersburg, MD). PGE$_2$-G, PGF$_{2\alpha}$-G, PGE$_2$-d$_4$, AA-d$_8$, AEA-d$_8$, 2-AG-d$_8$, and SAG-d$_8$, were purchased from Cayman Chemical (Ann Arbor, MI). 17:1 LPC, 37:4 PC, 17:1 LPI, 37:4 PI, 37:4 PE, 37:4 PS, 37:4 PA, and 37:4 PG were purchased from Avanti Polar Lipids (Alabaster, AL). Lipopolysaccharide (LPS), zymosan B, ionomycin, and interferon γ (IFNγ) were purchased from Sigma Aldrich (Milwaukee, WI). PGE$_2$-G-d$_5$ was synthesized as described previously using chemicals from Sigma Aldrich.[48] Macrophage colony stimulating factor (M-CSF) and granulocyte macrophage colony stimulating factor (GM-CSF) were purchased from R&D Systems (Minneapolis, MN). Giripladib was a kind gift from Alex Brown (Vanderbilt University).

Determination of the effects of AA on 2-AG oxygenation by mCOX-2

A fixed concentration of mCOX-2 (250 nM) was suspended in a 100 mM Tris-HCl buffer, pH = 8 with 500 μM phenol and 2 equivalents of heme were added, the solution was vigorously mixed and then aliquoted out at 195 μl per tube and pre-incubated for five minutes at 37°C. After pre-incubation, 5 μl of DMSO containing the specified amounts of AA and/or 2-AG was added in to the tube, vigorously mixed, and allowed to react for 30 seconds. The reaction was quenched after 30 seconds by adding 200 μl of ethyl acetate containing 0.1% glacial acetic acid, 300 pmol of PGE$_2$-d$_4$, and 300 pmol of PGE$_2$-G-d$_5$. Tubes were frozen and the organic layer was separated and evaporated to dryness under nitrogen gas. The samples were then reconstituted in 200 μl of 1:1 methanol:water and analyzed using liquid chromatography-tandem mass spectrometry (LC-MS/MS) analysis.

RAW 264.7 Cell Culture

Low passage RAW 264.7 cells (ATCC) were cultured in DMEM containing 10% HI-FBS. Cells were plated at 3x10^6 cells onto 100 mm plates. Cells were treated with 20 ng/ml GM-CSF for 24 hours and then the media was removed and replaced with serum-free DMEM containing 1 μg/ml LPS (E. coli 011:B4) and 20 units/ml IFNγ. At this time point cells were treated with inhibitor or DMSO vehicle as described in the text. 6 hours after LPS and IFNγ stimulation the cells were treated with 2 μM ionomycin or vehicle. 45 minutes after ionomycin

treatment the media was removed and extracted with 2 equivalents (v/v) of ethyl acetate containing PGE_2-d_4 and PGE_2-G-d_5. The cells were then scraped into 1 ml of ice-cold methanol containing AA-d_8, 2-AG-d_8, SAG-d_8, 17:1 LPC, 37:4 PC, 17:1 LPI, 37:4 PI, 37:4 PE, 37:4 PS, 37:4 PA, and 37:4 PG and added directly into the ethyl acetate solution. The solution was vigorously mixed and the organic layer was then removed and dried under a stream of nitrogen gas. The resultant film was then reconstituted in 200 μl of methanol and 100 μl of water for analysis by LC/MS/MS.

BMDM Harvesting and Culture

20-30g Female ICR (CD-1) cPLA$_2$$^{+/+}$, cPLA$_2$$^{-/-}$, *Ptgs2*$^{+/+}$ and *Ptgs2*$^{-/-}$ mice were bred and genotyped as described previously.[7] Mice were sacrificed by cervical dislocation and decapitation and the lower body was soaked in a 70% ethanol solution. The skin was removed from each hind leg and the femur was detached from the tibia at the knee joint. The femur and tibia of each leg were then detached and placed in ice-cold sterile Ca^{2+}- and Mg^{2+}-free phosphate-buffered saline (PBS). Under a tissue culture hood the soft tissue was removed from each bone using a sterile razor blade and forceps, the bone was rinsed in sterile PBS, and the ends were cut off using sterile scissors. The marrow was flushed from each bone with 5 ml of ice cold Minimum Essential Medium-Alpha with GlutaMAX (α-MEM, Gibco) using a syringe and 26 gauge needle. The resulting cell suspension was subjected to centrifugation at 1,000 rpm for 5 min, and the cells were resuspended in 1 ml/mouse of lysis buffer (155 mM ammonium chloride, 10 mM potassium bicarbonate, 0.1 mM EDTA, pH 7.2 − 7.4). Following a 2 minute incubation at room temperature, α-MEM (10 ml/mouse) was added and the cells were collected by centrifugation (1,000 rpm for 5 min). The resulting cell pellet was re-suspended in 42 ml/mouse of α-MEM containing 10% heat-inactivated fetal bovine serum (Atlas Biologicals, Norcross, GA) plus 100 Units/ml penicillin and 0.10 mg/ml streptomycin (Sigma, St. Louis, MO) (α-MEM/FCS) supplemented with 50 ng/ml of M-CSF (R&D Systems). The cells were then plated at 7 ml/dish onto 100 mm Fisherbrand untreated polystyrene tissue culture dishes (cat. #08-757-13) and incubated for 4 days at 37°C.

After 4 days colonies of adherent macrophages had developed. The dishes were washed once with α-MEM and overlaid with 10 ml of fresh α-MEM/FCS containing 50 ng/ml of m-CSF. Following an additional incubation of 2 days the cells were harvested. The dishes were washed once with 6 ml of PBS and overlaid with

162

6 ml of calcium- and magnesium-free Hanks Balanced Salt Solution containing 2 mM EDTA. The cells were incubated at 37°C for 30 min. The dishes then scraped and the cells from three dishes were combined into a 50 ml sterile tube containing 20 ml of α-MEM and were then subjected to centrifugation (1,000 rpm for 5 min). This procedure yielded between 20 and 40 million cells per mouse on the day of harvest.

After centrifugation the cells were re-suspended and diluted to 0.5×10^6 cells/ml in α-MEM/FCS containing 50 ng/ml of m-CSF and 20 ng/ml of GM-CSF and plated at 3×10^6 cells onto 100 mm dishes (6 ml/dish). The dishes were then incubated for 24 hours prior to experimental treatment. The following morning the media was removed and replaced with fresh serum-free α-MEM with LPS (1 µg/ml) and IFNγ (20 units/ml). At this point vehicle (DMSO) or inhibitors were added to the dishes. Cultures were then incubated as described in the text before the addition of zymosan (960 µg/dish) as indicated or ionomycin (2 µM) for 1 hour. The samples were then extracted in an identical fashion as described above for RAW 264.7 cells.

LC-MS/MS Analysis

Analyses of PGs, PG-Gs, 2-AG, AA, OEA, and 2-OG were performed as described previously.[49-51] DAGs and PCs were analyzed using a C4 column and mobile phases of 1:1 H_2O:MeOH with 5 mM ammonium acetate at pH 3.5 with formic acid (A) and 4:1 acetonitrile:2-propanol with 0.1% (v/v) formic acid (B). DAGs were analyzed with a Q1 of $[M+NH_4]^+$ (+18) and a Q3 of the loss of a fatty acid tail using 38:4 DAG-d_8 as an internal standard. PCs and LPCs were analyzed with a Q1 of $[M+H]^+$ and a Q3 of 184.1 using 37:4 PC and 17:1 LPC as internal standards. PAs, PGs, PEs, PSs, and PIs were analyzed using a C4 column and mobile phases of 1:1 H_2O:MeOH at pH 8.0 with piperidine (A) and 4:1 acetonitrile:2-propanol at pH 8.0 with piperidine (B). PAs were analyzed with a Q1 of $[M-H]^-$ and a Q3 of 153.1 using 37:4 PA as an internal standard, PGs were analyzed with a Q1 of $[M-H]^-$ and a Q3 of 153.1 using 37:4 PG as an internal standard, PEs were analyzed with a Q1 of $[M-H]^-$ and a Q3 of 196.1 using 37:4 PE as an internal standard, PSs were analyzed with a Q1 of $[M-H]^-$ and a Q3 of a loss of 87 using 37:4 PS as an internal standard, and PIs were analyzed with a Q1 of $[M-H]^-$ and a Q3 of 241.1 using 37:4 PI and 17:1 LPI as internal standards. Analytes were quantitated by integrating the areas of the analyte peaks and normalizing them to the areas of their respective internal standard peaks.

In vitro competition between AA and 2-AG

We first sought to analyze the potential of AA and 2-AG to inhibit each other's oxygenation by purified murine COX-2. To do this we analyzed the effect of adding increasing amounts of either AA or 2-AG to a fixed concentration of the other substrate (5 µM) with purified COX-2. While increasing concentrations of 2-AG had little effect on the production of PGs from AA, increasing the amounts of AA caused dramatic decreases in PG-G formation from 2-AG (Figure 3). Thus, it appears that AA acts as an inhibitor of 2-AG oxygenation, but 2-AG has little impact on the oxygenation of AA by COX-2 *in vitro*.
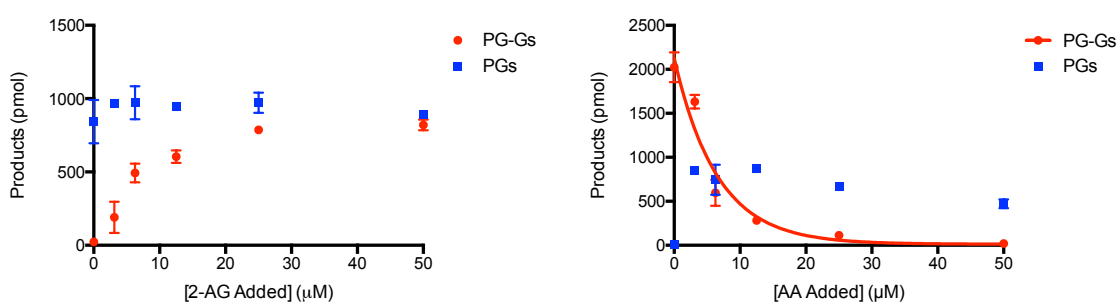
Figure 3: Effects of increasing concentrations of 2-AG or AA on oxygenation of 5 µM AA or 2-AG by COX-2. While the addition of increasing amounts of 2-AG had little effect on the turnover of AA, addition of increasing amounts of AA potently inhibited the turnover of 2-AG. Data shown are mean ± s.e.m., n = 6.

To characterize the inhibition of 2-AG turnover elicited by increasing amounts of AA we then performed kinetic analyses by varying the amounts of AA and 2-AG added into the enzyme mixture and analyzing the resultant PG and PG-G production. These kinetic analyses identified that 2-AG again had little impact on the oxygenation of AA by COX-2 (Figure 4). In contrast, AA appears to be a non-competitive inhibitor of 2-AG oxygenation by COX-2 *in vitro*. This finding was quite surprising, as COX-2 oxygenates the two substrates to comparable extents with comparable efficiencies.[52]
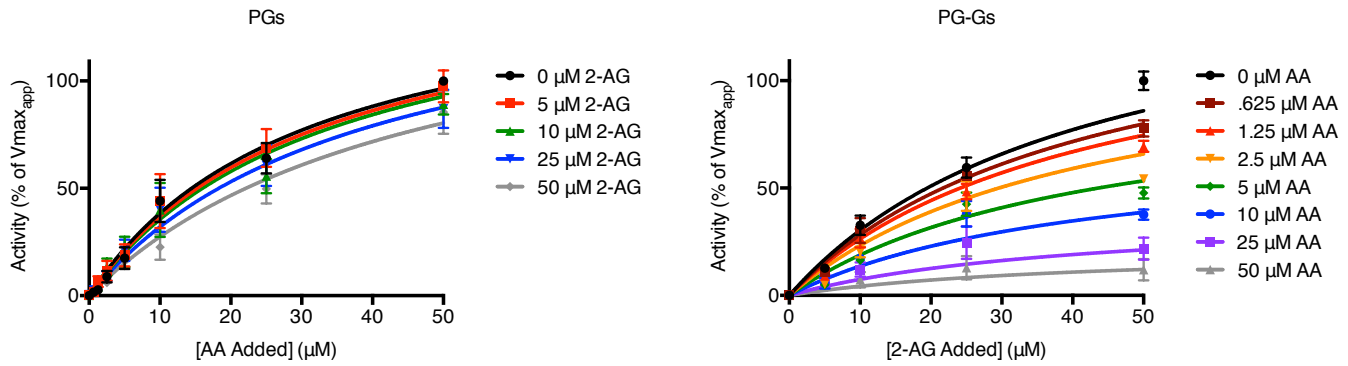
Figure 4: Kinetic analyses of the effects of 2-AG on AA oxygenation and AA on 2-AG oxygenation by COX-2. While 2-AG had little effect on AA oxygenation, AA exerts non-competitive inhibition of 2-AG oxygenation. Data shown are mean ± s.e.m., n = 6.

Modulation of cellular AA to augment PG-G formation in cells

The *in vitro* inhibition of 2-AG oxygenation by AA suggested that a potential method of increasing PG-G formation would be to inhibit AA production. Indeed, previous studies have found that inhibition of MAGL, which hydrolyzes 2-AG to AA, increases the amount of PG-Gs in carrageenan inflamed rat paws.[53] We first tested this hypothesis by culturing stimulated RAW 264.7 cells with DMSO vehicle or varying amounts of the cPLA$_2\alpha$ inhibitor giripladib and then analyzing their production of PGs and PG-Gs. Giripladib caused a concentration-dependent decrease in the production of PGs with significant effects at all concentrations (Figure 5). In contrast, giripladib increased the production of PG-Gs, with significant effects at 5, 10, 100 and 1000 nM. Consistent with its characterization as a cPLA$_2\alpha$ inhibitor, giripladib caused a significant decrease in AA levels with all concentrations used. In contrast, giripladib significantly increased the levels of 2-AG at 2.5 and 5 nM concentrations, but not at higher concentrations. Thus, inhibition of cPLA$_2\alpha$ by giripladib differentially modulates the levels of PGs and AA versus the levels of PG-Gs and 2-AG.
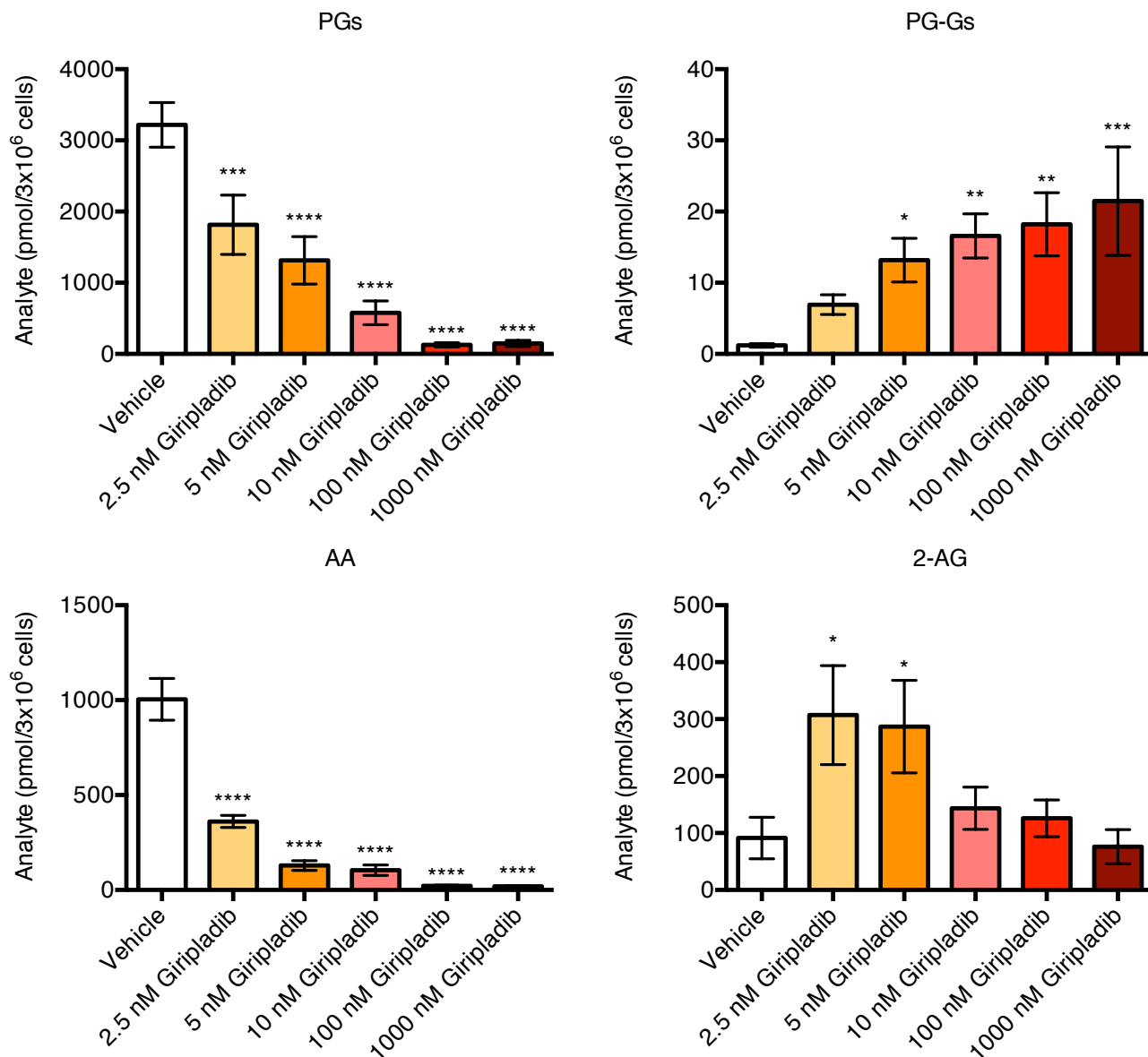
Figure 5: Concentration-dependent effects of giripladib on PGs, PG-Gs, AA, and 2-AG in stimulated RAW 264.7 cells. Inhibition of cPLA$_2$α by giripladib decreases the production of PGs by stimulated RAW 264.7 cells but increases the levels of PGGs. Giripladib decreases the levels of AA at all concentrations, but increases the levels of 2-AG at 2.5 nM but not higher concentrations. Values shown are mean ± s.e.m., n = 12. Significance was determined using a one-way ANOVA followed by a Holm-Sidak post-test.

To further characterize the effects of giripladib treatment in stimulated RAW 264.7 cells, we also performed a targeted lipidomic analysis of AA-containing phospholipids and DAGs, the biosynthetic precursors of AA and 2-AG. Giripladib treatment caused a significant concentration-dependent increase in the major AA-containing PI, 38:4 (Figure 6). While giripladib also increased the levels of 36:4 and 38:5 PI, these increases were not significant. The augmentation of AA-containing PI caused by increasing concentrations of giripladib was complemented by significant decreases in the levels of 18:1 and 18:0 LPI. Giripladib treatment also caused

166

a concentration-dependent increase in the levels of AA-containing PCs and decreased the levels of LPCs in a concentration-dependent manner (Figure 7). Thus, the inhibition of cPLA$_2\alpha$ by giripladib appears to inhibit the hydrolysis of AA-containing PIs or PCs to AA and LPI or LPC, respectively. While previous studies have identified AA-containing PI as a substrate for cPLA$_2\alpha$, it is not widely accepted as a major phospholipid precursor of AA.[54-57]
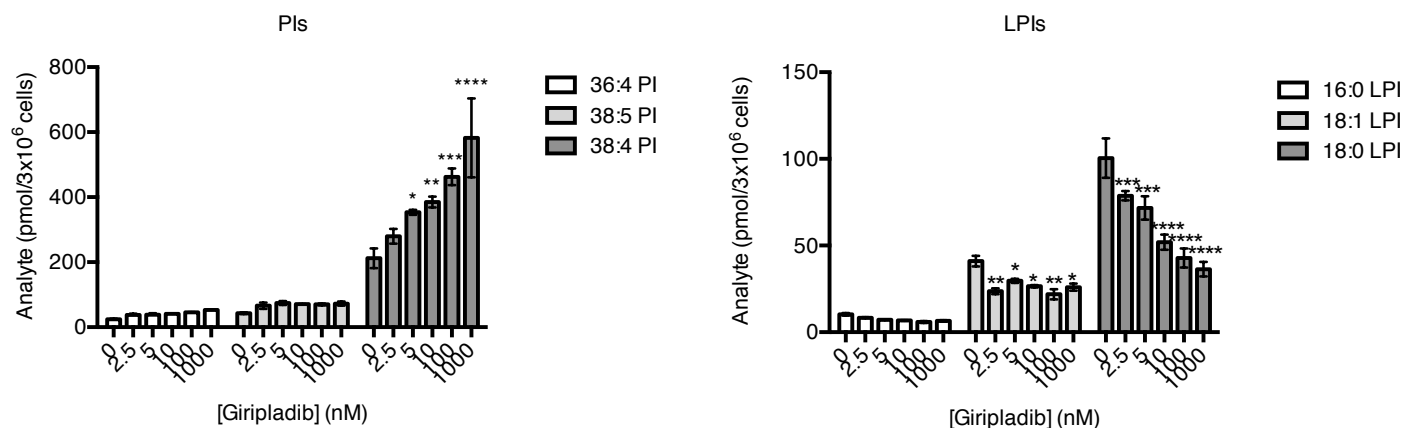
Figure 6: Concentration-dependent effects of giripladib on PIs and LPIs in stimulated RAW 264.7 cells. Inhibition of cPLA$_2\alpha$ by giripladib significantly increases the levels of 38:4 PI in a concentration-dependent manner with trending non-significant increases in 36:4 and 38:5 PI. Concomitantly, the levels of 18:1 and 18:0 LPI are significantly decreased. Values shown are mean ± s.e.m., n = 9. Significance was determined using a two-way ANOVA followed by a Holm-Sidak post-test.

Figure 7: Concentration-dependent effects of giripladib on PCs and LPCs in stimulated RAW 264.7 cells. Inhibition of cPLA$_2\alpha$ by giripladib significantly increases the levels of 38:4 and 38:5 PC in a concentration-dependent manner with trending non-significant increases in 36:4 PC. Additionally, the levels of 18:1 LPC are significantly decreased. Values shown are mean ± s.e.m., n = 9. Significance was determined using a two-way ANOVA followed by a Holm-Sidak post-test.

Given the increases in 2-AG and PG-Gs produced by treatment of stimulated RAW 264.7 macrophages with giripladib, we also analyzed the levels of AA-containing DAGs. DAGs are primarily formed through the hydrolysis of PIP$_2$ by PLC, but can also be formed through the cleavage of PC by PLC or other phospholipids through hydrolysis by PLD and a phosphatase.[37-39,42,43] Although the PL and phosphatase pathways have been described in other cell lines, the levels of AA-containing PA were below the limit of detection in our stimulated RAW 264.7 macrophages. Thus, we focused on measurement of the levels of AA-containing DAGs. Giripladib treatment resulted in a concentration-dependent increase in the levels of 38:4 DAG but not other AA-containing DAGs (Figure 8). These experiments reveal that inhibition of cPLA$_2\alpha$ in stimulated RAW 264.7 macrophages increases the production of PG-Gs and decreases the levels of PGs. This increase in PG-G production could be due to multiple factors including the increase in 2-AG synthesis or the decreased levels of AA.
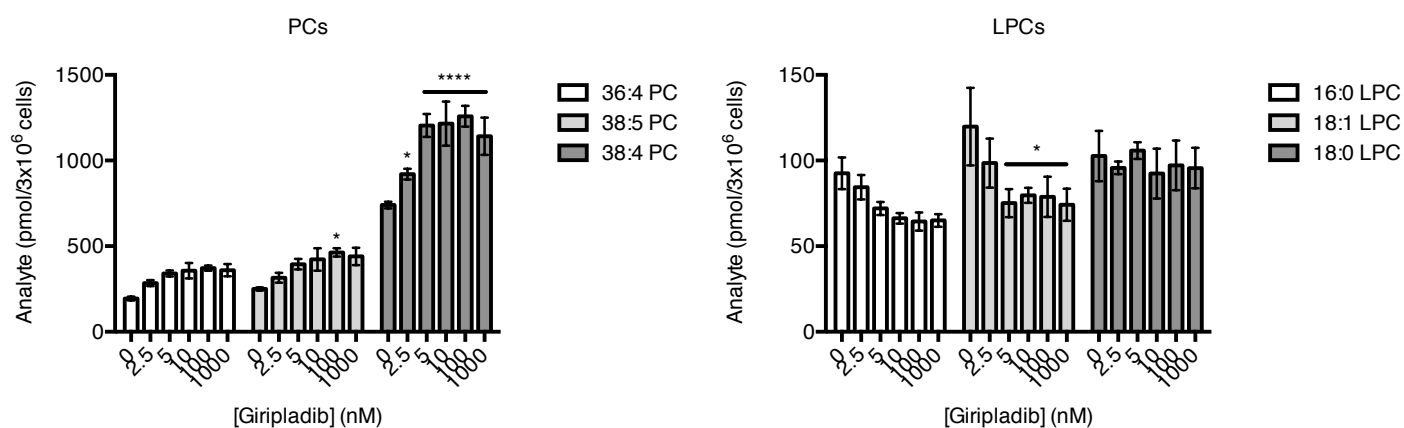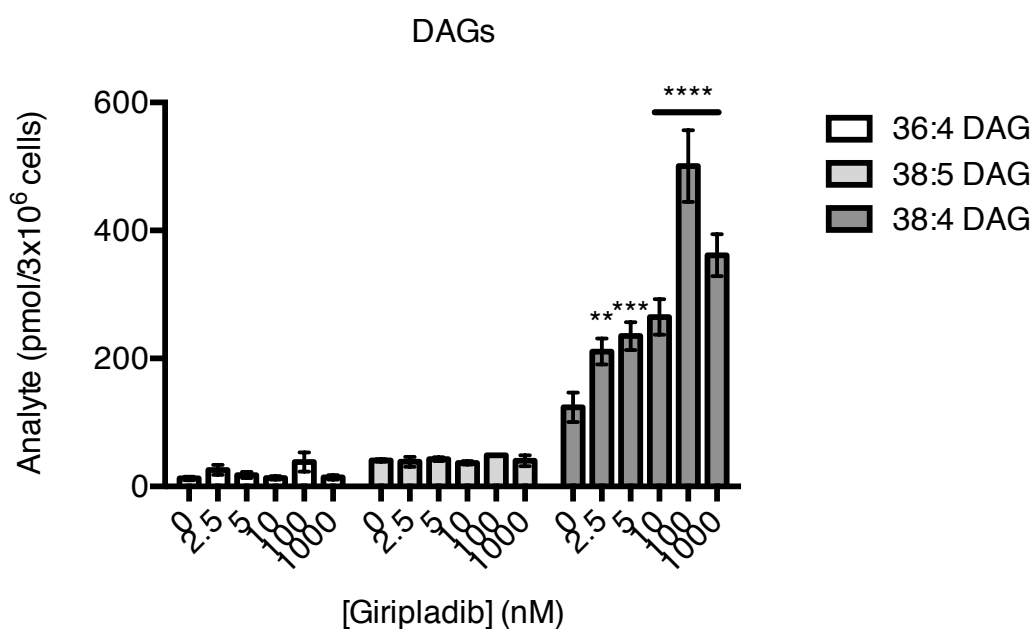

Figure 8: Concentration-dependent effects of giripladib on DAGs in stimulated RAW 264.7 cells. Inhibition of cPLA$_2\alpha$ by giripladib significantly increases the levels of 38:4 DAG in a concentration-dependent manner but has no effect on 36:4 or 38:5 DAG. Values shown are mean ± s.e.m., n = 9. Significance was determined using a two-way ANOVA followed by a Holm-Sidak post-test.

We next sought to determine the impact of genetic deletion of cPLA$_2\alpha$ on PG and PG-G production. To do this we utilized BMDMs harvested in parallel from either cPLA$_2\alpha^{+/+}$ or cPLA$_2\alpha^{-/-}$ mice. After overnight stimulation with GM-CSF, the BMDMs were stimulated with LPS and IFNγ followed by zymosan for varying amounts of time. In agreement with the studies performed in RAW 264.7 cells with giripladib, BMDMs derived

from cPLA$_2$α$^{-/-}$ mice produced fewer PGs and greater amounts of PG-Gs relative to BMDMs derived from cPLA$_2$α$^{+/+}$ mice in response to stimulation (Figure 9). While zymosan stimulation resulted in a robust synthesis of AA in wild-type derived BMDMs, the production of AA was blunted in cPLA$_2$α$^{-/-}$ BMDMs. Zymosan treatment also stimulated 2-AG synthesis in both cPLA$_2$α$^{+/+}$ and cPLA$_2$α$^{-/-}$ BMDMs, but the amount of 2-AG produced by the cPLA$_2$α$^{-/-}$ BMDMs was significantly higher. Thus, the effect of genetic deletion of cPLA2α in BMDMs mirrors the effect of giripladib in RAW 264.7 cells.
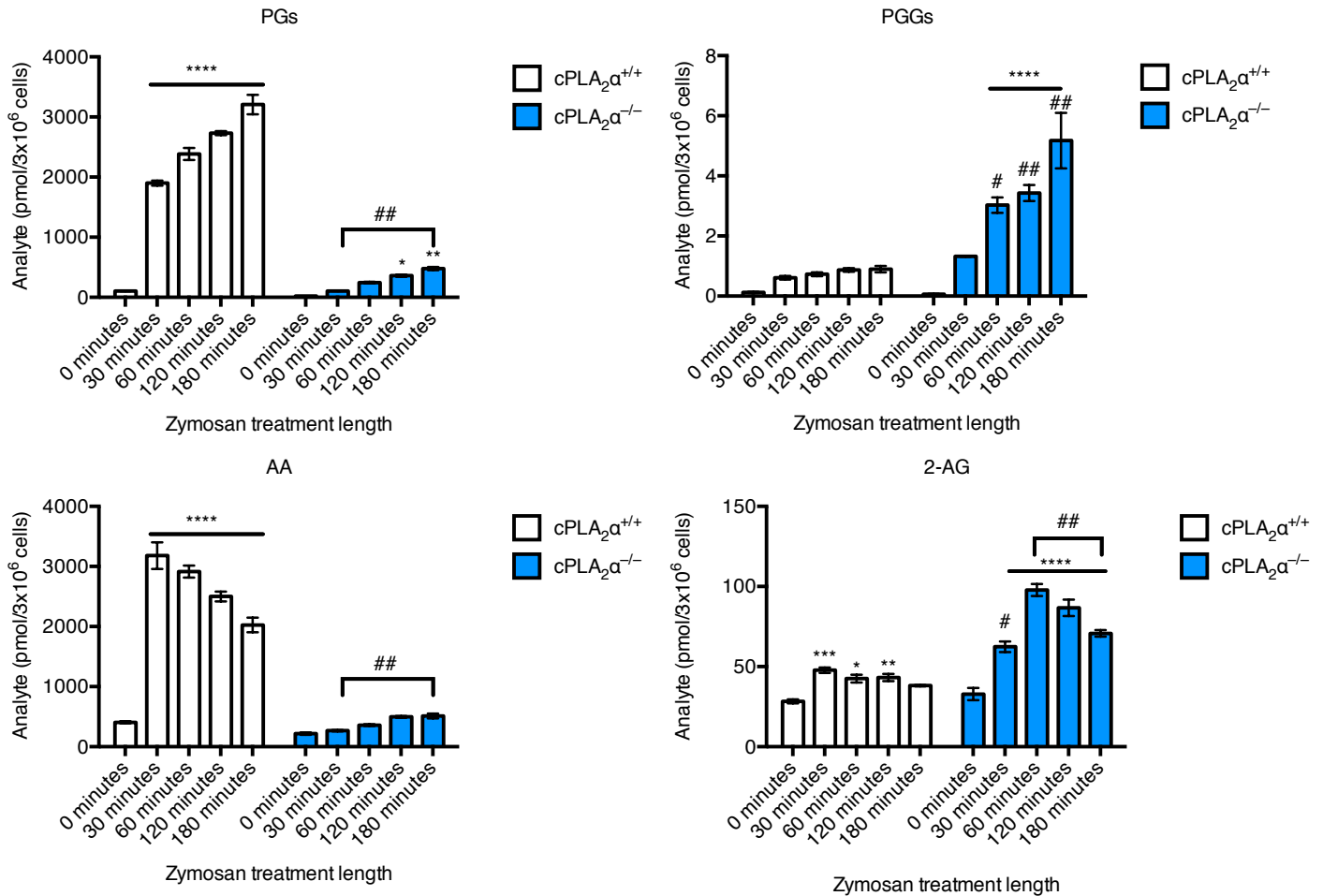
Figure 9: Effects of cPLA$_2$α deletion on PGs, PG-Gs, AA, and 2-AG in zymosan stimulated BMDMs. Zymosan causes significant PG production in cPLA$_2$α$^{+/+}$ BMDMs, but less pronounced production in cPLA$_2$α$^{-/-}$ BMDMs. Zymosan also caused PG-G production in both WT- and KO-derived BMDMs, but KO-derived BMDMs produced larger amounts of PG-Gs. Zymosan stimulated the synthesis of AA in cPLA$_2$α$^{+/+}$ but not cPLA$_2$α$^{-/-}$ BMDMs. Treatment with zymosan also increased the levels of 2-AG in KO-derived BMDMs to a greater extent than WT-derived BMDMs. Values shown are mean ± s.e.m., n = 6. Significance was determined using a two-way ANOVA followed by a Holm-Sidak post-test (* $p < .05$, ** $p < .01$, *** $p < .001$, and **** $p < .0001$ vs vehicle; # $p < .01$ and ## $p < .0001$ vs wild-type).

To further analyze the lipidomic consequences of genetic deletion of cPLA$_2$α, the levels of phospholipids and DAGs were analyzed in parallel. Zymosan caused an initial significant decrease in 38:4 PI at 30 minutes after treatment, which recovered back to non-zymosan treated levels at later time points in cPLA$_2$α$^{+/+}$ BMDMs (Figure 10). In contrast, in cPLA$_2$α$^{-/-}$ BMDMs zymosan decreased 38:4 PI at all time points relative to non-zymosan treated cells. Interestingly, cPLA$_2$α$^{+/+}$ BMDMs displayed a reduction in AA-containing DAGs with 30 minutes of zymosan stimulation but little effect at later time points. In stark contrast, cPLA$_2$α$^{-/-}$ BMDMs basally had much higher levels of DAGs relative to cPLA$_2$α$^{+/+}$ BMDMs and zymosan treatment caused a large increase in AA-derived DAGs.

Figure 10: Effects of cPLA$_2$α deletion on PIs and DAGs in zymosan stimulated BMDMs. Zymosan treatment causes an initial decrease in AA-containing PIs and DAGs in WT-derived BMDMs that recovers over time. In contrast, KO-derived BMDMs have decreased levels of 38:4 at all time points after zymosan stimulation but higher levels of DAGs after zymosan treatment at all time points. Values shown are mean ± s.e.m., n = 6. Significance was determined using a one-way ANOVA followed by a Holm-Sidak post-test (* $p < .05$, ** $p < .01$, *** $p < .001$, and **** $p < .0001$ vs vehicle).
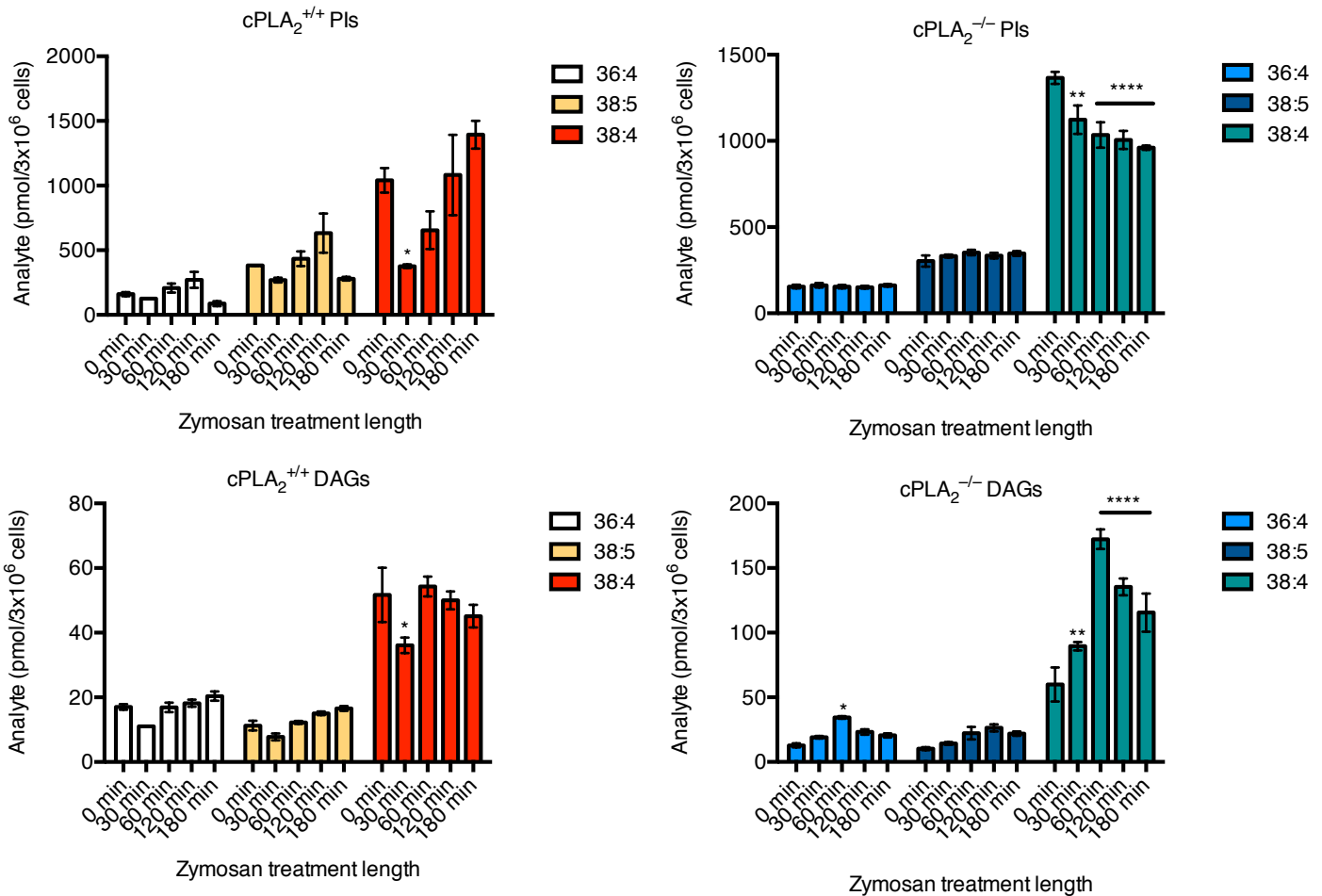
Surprisingly, zymosan treatment had no significant effect on AA-containing PC species in both cPLA$_2$α$^{+/+}$ and cPLA$_2$α$^{-/-}$BMDMs (Figure 11). However, it should be noted that the levels of AA-containing PIs and PCs in BMDMs are substantially higher than in RAW 264.7 cells, consistent with previous reports identifying RAW 264.7 cells as being relatively arachidonate-deficient.[58] Taken together, these data suggest that treatment of cPLA$_2$α$^{+/+}$ BMDMs with zymosan leads to rapid hydrolysis of 38:4 PI by cPLA$_2$α to form AA. In contrast, cPLA$_2$α$^{-/-}$ BMDMs treated with zymosan hydrolyze 38:4 PI via the PLC pathway to form DAGs, which are then converted to 2-AG and PG-Gs.
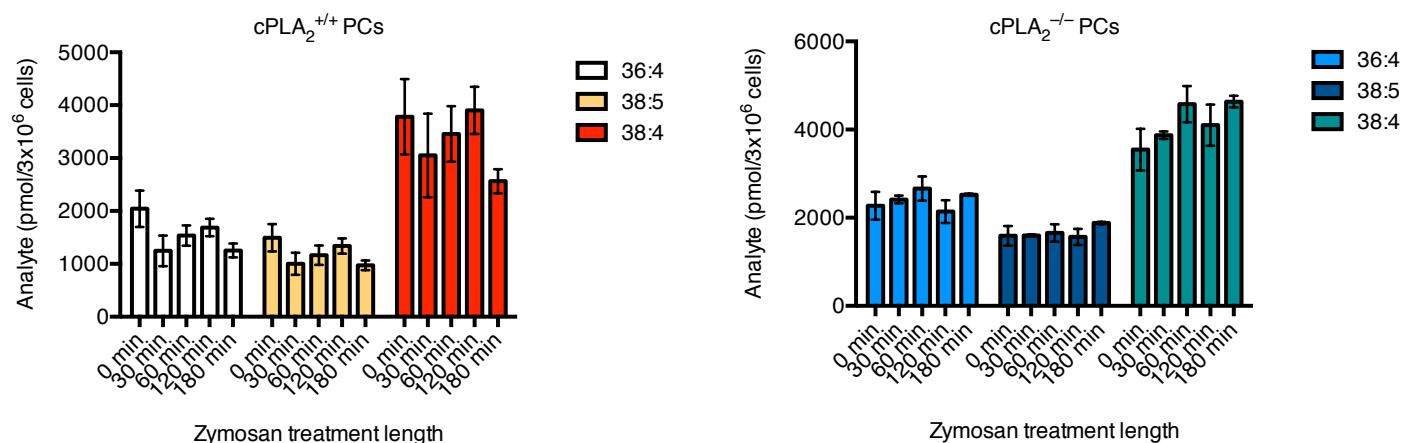
Figure 11: Effects of cPLA$_2$α deletion on PCs in zymosan stimulated BMDMs. Zymosan treatment causes no statistically significant effects on AA-containing PCs in either cPLA$_2$α$^{+/+}$ or cPLA$_2$α$^{-/-}$ BMDMs. Values shown are mean ± s.e.m., n = 6.

We next sought to validate the effects of giripladib as being mediated by cPLA$_2$α inhibition in BMDMs under multiple stimulation conditions. BMDMs derived from cPLA$_2$α$^{+/+}$ and cPLA$_2$α$^{-/-}$ mice were stimulated with either ionomycin for 1 hour or zymosan for 2 hours with and without giripladib. Both zymosan and ionomycin caused a robust production of PGs in cPLA$_2$α$^{+/+}$ BMDMs, which was significantly reduced by treatment with 100 nM giripladib (Figure 12). In contrast, cPLA$_2$α$^{-/-}$ BMDMs did not robustly produce PGs in response to either zymosan or ionomycin treatment and giripladib had no effect on the minimal production of PGs. Both zymosan and ionomycin induced the formation of PG-Gs in cPLA$_2$α$^{+/+}$ BMDMs, and giripladib significantly increased the levels of PG-Gs over the ionomycin alone stimulated values. In cPLA$_2$α$^{-/-}$ BMDMs stimulated with ionomycin there were larger amounts of PG-Gs relative to cPLA$_2$α$^{+/+}$ BMDMs treated with

ionomycin. Importantly, in cPLA$_2\alpha^{-/-}$ BMDMs giripladib treatment had no effect on the production of PG-Gs. In agreement with the reduction in AA release produced by giripladib in RAW 264.7 cells, it also significantly reduced the levels of AA in zymosan and ionomycin treated cPLA$_2\alpha^{+/+}$ BMDMs. Giripladib had no effect on AA in cPLA$_2\alpha^{-/-}$ BMDMs treated with either zymosan or ionomycin, although ionomycin treatment resulted in a significant increase in AA levels relative to vehicle treatment. Giripladib increased the levels of 2-AG in ionomycin-stimulated cPLA$_2\alpha^{+/+}$ BMDMs, but not zymosan treated cPLA$_2\alpha^{+/+}$ BMDMs, and had no effect on 2-AG levels under any stimulation conditions in cPLA$_2\alpha^{-/-}$ BMDMs. BMDMs treated with ionomycin had significantly higher levels of 2-AG when derived from cPLA$_2\alpha^{-/-}$ versus cPLA$_2\alpha^{+/+}$ mice.
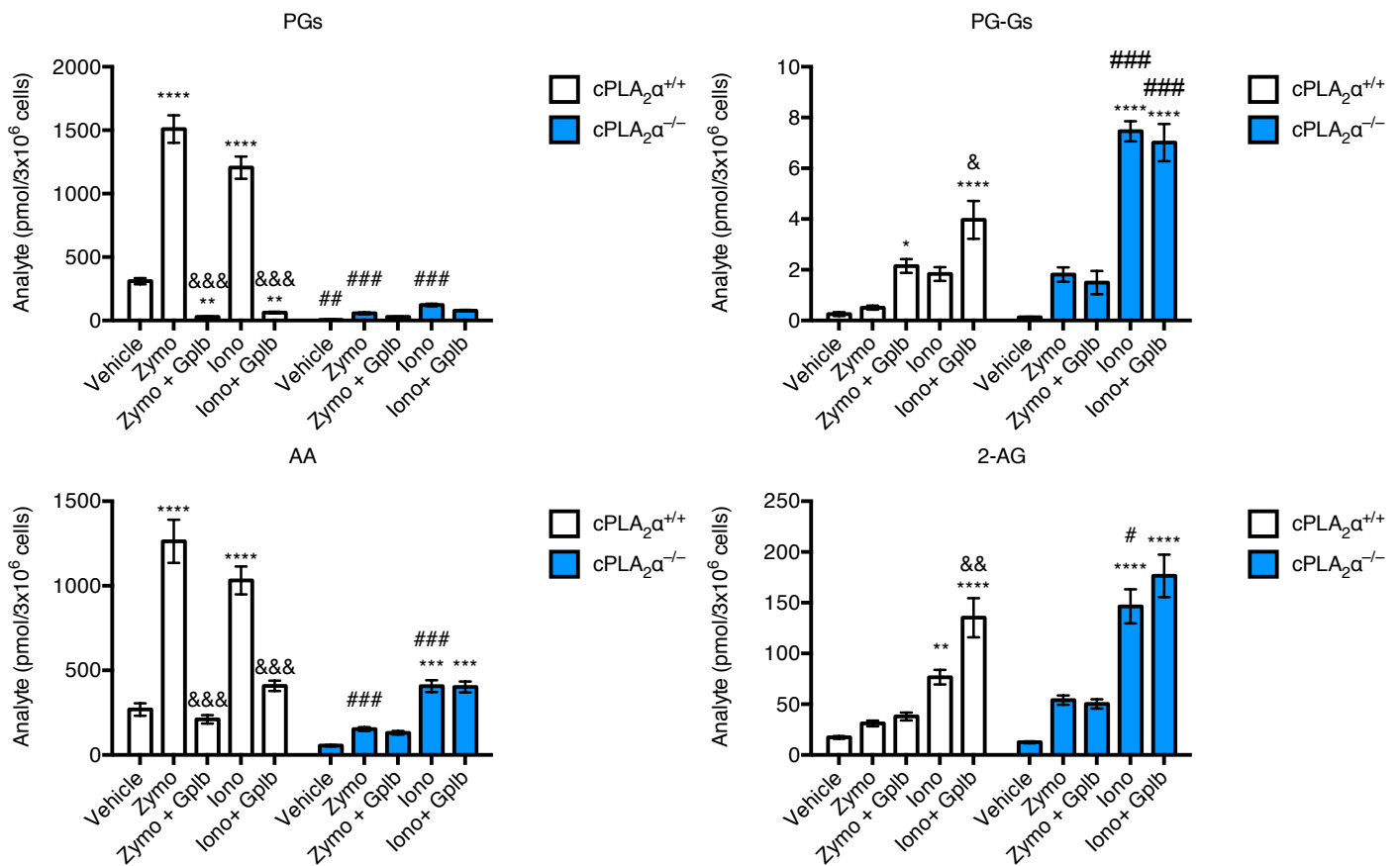
Figure 12: Effects of giripladib in cPLA$_2\alpha^{+/+}$ and cPLA$_2\alpha^{-/-}$ BMDMs. The effects of giripladib are abolished in cPLA$_2\alpha^{-/-}$ mice. Values shown are mean ± s.e.m., n = 6. Significance was determined using a two-way ANOVA followed by a Holm-Sidak post-test (* $p < .05$, ** $p < .01$, *** $p < .001$, and **** $p < .0001$ versus respective genotype vehicle; & $p < .05$, && $p < .01$, &&& $p < .0001$ versus stimulation with no giripladib; # $p < .01$, ## $p < .001$, ### $p < .0001$ versus cPLA$_2\alpha^{+/+}$).

To further assess effects of giripladib under different stimulation conditions in cPLA$_2\alpha^{+/+}$ and cPLA$_2\alpha^{-/-}$ BMDMs, full lipidomic analyses were performed in parallel. Giripladib (100 nM) demonstrated similar effects

in $cPLA_2\alpha^{+/+}$ BMDMs as previously seen in RAW 264.7 cells, as it increased 38:4 PI and DAG but had no effect in $cPLA_2\alpha^{-/-}$ BMDMs (Figure 13). The effects of giripladib compared to $cPLA_2\alpha^{+/+}$ were mirrored by $cPLA_2\alpha^{-/-}$ BMDMs, revealing they produce analogous effects. Thus, these data suggest that giripladib acts as a selective $cPLA_2\alpha$ inhibitor to block the hydrolysis of AA from the *sn*-2 position of 38:4 PI, which can then be phosphorylated to PIP_2 and cleaved by PLC to form 38:4 DAG. 38:4 DAG can then be hydrolyzed to 2-AG, which is oxygenated to form PG-Gs.
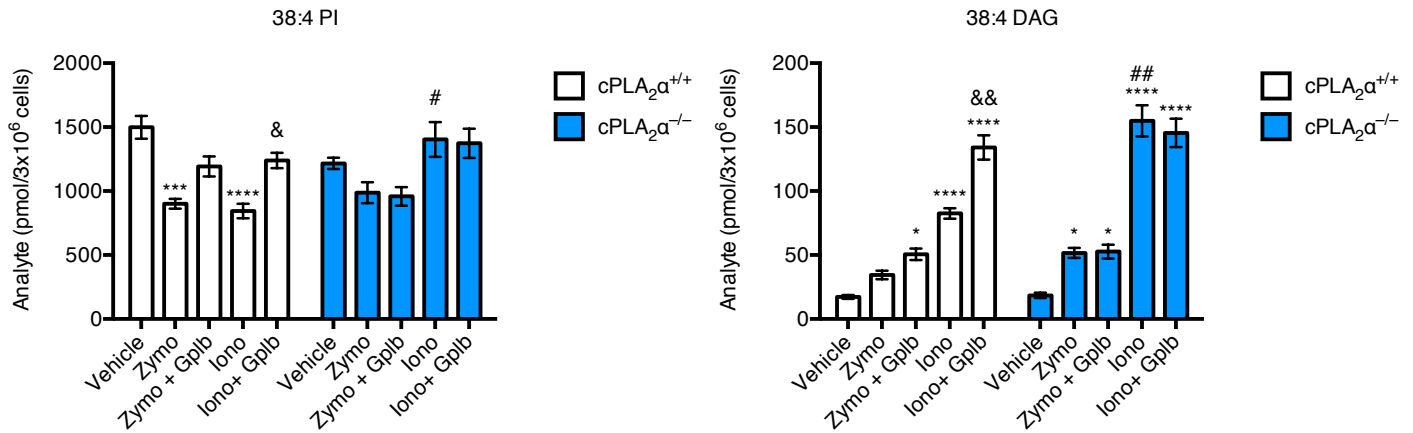
Figure 13: Effects of giripladib in $cPLA_2\alpha^{+/+}$ and $cPLA_2\alpha^{-/-}$ BMDMs. The effects of giripladib are abolished in $cPLA_2\alpha^{-/-}$ mice. Values shown are mean ± s.e.m., n = 6. Significance was determined using a two-way ANOVA followed by a Holm-Sidak post-test (* $p < .05$, *** $p < .001$, and **** $p < .0001$ versus respective genotype vehicle; & $p < .05$, && $p < .0001$ versus stimulation with no giripladib; # $p < .001$, ## $p < .0001$ versus $cPLA_2\alpha^{+/+}$).

Identification of the COX isoform responsible for PG-G production in BMDMs

As the final step in characterizing the biosynthetic pathway for PG-G production in BMDMs, we also sought to identify the enzyme responsible for the production of PG-Gs from 2-AG. While COX-1 does not utilize 2-AG as a substrate efficiently *in vitro*, previous studies identified COX-1 as the major mediator of PG-G formation in resident peritoneal macrophages.[7,52] To assess the relative contributions of COX-1 and COX-2 to PG and PG-G production in stimulated BMDMs we harvested cells from *Ptgs2*^{+/+} and *Ptgs2*^{-/-} mice. While *Ptgs2*^{+/+} BMDMs had robust production of both PGs and PG-Gs in response to zymosan or ionomycin stimulation, *Ptgs2*^{-/-} BMDMs produced significantly less PGs and trace amounts of PG-Gs (Figure 14). Giripladib treatment significantly reduced the levels of PGs in both *Ptgs2*^{+/+} and *Ptgs2*^{-/-} BMDMs. While giripladib treatment significantly increased the levels of PG-Gs in *Ptgs2*^{+/+} BMDMs relative to zymosan or

ionomycin alone, it was unable to rescue the lack of production of PG-Gs in *Ptgs2*$^{-/-}$ BMDMs. Thus, COX-2

appears to be the major producer of PGs and PG-Gs in BMDMs under these stimulation conditions.
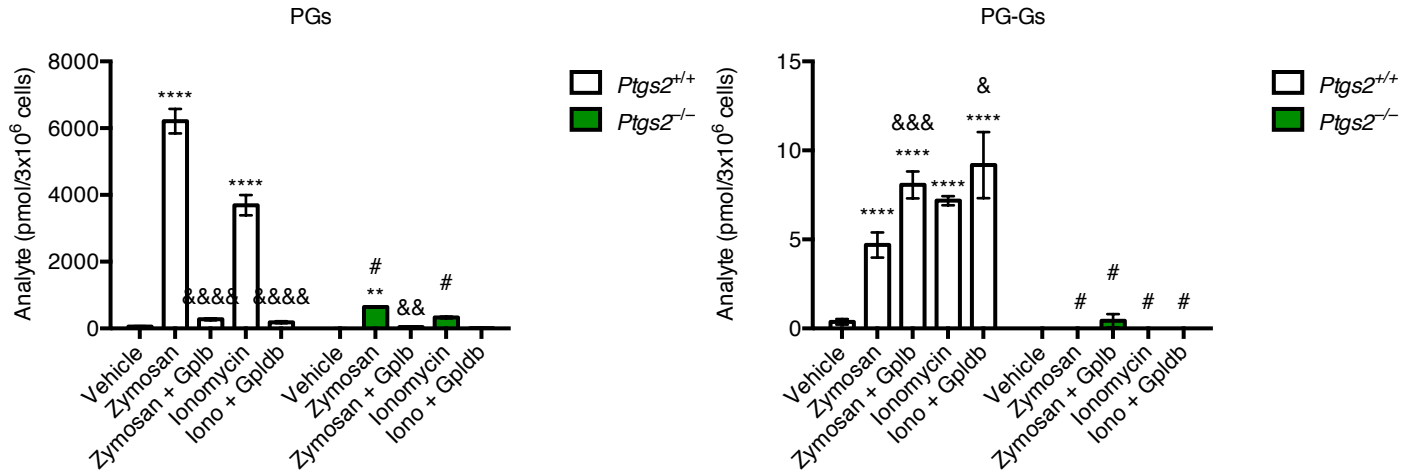
Figure 14: Effect of COX-2 genetic deletion on PG and PG-G production elicited by zymosan and ionomycin stimulation with and without giripladib treatment. While *Ptgs2*$^{+/+}$ BMDMs had robust production of both PGs and PG-Gs, *Ptgs2*$^{-/-}$ BMDMs produced significantly less PGs and trace amounts of PG-Gs. Giripladib treatment significantly reduced the levels of PGs in both *Ptgs2*$^{+/+}$ and *Ptgs2*$^{-/-}$ BMDMs. Giripladib treatment significantly increased the levels of PG-Gs in *Ptgs2*$^{+/+}$ BMDMs, but did not lead to robust PG-G production in *Ptgs2*$^{-/-}$ BMDMs. Values shown are mean ± s.e.m., n = 3. Significance was determined using a two-way ANOVA followed by a Holm-Sidak post-test (* $p < .05$, ** $p < .01$, and **** $p < .0001$ versus respective genotype vehicle; & $p < .05$, && $p < .01$, &&& $p < .001$, &&&& $p < .0001$ versus stimulation with no giripladib; # $p < .0001$ versus cPLA$_2$α$^{+/+}$).

To determine if the lack of effect of giripladib on PG-G production in *Ptgs2*$^{-/-}$ BMDMs was due to a

lack of inhibition of AA production, we also analyzed the levels of AA and 2-AG. Giripladib treatment

significantly inhibited the production of AA in *Ptgs2*$^{+/+}$ treated with zymosan and in *Ptgs2*$^{-/-}$ treated with either

zymosan or ionomycin (Figure 15). Interestingly, the levels of AA in *Ptgs2*$^{-/-}$ BMDMs were significantly

higher after zymosan or ionomycin treatment relative to the levels in *Ptgs2*$^{+/+}$ BMDMs treated with zymosan or

ionomycin. This suggests that COX-2 is a major determinant of AA levels in zymosan or ionomycin stimulated

BMDMs. Both zymosan and ionomycin caused significant increases in 2-AG levels in both *Ptgs2*$^{+/+}$ and *Ptgs2*$^{-}$

$^{/-}$ BMDMs. Giripladib treatment led to a further significant enhancement of 2-AG levels compared to zymosan

treatment alone in *Ptgs2*$^{+/+}$ BMDMs and compared to both zymosan and ionomycin treatment alone in *Ptgs2*$^{-/-}$

BMDMs. Taken together, these studies demonstrate that AA may serve as an inhibitor of 2-AG oxygenation by

COX-2. Pharmacological or genetic blockade of the hydrolysis of 38:4 PI by cPLA$_2$α leads to augmentation of

174

38:4 DAG and 2-AG levels in both RAW 264.7 and BMDMs. Thus, a shunting of AA-containing PI to form 2-AG occurs and a consequence of this is increased PG-G production by COX-2. The increase in PG-G production could be caused by multiple factors including release of inhibition of COX-2 oxygenation of 2-AG by reducing AA levels or an increase in 2-AG available to be oxygenated by COX-2. It is likely that both effects contribute to the increase in PG-G formation.
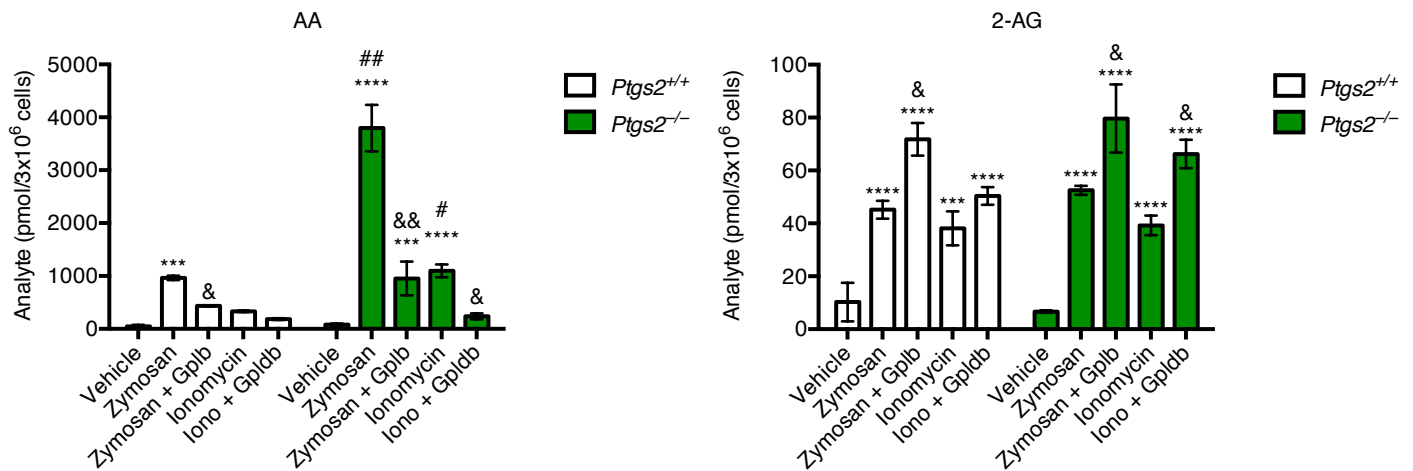
Figure 15: Effect of COX-2 genetic deletion on AA and 2-AG production elicited by zymosan and ionomycin stimulation with and without giripladib treatment. Giripladib treatment significantly inhibited the production of AA in both $Ptgs2^{+/+}$ and $Ptgs2^{-/-}$ BMDMs and significantly increased the levels of 2-AG in $Ptgs2^{+/+}$ and $Ptgs2^{-/-}$ BMDMs. Values shown are mean ± s.e.m., n = 3. Significance was determined using a two-way ANOVA followed by a Holm-Sidak post-test (*** $p < .001$ and **** $p < .0001$ versus respective genotype vehicle; & $p < .001$ and && $p < .0001$ versus stimulation with no giripladib; # $p < .01$ and ## $p < .0001$ versus cPLA$_2\alpha^{+/+}$).

In vivo production of PG-Gs

The increased production of PG-Gs in response to giripladib treatment in stimulated macrophages prompted us to explore the potential of increasing PG-G production *in vivo* by decreasing the levels of AA and increasing the levels of 2-AG. To do this, we utilized mice containing a human Thy-1-COX-2 transgene, which leads to expression of human COX-2 in neurons of the amygdala, striatum, cerebral cortex, and hippocampus.[59-61] These mice have PGE$_2$ levels that are 25-40-fold higher than non-transgenic controls. The mice also develop an age-dependent deficit in both spatial and non-spatial memory tasks due to increases in cortical neuron apoptosis and glial activation.[62] The mice also exhibit enhanced hippocampal long-term synaptic plasticity and

a lack of depolarization-induced suppression of inhibition, both of which are mediated by increased oxidative degradation of eCBs by COX-2.[63]

We first assessed the impact of overexpressing COX-2 by measuring the levels of PGs, AEA, 2-AG, and AA in the brain in transgenic COX-2 and wild-type littermates. The transgenic mice had significantly higher PG levels and significantly decreased AEA and 2-AG levels, with no change in AA (Figure 16). Thus, COX-2 overexpression decreases the levels of AEA and 2-AG in whole brain, consistent with the previous studies identifying deficits in eCB signaling.[63] These analyses also confirmed the striking increase in PG production in COX-2 transgenic mice compared to wild-type littermates.
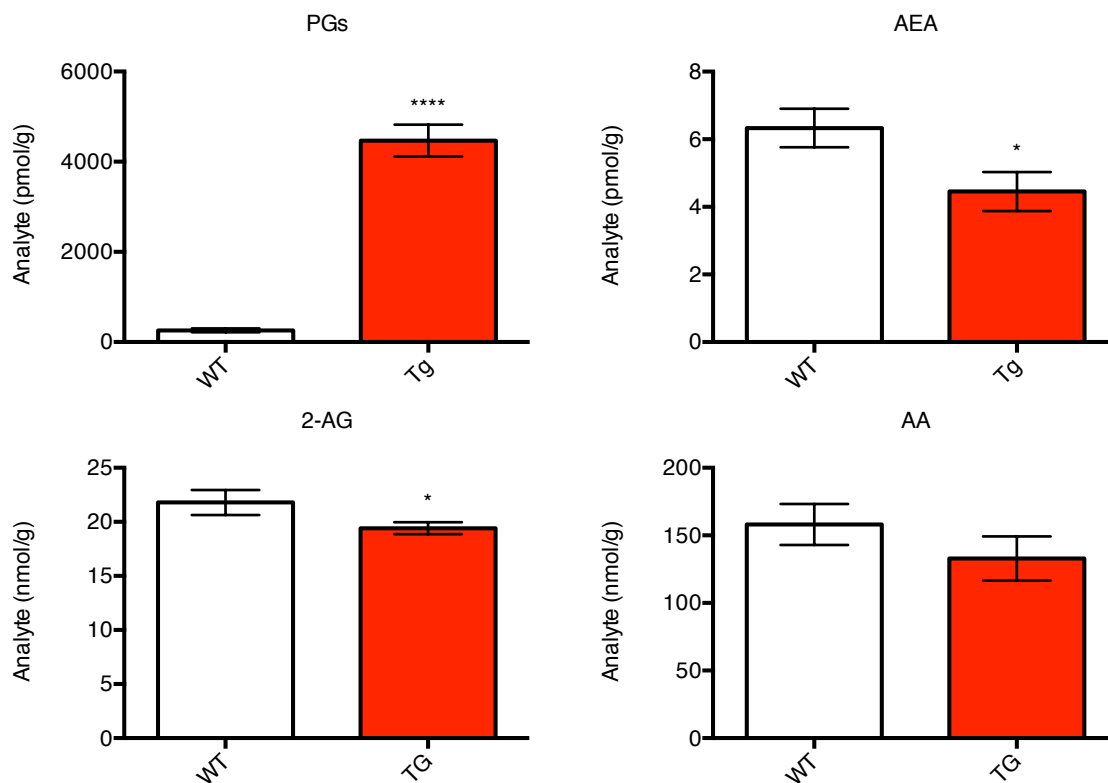
Figure 16: Effect of COX-2 overexpression on brain PGs, AEA, 2-AG, and AA. COX-2 transgenic mice have significantly increased PG levels in the brain. Overexpression of COX-2 in the brain also results in decreased AEA and 2-AG levels, but has no effect on AA levels. Values shown are mean ± s.e.m., vehicle n = 24 and transgenic n = 21. Significance was determined using a two-tailed t-test (* $p < .05$ and **** $p < .0001$).

We hypothesized that PG-G production could be induced in these mice by blocking the hydrolysis of 2-AG to AA in the brain by inhibiting MAGL with JZL-184. Previous studies have found that 2-AG is a major precursor for AA in the brain, suggesting that JZL-184 may produce similar effects in the brain to those elicited

by giripladib in macrophages.[36] Treatment of COX-2 overexpressing mice with JZL-184 resulted in the production of PG-Gs in the brain (Figure 17). This is notable as it is the first detection of PG-Gs in the brain. These studies are also in line with previous reports demonstrating that JZL-184 increases PG-G formation in carrageenan-treated rat footpads.[53] Thus, COX-2 overexpressing mice treated with JZL-184 could serve as an ideal *in vivo* platform to characterize substrate-selective COX-2 inhibitors for not just their effects on eCBs, but also with a direct measure of substrate-selective inhibition by monitoring PGs and PG-Gs.
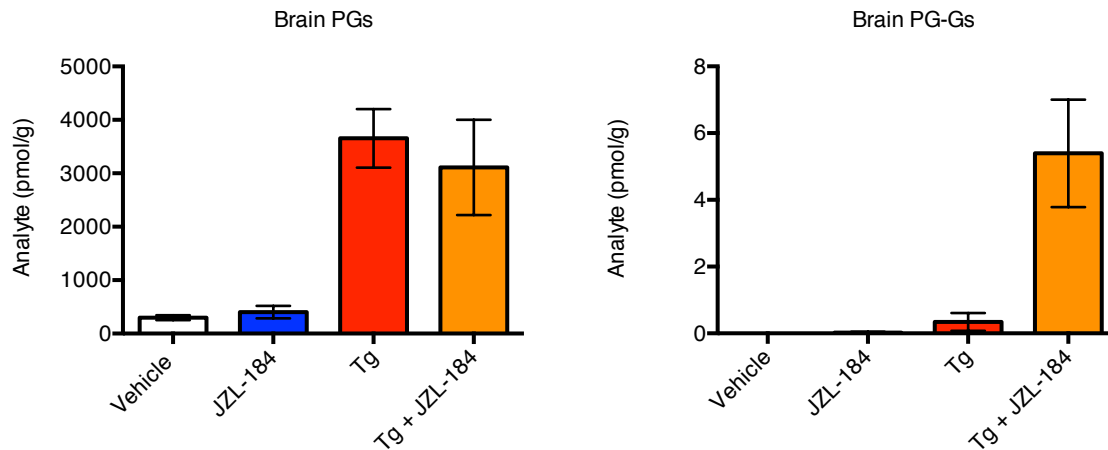
Figure 17: Effect of JZL-184 on production of PGs and PG-Gs in wild-type and COX-2 transgenic mice. While JZL-184 had no significant effect on PG production in either wild-type or COX-2 transgenic mice, it caused an increase in brain PG-Gs. Values shown are mean ± s.e.m., vehicle n = 8, JZL-184 n = 6, COX-2 transgenic n = 5, COX-2 transgenic + JZL-184 n = 7.

Discussion

These studies identify AA as a non-competitive inhibitor of 2-AG oxygenation by COX-2. The *in vitro* competition between the substrates for oxygenation by COX-2 appears to mirror the effects of substrate-selective inhibitors on 2-AG, which also display non-competitive inhibition.[64] Whether the mechanisms that give rise to the non-competitive inhibition of 2-AG by AA and substrate-selective inhibitors are identical is unknown, but given the fact that AA and substrate-selective inhibitors bind to COX-2 in similar fashions, it is likely that they inhibit AA oxygenation via similar structural perturbations.

We have extended the *in vitro* studies by utilizing two macrophage cell lines to characterize the impact of manipulating AA levels on PG-G production. PG-G production has been demonstrated in several cell lines, but the relatively abundant levels of PGs compared to a dearth of 2-AG derived PG-Gs, even when correcting for the relative amounts of AA and 2-AG, suggests that the two substrates are not equally utilized by COX-2.[5,6] Previous studies in our laboratory had identified that one mediator of this large difference between substrate utilization is based on the requirement of higher peroxide tone for 2-AG oxygenation.[8] We have now established AA levels as another determinant of 2-AG oxygenation. Although both of these factors clearly contribute to 2-AG turnover by COX-2, the production of PG-Gs in cells still is not comparable with the production of PGs. Although they are not produced in bulk amounts as PGs are, it is notable that PG-Gs have quite potent biological effects, suggesting that subtle manipulation of their levels may produce exponential biological effects, such as calcium mobilization, compared to similar perturbations of PGs.[65]

Beyond the characterization of PG-G biosynthesis, these studies identify 38:4 PI as a fundamentally limiting phospholipid precursor species in the synthesis of both AA and 2-AG in stimulated macrophages. 38:4 PI can be hydrolyzed by $cPLA_2\alpha$ to form AA and 18:0 LPI or alternatively can be hydrolyzed by PLC to form 38:4 DAG. 38:4 DAG can be further hydrolyzed by DAGL, which forms a free fatty acid and 2-AG. Thus, 38:4 PI serves as a source for AA and 2-AG in a mutually exclusive fashion at the phospholipid level, although 2-AG itself can also serve as a precursor to AA through hydrolytic enzymes. Inhibition or deletion of $cPLA_2\alpha$ leads to augmentation of 38:4 PI, which is then utilized by stimulated RAW 264.7 or BMDMs to form 38:4 DAG, 2-AG, and PG-Gs.

The increase in PG-G production could be due to a number of factors including the increase in 2-AG synthesis, but also through the removal of substrate competition from AA in the cellular milieu. Further studies defining the exact isoform(s) of PLC and DAGL that control this pathway and thorough examination of other pathways as possible routes to synthesize 2-AG for oxygenation by COX-2 are needed to fully elucidate biosynthetic pathway that produces PG-Gs.

To extend these cellular studies *in vivo* we also assessed the impact of the MAGL inhibitor JZL-184 on PG-G production in COX-2 transgenic mice. These mice produced significant amounts of PG-Gs when treated with JZL-184. Thus, inhibition of 2-AG hydrolysis to AA coupled with overexpression of COX-2 results in a robust production of PG-Gs in the brain *in vivo*. This system should prove valuable for future studies assessing substrate-selective inhibition, as it allows for a direct read out of PG-G inhibition as opposed to tangential measurements such as increases in AEA and 2-AG. Additionally, these COX-2 transgenic mice treated with JZL-184 could be useful for studying the biological effects of PG-Gs from behavioral responses to synaptic signaling.

References

1. Kozak, K.R.*, et al.* Metabolism of the endocannabinoids, 2-arachidonylglycerol and anandamide, into prostaglandin, thromboxane, and prostacyclin glycerol esters and ethanolamides. *J Biol Chem* **277**, 44877-44885 (2002).
2. Duggan, K.C.*, et al.* (R)-Profens are substrate-selective inhibitors of endocannabinoid oxygenation by COX-2. *Nat Chem Biol* **7**, 803-809 (2011).
3. Hermanson, D.J.*, et al.* Substrate-selective COX-2 inhibition decreases anxiety via endocannabinoid activation. *Nat Neurosci* **16**, 1291-U1176 (2013).
4. Rouzer, C.A. & Marnett, L.J. Endocannabinoid Oxygenation by Cyclooxygenases, Lipoxygenases, and Cytochromes P450: Cross-Talk between the Eicosanoid and Endocannabinoid Signaling Pathways. *Chem Rev* **111**, 5899-5921 (2011).
5. Rouzer, C.A. & Marnett, L.J. Glycerylprostaglandin synthesis by resident peritoneal macrophages in response to a zymosan stimulus. *J Biol Chem* **280**, 26690-26700 (2005).
6. Rouzer, C.A. & Marnett, L.J. Glyceryl prostaglandin synthesis in lipopolysaccharide-treated RAW264.7 cells is augmented by interferon-gamma and granulocytemacrophage colony stimulating factor. *Prostag Oth Lipid M* **79**, 146-147 (2006).
7. Rouzer, C.A.*, et al.* Zymosan-induced glycerylprostaglandin and prostaglandin synthesis in resident peritoneal macrophages: roles of cyclo-oxygenase-1 and-2. *Biochem J* **399**, 91-99 (2006).
8. Musee, J. & Marnett, L.J. Prostaglandin H synthase-2-catalyzed oxygenation of 2-arachidonoylglycerol is more sensitive to peroxide tone than oxygenation of arachidonic acid. *J Biol Chem* **287**, 37383-37394 (2012).
9. Dessen, A.*, et al.* Crystal structure of human cytosolic phospholipase A(2) reveals a novel topology and catalytic mechanism. *Cell* **97**, 349-360 (1999).
10. Clark, J.D.*, et al.* A Novel Arachidonic Acid-Selective Cytosolic Pla2 Contains a Ca2+-Dependent Translocation Domain with Homology to Pkc and Gap. *Cell* **65**, 1043-1051 (1991).
11. Lin, L.L.*, et al.* Cpla2 Is Phosphorylated and Activated by Map Kinase. *Cell* **72**, 269-278 (1993).
12. Nakamura, H., Hirabayashi, T., Shimizu, M. & Murayama, T. Ceramide-1-phosphate activates cytosolic phospholipase A2 alpha directly and by PKC pathway. *Biochem Pharmacol* **71**, 850-857 (2006).
13. Mosior, M., Six, D.A. & Dennis, E.A. Group IV cytosolic phospholipase A(2) binds with high affinity and specificity to phosphatidylinositol 4,5-bisphosphate resulting in dramatic increases in activity. *J Biol Chem* **273**, 2184-2191 (1998).
14. Leslie, C.C., Voelker, D.R., Channon, J.Y., Wall, M.M. & Zelarney, P.T. Properties and Purification of an Arachidonoyl-Hydrolyzing Phospholipase-A2 from a Macrophage Cell-Line, Raw-264.7. *Biochim Biophys Acta* **963**, 476-492 (1988).
15. Davidson, F.F. & Dennis, E.A. Evolutionary Relationships and Implications for the Regulation of Phospholipase-A2 from Snake-Venom to Human Secreted Forms. *J Mol Evol* **31**, 228-238 (1990).
16. Reynolds, L.J., Hughes, L.L., Louis, A.I., Kramer, R.M. & Dennis, E.A. Metal-Ion and Salt Effects on the Phospholipase-a(2), Lysophospholipase, and Transacylase Activities of Human Cytosolic Phospholipase-a(2). *Biochim Biophys Acta* **1167**, 272-280 (1993).
17. Buczynski, M.W., Dumlao, D.S. & Dennis, E.A. An integrated omics analysis of eicosanoid biology. *J Lipid Res* **50**, 1015-1038 (2009).
18. Vignola, M.J., Kashatus, D.F., Taylor, G.A., Counter, C.M. & Valdivia, R.H. cPLA(2) Regulates the Expression of Type I Interferons and Intracellular Immunity to Chlamydia trachomatis. *J Biol Chem* **285**, 21625-21635 (2010).
19. Nakanishi, M. & Rosenberg, D.W. Roles of cPLA(2)alpha and arachidonic acid in cancer. *Bba-Mol Cell Biol L* **1761**, 1335-1343 (2006).
20. Vanhoutte, P.M. COX-1 and Vascular Disease. *Clin Pharmacol Ther* **86**, 212-215 (2009).
21. Raichel, L.*, et al.* Reduction of cPLA(2 alpha) overexpression: An efficient anti-inflammatory therapy for collagen-induced arthritis. *Eur J Immunol* **38**, 2905-2915 (2008).

22. Street, I.P., *et al.* Slow-Binding and Tight-Binding Inhibitors of the 85-Kda Human Phospholipase-A2. *Biochemistry-Us* **32**, 5935-5940 (1993).

23. Svensson, C.I., *et al.* Spinal phospholipase A(2) in inflammatory hyperalgesia: Role of the small, secretory phospholipase A(2). *Neuroscience* **133**, 543-553 (2005).

24. Marinier, A., *et al.* Synthesis and biological activity of alpha and beta-substituted trifluoromethylketone derivatives as CPLA2 inhibitors. *Abstr Pap Am Chem S* **223**, A97-A97 (2002).

25. Banville, J., *et al.* Preparation and evaluation of BMS-229724 analogues as inhibitors of cytosolic phospholipase A(2). *Abstr Pap Am Chem S* **223**, A97-A97 (2002).

26. Flamand, N., *et al.* Effects of pyrrophenone, an inhibitor of group IVA phospholipase A(2), on eicosanoid and PAF biosynthesis in human neutrophils. *Brit J Pharmacol* **149**, 385-392 (2006).

27. Tai, N., *et al.* Cytosolic phospholipase A2 alpha inhibitor, pyrroxyphene, displays anti-arthritic and anti-bone destructive action in a murine arthritis model. *Inflammation research : official journal of the European Histamine Research Society ... [et al.]* **59**, 53-62 (2010).

28. Lee, K.L., *et al.* Discovery of Ecopladib, an indole inhibitor of cytosolic phospholipase A2alpha. *Journal of medicinal chemistry* **50**, 1380-1400 (2007).

29. McKew, J.C., *et al.* Indole cytosolic phospholipase A2 alpha inhibitors: discovery and in vitro and in vivo characterization of 4-{3-[5-chloro-2-(2-{[(3,4-dichlorobenzyl)sulfonyl]amino}ethyl)-1-(diphenylmethyl)-1H-indol-3-yl]propyl}benzoic acid, efipladib. *Journal of medicinal chemistry* **51**, 3388-3413 (2008).

30. Marusic, S., *et al.* Blockade of cytosolic phospholipase A2 alpha prevents experimental autoimmune encephalomyelitis and diminishes development of Th1 and Th17 responses. *Journal of neuroimmunology* **204**, 29-37 (2008).

31. Lee, K.L., *et al.* Benzenesulfonamide indole inhibitors of cytosolic phospholipase A2alpha: optimization of in vitro potency and rat pharmacokinetics for oral efficacy. *Bioorganic & medicinal chemistry* **16**, 1345-1358 (2008).

32. Lamothe, J., *et al.* Efficacy of Giripladib, a novel inhibitor of cytosolic phospholipase A2 alpha, in two different mouse models of rheumatoid arthritis. *Clin Immunol* **127**, S89-S90 (2008).

33. Chen, L., *et al.* Reactions of functionalized sulfonamides: application to lowering the lipophilicity of cytosolic phospholipase A2alpha inhibitors. *Journal of medicinal chemistry* **52**, 1156-1171 (2009).

34. Kirincich, S.J., *et al.* Benzhydrylquinazolinediones: Novel cytosolic phospholipase A(2)alpha inhibitors with improved physicochemical properties. *Bioorganic & medicinal chemistry* **17**, 4383-4405 (2009).

35. Gopalsamy, A., *et al.* 1,2,4-Oxadiazolidin-3,5-diones and 1,3,5-triazin-2,4,6-triones as cytosolic phospholipase A2alpha inhibitors. *Bioorganic & medicinal chemistry letters* **16**, 2978-2981 (2006).

36. Nomura, D.K., *et al.* Endocannabinoid hydrolysis generates brain prostaglandins that promote neuroinflammation. *Science* **334**, 809-813 (2011).

37. Prescott, S.M. & Majerus, P.W. Characterization of 1,2-diacylglycerol hydrolysis in human platelets. Demonstration of an arachidonoyl-monoacylglycerol intermediate. *J Biol Chem* **258**, 764-769 (1983).

38. Sugiura, T., Kishimoto, S., Oka, S. & Gokoh, M. Biochemistry, pharmacology and physiology of 2-arachidonoylglycerol, an endogenous cannabinoid receptor ligand. *Prog Lipid Res* **45**, 405-446 (2006).

39. Ueda, N., Tsuboi, K., Uyama, T. & Ohnishi, T. Biosynthesis and degradation of the endocannabinoid 2-arachidonoylglycerol. *BioFactors* **37**, 1-7 (2011).

40. Fukami, K., Inanobe, S., Kanemaru, K. & Nakamura, Y. Phospholipase C is a key enzyme regulating intracellular calcium and modulating the phosphoinositide balance. *Prog Lipid Res* **49**, 429-437 (2010).

41. Kano, M., Ohno-Shosaku, T., Hashimotodani, Y., Uchigashima, M. & Watanabe, M. Endocannabinoid-mediated control of synaptic transmission. *Physiological reviews* **89**, 309-380 (2009).

42. Bisogno, T., Melck, D., De Petrocellis, L. & Di Marzo, V. Phosphatidic acid as the biosynthetic precursor of the endocannabinoid 2-arachidonoylglycerol in intact mouse neuroblastoma cells stimulated with ionomycin. *Journal of neurochemistry* **72**, 2113-2119 (1999).

43. Oka, S., *et al.* Evidence for the involvement of the cannabinoid CB2 receptor and its endogenous ligand 2-arachidonoylglycerol in 12-O-tetradecanoylphorbol-13-acetate-induced acute inflammation in mouse ear. *J Biol Chem* **280**, 18488-18497 (2005).

44. Ueda, H., Kobayashi, T., Kishimoto, M., Tsutsumi, T. & Okuyama, H. A possible pathway of phosphoinositide metabolism through EDTA-insensitive phospholipase A1 followed by lysophosphoinositide-specific phospholipase C in rat brain. *Journal of neurochemistry* **61**, 1874-1881 (1993).

45. Tsutsumi, T*., et al.* Lysophosphoinositide-specific phospholipase C in rat brain synaptic plasma membranes. *Neurochemical research* **19**, 399-406 (1994).

46. Nakane, S*., et al.* 2-arachidonoyl-sn-glycero-3-phosphate, an arachidonic acid-containing lysophosphatidic acid: occurrence and rapid enzymatic conversion to 2-arachidonoyl-sn-glycerol, a cannabinoid receptor ligand, in rat brain. *Arch Biochem Biophys* **402**, 51-58 (2002).

47. Hsu, K.L*., et al.* DAGLbeta inhibition perturbs a lipid network involved in macrophage inflammatory responses. *Nat Chem Biol* **8**, 999-1007 (2012).

48. Kozak, K.R., Rowlinson, S.W. & Marnett, L.J. Oxygenation of the endocannabinoid, 2-arachidonylglycerol, to glyceryl prostaglandins by cyclooxygenase-2. *Journal of Biological Chemistry* **275**, 33744-33749 (2000).

49. Hermanson, D.J*., et al.* Substrate-selective COX-2 inhibition decreases anxiety via endocannabinoid activation. *Nat Neurosci* **16**, 1291-1298 (2013).

50. Kingsley, P.J. & Marnett, L.J. Analysis of endocannabinoids, their congeners and COX-2 metabolites. *Journal of chromatography. B, Analytical technologies in the biomedical and life sciences* **877**, 2746-2754 (2009).

51. Kingsley, P.J. & Marnett, L.J. LC-MS-MS analysis of neutral eicosanoids. *Methods in enzymology* **433**, 91-112 (2007).

52. Kozak, K.R., Rowlinson, S.W. & Marnett, L.J. Oxygenation of the endocannabinoid, 2-arachidonylglycerol, to glyceryl prostaglandins by cyclooxygenase-2. *J Biol Chem* **275**, 33744-33749 (2000).

53. Hu, S.S., Bradshaw, H.B., Chen, J.S., Tan, B. & Walker, J.M. Prostaglandin E2 glycerol ester, an endogenous COX-2 metabolite of 2-arachidonoylglycerol, induces hyperalgesia and modulates NFkappaB activity. *Br J Pharmacol* **153**, 1538-1549 (2008).

54. Leslie, C.C. & Detty, D.M. Arachidonic acid turnover in response to lipopolysaccharide and opsonized zymosan in human monocyte-derived macrophages. *Biochem J* **236**, 251-259 (1986).

55. Irvine, R.F., Hemington, N. & Dawson, R.M. The hydrolysis of phosphatidylinositol by lysosomal enzymes of rat liver and brain. *Biochem J* **176**, 475-484 (1978).

56. Billah, M.M. & Lapetina, E.G. Formation of lysophosphatidylinositol in platelets stimulated with thrombin or ionophore A23187. *J Biol Chem* **257**, 5196-5200 (1982).

57. Balsinde, J. Roles of various phospholipases A2 in providing lysophospholipid acceptors for fatty acid phospholipid incorporation and remodelling. *Biochem J* **364**, 695-702 (2002).

58. Rouzer, C.A*., et al.* Lipid profiling reveals arachidonate deficiency in RAW264.7 cells: Structural and functional implications. *Biochemistry-Us* **45**, 14795-14808 (2006).

59. Vidensky, S*., et al.* Neuronal overexpression of COX-2 results in dominant production of PGE2 and altered fever response. *Neuromolecular medicine* **3**, 15-28 (2003).

60. Dore, S*., et al.* Neuronal overexpression of cyclooxygenase-2 increases cerebral infarction. *Annals of neurology* **54**, 155-162 (2003).

61. Andreasson, K.I*., et al.* Age-dependent cognitive deficits and neuronal apoptosis in cyclooxygenase-2 transgenic mice. *The Journal of neuroscience : the official journal of the Society for Neuroscience* **21**, 8198-8209 (2001).

62. Melnikova, T*., et al.* Cycloxygenase-2 activity promotes cognitive deficits but not increased amyloid burden in a model of Alzheimer's disease in a sex-dimorphic pattern. *Neuroscience* **141**, 1149-1162 (2006).

63. Yang, H., Zhang, J., Andreasson, K. & Chen, C. COX-2 oxidative metabolism of endocannabinoids augments hippocampal synaptic plasticity. *Molecular and cellular neurosciences* **37**, 682-695 (2008).

64. Prusakiewicz, J.J., Duggan, K.C., Rouzer, C.A. & Marnett, L.J. Differential sensitivity and mechanism of inhibition of COX-2 oxygenation of arachidonic acid and 2-arachidonoylglycerol by ibuprofen and mefenamic acid. *Biochemistry-Us* **48**, 7353-7355 (2009).

65. Nirodi, C.S., Crews, B.C., Kozak, K.R., Morrow, J.D. & Marnett, L.J. The glyceryl ester of prostaglandin E2 mobilizes calcium and activates signal transduction in RAW264.7 cells. *Proceedings of the National Academy of Sciences of the United States of America* **101**, 1840-1845 (2004).

CHAPTER VIII

PERSPECTIVE AND FUTURE DIRECTIONS

Cyclooxygenase-2 (COX-2) catalyzes the *bis*-dioxygenation and cyclization of polyunsaturated fatty acid substrates such as arachidonic acid (AA), 2-arachidonoyl glycerol (2-AG), and arachidonoyl ethanolamide (AEA).[1,2] This is the committed step in the generation of prostaglandin H_2, prostaglandin H_2-glycerol, and prostaglandin H_2-ethanolamide, which are each then processed by downstream enzymes to form prostaglandins (PGs), prostaglandin glycerol esters (PG-Gs), and prostaglandin ethanolamides (PG-EAs). These bioactive species mediate a variety of physiological effects, including pain, inflammation, and fever, through their actions at G-protein coupled receptors (GPCRs). While the GPCRs that respond to PGs have been thoroughly studied, the receptors for PG-Gs and PG-EAs appear to be distinct from traditional prostanoid receptors.[3]

The oxygenation of AEA and 2-AG by COX-2 not only produces a distinct set of bioactive lipids, but it also modulates the levels of AEA and 2-AG. AEA and 2-AG are the endogenous ligands for the cannabinoid receptors 1 and 2 (CB_1 and CB_2), which mediate a variety of physiological and pathophysiological processes.[4,5] In addition to activating CB_1 and CB_2, they can also act at other targets including vanilloid receptor 1 (TRPV1), peroxisome proliferator-activated receptor (PPAR), and some ion channels.[4]

AEA and 2-AG are synthesized and degraded by discrete sets of enzymes.[6-8] Elucidation of the molecular regulation of eCB metabolism has led to the development of pharmacological tools to enhance eCB signaling and probe the therapeutic utility of eCB augmentation for a variety of pathological conditions.[9-11] AEA is primarily degraded by fatty acid amide hydrolase (FAAH), and pharmacological inhibition of FAAH causes robust increases in brain AEA levels.[12,13] However, FAAH also degrades a number of non-cannabinoid N-acylethanolamides (NAEs), which are elevated upon FAAH inhibition and are active at molecular targets such as PPARs.[14-16] In parallel to AEA, 2-AG is primarily degraded by monoacylglycerol lipase (MAGL), which also metabolizes a series of monoacylglycerols (MAGs).[17] Inhibition of FAAH or MAGL have demonstrated preclinical efficacy in models of neuropathic pain, neurodegeneration, anxiety and depression, pain, hyperemesis, and drug withdrawal syndromes, many of which are mediated by CB receptor-dependent

mechanisms.[9,18-21] These studies demonstrate the pleiotropic therapeutic potential of eCB augmentation via FAAH and MAGL inhibition and the resulting modulation of cannabinoid receptor signaling.

The studies discussed in this dissertation reveal that, in addition to FAAH and MAGL, COX-2 action modulates the levels of AEA and 2-AG. While a connection between COX-2 action and endocannabinoid inactivation has been suggested by a series of converging data, our studies have demonstrated for the first time that COX-2 action can modulate endocannabinoid levels in multiple settings and across a series of tissues. This discovery opens exciting new frontiers to study the mechanism of action of clinically used non-steroidal anti-inflammatory drugs (NSAIDs). Multiple studies have identified that CB1 receptor antagonists block the anti-nociceptive effects of NSAIDs in spinal injury models.[22-27]

A novel class of COX-2 inhibitors termed "substrate-selective" COX-2 inhibitors, which prevent AEA and 2-AG oxygenation by COX-2 without inhibiting the oxygenation of AA to PGs, offers a novel pharmacological strategy to increase endocannabinoid levels without affecting AA-derived PG formation.[28] The studies outlined in this dissertation have generalized that rapid, reversible COX-2 inhibitors are potent inhibitors of 2-AG oxygenation, but weak inhibitors of AA oxygenation. In contrast, slow, tight-binding COX-2 inhibitors inhibit AA and 2-AG oxygenation with comparable IC_{50} values. In addition, we have identified the (R)-profens as substrate-selective inhibitors in contrast to previous reports suggesting they are inactive against COX-2.

In addition to our identification of a series of novel substrate-selective inhibitors, we have identified a facile method of developing novel substrate-selective inhibitors. Our studies demonstrating that manipulation of hydrogen bonding and ion pairing between a slow, tight-binding inhibitor and active site residues of COX-2 can produce substrate-selective inhibition suggests that modification of slow, tight-binding inhibitors to reduce their capacity to hydrogen bond and/or ion pair with the active site can generate substrate-selective inhibitors. Given the plethora of scaffolds that have been identified as NSAIDs, substrate-selective inhibitors likely also exist in a vast chemical space. Along with rational design of substrate-selective inhibitors through modification of slow, tight-binding inhibitors, our studies suggest that a series of compounds previously identified as inactive against COX-2 may in fact be substrate-selective inhibitors. As significant libraries of NSAIDs and NSAID analogs have been developed through concerted drug discovery efforts, a method such as high throughput screening for

the ability of these compounds to act as substrate-selective inhibitors could rapidly identified these probes along with a series of scaffolds not previously characterized as having activities against COX-2 *in vitro*.

We have investigated the enzymatic mechanism of substrate-selective inhibition based on several studies examining the basic function of COX-2. While the two subunits of COX-2 are sequence homodimers, the heme prosthetic group binds to only a single monomer, creating functional heterodimers. The heme-containing subunit is the catalytic subunit, whereas the non-heme-containing subunit is the allosteric subunit.[29,30] Binding of substrates, activators, and inhibitors to the allosteric subunit alters binding in the catalytic subunit through subunit communication via the dimer interface.[31] Substrate-selective inhibitors bind in the allosteric subunit and induce a conformational change that blocks AEA and 2-AG oxidation in the catalytic subunit. Binding of a second inhibitor molecule in the catalytic subunit blocks AA oxygenation, but this typically occurs at inhibitor concentrations orders of magnitude higher than the concentrations that block AEA and 2-AG oxygenation.[28] In contrast, slow, tight-binding inhibitors bind in the catalytic subunit and block the oxygenation of all substrates at similar concentrations.[32,33]

Consistent with this hypothesis, we have identified Leu-531 as a key mediator of substrate-selective inhibition. Leu-531 lies adjacent to the glycerol-binding pocket of 2-AG and mutation of Leu-531 to Ala results in abrogation of substrate-selective inhibition. This suggests that binding of a substrate-selective inhibitor to the allosteric site causes rotation of Leu-531 into the active site and a steric clash with the glycerol of 2-AG, resulting in inhibition. The exact mechanism that gives rise to the rotation of Leu-531 is still under investigation. These studies will assess the determinants of Leu-531 rotation and dimer crosstalk. One critical experiment will be mutation of Tyr-544 to Phe, which may mediate the translocation of the helix containing Leu-531 via a change in hydrogen bonding interactions with Pro-127 at the dimer interface. Further insight into the dynamics of substrate-selective inhibition could be gleaned from experiments with heterodimers containing one monomer of COX-2 lacking the ability to bind heme and a second monomer containing Leu-531 to Ala mutations. This mutant would force the Leu-531 to Ala monomer to serve as the catalytic site, while the monomer lacking heme binding would serve as the allosteric site. Thus, the through-space effects of binding to the allosteric site could be probed selectively with this heterodimer. The dynamics of substrate-selective

inhibition could also be identified with crystal structures containing only one molecule of a substrate-selective inhibitor bound to one active site with no occupancy at the second active site. These crystal structures could identify the structural perturbations in the second active site, such as a rotation of Leu-531, that give rise to substrate-selective inhibition.

In addition to establishing the *in vitro* determinants of substrate-selective inhibition we have also developed multiple cellular systems to characterize substrate-selective inhibitors. Both stimulated RAW 264.7 macrophages and stimulated primary dorsal root ganglia cells (DRGs) produce PG-Gs. DRGs also produce PG-EAs when treated with the calcium ionophore, ionomycin. We have utilized these model systems to validate that substrate-selective inhibitors selectively decrease the production of PG-Gs and PG-EAs while having no inhibition of PGs. In addition, we have discovered that substrate-selective inhibition leads not only to a reduction in PG-Gs and PG-EAs, but also an increase in 2-AG and AEA. This suggests that substrate-selective inhibition not only decreases compounds that induce hyperalgesia and mechanical allodynia, but also increases the levels of analgesic agents.[34-36] These cellular systems, particularly RAW 264.7 macrophages, also provide a convenient and rapid system to assess potential substrate-selective inhibitors for activity prior to *in vivo* testing.

Despite our successes with the (*R*)-profens in cellular systems, their one-way conversion to (*S*)-profens in mice necessitated the development of novel substrate-selective inhibitors. We identified a facile method of converting slow, tight-binding inhibitors to substrate-selective inhibitors by removing binding interactions between the inhibitor and the COX-2 active site. These studies lead to LM-4131, which we validated as a substrate-selective inhibitor against purified COX-2, in cellular systems, and *in vivo*. LM-4131 treatment increased the levels of AEA and 2-AG in the brain and several peripheral organs without having any effect on AA or PG production. Thus, we have identified the biochemical effects of a substrate-selective inhibitor *in vivo*.

The effect of LM-4131 on brain AEA and 2-AG prompted us to test its effects in several behavioral paradigms. Of particular importance, LM-4131 demonstrated anxiolytic effects in several pre-clinical models of anxiety. While the use of COX inhibitors in the treatment of pain and inflammation dates back over three thousand years, the anxiolytic effects of LM-4131 suggest a novel potential therapeutic effect. Thus, substrate-selective inhibition exhibits a novel therapeutic effect *in vivo*, although we clearly have not established the

187

scope of the potential therapeutic effects of substrate-selective inhibitors compared to traditional NSAIDs or endocannabinoid augmenting agents such as FAAH or MAGL inhibitors.

While substrate-selective inhibition exhibits anxiolytic effects in pre-clinical models of anxiety, we also sought to determine if they have reduced side effects relative to traditional NSAIDs and endocannabinoid augmenting agents. The potential side effects of substrate-selective COX-2 inhibitors could be produced from two biochemical effects. First, adverse effects such as gastrointestinal and cardiovascular or cerebrovascular toxicity are associated with most NSAIDs and are mediated by the inhibition of PG synthesis by COX-1, COX-2, or both enzymes.[37-40] Second, adverse cognitive, metabolic, and locomotor side effects are associated with direct CB_1 receptor activation.

A major clinical concern for the chronic use of COX inhibitors is cardiovascular and cerebrovascular toxicity manifested by an increased incidence of heart attack and stroke. Cardiovascular side effects are exhibited by most NSAIDs, regardless of their selectivity for COX-2, due to a reduction in vascular PGI_2 biosynthesis.[41,42] As LM-4131 did not affect central or peripheral levels of PGs, including PGI_2, it is possible that this pharmacological class of inhibitors could be devoid of or exhibit significantly reduced cardio/cerebrovascular toxicity compared to NSAIDs. Indeed, clinical trials conducted with the substrate-selective COX-2 inhibitor (R)-flurbiprofen suggest that it does not increase cardiovascular events.[43,44]

Gastrointestinal bleeding is also a well-known adverse effect of COX inhibition and is mediated by inhibition of gastroprotective PG synthesis in the gut.[45,46] LM-4131 does not cause overt gastrointestinal bleeding after acute administration, whereas indomethacin causes significant overt bleeding at the same dose. Additionally, (R)-flurbiprofen does not display gastrointestinal toxicity in humans.[43,44] These studies suggest that substrate-selective COX-2 inhibitors lack of an effect on PG synthesis may render them less prone to or even devoid of the complicating side effects of traditional COX inhibitors.

Since LM-4131 leads to CB_1 receptor activation in the central nervous system, and possibly in other tissues, cannabimimetic side effects could occur. Common adverse effects of direct acting cannabinoid agonists include motor suppression, cognitive impairment, hyperphagia, and dependence liability. LM-4131 does not cause motor suppression or object recognition memory deficits.[47] This may be in part be due to the relative

188

preference to elevate AEA over 2-AG, since MAGL inhibition or combined MAGL and FAAH inhibition produces cannabimimetic effects such as pronounced motoric inhibition.[48]

In addition to the potential lack of adverse cannabimimetic effects of LM-4131, distinct differences in the tissue-specificity of LM-4131 relative to FAAH inhibition suggest that it may lack some of the side effects of FAAH inhibition. FAAH inhibition in the liver causes robust increases in AEA and non-endocannabinoid NAE levels.[47] In contrast, LM-4131 does not affect liver AEA or NAE levels.[47] Activation of hepatic CB_1 receptors contributes to diet-induced metabolic pathology [49,50] and genetic FAAH deletion promotes a pre-diabetic state and adversely affects energy metabolism.[49,50,51] The lack of effect of LM-4131 on hepatic AEA indicates that substrate-selective COX-2 inhibitors may lack adverse metabolic side effects relative to other indirect or direct acting cannabinoid agonists.[47] Ongoing studies aimed at comparing and contrasting the relative cannabimimetic profiles of the three distinct endocannabinoid augmentation strategies will clarify the relative side-effect profiles of the three different enzymatic inhibition strategies.

Despite the promising initial studies with LM-4131, further characterization uncovered critical problems with its use *in vivo*. Although LM-4131 acted as a substrate-selective COX-2 inhibitor 2 hours after administration, at later time points it underwent hydrolysis to indomethacin. This metabolism to indomethacin results in the inhibition of PGs and a lack of substrate-selectivity over time. Thus, LM-4131 is not a good probe for acute studies lasting over 2 hours or for chronic studies.

To overcome the limitations of LM-4131 for *in vivo* time-course studies we turned to lumiracoxib. Lumiracoxib displayed robust substrate-selective inhibition *in vitro*, in cellular systems, and *in vivo*. In contrast to LM-4131, it has a long duration of action and is effective in chronic settings. However, lumiracoxib also displays a different biochemical profile than LM-4131 with significant increases in 2-OG and AA. Both of these increases are MAGL-dependent, as co-treatment of JZL-184 and lumiracoxib does not result in an additive increase of 2-OG and abolishes the increase in AA produced by lumiracoxib alone. While lumiracoxib does not display potent inhibition of MAGL *in vitro*, it is possible that lumiracoxib inhibits MAGL *in vivo*. Further determinations of the molecular mechanisms of lumiracoxib are required to define the parameters under which it would act exclusively as a substrate-selective COX-2 inhibitor. Although lumiracoxib does show initial

promise, further efforts to optimize the selectivity and pharmacological profile of *in vivo* substrate-selective inhibitors is needed.

Future studies utilizing the probes we have developed aimed at examining the therapeutic landscape of substrate-selective inhibition will provide a comparison of the therapeutic potential of substrate-selective inhibitors compared to traditional NSAIDs along with FAAH or MAGL inhibitors. Given the vast array of effects mediated by endocannabinoids and the identified beneficial effects of NSAIDs, substrate-selective inhibitors could represent an important novel class of therapeutic agents. Of primary importance, the ability of substrate-selective inhibitors to act as analgesic and anti-inflammatory agents has not yet been directly evaluated, although (*R*)-flurbiprofen has shown some initial promise as both an analgesic and anti-inflammatory agent. The probes developed in our laboratory coupled with other tools, such as prostanoid receptor knockout mice, will serve as invaluable tools to pinpoint the biochemical basis of the therapeutic effects of substrate-selective inhibitors.

We have also explored the biosynthetic pathway of PG-Gs in stimulated macrophages. Our finding that AA is a non-competitive inhibitor of 2-AG oxygenation by COX-2 *in vitro* was quite surprising. However, we leveraged the *in vitro* studies by using pharmacological inhibition or genetic deletion of cPLA$_2\alpha$ in macrophages, which resulted in significant decreases in PG production and significant increases in PG-G production. While these studies identified the 38:4 PI, 38:4 DAG, 2-AG, PG-G pathway as the likely source for increased PG-G production, further experiments identifying the enzymes responsible for the lipid remodeling are clearly required. While enrichment of 38:4 PI, 38:4 DAG, and 2-AG were readily apparent upon inhibition or deletion of cPLA$_2\alpha$, whether this pathway is actually directly coupled to COX-2 for oxygenation is unclear as the increases in these species is much larger than the increase in PG-G production. Additionally, whether 38:4 PI itself is the substrate for PLC or whether it is phosphorylated to generate PIP species that are then hydrolyzed to DAGs is unknown at this point. Previous studies have identified that while PIP$_2$ and PIP are preferred substrates for PLC, PI can also be hydrolyzed, albeit at a lower efficiency.[52-54] Given the much larger pool of 38:4 PI relative to 38:4 PIP and 38:4 PIP$_2$, it is possible that the major precursor for 38:4 DAG is in fact 38:4 PI. Further identification of the phospholipases involved in the biosynthesis of PG-Gs will also be necessary. While

the PLC and DAGL pathway appears to be the most enriched pathway upon inhibition or deletion of cPLA$_2\alpha$, it is possible that other pathways, such as the PLD pathway, may actually be directly involved in the increase of PG-G production. Selective inhibition of PLD1, PLD2, and DAGLβ, the major enzymatic isoforms mediating these pathways in RAW 264.7 cells and BMDMs, will provide further insight into the exact biosynthetic pathway of PG-Gs.

We also have not yet established a complete coverage of manipulating the production of AA in either RAW 264.7 macrophages or BMDMs. While cPLA$_2\alpha$ is the major source of AA, it can also be produced through hydrolysis of 2-AG by ABHD6, MAGL, and ABHD12. Further experiments examining the impact of ABHD6 and/or MAGL inhibition with and without cPLA$_2\alpha$ inhibition or deletion will provide a more complete picture of the interplay between 2-AG and AA oxygenation by COX-2. While no selective inhibitors of ABHD12 have been reported, previous studies have suggested that ABHD6 and MAGL are the major hydrolytic enzymes for 2-AG in macrophages. While we have not established each of the nodes of PG-G biosynthesis, we have identified that PG and PG-G production in stimulated BMDMs is mediated primarily by COX-2, as opposed to COX-1 in resident peritoneal macrophages.[55] Thus, future studies examining the biology of PG-Gs in a COX-2-dependent manner should focus on BMDMs rather than RPMs.

Taken together, these studies have identified and expanded our knowledge of the impact of COX-2 action on endocannabinoids and endocannabinoid-derived prostaglandin products. The development and characterization of novel substrate-selective COX-2 inhibitors for use *in vitro*, in cellular systems, and *in vivo* has produced valuable probes for studying the role of COX-2 in endocannabinoid metabolism and for elucidating the function of PG-Gs and PG-EAs. Substrate-selective COX-2 inhibitors provide a novel pharmacological strategy to augment endocannabinoid signaling without affecting PG formation. Substrate-selective inhibitors offer a novel mechanism for augmenting endocannabinoids and provide a valuable set of tools to elucidate the differential fundamental biology of endocannabinoid- and AA-derived COX-2 products.

Further studies optimizing the *in vivo* pharmacological profile of substrate-selective inhibitors and elucidating the therapeutic potential of this class of compounds could have broad implications. The potential to develop a novel class of NSAIDs with therapeutic effects and reduced side effect profiles is quite promising.

The studies discussed in this dissertation put forward the basic biochemical principles that mediate substrate-selective COX-2 inhibition, a series of probes to test the therapeutic potential and biological effects of substrate-selective COX-2 inhibition, and a fundamental understanding of how substrate-selective COX-2 inhibition interacts with the endocannabinoid system.

References

1. Yu, M., Ives, D. & Ramesha, C.S. Synthesis of prostaglandin E2 ethanolamide from anandamide by cyclooxygenase-2. *The Journal of biological chemistry* **272**, 21181-21186 (1997).
2. Kozak, K.R., Rowlinson, S.W. & Marnett, L.J. Oxygenation of the endocannabinoid, 2-arachidonylglycerol, to glyceryl prostaglandins by cyclooxygenase-2. *The Journal of biological chemistry* **275**, 33744-33749 (2000).
3. Woodward, D.F., Wang, J.W. & Poloso, N.J. Recent progress in prostaglandin F2alpha ethanolamide (prostamide F2alpha) research and therapeutics. *Pharmacological reviews* **65**, 1135-1147 (2013).
4. Kano, M., Ohno-Shosaku, T., Hashimotodani, Y., Uchigashima, M. & Watanabe, M. Endocannabinoid-mediated control of synaptic transmission. *Physiol Rev* **89**, 309-380 (2009).
5. Mechoulam, R. & Parker, L.A. The endocannabinoid system and the brain. *Annual review of psychology* **64**, 21-47 (2013).
6. Ahn, K., McKinney, M.K. & Cravatt, B.F. Enzymatic pathways that regulate endocannabinoid signaling in the nervous system. *Chem Rev* **108**, 1687-1707 (2008).
7. Piomelli, D. The molecular logic of endocannabinoid signalling. *Nat Rev Neurosci* **4**, 873-884 (2003).
8. Di Marzo, V. Endocannabinoids: synthesis and degradation. *Reviews of physiology, biochemistry and pharmacology* **160**, 1-24 (2008).
9. Petrosino, S. & Di Marzo, V. FAAH and MAGL inhibitors: therapeutic opportunities from regulating endocannabinoid levels. *Curr Opin Investig Drugs* **11**, 51-62 (2010).
10. Piomelli, D. The endocannabinoid system: a drug discovery perspective. *Curr Opin Investig Drugs* **6**, 672-679 (2005).
11. Blankman, J.L. & Cravatt, B.F. Chemical probes of endocannabinoid metabolism. *Pharmacological reviews* **65**, 849-871 (2013).
12. Cravatt, B.F.*, et al.* Supersensitivity to anandamide and enhanced endogenous cannabinoid signaling in mice lacking fatty acid amide hydrolase. *Proceedings of the National Academy of Sciences of the United States of America* **98**, 9371-9376 (2001).
13. Kathuria, S.*, et al.* Modulation of anxiety through blockade of anandamide hydrolysis. *Nature medicine* **9**, 76-81 (2003).
14. Khasabova, I.A., Xiong, Y., Coicou, L.G., Piomelli, D. & Seybold, V. Peroxisome proliferator-activated receptor alpha mediates acute effects of palmitoylethanolamide on sensory neurons. *The Journal of neuroscience : the official journal of the Society for Neuroscience* **32**, 12735-12743 (2012).
15. Fu, J.*, et al.* Oleylethanolamide regulates feeding and body weight through activation of the nuclear receptor PPAR-alpha. *Nature* **425**, 90-93 (2003).
16. O'Sullivan, S.E. & Kendall, D.A. Cannabinoid activation of peroxisome proliferator-activated receptors: potential for modulation of inflammatory disease. *Immunobiology* **215**, 611-616 (2010).
17. Dinh, T.P.*, et al.* Brain monoglyceride lipase participating in endocannabinoid inactivation. *Proceedings of the National Academy of Sciences of the United States of America* **99**, 10819-10824 (2002).
18. Hill, M.N.*, et al.* The therapeutic potential of the endocannabinoid system for the development of a novel class of antidepressants. *Trends Pharmacol Sci* **30**, 484-493 (2009).
19. Roques, B.P., Fournie-Zaluski, M.C. & Wurm, M. Inhibiting the breakdown of endogenous opioids and cannabinoids to alleviate pain. *Nature reviews. Drug discovery* **11**, 292-310 (2012).

20. Mulvihill, M.M. & Nomura, D.K. Therapeutic potential of monoacylglycerol lipase inhibitors. *Life sciences* **92**, 492-497 (2013).

21. Bari, M., Battista, N., Fezza, F., Gasperi, V. & Maccarrone, M. New insights into endocannabinoid degradation and its therapeutic potential. *Mini reviews in medicinal chemistry* **6**, 257-268 (2006).

22. Ghilardi, J.R., Svensson, C.I., Rogers, S.D., Yaksh, T.L. & Mantyh, P.W. Constitutive spinal cyclooxygenase-2 participates in the initiation of tissue injury-induced hyperalgesia. *The Journal of neuroscience : the official journal of the Society for Neuroscience* **24**, 2727-2732 (2004).

23. Guhring, H.*, et al.* A role for endocannabinoids in indomethacin-induced spinal antinociception. *European journal of pharmacology* **454**, 153-163 (2002).

24. Staniaszek, L.E., Norris, L.M., Kendall, D.A., Barrett, D.A. & Chapman, V. Effects of COX-2 inhibition on spinal nociception: the role of endocannabinoids. *British journal of pharmacology* **160**, 669-676 (2010).

25. Guindon, J., LoVerme, J., De Lean, A., Piomelli, D. & Beaulieu, P. Synergistic antinociceptive effects of anandamide, an endocannabinoid, and nonsteroidal anti-inflammatory drugs in peripheral tissue: a role for endogenous fatty-acid ethanolamides? *European journal of pharmacology* **550**, 68-77 (2006).

26. Guindon, J., De Lean, A. & Beaulieu, P. Local interactions between anandamide, an endocannabinoid, and ibuprofen, a nonsteroidal anti-inflammatory drug, in acute and inflammatory pain. *Pain* **121**, 85-93 (2006).

27. Telleria-Diaz, A.*, et al.* Spinal antinociceptive effects of cyclooxygenase inhibition during inflammation: Involvement of prostaglandins and endocannabinoids. *Pain* **148**, 26-35 (2010).

28. Prusakiewicz, J.J., Duggan, K.C., Rouzer, C.A. & Marnett, L.J. Differential sensitivity and mechanism of inhibition of COX-2 oxygenation of arachidonic acid and 2-arachidonoylglycerol by ibuprofen and mefenamic acid. *Biochemistry* **48**, 7353-7355 (2009).

29. Dong, L.*, et al.* Human Cyclooxygenase-2 Is a Sequence Homodimer That Functions as a Conformational Heterodimer. *Journal of Biological Chemistry* **286**, 19035-19046 (2011).

30. Kulmacz, R.J. & Lands, W.E.M. Prostaglandin-H Synthase - Stoichiometry of Heme Cofactor. *Journal of Biological Chemistry* **259**, 6358-6363 (1984).

31. Yuan, C.*, et al.* Cyclooxygenase Allosterism, Fatty Acid-mediated Cross-talk between Monomers of Cyclooxygenase Homodimers. *The Journal of biological chemistry* **284**, 10046-10055 (2009).

32. Duggan, K.C.*, et al.* Molecular basis for cyclooxygenase inhibition by the non-steroidal anti-inflammatory drug naproxen. *The Journal of biological chemistry* **285**, 34950-34959 (2010).

33. Kulmacz, R.J. & Lands, W.E. Stoichiometry and kinetics of the interaction of prostaglandin H synthase with anti-inflammatory agents. *The Journal of biological chemistry* **260**, 12572-12578 (1985).

34. Nirodi, C.S., Crews, B.C., Kozak, K.R., Morrow, J.D. & Marnett, L.J. The glyceryl ester of prostaglandin E2 mobilizes calcium and activates signal transduction in RAW264.7 cells. *Proceedings of the National Academy of Sciences of the United States of America* **101**, 1840-1845 (2004).

35. Richie-Jannetta, R.*, et al.* Structural determinants for calcium mobilization by prostaglandin E2 and prostaglandin F2alpha glyceryl esters in RAW 264.7 cells and H1819 cells. *Prostaglandins Other Lipid Mediat* **92**, 19-24 (2010).

36. Hu, S.S., Bradshaw, H.B., Chen, J.S., Tan, B. & Walker, J.M. Prostaglandin E(2) glycerol ester, an endogenous COX-2 metabolite of 2-arachidonoylglycerol, induces hyperalgesia and modulates NFkappaB activity. *British journal of pharmacology* (2008).

37. Patrono, C. Molecular and clinical determinants of the cardiovascular effects of selective COX-isozyme inhibition. *Ann Rheum Dis* **64**, 39-40 (2005).

38. Fitzgerald, G.A.*, et al.* COX-2 and mPGES-1 derived eicosanoids and cardiovascular function. *Prostag Oth Lipid M* **79**, 157-157 (2006).

39. Mitchell, J.A. & Warner, T.D. COX isoforms in the cardiovascular system: understanding the activities of non-steroidal anti-inflammatory drugs. *Nature Reviews Drug Discovery* **5**, 75-85 (2006).

40. Cannon, C.P. & Cannon, P.J. COX-2 Inhibitors and Cardiovascular Risk. *Science* **336**, 1386-1387 (2012).

41.   Yu, Y*., et al.* Vascular COX-2 modulates blood pressure and thrombosis in mice. *Science translational medicine* **4**, 132ra154 (2012).

42.   Warner, T.D. & Mitchell, J.A. COX-2 selectivity alone does not define the cardiovascular risks associated with non-steroidal anti-inflammatory drugs. *Lancet* **371**, 270-273 (2008).

43.   Wilcock, G.K. Disease-modifying treatments for Alzheimer's disease: a perspective based on experience with R-Flurbiprofen. *Alzheimer's & dementia : the journal of the Alzheimer's Association* **2**, 150-152 (2006).

44.   Wilcock, G.K*., et al.* Efficacy and safety of tarenflurbil in mild to moderate Alzheimer's disease: a randomised phase II trial. *Lancet neurology* **7**, 483-493 (2008).

45.   Goldstein, J.L*., et al.* Significantly improved upper gastrointestinal (UGI) tolerability with celecoxib, a COX-2 specific inhibitor, compared with conventional NSAIDs. The SUCCESS trial. *Gastroenterology* **120**, A105-A105 (2001).

46.   Burkhardt, F., Dammann, H.G. & Walter, T.A. COX-2 selectivity: Its clinical relevance for NSAID-gastrointestinal toxicity. *Clin Pharmacol Ther* **61**, Pii13-Pii13 (1997).

47.   Hermanson, D.J*., et al.* Substrate-selective COX-2 inhibition decreases anxiety via endocannabinoid activation. *Nature neuroscience* **16**, 1291-1298 (2013).

48.   Long, J.Z*., et al.* Dual blockade of FAAH and MAGL identifies behavioral processes regulated by endocannabinoid crosstalk in vivo. *Proceedings of the National Academy of Sciences of the United States of America* **106**, 20270-20275 (2009).

49.   Liu, J*., et al.* Hepatic cannabinoid receptor-1 mediates diet-induced insulin resistance via inhibition of insulin signaling and clearance in mice. *Gastroenterology* **142**, 1218-1228 e1211 (2012).

50.   Cinar, R*., et al.* Hepatic cannabinoid-1 receptors mediate diet-induced insulin resistance by increasing de novo synthesis of long-chain ceramides. *Hepatology* **59**, 143-153 (2014).

51.   Liu, J*., et al.* Monounsaturated fatty acids generated via stearoyl CoA desaturase-1 are endogenous inhibitors of fatty acid amide hydrolase. *Proceedings of the National Academy of Sciences of the United States of America* **110**, 18832-18837 (2013).

52.   Lee, K.Y., Ryu, S.H., Suh, P.G., Choi, W.C. & Rhee, S.G. Phospholipase C associated with particulate fractions of bovine brain. *Proceedings of the National Academy of Sciences of the United States of America* **84**, 5540-5544 (1987).

53.   Ryu, S.H., Cho, K.S., Lee, K.Y., Suh, P.G. & Rhee, S.G. Purification and characterization of two immunologically distinct phosphoinositide-specific phospholipases C from bovine brain. *The Journal of biological chemistry* **262**, 12511-12518 (1987).

54.   Ryu, S.H., Suh, P.G., Cho, K.S., Lee, K.Y. & Rhee, S.G. Bovine brain cytosol contains three immunologically distinct forms of inositolphospholipid-specific phospholipase C. *Proceedings of the National Academy of Sciences of the United States of America* **84**, 6649-6653 (1987).

55.   Rouzer, C.A*., et al.* Zymosan-induced glycerylprostaglandin and prostaglandin synthesis in resident peritoneal macrophages: roles of cyclo-oxygenase-1 and -2. *The Biochemical journal* **399**, 91-99 (2006).